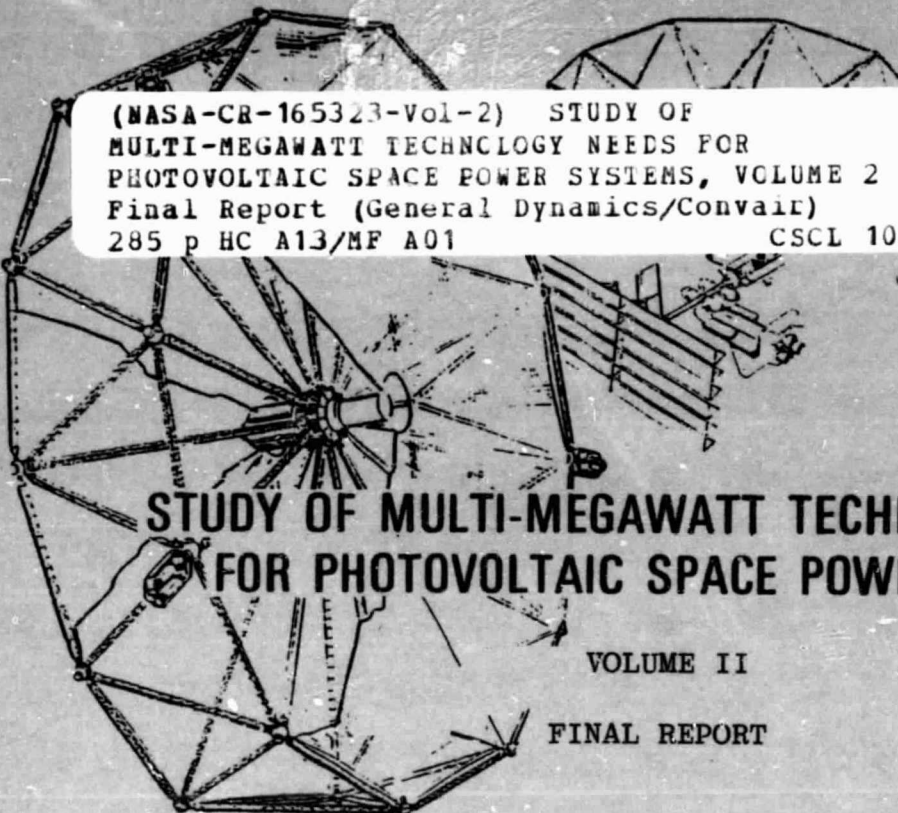


## N O T I C E

THIS DOCUMENT HAS BEEN REPRODUCED FROM  
MICROFICHE. ALTHOUGH IT IS RECOGNIZED THAT  
CERTAIN PORTIONS ARE ILLEGIBLE, IT IS BEING RELEASED  
IN THE INTEREST OF MAKING AVAILABLE AS MUCH  
INFORMATION AS POSSIBLE

REPORT NO. GDC-AST-81-019

CR 165323



(NASA-CR-165323-Vol-2) STUDY OF  
MULTI-MEGAWATT TECHNOLOGY NEEDS FOR  
PHOTOVOLTAIC SPACE POWER SYSTEMS, VOLUME 2  
Final Report (General Dynamics/Convair)  
285 p HC A13/MF A01

N82-14637

Unclas

CSSL 10A G3/44 08691

# STUDY OF MULTI-MEGAWATT TECHNOLOGY NEEDS FOR PHOTOVOLTAIC SPACE POWER SYSTEMS

VOLUME II

FINAL REPORT

May 1981

FOR  
NATIONAL AERONAUTICS AND SPACE ADMINISTRATION  
LEWIS RESEARCH CENTER

CONTRACT NAS3-21951



**GENERAL DYNAMICS**  
Convair Division

**PRECEDING PAGE BLANK NOT FILMED**

1. Report No. CR 165323	2. Government Accession No.	3. Recipient's Catalog No.	
4. Title and Subtitle Study of Multi-Megawatt Technology Needs for Photovoltaic Space Power Systems		5. Report Date 19 March 1981	
		6. Performing Organization Code	
7. Author(s) D. M. Peterson, R. L. Pleasant		8. Performing Organization Report No. GDC-ASP-81-019	
		10. Work Unit No.	
9. Performing Organization Name and Address		11. Contract or Grant No. NAS 3-21951	
		13. Type of Report and Period Covered Contractor Report	
12. Sponsoring Agency Name and Address National Aeronautics and Space Administration Lewis Research Center Cleveland, Ohio		14. Sponsoring Agency Code	
		15. Supplementary Notes	
16. Abstract			
<p>This study examines possible beneficial missions requiring multi-megawatt photovoltaic space power systems in the 1990s time frame and the power system technology needs associated with these missions.</p> <p>To develop the required technology plan, LEO and GEO missions are postulated, along with various orbital constraints and operational alternatives. Representative GEO Radar and LEO Construction Facility missions are selected for further study and the power requirements defined.</p> <p>Concepts for photovoltaic power approaches are considered, including planar arrays, concentrating arrays, hybrid systems using Rankine engines, thermophotovoltaic approaches; all with various photovoltaic cell component technologies. AC and DC power management approaches, and battery, fuel cell, and flywheel energy storage concepts are evaluated. Interactions with the electrical ion engine injection and stationkeeping system are considered.</p> <p>The levels of modularity for efficient, safe, constructable, serviceable, and cost effective system design are analyzed, and the benefits of alternate approaches developed. A technology plan for technology development which would not otherwise occur is presented. Also, technology developments applicable to power systems which appear to have benefits independent of the absolute power level are suggested.</p>			
17. Key Words (Suggested by Author(s)) Space Power, Solar Concentrators, Planar Arrays, Space Missions, Space Batteries, Space Flywheels		18. Distribution Statement Unclassified - Unlimited	
19. Security Classif. (of this report) Unclassified	20. Security Classif. (of this page) Unclassified	21. No. of Pages	22. Price*

\* For sale by the National Technical Information Service, Springfield Virginia 22161

PRECEDING PAGE BLANK NOT FILMED

FOREWORD

This final report was prepared by General Dynamics Convair Division for NASA Lewis Research Center in compliance with Contract NAS3-21951.

The principal results were developed throughout 1980 with reviews at LeRC on 7 May 1980, 4 September 1980, and 17 December 1980.

Because of the scope of the study, many individuals contributed technical assistance. General Dynamics Convair personnel who significantly contributed to the study include:

Study Manager	D.M. Peterson
Mission Orbital Constraints	L.A. Cowgill
Systems Thermal Analyses	R.L. Pleasant
Cost Analysis	R.C. Risley
Component Design Analysis	T.G. Stern J.W. Mildice C.G. Foster A.T. Wells
Concept Design and Trade Analysis Studies	D.M. Peterson T.G. Stern J.W. Mildice
Dynamics Analysis	R.V. Haltzenberg
Technical Review	M. Cornwall J.G. Fisher

In addition to the General Dynamics personnel involved, information pertaining to advanced photovoltaic cell projections was developed by T.J. Maloney and B.R. Cairns of Varian. They provided Appendix C to this report and their data is used for portions of the projections in Volumes I and II.

The study was conducted in Convair's Advanced Space Programs Department, headed by Vice President W. Rector. The NASA Project Manager is M. Valgora of the Space Propulsion Division.

For further information contact:

M. Valgora  
NASA/LeRC  
Cleveland, Ohio  
(216) 433-4000, Ext. 5186

D.M. Peterson  
General Dynamics Convair Division  
San Diego, CA 92117  
(714) 277-8900, Ext. 2204

This is the second of two volumes comprising the total report. Volume one is the Executive Summary.

## TABLE OF CONTENTS

<u>Section</u>		<u>Page</u>
1	INTRODUCTION	1-1
2	STUDY RESULTS	2-1
2.1	TASK I, BASELINE MISSION IDENTIFICATION	2-1
2.1.1	Identify Potential Missions	2-1
2.1.2	Solar Power Satellite (SPS) Technology Demonstration	2-1
2.1.3	Material Processing in Space (MPS)	2-4
2.1.4	Propellant Processor	2-4
2.1.5	LEO Space Construction Facility	2-7
2.1.6	Orbiting Space Sciences Observatory	2-10
2.1.7	Fast Electric Transfer	2-12
2.1.8	Air Traffic Control Radar Illuminator	2-17
2.1.9	RF Power Beaming Satellite in GEO	2-22
2.1.10	Orbital Constraints	2-22
2.1.11	Mission Selection and Grouping	2-29
2.1.12	Power Requirements	2-30
2.2	TASK II, CANDIDATE POWER SYSTEM CONCEPTS. AND COMPONENT TECHNOLOGIES	2-30
2.2.1	Concept Identification	2-30
2.2.2	Planar Array or Low Concentration about Gimbaled Axis (Concentration Ratio, CR, =2)	2-36
2.2.3	Large Trough Concentrators	2-51
2.2.4	Thermal Management Requirements	2-51
2.2.5	Operating Options	2-63
2.2.6	Geosynchronous Operational Modes	2-68
2.2.7	Operating Options - Planar Silicon Arrays	2-68
2.2.8	Power Generation Synthesis and Evaluation	2-69
2.2.9	Large Parabolic Troughs	2-76
2.2.10	Modular Trough Concentrators	2-78
2.2.11	Efficiency Chains	2-88
2.2.12	Mass Properties	2-93
2.2.13	Costs	2-93
2.2.14	Energy Storage	2-93
2.2.15	10-Megawatt Radar Power System Synthesis	2-93
2.3	TECHNOLOGY GOALS - SENSITIVITY TRADES AND ANALYSES	2-107
2.3.1	Thermal Management	2-107
2.3.2	Environmental Interactions	2-115
2.3.3	Storage, Development and Assembly	2-122
2.3.4	Safety	2-122
2.3.5	Modularity and Benefits Analysis	2-123

TABLE OF CONTENTS, Contd

<u>Section</u>		<u>Page</u>
2.4	TECHNOLOGY RECOMMENDATIONS	2-138
2.4.1	Power Generation Technology Gap Identification	2-138
2.4.2	Technology Requirements Definition	2-139
2.4.3	Critical Long Lead Technology Identification	2-139
3	CONCLUSIONS	3-1
4	REFERENCES	4-1
Appendix		
A	MULTIMEGAWATT POWER SYSTEM (MMPS) APPLICATION AND PERFORMANCE SHEETS	A-1
B	DEFINITION OF TECHNOLOGY REQUIREMENTS AND TECHNOLOGY PLANS	B-1
C	TECHNOLOGY PLANS	C-1

## LIST OF FIGURES

<u>Figure</u>	<u>Page</u>	
2-1	Baseline Mission Identification	2-1
2-2	Potential Missions	2-2
2-3	Satellite Power System - Demonstration Article	2-3
2-4	Material Processing in Space - Processing Cluster	2-5
2-5	Typical Propellant Processor System Schematic	2-6
2-6	Propellant Processor	2-7
2-7	LEO Mission Concept Space Construction Facility	2-8
2-8	Orbiting Space Sciences Observatory (OSSO)	2-11
2-9	Fast Electric Transfer System	2-15
2-10	Foldout Truss Deployable Antenna	2-16
2-11	160 Kilowatt System, 5 Years, $P(o) = 0.22$ (System)	2-18
2-12	Recommended Mission Concept Provides Conus Redundancy with Only Two Spacecraft	2-19
2-13	Air Traffic Control Bistatic Radar Power Allocation	2-21
2-14	FAA Traffic Control Alternatives	2-23
2-15	RF Power Beaming Satellite	2-24
2-16	Spacecraft Geometry and Definitions	2-25
2-17	Inertial Orientation of Spacecraft	2-27
2-18	Effect of Drag on a Large Planar Array	2-28
2-19	The Power and Array Sizing Chain — LEO Mission Varies with Energy Storage	2-31
2-20	Power System Concepts and Component Technologies	2-30
2-21	Multi-Bandgap Cells Utilize more of the Available Energy	2-33
2-22	Multi-Bandgap Cell Projections were Based on Detailed Cell Analysis	2-34
2-23	A Dual-Band Reflecting Concept for Higher Efficiency	2-35
2-23A	Various Cell Technologies Will Be Possible	2-37
2-24	Planar Array/Antenna Configuration for Radar Spacecraft	2-38
2-25	Space Construction Planar Array	2-39

## LIST OF FIGURES, Contd

<u>Figure</u>		<u>Page</u>
2-26	Parabolic Trough Collector for 10 MW Mission	2-40
2-27	Space Construction Facility Utilizing Large Parabolic Trough	2-41
2-28	The Second Configuration Uses a Planar Structure to Support Modularized Concentrators	2-42
2-29	Space Construction Semi-Parabolic Concentrator/Heat Pipe	2-43
2-30	Rectangular Deployable Truss Beam with Tensioned Solar Blankets for GEO Space Radar	2-44
2-31	Space-Fabricated Truss Beam	2-45
2-32	Planar Array and Antenna Configuration for Radar Spacecraft	2-46
2-33	Space Construction Planar Array	2-47
2-34	Mass Properties for Space Construction Facility	2-48
2-35	Ten Megawatt Planar Construction Using On Orbit Assembly-Construction Approach	2-49
2-36	Deployment of Hexagonal Array	2-50
2-37	Radar Modifications to Basic Parabolic Trough	2-52
2-38	Space Construction Facility Utilizing Large Parabolic Trough	2-53
2-39	Parabolic Concentrator with Pumped Coolant System	2-54
2-40	Spacecraft Thermal Model for Pumped Coolant System	2-54
2-41	Solar Cell/Coolant Tube Wall/Coolant Cross-Section	2-55
2-42	Heat Transfer Coefficient Versus Velocity for FC-75	2-57
2-43	Temperature Difference Across Coolant Boundary Layer Versus Heat Transfer Coefficient	2-57
2-44	Solar Cell Substrate $\Delta T$ s for Typical Low-k Semiconductor	2-58
2-45	Solar Concentrator Concept Suited to Heat Pipe Use	2-59
2-46	Heat Pipe Arrangement Assumed for Analysis	2-60
2-47	LEO Mission Concept Space Construction Facility	2-67
2-48	Three Geosynchronous Operational Modes are Feasible	2-68
2-49	Maximum Power Versus 1 MEV Electron Fluence for 2 Ohm-cm n/p Textured Silicon Cells. At 135.3 MW/cm <sup>2</sup> AMO Illumination, 30°C from Reference 20	2-72
2-50	Efficiency Chains GEO Planar Array	2-73

## LIST OF FIGURES, Contd

<u>Figure</u>		<u>Page</u>
2-51	CR=2 Geometry	2-75
2-52	Parabolic Trough Collector	2-77
2-53	Mass Extrapolation - Rankine Cycle Turbine-Generator	2-77
2-54	Hybrid Concentrator - Efficiency Chain	2-79
2-55	Block Diagram and Mass Properties Hybrid Concentrator with Cells at Secondary Focus	2-81
2-56	Efficiency Chain-Hybrid Concentrator with Cells at Secondary Focus	2-82
2-57	Advanced Goal (50% Efficient) Photovoltaic Array	2-83
2-58	Thermophotovoltaic Efficiency Chain	2-84
2-59	Small, Modular Trough Assembly	2-85
2-60	Orbital Geometry	2-87
2-61	Efficiency Chains - LEO Planar Array	2-89
2-62	Efficiency Chains - GEO Planar Array	2-90
2-63	Efficiency Chain - LEO Concentrators	2-91
2-64	Efficiency Chain - GEO Concentrators	2-92
2-65	10-Megawatt Radar Sizing - Planar Arrays and Large Concentrators	2-94
2-66	LEO Planar Array Sizing & Mass	2-95
2-67	2.5 Megawatt Sizing Modular Concentrator (CR=50)	2-96
2-68	10 Megawatt Sizing Modular Concentrator (CR=50)	2-97
2-69	Comparison of Estimates for the Three Power Generation Options (10 MW Space Radar)	2-98
2-70	Cost Comparison - LEO Power Generation	2-99
2-71	Six Energy Storage Technologies were Considered	2-100
2-72	Task II Comparison of Estimates for Alternative Storage Options	2-101
2-73	Typical Multi-Driver, Multi-Receiver System	2-105
2-74	Hybrid Power Management and Control Block Diagram - GEO Radar System	2-106
2-75	Technology Goals	2-107

## LIST OF FIGURES, Contd

<u>Figure</u>		<u>Page</u>
2-76	Variation of Coolant Temperature Rise with Passage Height and Velocity	2-109
2-77	Spacecraft Thermal Model for Heat Pipe System	2-111
2-78	Weight/Aperture Area as a Function of Sheet Reflector Thickness and Heat Pipe Spacing	2-112
2-79	Primary Reflector Temperature Distribution as a Function of Heat Pipe Spacing	2-113
2-80	Heat Pipe Temperature as a Function of Heat Pipe Spacing and Reflector Thickness	2-114
2-81	Radiator Heat Rejection View Factor Blockages for Two Representative Small Concentrators	2-116
2-82	Efficiency Chains LEO Planar Array	2-118
2-83	Geometrical Performance - 3 Mini-concentrators	2-124
2-84	Energy Storage - Flywheels and Sodium Sulfur Batteries could Support 30,000-120,000 LEO Cycles over 20-Year Life	2-129
2-85	Hybrid Power Management and Control Block Diagram -- LEO SCF System	2-131
2-86	Suggested Potential Distribution	2-133
2-87	GEO Mission - Radar Power Management and Control Approaches	2-137
2-88	Technology Recommendations	2-138

## LIST OF TABLES

<u>Table</u>		<u>Page</u>
2-1	Weight Breakdown for Propellant Processor	2-5
2-2	Mass Properties for Space Construction Facility	2-9
2-3	Functional Interface Requirements at Sensor Platform Docking Points	2-12
2-4	Preliminary Weight Statement (OSSO)	2-13
2-5	Fast Electric Transfer System Weight Targets, kg	2-14
2-6	Mass Properties for the 10 Megawatt Radar - Electrical Ion Engine Propulsion Injection with an AC Power Management System	2-65
2-7	Mass Properties for the 10 Megawatt Radar - Chemical Propulsion Injection	2-65
2-8	Annual Equivalent 1 MEV Electron Fluence for $V_{oc}$ and $P_{max}$ Due to Trapped Protons, Circular Orbits, Inclination 0 Degree, Infinite Backshielding Assumed from Reference 20	2-71
2-9	Mass Properties, Hybrid Concentrator	2-80
2-10	Power Management Major Components Considered	2-102
2-11	Assumptions for Calculating Radiator Sink Temperatures	2-110
2-12	Summary of Radiator Heat Rejection Fluxes, $W/m^2$ (Btu/hr-ft <sup>2</sup> )	2-110
2-13	Summary of Required Radiator Areas, $m^2$ (ft <sup>2</sup> )	2-111
2-14	BOL Performance - Three Mini-Concentrators	2-125
2-15	Final Trades Support the Minitrough	2-125
2-16	Cost Comparison LEO Power Generation	2-126
2-17	10 MW GEO Radar Mass and Cost Estimates	2-127
2-18	Costs and Benefits of Alternative Energy Storage Options	2-128
2-19	Comparison of Alternative Power Management Options	2-136
2-20	Technology Gap Identification	2-140

SECTION 1

INTRODUCTION

The ability of man to exploit space will be a function of availability of power and energy in space and the cost of that power. Programs (such as the 25 kW power system) are presently underway to develop and orbit space power ranging in the tens of kilowatts, and new studies are pursuing systems ranging to hundreds of kilowatts. It is envisioned that by the end of the century megawatt capability will power missions which will offer significant benefits to society. This study was constructed to survey possible beneficial missions and identify crucial technologies that must be developed to enable multimegawatt photovoltaic space power systems.

Both Low Earth Orbit (LEO) and Geosynchronous Earth Orbit (GEO) applications were examined. LEO orbits offered the obvious advantage of lower insertion costs and initial manned serviceability and constructability, while GEO orbits enable single or dual satellites to support services tied to one terrestrial area.

This study assumes that power levels in the low megawatt range can be realized by the year 2000 if technology development is started early enough to permit an orderly, well planned development approach. Such an approach would also aid in making programmatic decisions on current and near term technology efforts to direct those technologies toward a multimegawatt capability.

By contractual ground rule, a photovoltaic source was selected for the baseline power generation system, rather than solar thermodynamics or nuclear systems. However, to assure that possible beneficial solutions were not overlooked, two alternates employing hybrid photovoltaic/thermodynamic approaches were included for completeness.

The study was divided into four separate tasks:

Potential beneficial missions which require power in the 1 to 10 megawatt average power region were developed in Task I. Based on benefits, two types of missions were selected as study baselines and their power requirements developed.

In Task II, alternative power system concepts and operating options, including alternative component technologies, were identified and compared. One high-risk concept and a low-risk backup approach were selected for further study.

In Task III, the concepts were refined by performing trades and analysis, with particular attention to environmental interactions and modularity and safety, to establish technology goals. Benefits of the goals were established.

In Task IV, technology efforts which enable megawatt capability were identified and, based on benefit criteria, ranked and recommended.

## SECTION 2

## STUDY RESULTS

## 2.1 TASK 1, BASELINE MISSION IDENTIFICATION

This part of the study was performed as shown in Figure 2-1.

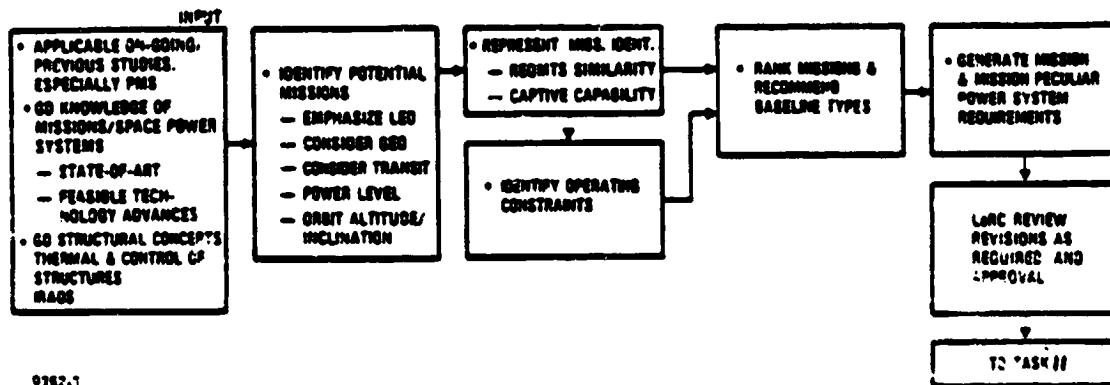


Figure 2-1. Baseline Mission Identification.

**2.1.1 IDENTIFY POTENTIAL MISSIONS.** The first step of the study identifies potential missions. Figure 2-2 indicates several of the potential missions which were considered. In addition to those listed in Figure 2-2, one other mission was considered; RF and laser GEO power beaming to LEO user satellites.

**2.1.2 SOLAR POWER SATELLITE (SPS) TECHNOLOGY DEMONSTRATION.** The prospect of converting solar energy at geosynchronous orbit continues to represent one of the more likely major future technological/energy thrusts. Its viability is enhanced by its 4 to 1 advantage over terrestrial solar power sources from its locations, and its potential for lower environmental risks than fusion, fission, or coal systems. The major obstacles to a funded SPS program are posed by technical uncertainties, public acceptance of environmental impacts, and skepticism about current economic analyses based on tentative assumptions. Like fusion, the technological approaches involved are varied, and all the effects and impacts of the various alternates have not been fully assessed or demonstrated. Several SPS technology demonstration approaches are viable, including non-photovoltaic systems which are not part of this study.

Capture probability of the SPS demonstration mission is rated high (Figure 2-3). While it can be argued that some major segments of the SPS, such as the required heavy launch vehicles and space construction techniques, would not be demonstrated

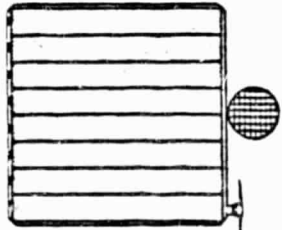
	<b>SPS CONCEPT PROOFING</b>	<b>MANUFACTURING ENERGY INTENSIVE</b>	<b>PROCESSING PROPELLANTS FROM H<sub>2</sub>O</b>	<b>EXPERIMENTS HIGH-ENERGY SCIENCE</b>	<b>TRANSPORTATION FAST ELECTRIC TRANSFER SYST</b>	<b>AIRPORT RADAR DOMESTIC SERVICES</b>
1 MW 250 NM 28.5 INTERMITTENT 2 YRS	1-10 MW 300 NM 28.5 INTERMITTENT 20 YRS	1.5 MW 260 NM 31 INTERMITTENT 20 YRS	1-5 MW 300 NM 28.5 CONSTANT 20 YRS	5 KW ALL ALL INTERMITTENT 10 YRS	10 MW GEOSTATIONARY 0 CONSTANT/EXCEPT MIDNIGHT 20 YRS	1890 - 2000

Figure 2-2. Potential Missions.

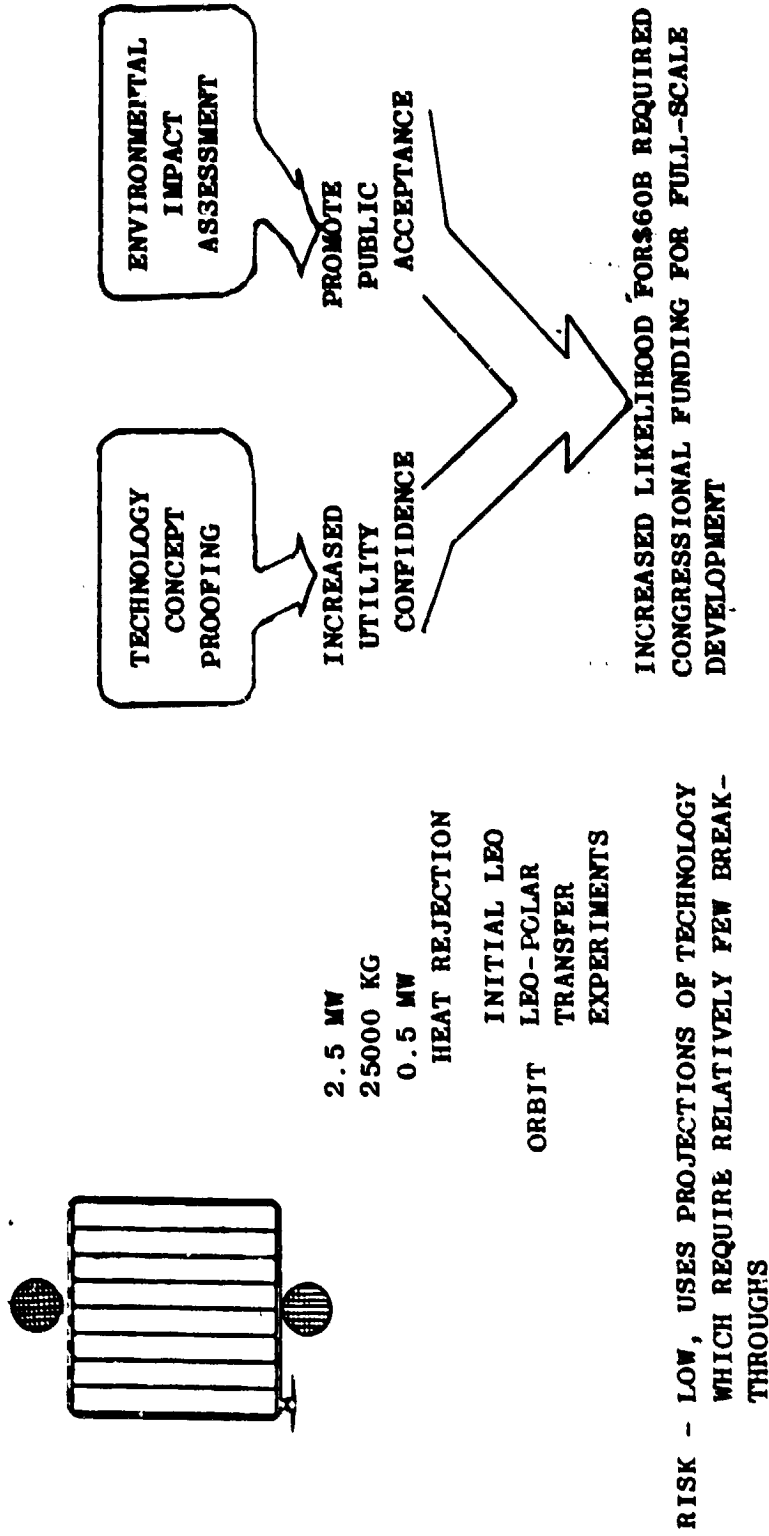


Figure 2-3. Satellite Power System - Demonstration Article.

with a shuttle launch demonstrator, the operational environment of high power and high voltage arrays and large, relatively flexible structures differs enough from present or future GEO satellite plans to warrant demonstration up to the limits of shuttle capability. Further, efficient RF conversion, transmissions, and rectification, and concerns about RFI/sidelobe environmental impacts should be addressed with test data for a GEO stabilized large structure. Without the data, environmental skepticism will remain too high for the full public support needed for the program.

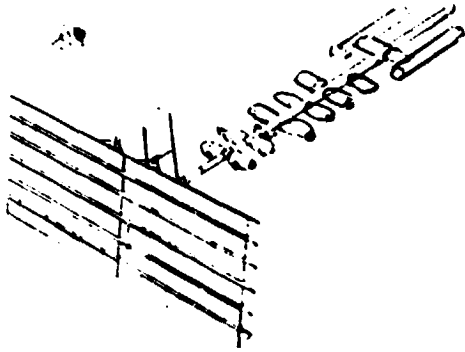
This study, therefore, includes the SPS demonstration mission. Orbital inclination is the recommended zero degrees (Ref. 1), weight is  $2.5 \times 10^4$  Kg, with 2.0 megawatts useful power delivered to a potential load. Although the two pure photovoltaic SPS concept baselines do not include active heat rejection, it is included here as a contingency that may be deleted later. Mission objectives include the demonstration of concept viability, measurements of efficiency and reliability, and data gathering on environmental interaction. These data would increase the credibility of studies leading to full-scale SPS development.

**2.1.3 MATERIAL PROCESSING IN SPACE (MPS).** With the advent of the space transportation system, it becomes feasible to consider the manufacturing of high technology drugs, perishable cutting tools, and semiconductor electronics, whenever zero "g" can significantly increase quality or yields. Science Applications, Inc. (SAI) estimated in 1977 (Ref. 2) that up to 25% of the drug market, 50% of the current tool market, and 10% of the semiconductor market (with space segment sales of 15, 38, and 17 billion dollars, respectively) might be economically justifiable. These processes have not yet been proven, but the potential is there. Certainly, if they can be developed, they will provide a significant encouragement for public support of space activities which is now lukewarm because the benefits are not clearly evident.

NASA plans to begin the development of MPS activity in the near future, and some contractor studies have suggested that material-processing clusters could be developed by the late 1990s to meet the needs for material processing in an efficient manner.

Unfortunately, in evaluating a cluster concept for materials processing (Figure 2-4), the conflicting needs of the different processes make a single integrated facility impractical, at least at this time when much basic research is still needed to prove the feasibility of manufacturing in space. Specific issues would be contamination and different basic operational points. Materials processing is a "hot" activity, while bio-processing (drugs) tends to be cold or at room temperature. All the processes require low "g" levels, and clustering complicates the environmental interaction.

**2.1.4 PROPELLANT PROCESSOR.** In the event that electric propulsion technology is unable to fulfill the requirements for transfer or interplanetary missions in the 1990s because of technical or economic considerations, an orbiting propellant processor was considered as a possible approach processing a high probability



ORBIT LEO, LATE 1990's  
20 YEAR LIFE,

$5 \times 10^{-5}$  G's

100-200 GROUPED CLUSTER @  
15-30 KW=1.5-6 MEGAWATTS

INTERMITTANT SERVICE OK FOR  
RE-SUPPLY

RISKS - CLUSTER INTEGRATION

DESIRED WEIGHT NOT  
INCLUDING MPS UNITS . 25000 Kg

Figure 2-4. Material Processing in Space - Processing Cluster.

of success and the ability for alternative functions. The major advantages of processing  $LH_2$  and  $LO_2$  fuels in LEO include the ability to avoid expenditure of fossil fuels on Earth for electrolysis, the high power density achievable with these more conventional thrusters and the ability to provide full-time multi-100kW power by later incorporating banks of nonregenerative fuel-cells, using the liquified gasses as a power storage medium.

A typical system configuration is shown in Figure 2-5, from which it can be seen that the high power level arises primarily from the requirements for electrolysis and the low coefficient of performance attained in cryogenic cooling. The weight breakdown shown in Table 2-1 indicates that the primary component of mass is the  $LO_2$  tank, and that multiple Shuttle launches or Heavy Lift Launch Vehicle (HLLV) Shuttle derivative would be required.

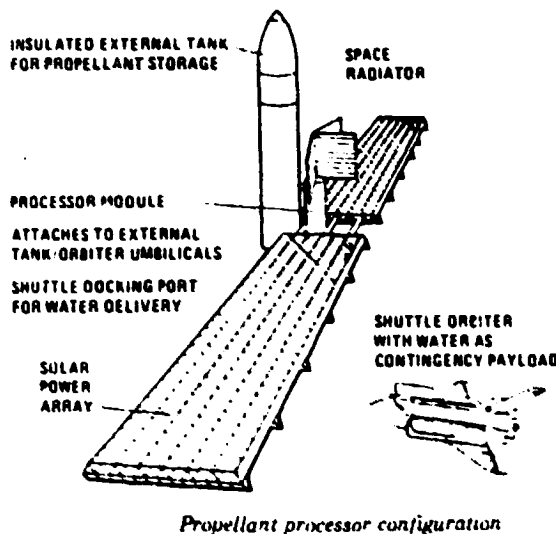
Table 2-1. Weight Breakdown for Propellant Processor.

$LH_2$ Tank	3,600 kg
$LO_2$ Tank	21,800
Radiators ( $2.4 \text{ kg/m}^2$ )	1,000
Stirling Cycle Refrigerators (2)	4,100
$H_2O$ Tank	250
Electrolyzer	900
Array (1 mw @ 430 w/kg)	2,300
Pumps, Piping, Insulation	2,250
<b>TOTAL SYSTEM</b>	<b>36,200 kg</b>
Initial Water Fill	25,400
<b>Total Operational Weight</b>	<b>61,600 kg</b>



The capture probability of this mission is considered to be low (Figure 2-6) for the following reasons:

- a. Ion and Magneto Plasma Discharge (MPD) thrusters are in an advanced state of technology development, and although there are uncertainties, it can be expected that these will be reduced in the time frame considered.
- b. Micro-meteoroid protection of the tanks makes them very heavy, leading to high transportation costs. Completely fail-safe protection is considered unlikely.
- c. The considerable masses of the oxygen tank and the water fuel would require multiple Shuttle launches to implement this system.



POWER LEVEL: 1 MW BASELINE  
COULD BE SCALED TO ANY SIZE

LIFE - 20-30 YEARS

LEO ORBIT FUELING STATION  
FOR TRANSFER, INTERPLANETARY,  
REBOOST OR LONG-TERM MISSIONS

SYSTEM MASS INCLUDING FUEL -  
61600 KG

RISK - CATASTROPHIC FAILURE IN  
EVENT OF METEOROID OR STRAY  
SATELLITE IMPACT RESULTING IN  
BREACH OF CONTAINMENT

Figure 2-6. Propellant Processor.

**2.1.5 LEO SPACE CONSTRUCTION FACILITY.** There are two major thrusts that encourage the development of space construction capability. The first arises from the results of many studies that are concluding that the Shuttle System payload capability is volume-limited rather than weight-limited. This implies that more efficient use of STS will result from the ability to load the cargo bay with a dense array of raw materials and then to perform construction and deployment of basic building blocks using an orbiting construction facility. This will allow a variety of structures to be implemented without incurring the penalty of

transporting a separate deployment mechanism to orbit for each. The planar structure of Figure 2-7 is an example. This would be especially true as shuttle performance increases in the 1990s.

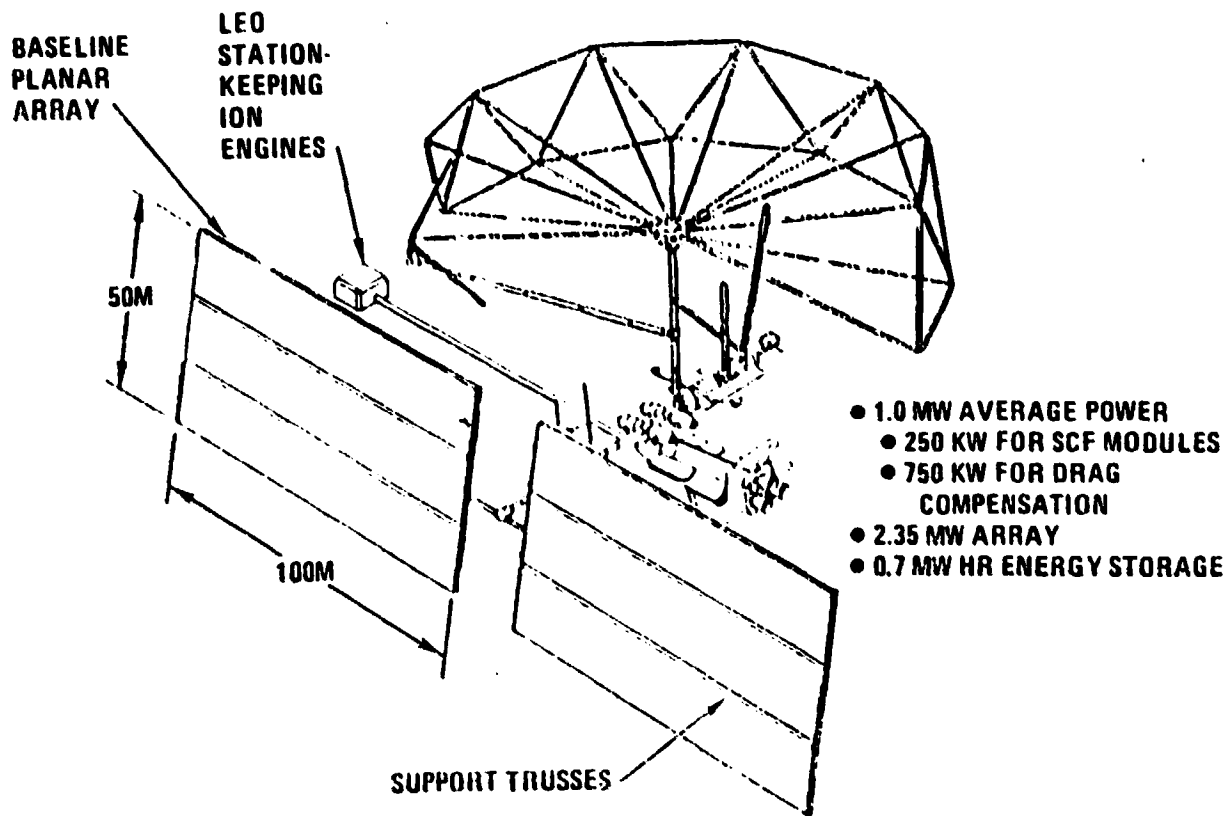


Figure 2-7. LEO Mission Concept Space Construction Facility.

The second thrust is the fact that deeper structures can be more maneuverable and transportable. Perhaps they can be erected in LEO, fully tested, and then deployed intact more easily with this facility. Later in this study, concentrating arrays are shown to have greater benefits (lower cost, higher efficiency) than planar arrays. This also may be true at lower power levels for different missions (Ref. 3). The technology for assembly may be significantly aided by utilizing space-aided construction.

Because of these issues, a space construction facility was selected as a baseline LEO mission.

Since the facility would be used to assemble larger spacecraft, such as those eventually to be stationed at GEO, the baseline design includes ion engines and their propellants required for stationkeeping, as described in the following section on orbital constraints. Final trades could substitute more engines and array

than included in the baseline; these would fire only when the spacecraft is isolated by sunlight, and the energy storage requirement would be decreased accordingly.

A set of baseline design SCF mass properties were developed to be used as input to the stationkeeping analysis. Table 2-2 lists the major components of the facility and their masses. A minimal facility could consist of a beam builder, a manipulator, a device for sheathing the structure in some manner dependent upon the particular application; for example, the construction of solar arrays, or manned stations requiring radiation shielding, pressurized "cherry-pickers" for manned operations, and crew quarters. Capture probability for the mission is high because it will be prerequisite to the deployment of very large space structures, and should enable more effective use of STS.

Table 2-2. Mass Properties for Space Construction Facility.

<u>MASS PROPERTIES</u>		<u>WEIGHT BREAKDOWN</u>	
Required Power	1.00 MW AVG	Beam Builder	15,000 kg
Energy Storage	0.64 MWH	Crane/Manipulator	20,000
Array for Energy Storage	0.7 MW	Sheather	5,000
Total Array	1.7	"Cherry-Pickers"	12,000
With Safety Factor (0.9)	2.35 MW	Crew Quarters	10,000
Distribution (0.9) and EOL (0.9)		2.5 MW Array	12,500**
		Energy Storage	<u>10,000**</u>
			84,500 kg
Array Area Required (0.17 η)	10,000 m <sup>2</sup>	<u>ALTERNATE BREAKDOWN</u>	
Solar Blanket Mass (10,000 x 0.8)	8,000 kg	Robotic Beam Extender(s)	15,000 kg
Truss Mass (4300 m x 0.87 kg/m)	3,700	Crane/Manipulator	20,000
Odapt* Mass	<u>800</u>	Crew Quarters	20,000
Total	12,500 kg	2.5 MW Array	12,500**
Electrical Propulsion Mass	100,000 kg	Energy Storage	<u>10,000**</u>
			77,500 kg

\* Orientation Drive and Power Transfer.

\*\* Depended upon Study Outputs — Final Estimates Higher.

**2.1.6 ORBITING SPACE SCIENCES OBSERVATORY.** The Orbiting Space Sciences Observatory (OSSO) (Figure 2-8) is a large, orbital laboratory facility that could be used by international scientists to increase man's knowledge and understanding of the earth's space environment, the sun, stars, and other celestial bodies. Specifically, OSSO would be employed for research to investigate the earth's upper atmosphere, the ionosphere, the magnetosphere, the interplanetary medium, and their coupling links; and to make observations of solar cosmic ray, X-ray, gamma ray, ultra violet, infrared, and radio emissions not possible from ground-based observatories.

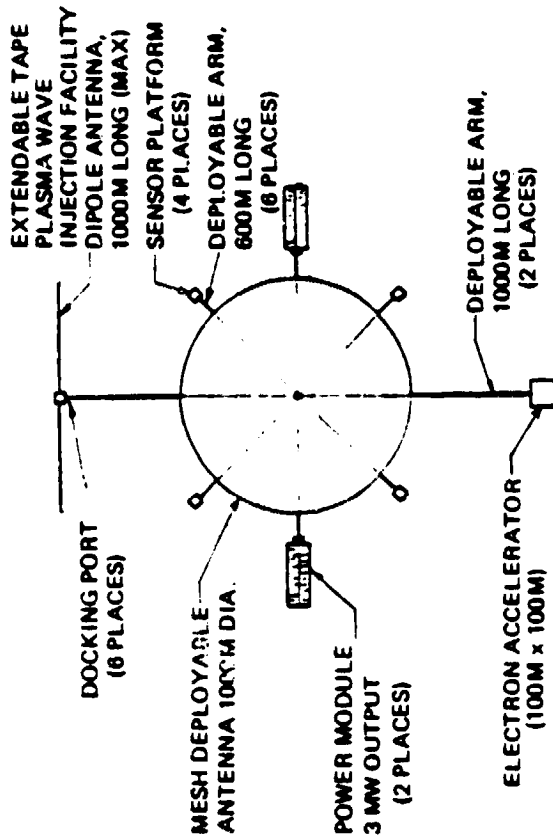
This large orbital facility is an unmanned, multi-purpose scientific observatory that provides central subsystem support (power generation and storage, propulsion, attitude control, telemetry and control communications, computation, and data handling) for a wide variety of user-provided scientific payloads in the Astrophysics and Solar Terrestrial Programs, thereby providing the scientific community with both economic benefits and expanded technological capabilities; e.g., high power, large area sensors, and a wide range of orbit altitudes and inclinations.

The OSSO will be a long-life facility that is initially assembled in low earth orbit (LEO) and is thereafter periodically serviced and refurbished in LEO using the Space Shuttle. Typical mission durations might range from 1 to 2 years. Some of the scientific instruments would stay aboard for multiple mission periods. Others would be updated in accordance with new mission requirements and as new technology evolves.

An advanced electric propulsion system provides the capability to operate over a wide range of earth orbit altitudes and inclinations. Each mission begins and ends in Shuttle-compatible low earth orbit; e.g., 300-500 km altitude and 28.5 to 56 degrees inclination. The electric propulsion system provides the capability for plane changes (range 0 to 104°) and orbit altitude changes (range 300-100,000 km), depending upon the specific mission requirements.

The facility includes a 1000m diameter antenna that is used for radio astronomy, gravity wave experiments, inner magnetosphere cold electron dynamics investigations, and various radar applications. The antenna size and figure should make it usable up to about 0.2 GHz.

The large size of the facility makes possible the use of very large experiment equipment items such as the 1000m long dipole antenna of the plasma wave injection facility (PWIF). Figure 2-8 shows the OSSO typically configured for a plasma Physics investigation mission. The extendable tape dipole antenna is used for investigations of magnetic pulsations and wave-particle interaction, and the electron accelerator is used for particle beam injection experiments. Diagnostic instruments such as rf receivers, energetic particle detectors, optical imagers & photometers, magnetometers, and wave detectors are mounted on sensor platforms at the ends of four 600m long experiment mounting arms. For other types of missions, these sensor platforms would carry telescopes, spectrometers, polarimeters, high-energy detectors, and



- ELECTRIC PROPULSION MODULE:  
USES 37 60-CM THRUSTERS WITH 4.1 N THRUST EACH.  
ARGON WORKING FLUID.  
 $I_{sp}$  3000 SEC.
- THE 8 EXPERIMENT EQUIPMENT MOUNTING ARMS EACH HAVE DOCKING PORTS WHICH PROVIDE THE STRUCTURAL AND FUNCTIONAL INTERFACE FOR SENSOR PLATFORMS, ANTENNAS, ETC.
- THE OBSERVATORY IS ASSEMBLED, SERVICED AND REFURBISHED IN LEO USING THE SPACE SHUTTLE.
- THE OBSERVATORY IS UNMANNED WHILE OPERATING.

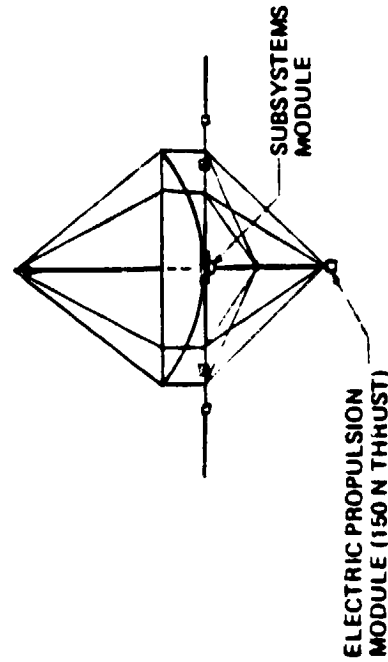
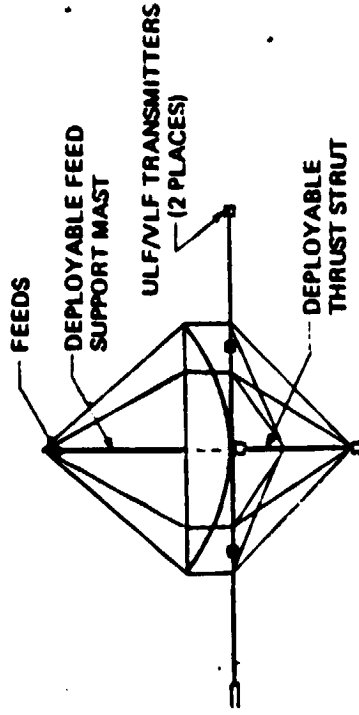


Figure 2-8. Orbiting Space Sciences Observatory (OSSO).

their supporting electronics. Some of the telescopes and/or detectors will be cooled to LHe or LH<sub>2</sub> temperatures and will require closed-loop refrigeration for these long term missions.

Standard docking ports are provided at the ends of the six 600m long experiment mounting arms. These provide the structural and functional interface for interchangeable platforms that house the user-supplied scientific experiment equipment. The functional interfaces to be accommodated are listed in Table 2-3.

Table 2-3. Functional Interface Requirements at Sensor Platform Docking Points.

---

Structural:	Maximum sensor platform mass = 5,000 kg (each of six)
Electrical Power:	Up to 3 mw at any location (not simultaneously)  4 mw total power during operation of experiments
NOTE: High power experiments do not operate while propulsion system is operating.	
Data Handling:	Digital = 50 mbps TV = 4.5 MHz, 2 channels simultaneously
Pointing/Attitude Control:	±5 degrees for photovoltaics
NOTE: 1000 m antenna pointing/attitude control = ±0.2 deg.	

---

The design of the OSSO must assure that the facility will not contaminate or otherwise perturb the local environment and thus invalidate the results of the investigations underway. For this reason, fine pointing control is accomplished using reaction wheels rather than mass-expulsion devices, and the electric propulsion system employs argon as the working fluid. Magnetic fields produced by the electrical power generation and distribution system must also be controlled to acceptably low values.

The total facility is estimated to weigh approximately 80,000 kg at the beginning of a typical mission. A preliminary weight estimate is presented in Table 2-4.

**2.1.7 FAST ELECTRIC TRANSFER.** The development of larger ion or MPD engines (References 4 and 5) could offer the prospect of relatively fast electric transfer from LEO to GEO.

The number of shuttle flights for propellant transfer would be reduced with this development, and thus the domain of less expensive space transportation extended to GEO altitudes. Even lunar transfer could become less expensive should lunar resources become needed in space.

Table 2-4. Preliminary Weight Statement (OSSO).

ELEMENT	MASS, kg
Structure	5,400
Electrical Generation & Storage	18,000
1000m Antenna	2,800
TCC	200
ACS	2,000
Propulsion, dry	7,600
Argon	12,000
Payload Equipment	30,000
Total	78,000

Successful pursuit of the fast electric transfer system (FETS) concept must recognize a need for technology developments along several lines of effort, including:

- a. Advanced photovoltaic arrays
- b. Light-weight, efficient support structures
- c. Light-weight power bussing
- d. DC to DC power conversion at MW levels, including possible on-array conditioning
- e. Thermal heat rejection
- f. Long life ion or MPD thrusters

By reason of high specific impulse (5,000 to 10,000 seconds), possible large cost savings are foreseen due to fewer shuttle flights needed for carrying propellants into orbit. Propellant requirements can be ideally determined by the ratio of the ISPs of the various propellants under consideration, but in practice, reduction of total system mass is not this large because the self-powered electric stage is heavier than its counterpart in a chemical OTV.

It is useful to examine a hypothetical design to better reveal the target areas for development to achieve fast electric transfer. Identification and study of the vehicle systems that use and service electrical thrusters may uncover information that is critical to the development of the thruster itself.

For this preliminary examination, Reference 4 was used to estimate thruster performance.

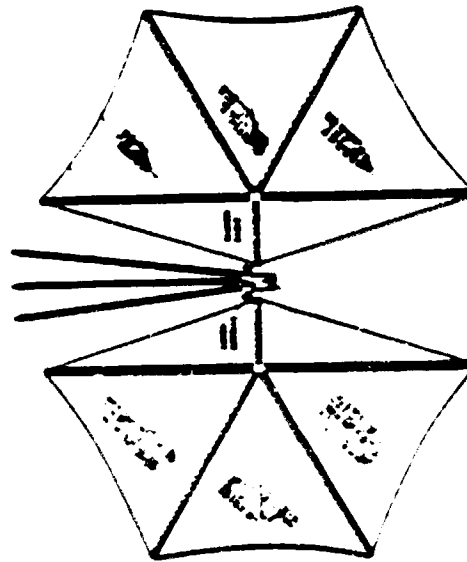
An overall concept for a FETS is shown in Figure 2-9. Two large solar arrays are coupled to the equipment and propulsion module through rotating joints. The structural subsystem is derived from a truss concept patented by General Dynamics in 1974 and from work accomplished during 1977 and 1978 under an Air Force study for On-Orbit Assembly of a large space antenna. During this study, a lightweight, deployable truss was defined (Figure 2-10). Linear packaging ratios of 10:1 and volumetric ratios of 40:1 are achievable with this concept. For the FETS structure, truss weights of 0.566 lb/ft are projected. Concepts for unfurling and tensioning very large membranes were also defined.

Important to the concept is a photovoltaic array of an advanced design. Lightweight, high efficiency, and long life are all important considerations. Studies by General Electric for NASA have shown potential for constructing arrays for approximately 450 watts/kg (array only). For this preliminary definition, array performance is targeted for 430 watts/kg at 260 watts/sq. meter.

Table 2-5 summarizes subsystem weights used to arrive at a total system weight. One of the important tradeoffs recognized is in the area of power conversion. DC to DC converters built to current technology would weigh three or four pounds per kilowatt, which would result in the single heaviest subsystem. A converter appears to be necessary, since the supply voltages for the ion and MPD thrusters are varied, whereas for maximum efficiency the supply voltage array may be 1000 volts. An ideal system might be designed to operate without power conversion. Trades at a system level can reveal information on this possibility. For the purpose of this estimate, a target weight of 1 kg/kw was inserted in the table for power conversion.

Table 2-5. Fast Electric Transfer System Weight Targets, kg.

Array Support Trusses 800m at 0.836 kg/m	640	Central Module	800
Payload Transfer Trusses 360m at 0.836/m Berthing devices and fittings 300 kg	300 300	Electronics	300
Array 5.1 mw at 430 w/kg	12,000	Batteries and Power Control	300
Array Deployment Drums Drums (2) 200 kg cable 2500m 160 kg motors 40 kg mechanism 40 kg	440	Auxiliary Propulsion	500
Main Support Truss 110m at 2.2/m	220	Argon Containers 15,000 lb capacity	1,000
Rotating Machinery est 5% of array weight	550	Thrusters 30 at 20 kg each	600
Bussing est 5% of array weight	550	DC to DC Converters/on Array Conditioning 1 kg/kw	5,000
		Radiator est. 98% power conversion 20 kg/kw	2,000
		<b>TOTAL</b>	<b>25,500</b> dry



RISKS - THE ATTACHED DESCRIPTION BREAK-DOWN SHOWS SOME RISKS IN THE AREA OF THRUSTER TEMPERATURE/ION ENGINE DEVELOPMENT, AND IN HOW POWER CONVERSION EFFICIENCIES CAN BE INCREASED.

**ORBITAL/TRAJECTORY REQUIREMENTS**

DELTA V- 5,800 M/SEC (19,000 FT/SEC)  
 TIME FOR XFER 30 DAYS  
 WEIGHT BOGIE - 25,000 KG  
 COST BOGIE - \$100,000,000 VEHICLE COST

POWER DURING  
 THRUST - 5.1 MW

**RADIATION DOSAGES TBS**

ACCELERATION - .0002 g's.  
 DRAG NEGLIGIBLE  
 SHADOWING 10%  
 LIFE 10 YEARS  
 HEAT REJECTION - NOT REQUIRED - TO BE FURTHER INVESTIGATED IN TASK III.  
 CAPTURE PROBABILITY - HIGH

Figure 2-9. Fast Electric Transfer System.

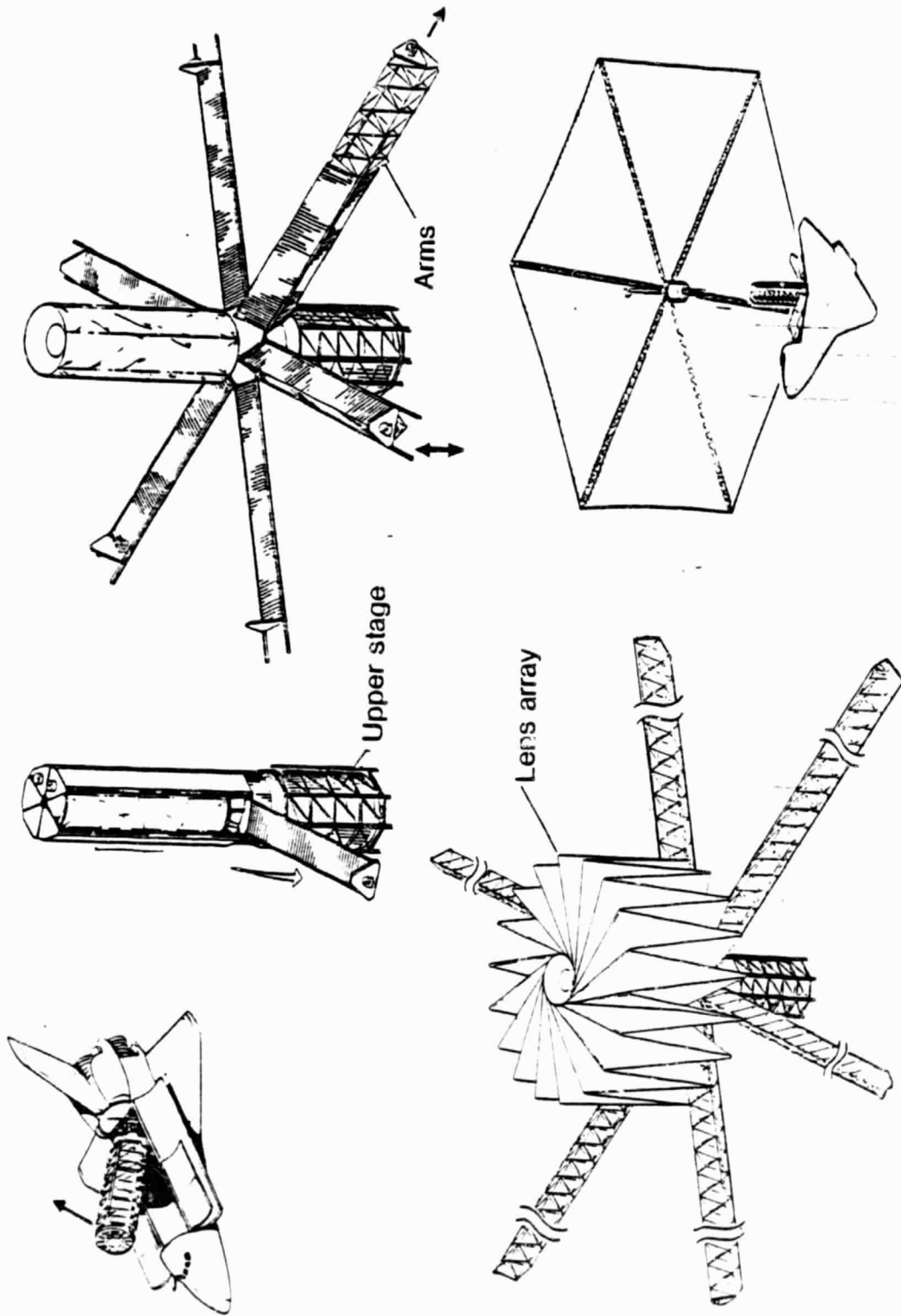


Figure 2-10. Foldout Truss Deployable Antenna.

A second major area of concern is heat rejection for the thrusters. No weight has been included in the table for radiators. Reference 5 estimates that it can be done for 700 kg per thruster. This may be conservative, and may also impose undue penalty in the event that multiple thrusters are used to unsure long life for the system. Some other way might be studied to solve the heat rejection problem. A bank of sixty MPD thrusters operating at one second on and fifty-nine off, might be self-cooled. If this works, it could also prolong thruster life, by distributing firing time across sixty thrusters. An additional system trade is required to establish whether the projected ion engine efficiency and array weight savings are worth the added complication.

Assuming the target weights indicated in Table 2-5 are achievable, the FETS can become an efficient and useful tool for both orbital transfer and planetary exploration. The weights are felt to be realistic, and in some cases conservative. For example, a radiator weight of 2000 kg, could be as low as 900 kg, according to some parametric information produced by the Vought Corporation (Figure 2-11).

With the fast electric transfer system, a GEO transfer time of 30 days is the goal. For the configuration outlined herein, preliminary estimates show a payload transfer capability of 20,000 kg to GEO, carrying sufficient propellants for return to LEO.

Conclusion: Although the Fast Electric transfer stage does provide significant benefits as a vehicle stage, it was not selected as a baseline mission for the study. It was felt that it would be better to select a mission which, in itself, provided new benefits to the public in terms of the actual use of power in orbit for extended time periods.

**2.1.8 AIR TRAFFIC CONTROL RADAR ILLUMINATOR.** There are approximately 13,000 commercial airports in the United States today. At this time, they have varying degrees of radar coverage for air traffic control/collision avoidance. There are indications from news media reports that the air traffic control and collision avoidance system could benefit from increased accuracy and awareness of the proximity of air traffic. Two ground station transmitters would be required to reliably assure that the area of each airport is illuminated, so that single point failures leave the system operational.

Further, each radar requires its own power, which is generated terrestrially. This generation adds to terrestrial energy usage; and, since beam field strength is relatively high, poses a possible health risk to personnel in close proximity to the transmitter. The above deficiencies can be overcome by careful control, but an alternative is the space generation of energy in the form desired.

Figure 2-12 shows the basic system approach for such a bistatic illuminator, and a baseline spacecraft configuration using planar arrays. A space radar transmitter operating in a bistatic mode would sequentially illuminate the area surrounding up to 1,000 airports. Surrounding the airport, several bistatic receivers would use inexpensive high-speed data processors which will be available in the



ORIGINAL PAGE IS  
OF POOR QUALITY

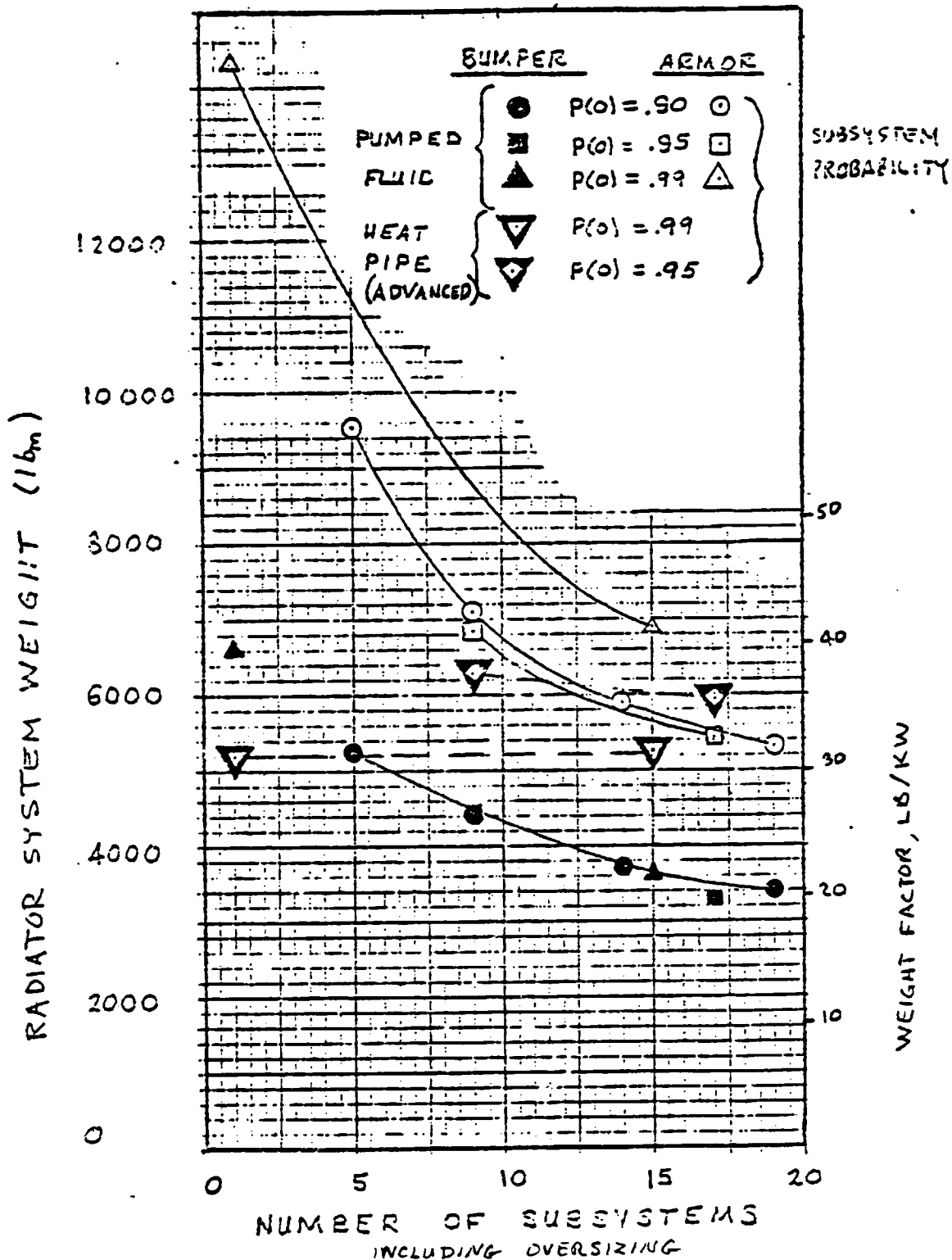


Figure 2-11. 160 Kilowatt System, 5 Years,  $P(o) = 0.22$  (System).

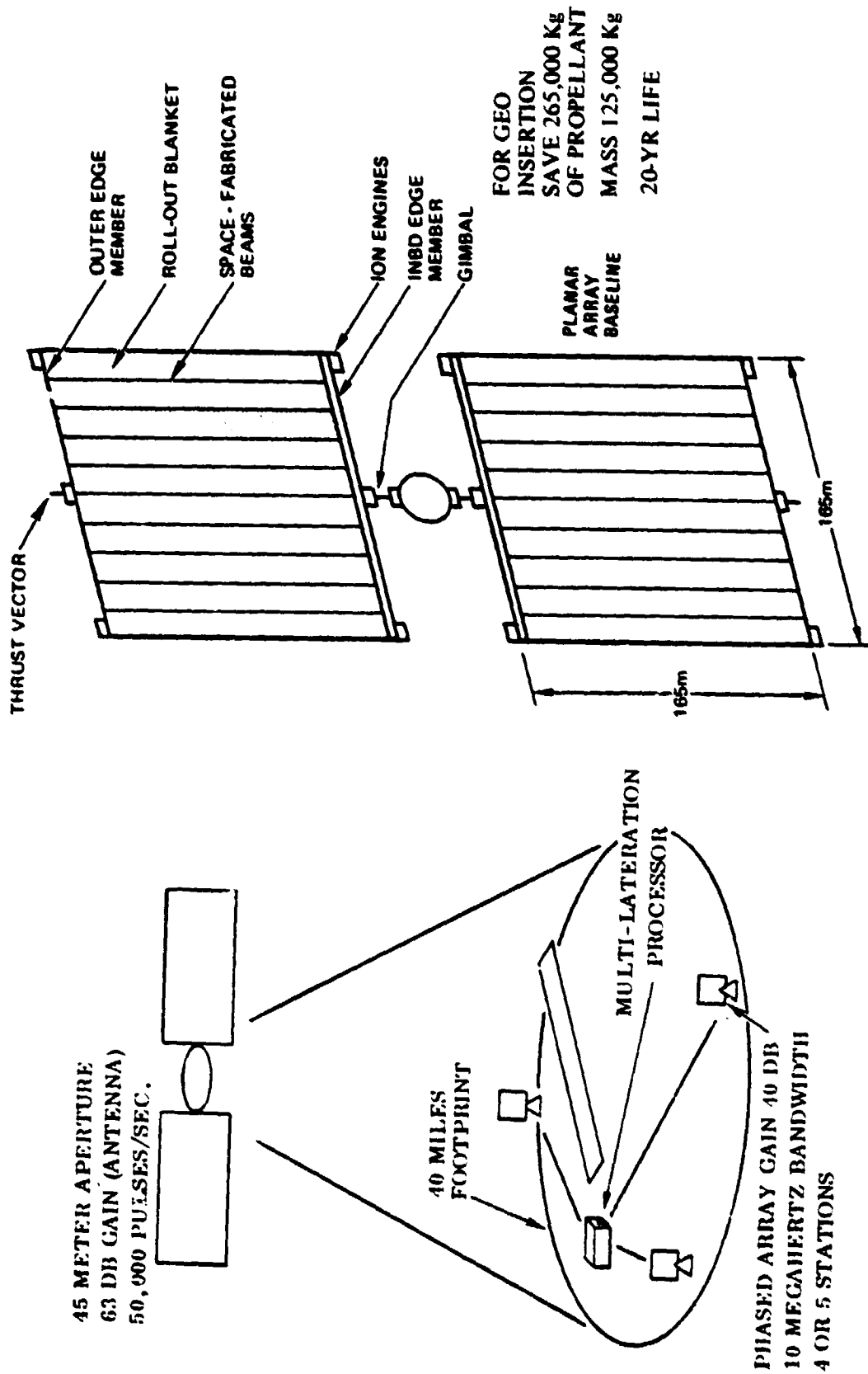


Figure 2-12. Recommended Mission Concept Provides Conus Redundancy With Only Two Spacecraft.

1990s, along with techniques from modern information theory to establish the location of the airplanes within a required error interval. The redundant set of ground system radars would be redistributed to other airports, since the space radar provides redundancy to protect against random or overtly caused failures of the ground radar or power systems. The ground system would provide redundancy in the event of hostile action against the space radar, or some highly improbable catastrophic failure. Airplane transponders would not be required.

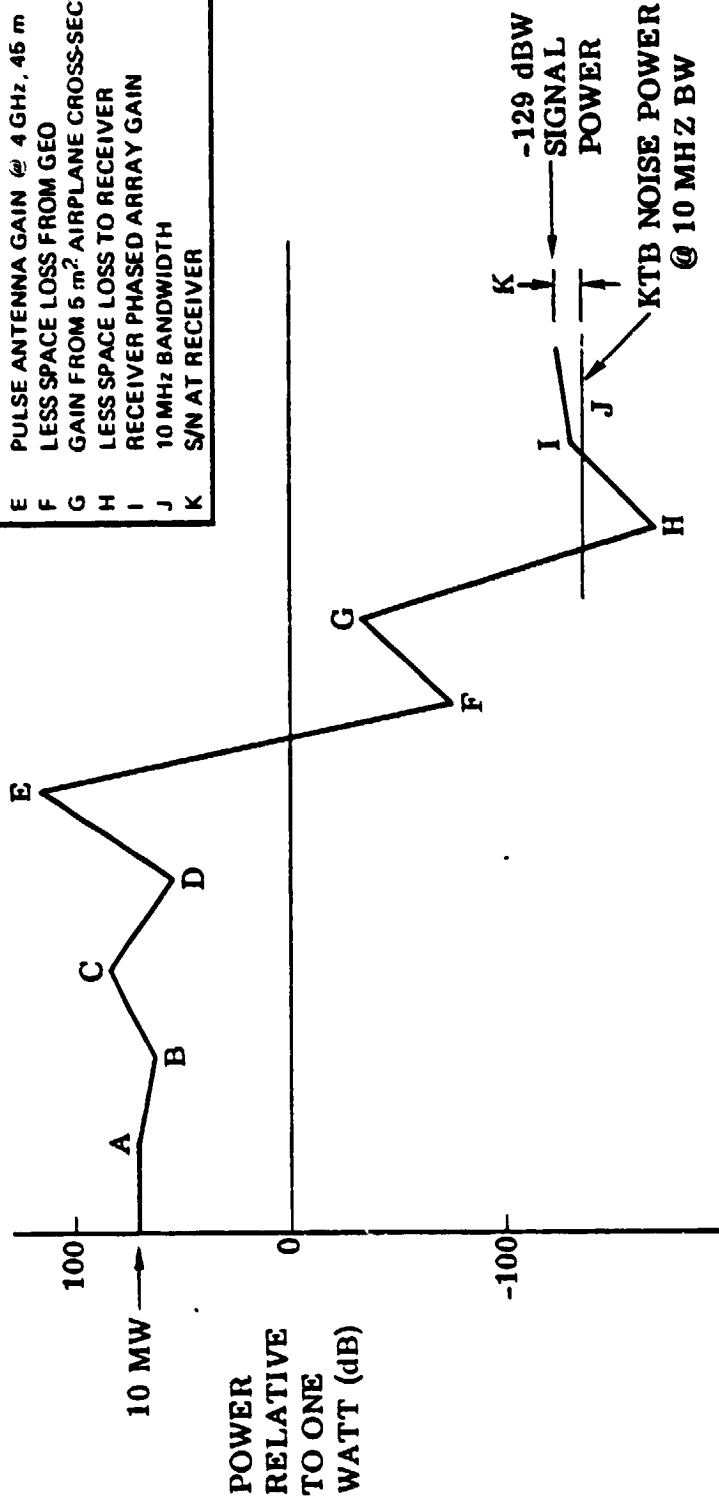
Two spacecraft would be spaced so that only one was eclipsed during the spring and fall eclipse periods. This is acceptable because traffic is reduced later at night. The two 15-megawatt solar arrays supply 10 MW to the radar antenna. The 45-meter aperture antenna uses phased array technology to direct the radar beam to up to 1,000 airport areas over the continental United States. The 45-meter aperture provides spot sizes of approximately 40-mile diameter from geosynchronous orbit. Using the 10 megawatts from the arrays provides enough energy for a signal-to-noise ratio of about 10 db at the bistatic receivers, for targets with a 5 sq. meter cross-section, which also requires a 10 MHz bandwidth to estimate the velocity and position within 100 ft. Figure 2-13 provides the preliminary link analysis. When the design is done, the bandwidth may be reduced by applying correlation and Kalman filtering to the video and state data, but this analysis assumes further study would be required to analyze these effects more completely to establish final link budgets.

The technology for the planar array baseline radar uses trusses to construct a gridwork upon which solar blankets are mounted; the 45-meter radar antenna concept uses Convair-developed deployable trusses and radar membrane blankets for its construction (Figure 2-10). The membrane, which consists of about one million transmitter modules spaced at intervals of  $0.6\lambda$ , can be used as a phased array and is also under development at Convair. Each module would radiate 3 watts of power.

The socio-economics of such a system are somewhat similar to the proposed SPS, with some exceptions:

- a. The environmental concerns, costs, and risks of the system on the terrestrial RF radiation environment are significantly reduced, because the average energy density can be held below even the Russian safety level of  $0.01 \text{ mw/cm}^2$ , and far below the postulated  $25 \text{ mw/cm}^2$  of the U.S. SPS.
- b. Shuttle launch costs per kilogram of payload are greater than the postulated SPS heavy launch vehicles. Therefore, the system effectiveness equations must show gains sufficient to overcome the transportation expenses. The preliminary analysis conducted by Convair for NASA has indicated that the cost of the space-based radar can reduce transportation costs by utilizing centralization to achieve economics of scale. These come about primarily because individual ground radars require at every airport separate backup systems which are operated only intermittently, while the space systems level of redundancy can be multiplexed in such a way as to be operational without

- A POWER FROM SOLAR POWER SYSTEM
- B LESS TRANSMITTER MODULE EFFICIENCY
- C PULSE COMPRESSION OF TRANSMITTER
- D LESS DISTRIBUTION TO 1000 AIRPORTS
- E PULSE ANTENNA GAIN @ 4 GHz, 45 m
- F LESS SPACE LOSS FROM GEO
- G GAIN FROM 5 m<sup>2</sup> AIRPLANE CROSS-SECTION
- H LESS SPACE LOSS TO RECEIVER
- I RECEIVER PHASED ARRAY GAIN
- J 10 MHz BANDWIDTH
- K S/N AT RECEIVER



A POSITIVE SIGNAL-TO-NOISE RATIO CAN BE OBTAINED.  
 10 MW IS FEASIBLE FOR 1000 AIRPORTS.

Figure 2-13. Air Traffic Control Bistatic Radar Power Allocation

a completely separate additional spacecraft. Low cost is essential however, for the concept to be viable. Figure 2-14 summarizes these considerations.

This analysis of the susceptibility of the two alternate approaches to catastrophic and overt destruction has not been completely developed, since it is dependent on the assumed threat and on detailed design.

**2.1.9 RF POWER BEAMING SATELLITE IN GEO.** The Solar Power Satellite (SPS) is economically viable because satellites in GEO receive insolation almost the entire orbital period and thus the photovoltaics have nearly 100% duty cycle. Use of these GEO SPS satellites to beam rf power to LEO satellites provides potential benefits to the space program. Because such satellites (Figure 2-15) would generate the beam power at GEO, the LEO satellites receiving power would:

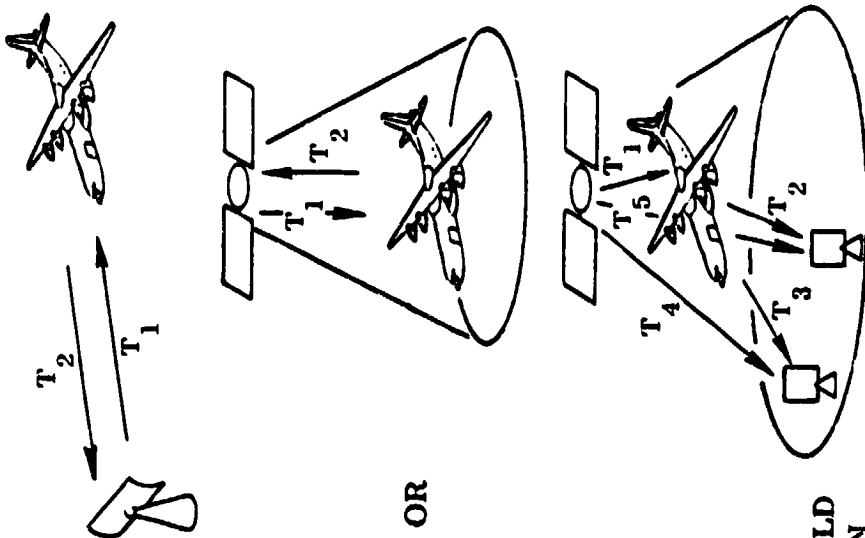
- a. Require a lower cost rectenna compared to a higher cost solar array. The rectenna would have a 100% duty cycle as compared to the 67% duty cycle the solar array eclipsed LEO satellites may have. The photovoltaic costs associated with LEO energy storage/power generation would also be avoided.
- b. Not require the significant energy storage systems which LEO satellites now need to accommodate the eclipse period.

The weight and cost of energy storage systems such as NICAD batteries, nickel hydrogen batteries, or fuel cells would be avoided.

Initially, the capture probability of such a system is thought to be small. User resistance will probably be high because LEO users would be dependent on the laser power beaming satellite for their energy. However, the benefit of such a satellite strongly depends upon the configuration and design concept which eventually evolves. If a concept could be developed which features an extremely light weight deployable structure for the rectennas and perhaps for the transmitting antenna, the concept might have more viability than appears on first examination. Because the air traffic control radar satellite has much higher capture probability, the RF power beaming satellite will not be considered further.

**2.1.10 ORBITAL CONSTRAINTS.** The deceleration of structures whose cross-sectional area is large increases as their mass decreases and may cause significant orbital decay in LEO. To evaluate these effects for a typical multimewatt configuration, an analysis of the effects of atmospheric drag was conducted for the spacecraft illustrated in Figure 2-16. The spacecraft configuration is one design concept for a 5-megawatt solar power demonstrator. Components would be delivered into low earth orbit by the Space Shuttle, where they would be assembled into the configuration illustrated.

The General Dynamics program TRAJEX was used to generate a parametric set of orbital flight simulations in which the only perturbing force acting on the spacecraft was atmospheric drag. The effects of rarefied flow aerodynamic forces normal to drag were not simulated. Since these forces act normal to the velocity



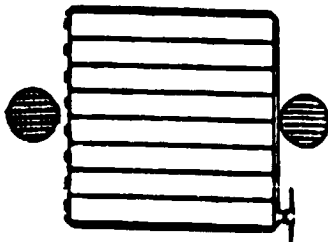
- **CURRENT GROUND CONTROL RADARS**
  - ▲ ASR-8: \$1.1M (1979 \$)
  - ▲ ARTS - 2
  - ▲ ARTS - 3
  - ▲ 3RD GENERATION
  - ▲ TRANSPONDERS
- **SPACE BASED MONO-STATIC RADAR**
  - ▲ RETURN TRIP SPACE LOSS SIGNIFICANT
  - ▲ MULTIPLE TARGETS FROM GEO REQUIRE:
    - (1) VERY CAREFUL PULSE INTERLEAVING, OR
    - (2) VERY LOW PULSE REPETITION FREQUENCY (5 PPS), OR
    - (3) HIGH RECEIVER DYNAMIC RANGE
  - ▲ LARGE FOOTPRINT
  - ▲ TRANSPONDERS
- **BI-STATIC RADAR**
  - ▲ SPACE BASED TRANSMITTER TO 1000 AIRPORTS
  - ▲ LOCAL GROUND BASED RECEIVERS
  - ▲ NO AIRPLANE TRANSPONDERS
  - ▲ LOWER TRIP LOSS TO RECEIVER
  - ▲ PULSE REPETITION TIMING BASED ON EASILY UNDERSTOOD ALGORITHMS
  - ▲ TRILATERATION AND INTERFEROMETRIC TECHNIQUES SHOULD PERMIT ACCURATE RANGE AND ELEVATION DETERMINATION

THE PRELIMINARY ANALYSIS INDICATES THE BI-STATIC MISSION APPROACH IS FEASIBLE FOR TRAFFIC CONTROL

Figure 2-14. FAA Traffic Control Alternatives.

ORBIT

- QUASI-GEOSYNCHRONOUS
- WEIGHT OBJECTIVE - 25 kg
- COST - TBS
- POWER REQUIRED - TBS
- SHADOWING - NONE
- POINTING ACCURACY
  - ▲ ANTENNA PATTERN - 1 ARC MINUTE
  - ▲ SPACECRAFT - 5°



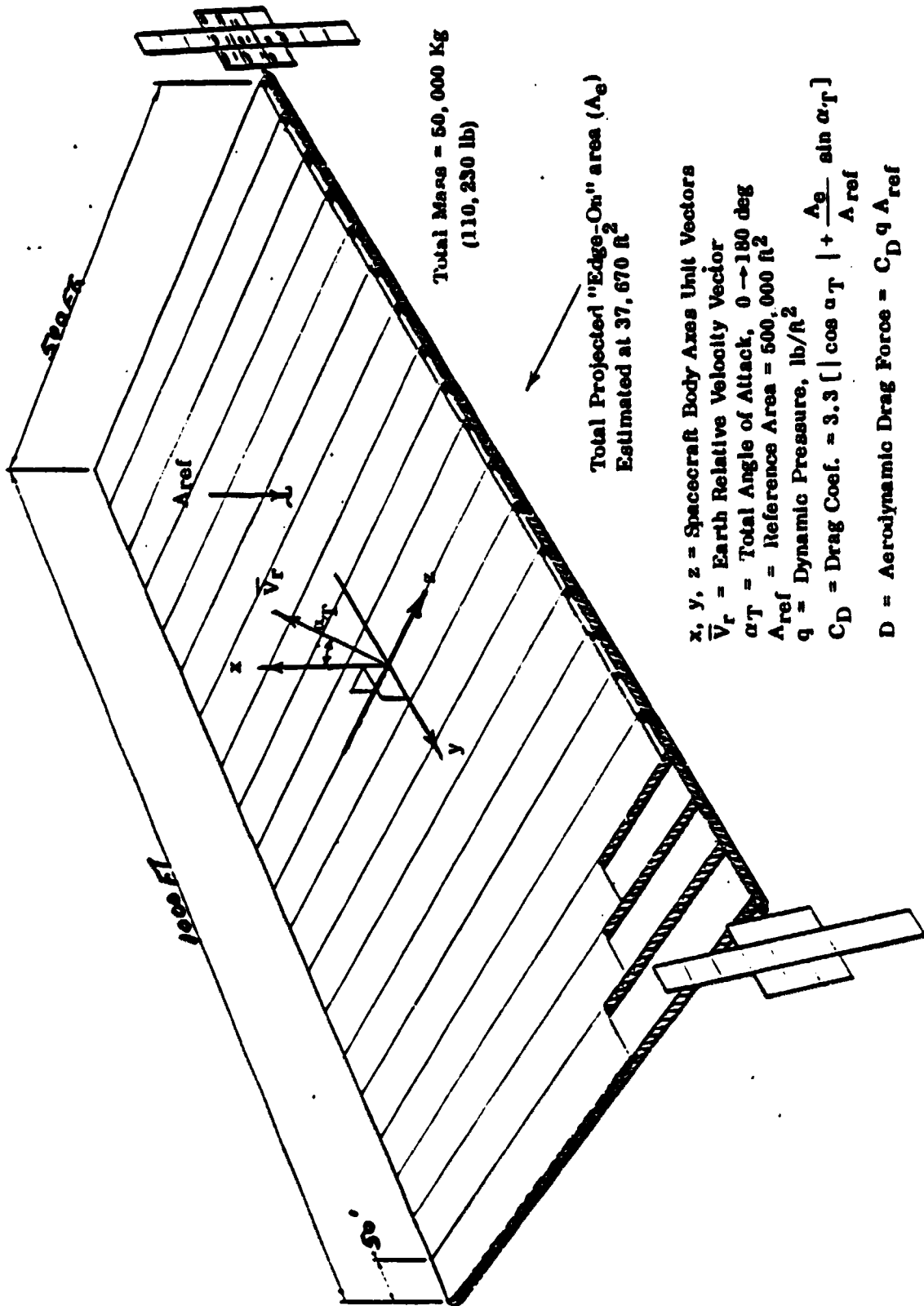
BENEFITS

- POWER SATELLITE IN GEO
- ENERGY STORAGE FOR EMERGENCY CONTROL
- ‡ SMALLER PHOTOVOLTAIC ARRAYS
- ECONOMIES OF SCALE

RISKS

- COST OF BEAMING CONVERSION AND TRANSPORTATION MAY OFFSET ENERGY STORAGE SAVINGS
- USERS DEPEND ON A FEW SATELLITES
  - ATTITUDE CONTROL/TRACKING NEEDS TRANSFERRED TO POWER BEAMING SATELLITE

Figure 2-15. RF Power Beaming Satellite.



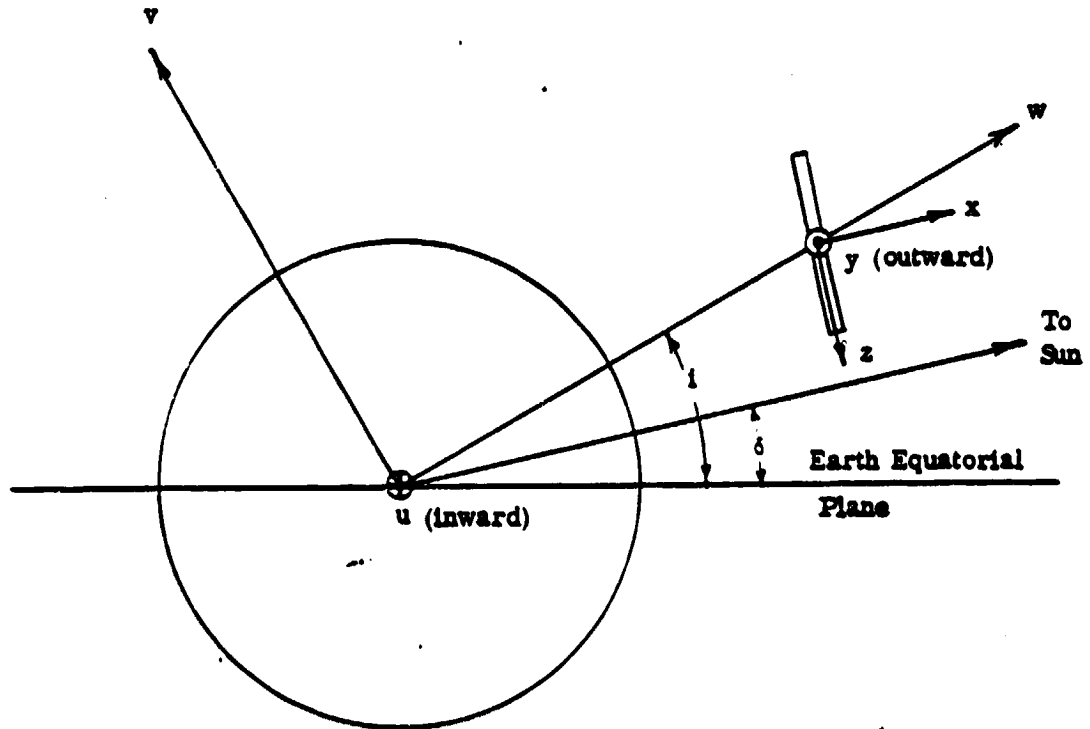
- $x, y, z$  = Spacecraft Body Axes Unit Vectors
- $\vec{V}_r$  = Earth Relative Velocity Vector
- $\alpha_T$  = Total Angle of Attack,  $0 \rightarrow 180$  deg
- $A_{ref}$  = Reference Area = 500,000 ft<sup>2</sup>
- $q$  = Dynamic Pressure, lb/ft<sup>2</sup>
- $C_D$  = Drag Coef. =  $3.3 \left[ \left| \cos \alpha_T \right| + \frac{A_e}{A_{ref}} \sin \alpha_T \right]$
- $D$  = Aerodynamic Drag Force =  $C_D q A_{ref}$

Figure 2-16. Spacecraft Geometry and Definitions.

vector, their effect would be to perturb orbital inclination and/or eccentricity without changing orbital energy. The corresponding station-keeping velocity corrections are believed to be small compared to the corrections for drag. The oblate earth terms in the gravitation function were set to zero to isolate the effects of atmospheric drag. The effect of solar radiation pressure was not included in this analysis since it is small compared to the effect of aerodynamic pressure. Reference 6 gives a value of about  $9 \times 10^{-8}$  lb/ft<sup>2</sup> for solar radiation pressure at earth, whereas a nominal aerodynamic pressure of about  $1 \times 10^{-6}$  lb/ft<sup>2</sup> is indicated for the highest circular orbit considered in this analysis (225 nautical miles). The nominal upper atmosphere densities defined by the 1976 U.S. Standard Atmosphere of Reference 7 were simulated by applying a correction factor to the densities computed by the older atmosphere model (Reference 8) used in the TRAJEX Computer Program. The densities defined by the 3-sigma cold atmosphere model of Section 7 of Reference 9 were used to compute data for maximum drag.

Drag characteristics of the spacecraft are based on data obtained from Chapter V of Reference 10. Drag coefficient was implemented as a function of total angle of attack as defined in Figure 2-16. A flat plate drag coefficient,  $C_D = 3.3$ , was assumed where  $C_D$  is based on projected area perpendicular to the free stream. Free molecular flow, a non-tumbling spacecraft, and diffuse reflection of impinging gas particles were assumed. The computed drag force was applied in the direction of the negative relative velocity vector in the TRAJEX simulations. Figure 2-17 defines the alignment of the spacecraft body axes with respect to the TRAJEX inertial  $u, v, w$  coordinate system (Reference 11). The matrix of direction cosines relating the spacecraft body axes to the inertial coordinate system is shown. The inertially fixed spacecraft attitude is defined as a function of orbit inclination and solar declination such that the flat plane of the spacecraft is always normal to the earth-sun line.

Figure 2-18 summarizes the results of this study. Each data point on the nominal atmosphere curves corresponds to a TRAJEX simulation. These simulations included a range of orbit inclinations from zero to 90 degrees, solar declinations of -23.5 degrees and +23.5 degrees, and altitudes of 150 nautical miles and 225 nautical miles. The 3-sigma dense atmosphere curves were obtained by multiplying the nominal drag loss values from the computer simulations by the ratio of the dispersed atmosphere density to nominal density, since drag loss is directly proportional to atmospheric density for the cases considered here. Note that minimum drag losses occur when the difference between orbital inclination and solar declination is equal to 90 degrees. Reference to Figure 2-17 shows that this corresponds to the case in which the spacecraft is always aligned in the minimum drag attitude, that is, "edge-on" to the direction of motion. It should be noted that, for simplicity, the projected frontal area for the "edge-on" case was conservatively assumed to be 37,670 ft<sup>2</sup>, corresponding to the long dimension of the rectangular spacecraft. In reality, the average projected area of the leading edge will be somewhat smaller over a full orbit because of the apparent spacecraft rotation with respect to the earth-relative velocity vector.



- x, y, z = Spacecraft Body Axes Unit Vectors**
- u, v, w = Earth Centered Inertial Coordinate System Unit Vectors**
- i = Orbital Inclination**
- δ = Solar Declination**

**Direction Cosines of the Spacecraft x, y, z Body Axes with the Inertial u, v, w Axes (TRAJEX Input Format):**

$$\text{SMS}(1) = \cos(x, u), \cos(x, v), \cos(x, w),$$

$$\text{SMS}(4) = \cos(y, u), \cos(y, v), \cos(y, w),$$

$$\text{SMS}(7) = \cos(z, u), \cos(z, v), \cos(z, w),$$



$$0, -\sin(i - \delta), \cos(i - \delta),$$

$$-1, 0, 0,$$

$$0, -\cos(i - \delta), -\sin(i - \delta),$$

**Figure 2-17. Inertial Orientation of Spacecraft.**

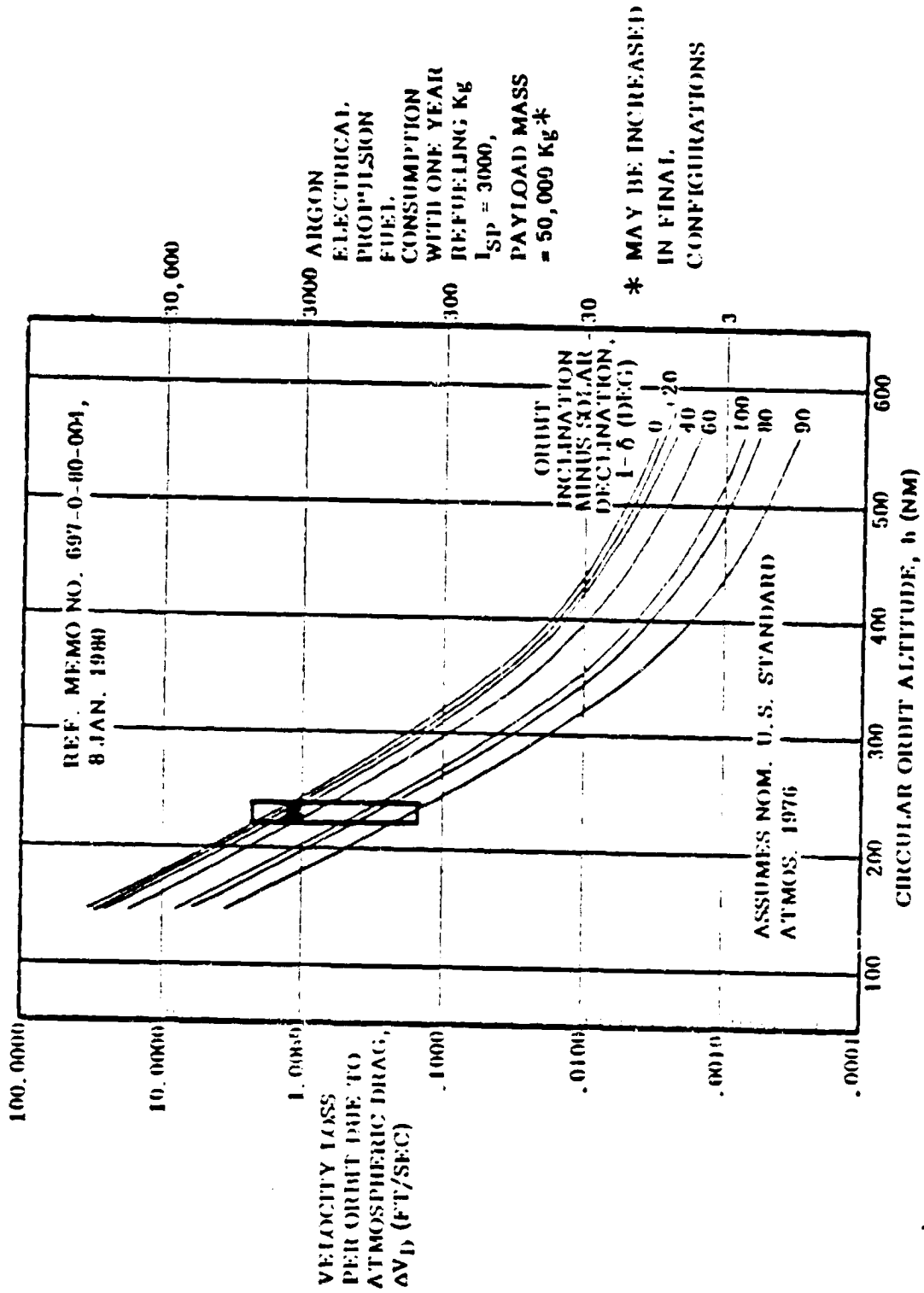


Figure 2-18. Effect of Drag on a Large Planar Array.

Maximum drag loss occurs when the orbit inclination is equal to the solar declination. Figure 2-17 shows that in this configuration, the spacecraft is alternately moving from "broadside" to "edge-on" with respect to its attitude relative to the direction of motion. This is the expected position for large structures hanging down from the Space Construction Facility, to minimize gravity gradient torques.

In sizing the stationkeeping propulsion system for the spacecraft, the minimum required thrust level would be determined by the maximum drag force expected to be encountered during the lifetime of the spacecraft. For a 150 nautical mile circular orbit, the maximum drag force would be about 93 pounds. This corresponds to a three-sigma dense atmosphere and maximum projected frontal area. For 225 nautical miles, the corresponding maximum drag force would be about 15 pounds. For preliminary estimates of propellant loading requirements, a velocity correction capability somewhere between those shown in Figure 2-18 for 3-sigma dense and nominal atmospheres should be used; to assume a nominal atmosphere would be nonconservative since drag force dispersions resulting from a 3-sigma cold (dense) atmosphere are greater than those resulting from a 3-sigma hot atmosphere. (See Section 7 of Reference 11.)

When the data for drag were used to calculate the propellant mass required for a 20-year mission life, up to  $2 \times 10^6$  kg of chemical stationkeeping propellant mass were found to be required (Hydrazine, ISP = 225), whereas only 100,000 kg of mass would be required for electric propulsion, with an assumed Ion Engine ISP of 5000 and a 225 mile altitude.

It should be noted that the amount of propellant required for stationkeeping depends on engine specific impulse, altitude, and spacecraft mass. This study assumed a 225 n.mi. shuttle orbit, an engine ISP of 5,000 and without Orbital Maneuvering System (OMS) Kits installed. Spacecraft mass was 50,000 Kg. This mass influences propellant usage, because the velocity loss per orbit is the integral of acceleration, and the more massive the spacecraft, the smaller the velocity loss per orbit. For a fully configured space construction facility with five times the 50,000 Kg mass for which Figure 2-3 applies, and for a higher OMS-aided 300-mile orbit and an ISP of 5,000, the chemical propellants required could decrease to as low as 40,000 Kg. However, the electrical propulsion propellant mass would still be about 5% of this value, and even with these lower masses of propellants, the expected chemical propellant transportation costs are approximately equal to the extra array costs, and therefore ion engine stationkeeping is viable.

**2.1.11 MISSION SELECTION AND GROUPING.** The foregoing discussion highlights the fact that two GEO missions emerged as potentially very beneficial to the needs of the country in the 1990s. They were the Radar illuminator and the Solar Power Satellite (SPS) demonstrator. Both beam R.F. power to a relatively small area on earth.

Because the SPS is being studied extensively elsewhere, it was decided to focus this study effort on the Radar illuminator mission. The Radar mission also has the attractiveness of focusing on a problem of concern to all who fly: assuring the safety of the traveling public.

The selection of a LEO Space Construction Facility to implement the GEO power beaming missions was a corollary to the LEO selection.

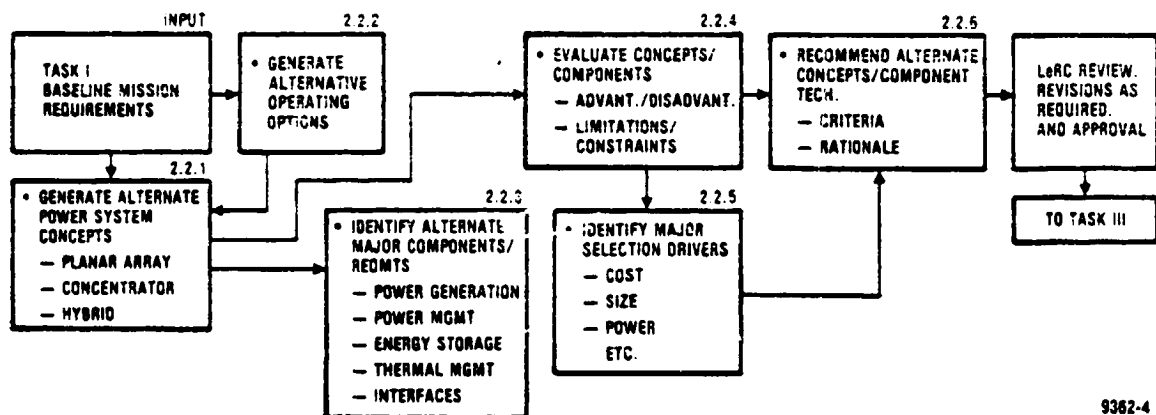
**2.1.12 POWER REQUIREMENTS.** As described above, the power requirements for the radar satellites were established so that one or two satellites could handle up to 1,000 airports. Final requirements would be dependent on the operational planning. However, to minimize wasted orbital slots, the satellites were sized at the high end of the power range studied -- 10 mW each.

The power requirements developed for the space construction facility assumed that the drag caused by the interaction of the atmosphere at LEO with the array frontal aperture was compensated for by electrical propulsion, with shuttle-supplied, stationkeeping propellants. Further, compensation for the drag caused by the interaction between the atmosphere and the item being assembled by the station was also supplied by electrical propulsion.

For ion engines, a 1.0 megawatt requirement will provide the stationkeeping with electrical propulsion at 225 n.mi. These power requirements interact with the energy storage component characteristics, as shown in Figure 2-19 (on the following page) which specifies the power generation capability for the various storage technologies. To accommodate any option, a 2.5 megawatt sizing was used.

## 2.2 TASK II, CANDIDATE POWER SYSTEM CONCEPTS AND COMPONENT TECHNOLOGIES

Figure 2-20 shows how candidate power system concepts were developed, components were identified, and preliminary system synthesis were accomplished.



9362-4

Figure 2-20. Power System Concepts and Component Technologies.

**2.2.1 CONCEPT IDENTIFICATION.** Three types of power generation concepts were developed: planar array, pure photovoltaic concentrator, and hybrid photovoltaic/thermal heat engine concepts. They were considered in conjunction

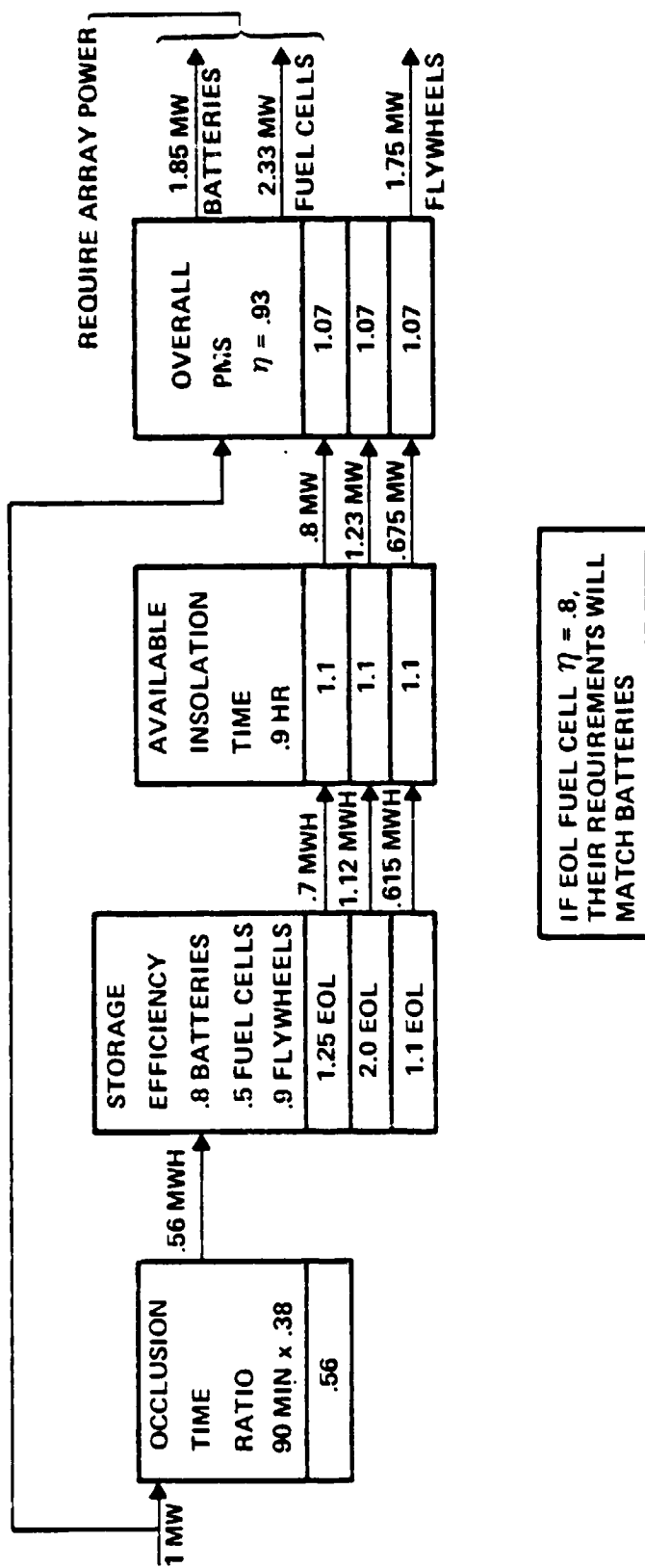


Figure 2-19. The Power and Array Sizing Chain — LEO Mission Varies with Energy Storage.

with two types of power management and distribution systems, ac and dc; and three types of energy storage systems: batteries, fuel cell/electrolysis, and inertial (flywheel) storage.

**2.2.1.1 Cell Configurations Considered.** Three configurations of photovoltaic cells were considered for power generation use:

- a. Multi-bandgap (three bandgaps) cells with high projected efficiencies. (Figure 2-21.)
- b. Two cells or two-bandgap cells, with some form of spectrum splitting or dual energy used.
- c. Single-bandgap cells such as today's silicon and gallium aluminum arsenide.

**2.2.1.1.1 Multi-Bandgap Cell Data.** The analysis accomplished by this study was performed using data provided to General Dynamics by the Varian Corporation as part of a trade-off data agreement between the two corporations. Figure 2-22 shows the performance predicted for three junction Gallium Arsenide cells with three-micron diffusion lengths for various concentration ratios and temperatures. Appendix C describes the approaches and expected performance in more detail.

**2.2.1.1.2 Two-Cell Configurations.** There is some concern that multi-bandgap cell technology will never really achieve its ultimate desired goals. To provide a viable plan, this study also projected an approach which uses two cells as a backup to provide two-band operation. Two possible configurations for two-cell systems were considered. In one configuration, a high-bandgap Gallium Arsenide cell floats on top of a lower-bandgap Gallium Arsenide or silicon cell. These type cells have been referred to as "Gallicon" cells in the literature. Basically, the spectral splitting is achieved inherently by the design; the two cells are bonded together with a transparent bonding material which can survive the temperature extremes of space. A second approach considered involves using energy which the high-bandgap cell does not use, and reflecting it because of the geometrical configuration on to the lower-bandgap cell. A typical configuration for such a reflection is shown in Figure 2-23. This figure also shows what the ideal energy utilization might be from the high-bandgap Gallium Arsenide cell when combined with the lower-bandgap Gallium Arsenide or silicon cell. In the figure, the lower-bandgap cell is a silicon cell. If the lower-bandgap cell were to be a Gallium Arsenide cell, the cutoff point for the infrared energy might be at a slightly lower wavelength (around 650 millimicrons) and the second lower-bandgap cell would probably cease performance between 900 millimicrons and 1 micrometer.

The data used for this two-cell Gallium Arsenide configuration was provided by Varian as part of the interchange agreement, and is also further described in Appendix C.

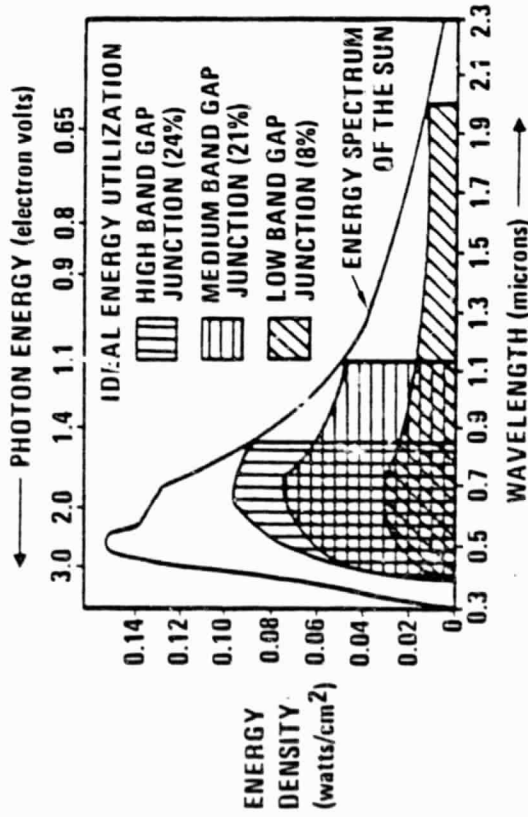
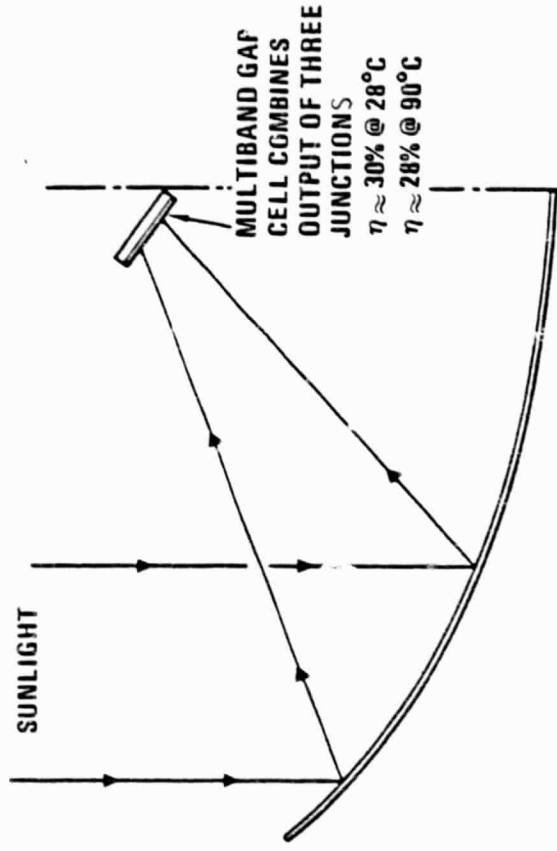


Figure 2-21. Multi-Bandgap Cells Utilize more of the Available Energy.

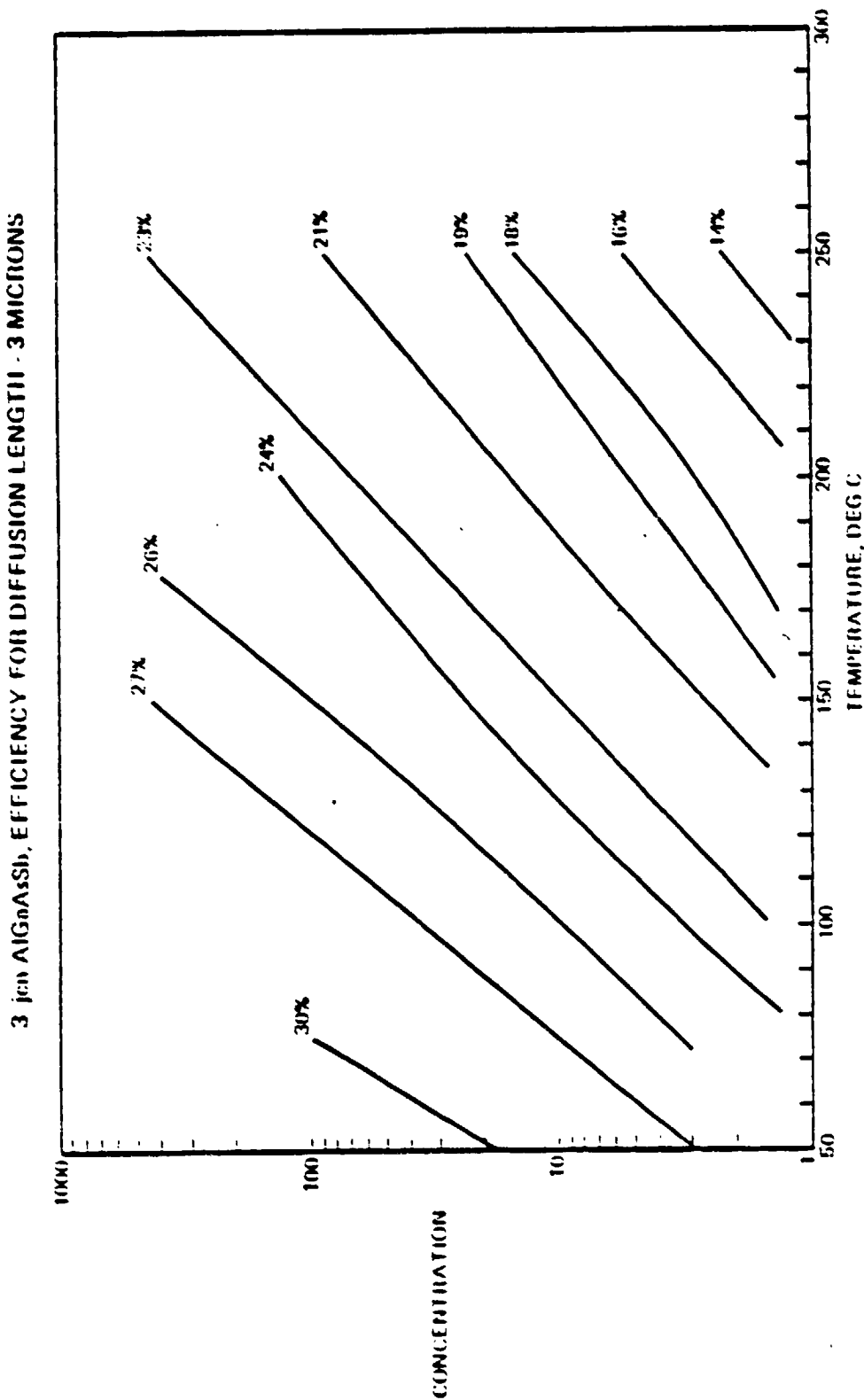


Figure 2-22. Multi-Bandgap Cell Projections were Based on Detailed Cell Analysis.

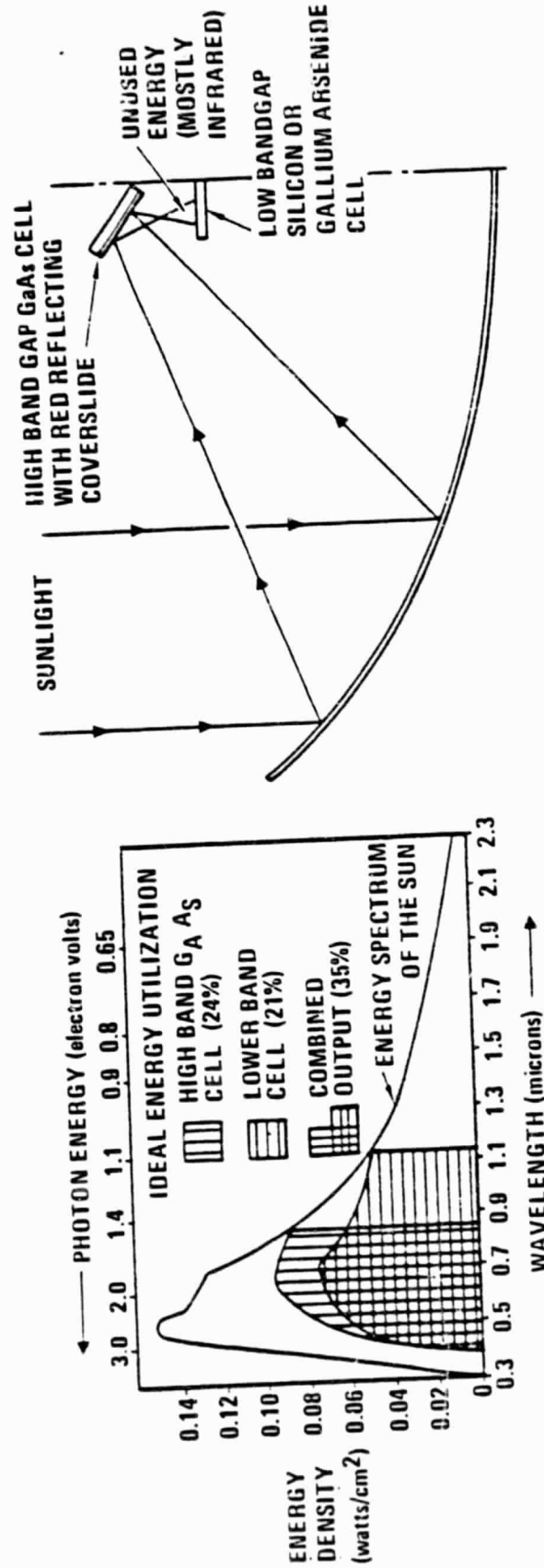


Figure 2-23. A Dual-Band Reflecting Concept for Higher Efficiency.

2.2.1.1.3 Single-Band Cells. The single-bandgap cells considered were those emerging from the laboratory today, but with slightly higher efficiency projections. Back surface reflectors were employed to eliminate the unused infrared energy, a "low cost", lower efficiency, silicon cell was also considered, since such cells may be available from the DOE "low cost" photovoltaic program.

2.2.1.1.4 Cell Configuration Summary. Figure 2-23a summaries the various cell technologies which will be available for use in planar arrays and concentrators. The projected characteristics are summaries from the Component Application and Performance estimates which are presented in Appendix A. These estimates were developed from Vendor discussions and consultations with NASA component engineers.

2.2.1.2 Power Generation Configuration Geometries. Six alternate geometrical configurations of spacecraft were investigated. They are shown in Figures 2-24 through 2-29. Three configurations satisfied the requirements of a 10-megawatt radar satellite operating in geosynchronous orbit (23.5 degrees). Three satisfied a LEO space construction mission objective at 28-degree inclination. Preliminary study of another configuration, the very-high-concentration-ratio (CR=2000) spherical paraboloid, revealed a concern which weighs against its selection: if the spacecraft should accidentally tip off the sun line, the truss structure attaching the focal electronics to the spacecraft could be destroyed by the concentrated solar beam. Further, the thermal analysis indicates thermal impedance of the high concentration ( $\geq 200$ ) systems is significant, and, very high velocity ( $> 50$  ft/sec) liquid cooling is required. The spherical paraboloid was therefore dropped from consideration.

2.2.2 PLANAR ARRAY OR LOW CONCENTRATION ABOUT GIMBALED AXIS (CONCENTRATION RATIO, CR, =2). These types of systems are extensions of today's technology. A truss structure is used to hold solar cell blankets, and (in the case of the CR=2 concentrator) the blanket and two flat mirrors are positioned so that their surface is at an angle of 60 degrees with respect to the sun line, doubling the solar blanket insolation. Several alternate truss approaches exist. Figure 2-30 shows a deployable space truss beam utilized in a rectangular configuration over which rows of solar blankets are tensioned.

An alternate, space-fabricated, composite truss, (Figure 2-31), can also be used to build up the rectangular structure, tension the blankets, and hold the mirrors.

Figure 2-32 indicates the configuration to be studied for the radar satellite with the antenna installation splitting the planar array into two equal rectangular sections. Figures 2-33 and 2-34 show the space construction configuration with the same type of split array, the differences being in the dimensions of the arrays and mass properties of the central construction module compared to the radar core antenna.

TECHNOLOGY	CHARACTERISTICS	REMARKS	RISKS
<u>PLANAR</u> SINGLE CRYSTAL CZ SILICON	5 cm X 5 cm X 50μ η = 14-16% BOL	WELDABLE, NOT ANNEALABLE, MATURE TECHNOLOGY.	<b>[MEDIUM]</b> FOR RADIATION RESISTANT, WELDABLE CELLS
EFG/DENDRITIC WEB RIBBON SILICON	5 cm X 8 cm X 300μ η = 13 -15% (BOL)	EFFICIENCY VIA LASER RECRYSTAL- IZATION. LOWER COST THAN CZ.	<b>[MEDIUM]</b> NO EXPERIENCE WITH SPACE APPLICATION
AMORPHOUS SILICON	η = 6%	EFFICIENCY UP TO 16% VIA LASERS OR TANDEM JUNCTIONS NOT ANNEALABLE,	<b>[MEDIUM]</b> SPACE QUALIFICATION REQUIRED
GaAs	2 cm X 4 cm X 50μ η = 16-20%	RADIATION RESISTANT BUT ALSO GREATER COST. ANNEALABLE LOW TEMPERATURE	<b>[MEDIUM]</b> FOR 50μ, WELDABLE CELLS
MULTIBANDGAP	η = 23-25%	MULTIPLE LAYER CONSTRUCTION. COST UNLIKELY TO BE OFFSET BY HIGHER EFFICIENCY. COMPLEXITY REQUIRED THICKER CELLS FOR YIELD.	<b>[HIGH]</b> EARLY STAGE OF DEVELOPMENT
<u>CONCENTRATOR</u> ETCHED GROOVE SILICON	η = 16-19% @ 50-1000 SUNS	HIGH CONCENTRATION RATIOS ALLOW HIGHER CELL COSTS WHILE REDUCING SYSTEM COSTS	<b>[MEDIUM]</b> REQUIRES SPACE DEMONSTRATION
GaAs	η = 16-19% @ 1000 SUNS	LOWER TEMPERATURE COEFFICIENT AND CONTINUOUS ANNEALING AT LOW TEMPERATURE ALLOW BENEFITS FROM HIGHER CONCENTRATION	<b>[MEDIUM]</b> REQUIRES SPACE DEMONSTRATION
MULTIBAND GAP	= 25-28%	MULTIPLE LAYER STRUCTURE	<b>[HIGH]</b> COSTS, RELIABILITY UNCERTAIN
GaAs TWO CELL	= 23%	ANNEALABLE	<b>[MEDIUM]</b> REQUIRES SPACE DEMONSTRATION
SILICON VERTICAL JUNCTION	= 18%	NOT ANNEALABLE	<b>[HIGH]</b> THERMOCYCLING TESTING NEEDED
SILICON-THERMO- CONCENTRATOR	= 20%	NOT ANNEALABLE	<b>[HIGH]</b> REQUIRES SIGNIFI- CANT DEVELOPMENT

Figure 2-23a. Various Cell Technologies Will Be Possible.

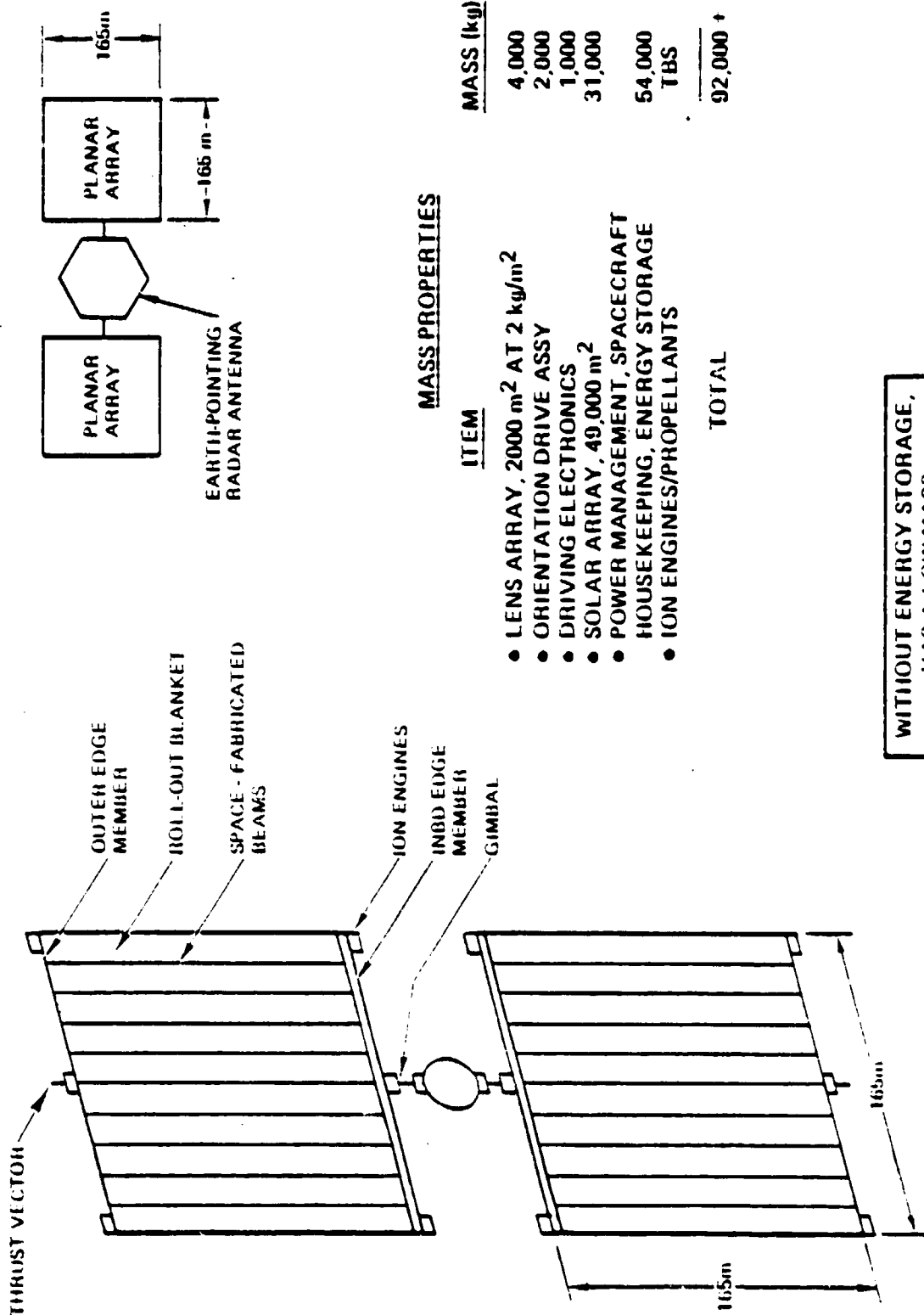


Figure 2-24. Planar Array/Antenna Configuration for Radar Spacecraft.

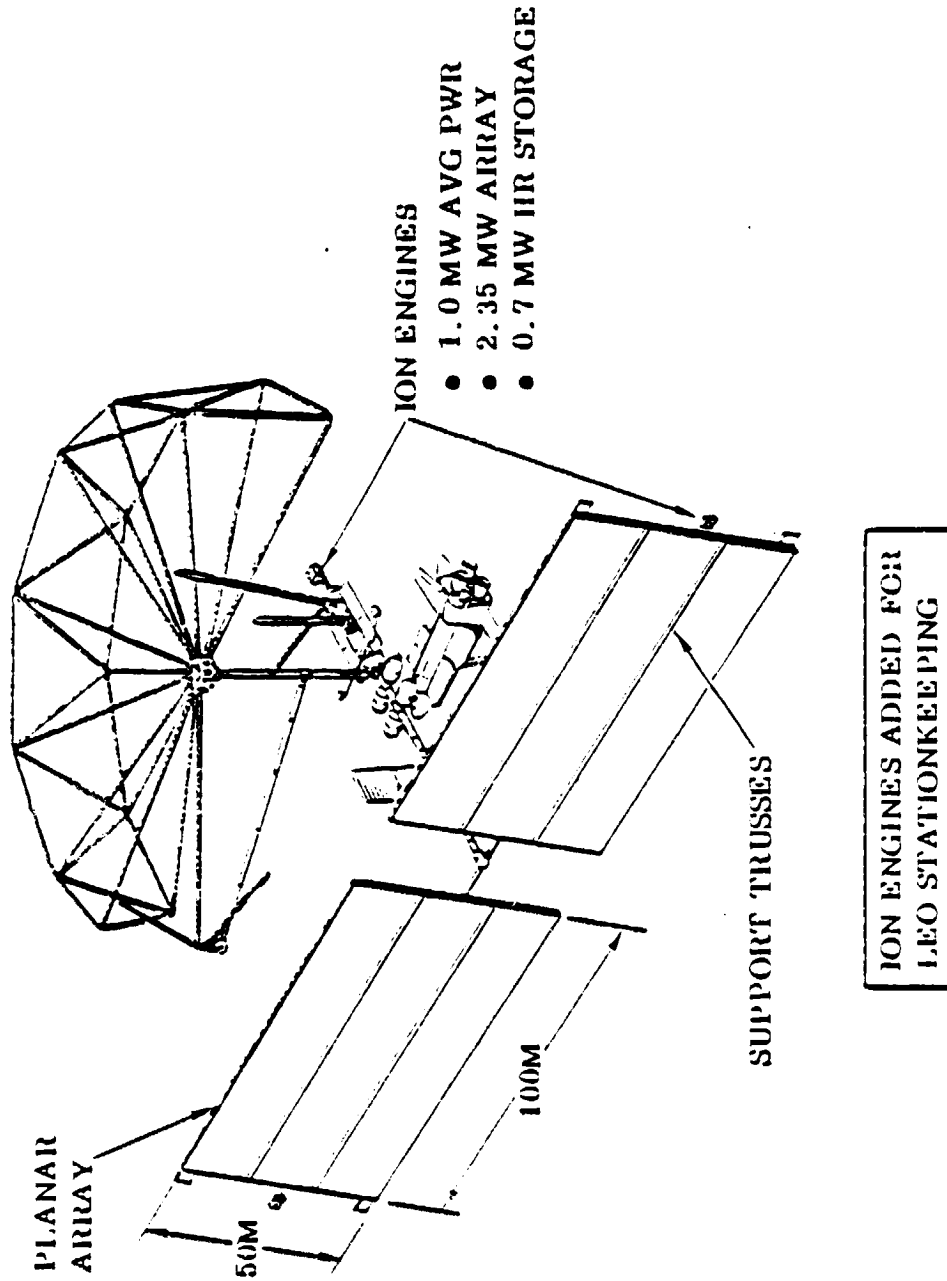


Figure 2-25. Space Construction Planar Array.

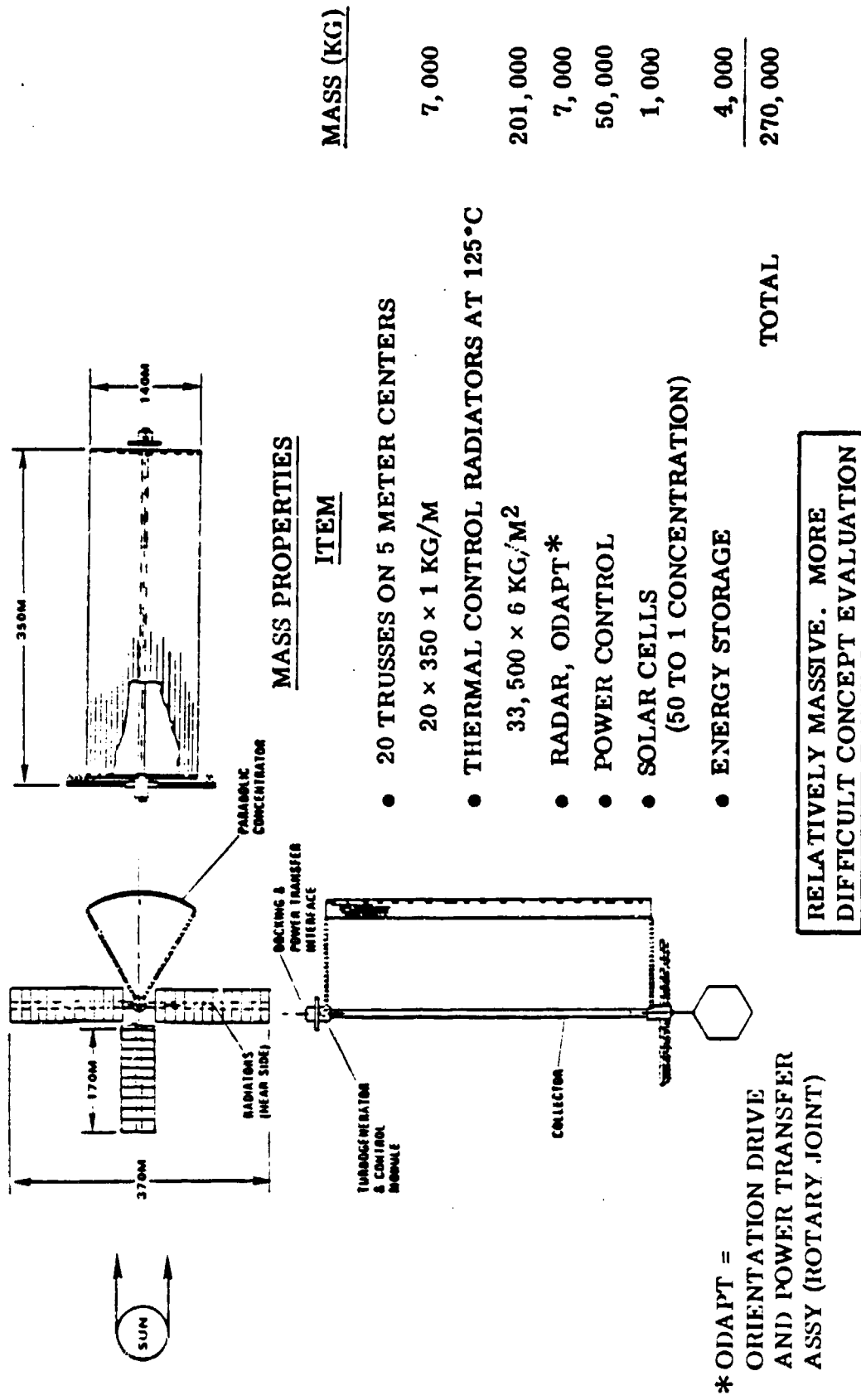
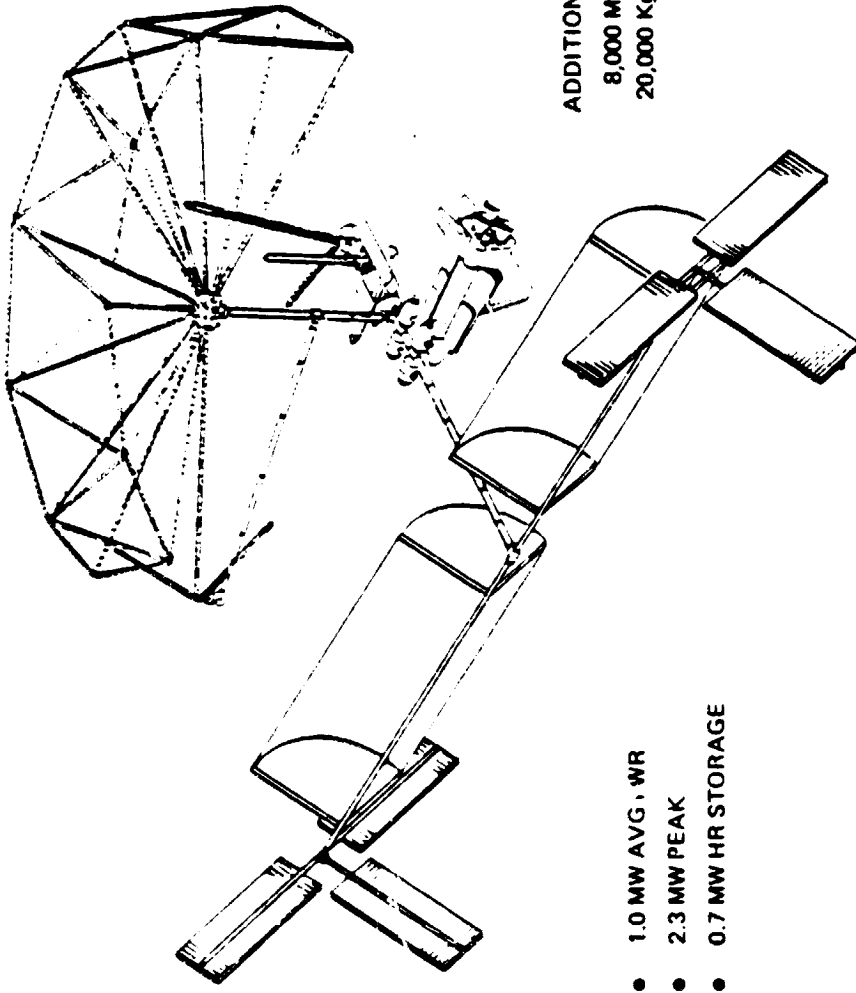


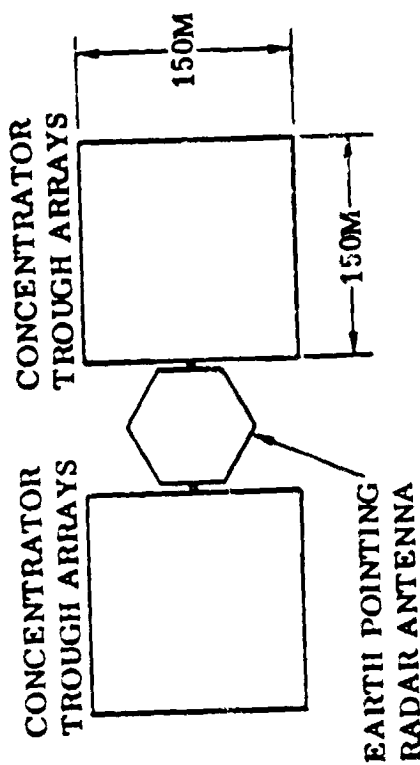
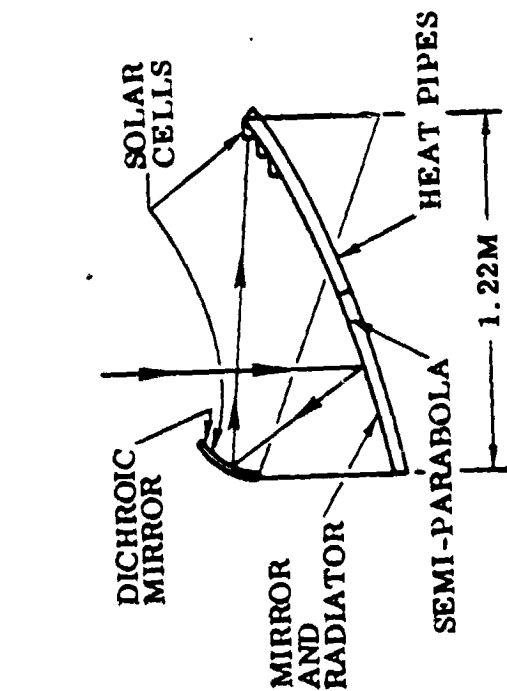
Figure 2-26. Parabolic Trough Collector for 10 MW Mission.

ARRAY AREA REQUIRED @ 2.35 MWATTS	
22% 1,8000 m <sup>2</sup>	
MASS OF COLLECTOR/RADIATOR	
8,000 m <sup>2</sup> x 3.5 kg/m <sup>2</sup>	28,000 kg
BEAM BUILDERS (3 @ 2400 kg)	10,200 kg
CRANE MANIPULATORS	20,000 kg
SHEATHER (INSTALLS BLANKETS)	5,000 kg
CHERRY - PICKERS	12,000 kg
CREW QUARTERS	10,000 kg
POWER MANAGEMENT	5,000 kg
ENERGY STORAGE	10,000 kg
	<hr/>
	100,200 kg



ALSO MASSIVE. AGAIN DIFFICULT TO TEST PRIOR TO LAUNCH.

Figure 2-27. Space Construction Facility Utilizing Large Parabolic Trough.



<u>MASS PROPERTIES</u>		<u>MASS (KG)</u>
<u>ITEM</u>		
● RADIATOR MIRROR	40,000 M <sup>2</sup> AT 3.5 KG/M <sup>2</sup>	140,000
● ANTENNA AND ELECTRONICS		7,000
● MISC. POWER MGMT.		51,000
● ENERGY STORAGE		4,000
	<b>TOTAL</b>	<b>202,000</b>

- 10 MW ARRAY POWER
- 12 MW HOURS ENERGY STORAGE

TERRESTRIALLY TESTABLE  
 LOW ARRAY MASS  
 LOW ARRAY COST

Figure 2-28. The Second Configuration uses a Planar Structure to Support Modularized Concentrators.

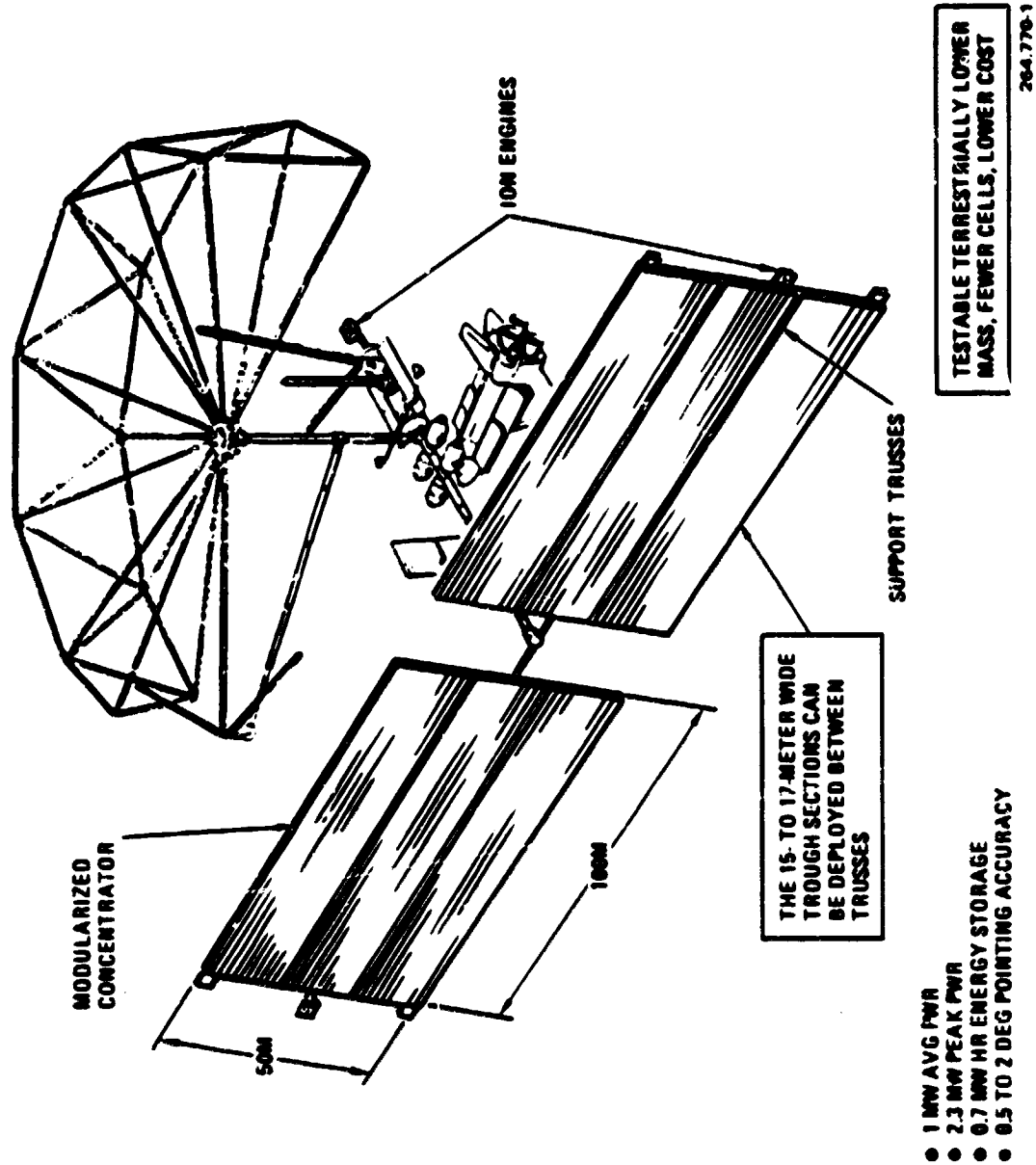


Figure 2-29. Space Construction Semi-Parabolic Concentrator/Heat Pipe.

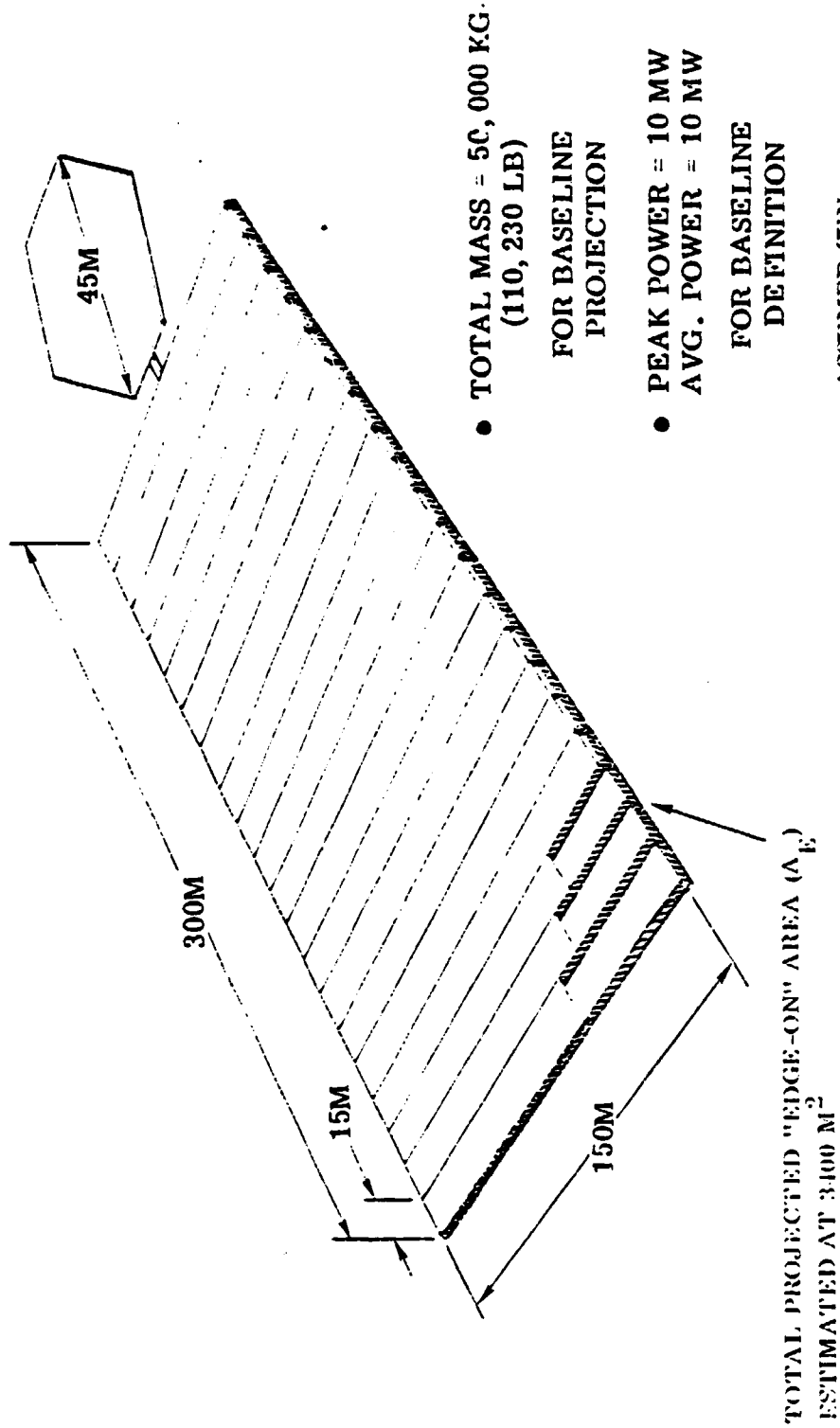
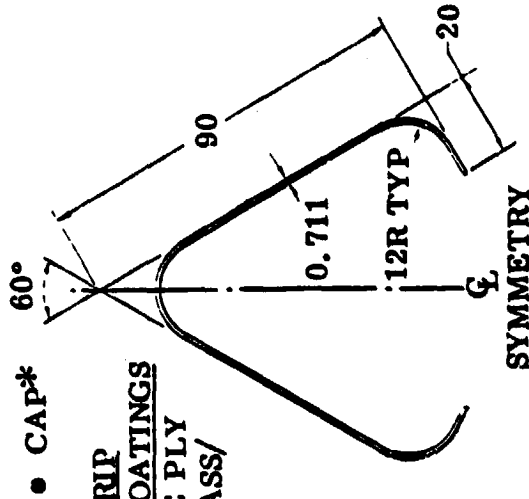
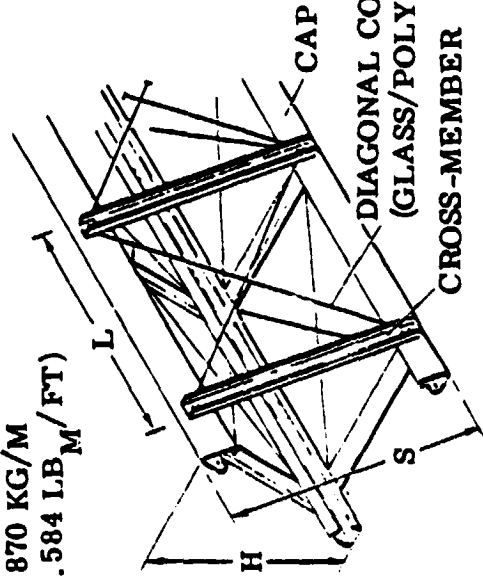


Figure 2-30. Rectangular Deployable Truss Beam with Tensioned Solar Blankets for GEO Space Radar.

● BEAM CHARACTERISTICS

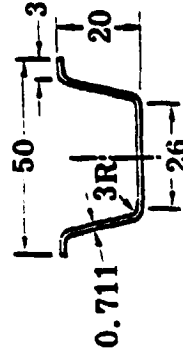
PHYSICAL

- L = 1.434M
- H = 1.180M
- S = 1.362M
- MASS = 0.870 KG/M  
(0.584 LB<sub>M</sub>/FT)



● CAP\*  
COMPOSITE STRIP  
WITH PIGMENTED COATINGS  
 ▲ WOVEN SINGLE PLY  
 ▲ GRAPHITE/GLASS/  
 POLYSULFONE

● CROSS MEMBER\*

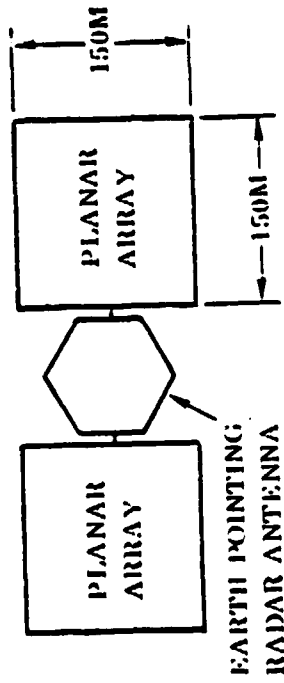


\*DIMENSIONS: MILLIMETERS

MECHANICAL

CAP	A	1.161	0.180	IN <sup>2</sup>
	E	1.317 E11	1.910 E7	LB/IN <sup>2</sup>
BEAM	AE	4.586 E7	1.031 E7	LB <sub>1</sub>
	I	1.078 E4	2.591 E2	IN <sup>4</sup>
	EI	1.420 E7	4.949 E9	LB <sub>1</sub> -IN <sup>2</sup>
	KG	1.111 E4	3.871 E6	LB <sub>1</sub> -IN <sup>2</sup>

Figure 2-31. Space-Fabricated Truss Beam.



MASS PROPERTIES

<u>ITEM</u>	<u>MASS (KG)</u>
• LENS ARRAY, 2000 M <sup>2</sup> AT 2 KG/M <sup>2</sup>	4, 000
• TRUSSES AND ODAPTS, 600 + 1400	.2, 000
• DRIVING ELECTRONICS	1, 000
• SOLAR ARRAY, 50, 000 M <sup>2</sup> AT .8 KG/M <sup>2</sup>	40, 000
• POWER MANAGEMENT/SPACECRAFT HOUSEKEEPING, ENERGY STORAGE	84, 000
<b>TOTAL</b>	<b>131, 000</b>

Figure 2-32. Planar Array and Antenna Configuration for Radar Spacecraft.

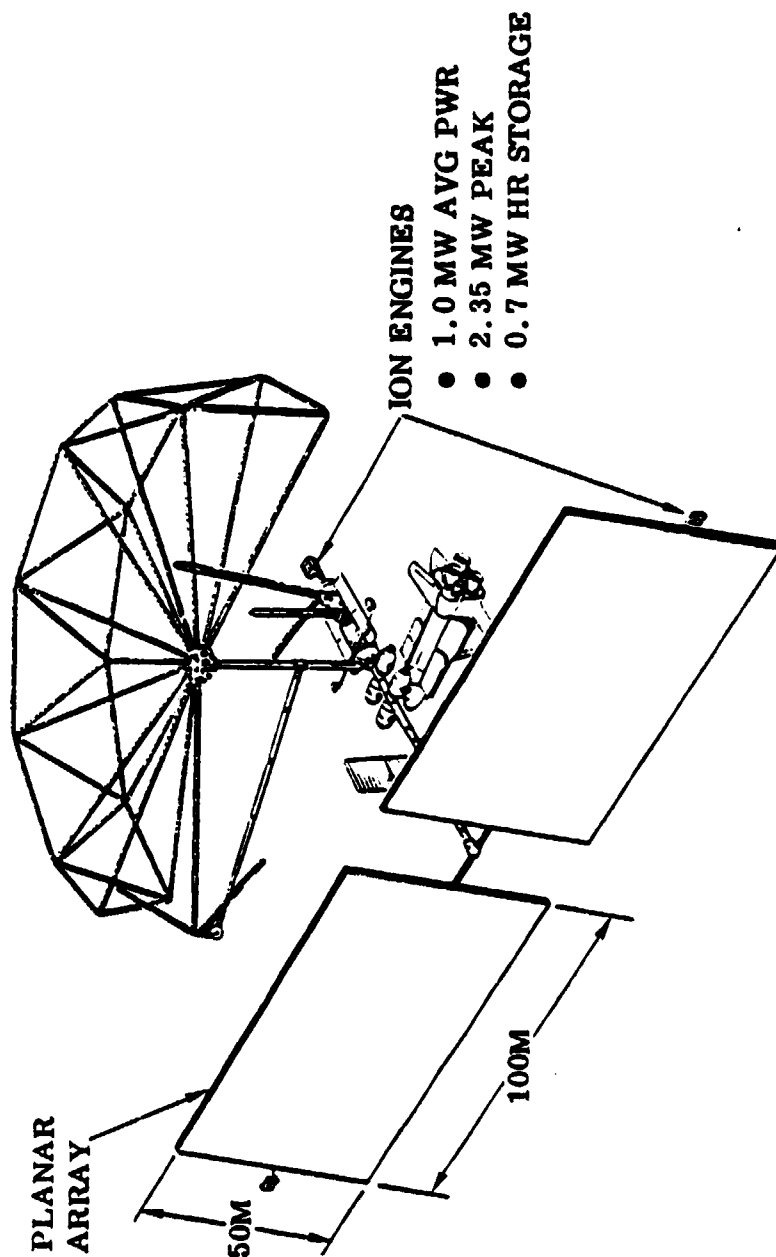


Figure 2-33. Space Construction Planar Array.

MASS PROPERTIES - SPACE CONSTRUCTION STATION		WEIGHT BREAKDOWN FOR SPACE CONSTRUCTION FACILITY	
REQUIRED POWER	1.00 M WATTS AVG.	BEAM BUILDER	15000 Kg
ENERGY STORAGE	.64 M WT. HRS	CRANE/MANIPULATOR	20000
ARRAY FOR ENERGY STORAGE	.7 M WATTS	SHEATH	5000
TOTAL ARRAY	1.7	"CHERRY - PICKERS"	12000
		CREW QUARTERS	10000
		2.5 MW ARRAY	12500 *
		ENERGY STORAGE	10000 *
			84500
WITH SAFETY FACTOR (.9)	2.35 M WATTS		
DISTRIBUTION (.9) AND EOL (.9)		<u>ALTERNATE BREAKDOWN</u>	
ARRAY AREA REQUIRED	10000 M <sup>2</sup>	ROBOTIC BEAM EXTENDER(S)	15000 Kg
(.17M)		CRANE/MANIPULATOR	20000
		CREW QUARTERS	20000
SOLAR BLANKET MASS (10,000 x .8)	8,000 Kg	2.5 MW ARRAY	12500 *
TRUSS MASS (4300 x .87 Kg/M)	3,700 Kg	ENERGY STORAGE	10000 *
ADAPT MASS **	<u>800 Kg</u>		77500
	12,500 Kg		
		* DEPEND ON STUDY OUTPUTS - SUBJECT TO CHANGE	

\*\* ORIENTATION DRIVE AND POWER TRANSFER ASSEMBLY

Figure 2-34. Mass Properties for Space Construction Facility.

In addition to the rectangular structure, the hexagonal shape and construction approach developed during Contract F04701-77-C-0178 (DOD/STS On-Orbit Assembly Concept Design Study) was examined for use as the structural backbone (Figure 2-35). The system employs a center shaft to hold the solar blankets during shuttle orbital insertion. During deployment, the arrays are then spooled from the shaft by arms which extend and pull the blankets away from the center shaft (Figure 2-36). Six shuttle flights would be required to complete the spacecraft deployment into LEO, and the spool shafts become a superfluous weight penalty of approximately 6000 kg after deployment. Also, the star configuration is usable for planar blanket approach but not the linear (x2) concentrator. Because of this added mass for the star system, it has been ruled out as a candidate for planar arrays in the multimewatt range.

In developing the planar configurations, it is apparent that consideration should have been given to the alternate material concepts for solar cells being developed for terrestrial application by various university and industrial groups for DCE. This approach was excluded at this time, for the following reasons: The only driver which will be influential in this approach is cost. Certainly risk, radiation sensitivity, LEO drag, and mass/volume are significantly increased. The viability of a 20-30 year life is extremely hard to evaluate. It does mean that risk would be significantly increased with little prospect for achieving significantly better. This does not mean the edge-defined film grown, dendritic web, or amorphous cells have been rejected. They will be considered as a part of Tasks 2.2.4 and 2.2.5.

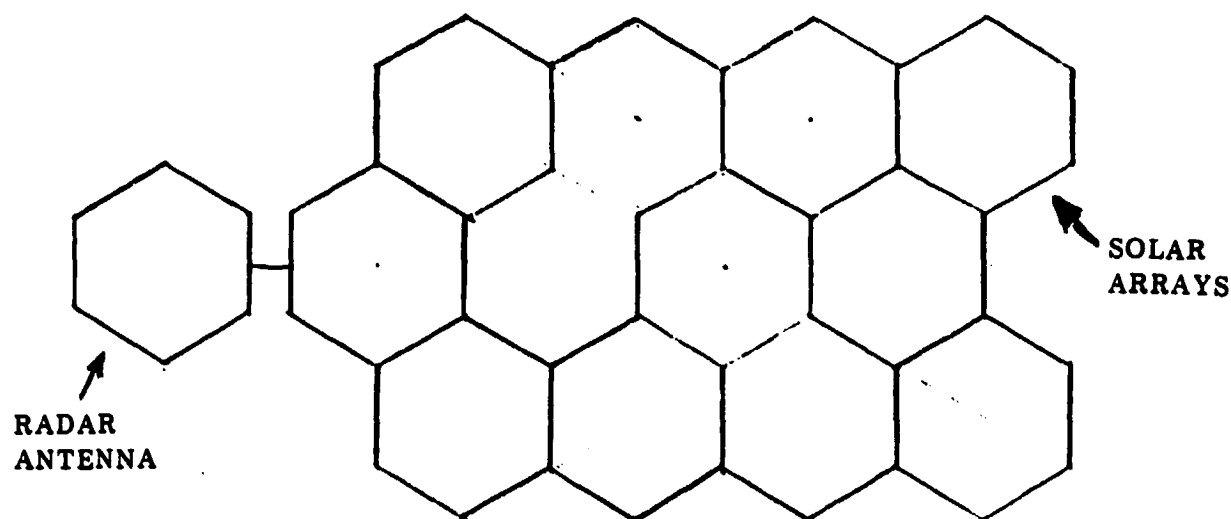


Figure 2-35. Ten Megawatt Planar Construction using On Orbit Assembly-Construction Approach.

ORIGINAL PAGE IS  
OF POOR QUALITY

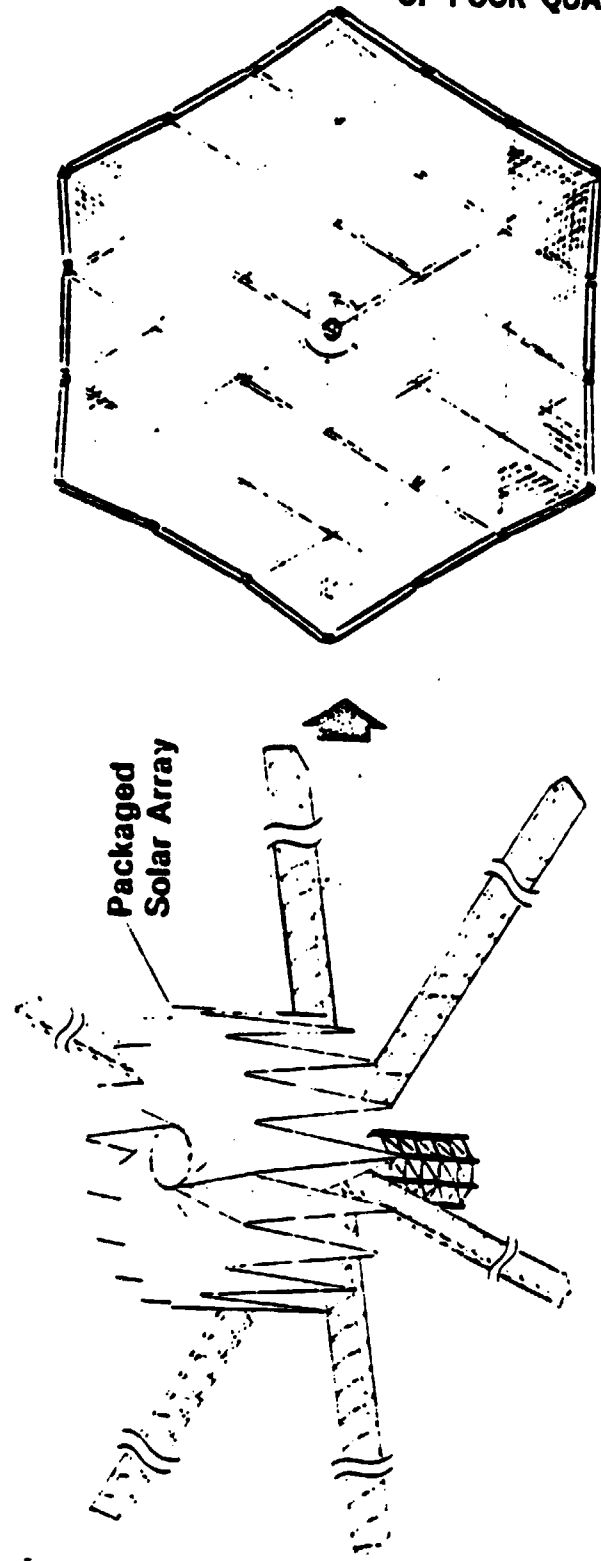


Figure 2-36. Deployment of Hexagonal Array.

**2.2.3 LARGE TROUGH CONCENTRATORS.** These designs use parabolic concentrators modified to accommodate the basic missions (antennas or construction module added). The concentrator (shown in Figure 2-37) has a blanket of aluminized Mylar attached to a truss frame which is parabolic when viewed from the end. To establish the mass properties and dimensions of the configuration for the two missions (those specified by Figures 2-37 and 2-38), the thermal aspects of the problem were first analyzed.

**2.2.4 THERMAL MANAGEMENT REQUIREMENTS.** Multimegawatt photovoltaic space power systems will require thermal management of the collected heat energy. Cooling and temperature control are required for the solar cells, the mission-specific payload equipment, and subsystem equipment. Thermal management requirements for orbiting spacecraft equipment have been well studied and thoroughly documented in the literature. The thermal analysis performed for this study therefore addresses only thermal management of the solar cells.

Solar cells used in planar space solar arrays (without solar concentration) tend to operate near 60°C (140°F). The portion of absorbed solar energy not converted to electrical energy (approx. 85%) is radiated back to space from front and back sides of the array. Use of a high emittance coating on the array back side provides sufficient cooling. No liquid cooling or other heat removal is required.

It was initially assumed that fluid cooling is required for solar cells used in space solar concentration systems, at least for large paraboloids. The cooling system which removes heat from the cells and transports it to a radiator where it is radiated to space can be either a pumped fluid or a heat pipe system. In both cases, the cooling liquid is required to be as close to the cell as possible to prevent excessive cell temperatures. Effectiveness and limitations of each of the heat transport methods are discussed in the following sections.

**2.2.4.1 Pumped Liquid Heat Removal.** The parabolic concentrator system shown in Figure 2-39 is a representative application for a pumped coolant system and will be used as a basis for the following discussion.

The coolant is pumped in parallel tubes across the solar cells in the short direction to minimize pressure drop and coolant temperature rise. The coolant then flows in larger manifolds along the long edge of the solar cells to the radiators at the end of the concentrator. Fluid routing is not defined beyond that described above.

Evaluation of the pumped coolant approach will be based on the coolant-to-solar cell temperature difference, with emphasis on convective heat transfer at the coolant/tube wall interface. The latter analysis will investigate fluid velocities, convective heat transfer coefficients, and resulting temperature differences across the coolant convective boundary layer.

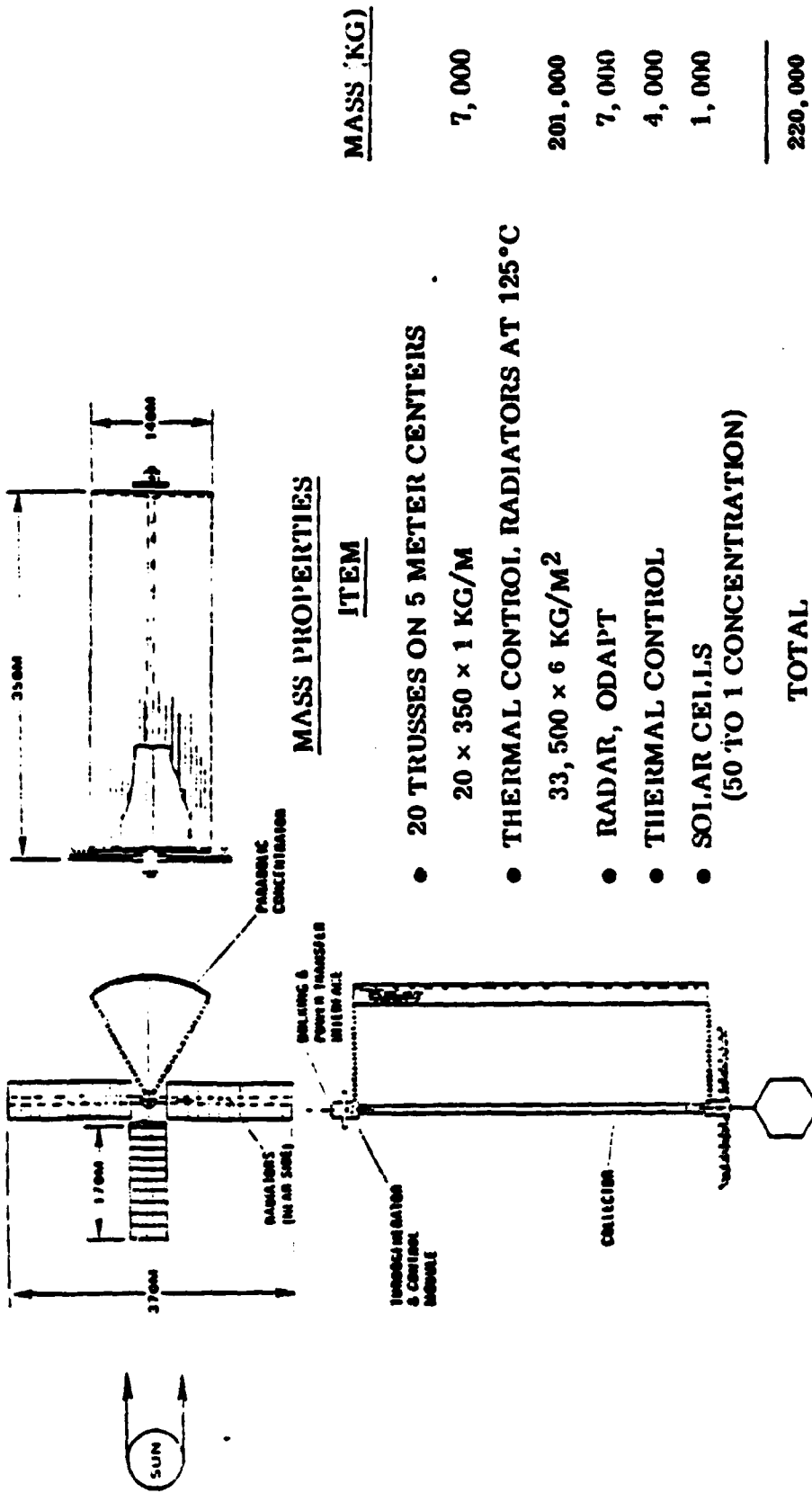
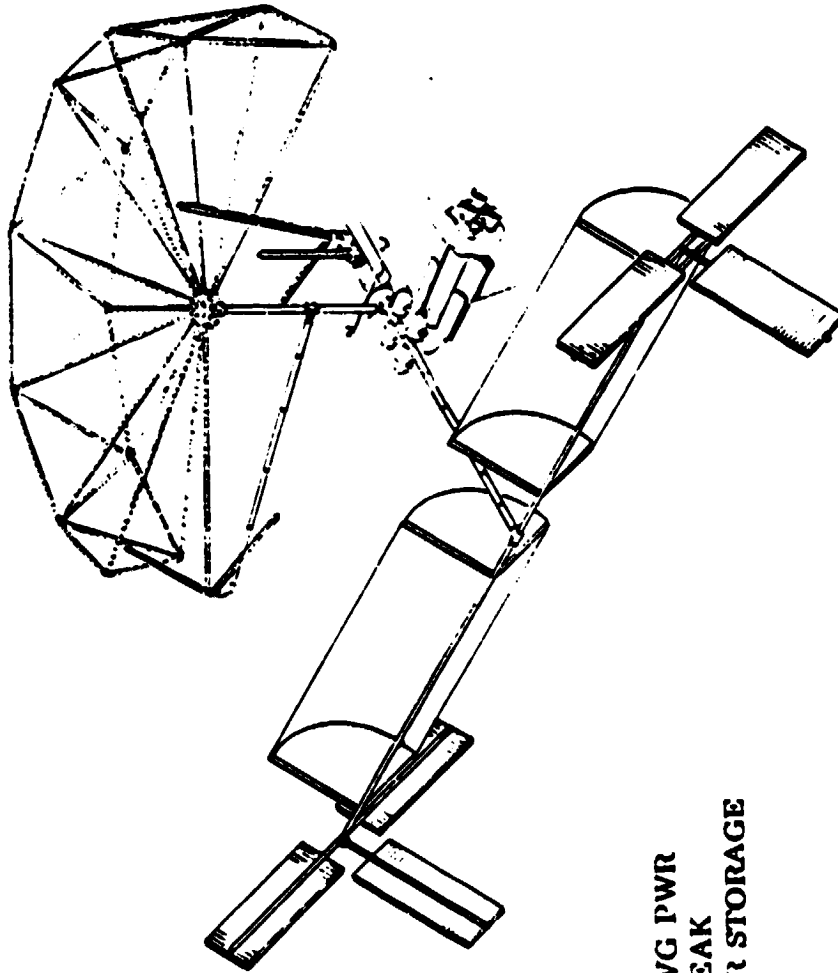


Figure 2-37. Radar Modifications to Basic Parabolic Trough.



- 1.0 MW AVG PWR
- 2.3 MW PEAK
- 0.7 MW IIR STORAGE

ADDITIONAL  
MASS FOR  
RADIATORS  
 $8,000 \text{ m}^2 \times 2.5 \text{ Kg/m}$   
20,000 Kg

Figure 2-38. Space Construction Facility Utilizing Large Parabolic Trough.

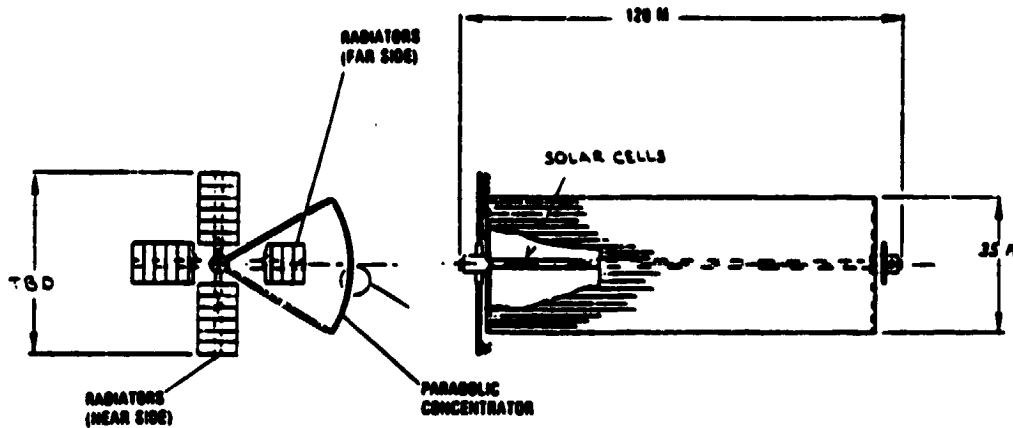


Figure 2-39. Parabolic Concentrator with Pumped Coolant System.

2.2.4.1.1 Heat Load Model. The spacecraft thermal model employed to determine the heat load on the pumped coolant system solar cells is shown in Figure 2-40. The solar cell flux to be removed by the heat rejection system  $Q_{rej}$ , is related to the concentration ratio,  $C_T$ , by:

$$Q_{rej} = 1000 C_T \text{ Watts/M}^2 \quad (\text{Eq. 1})$$

$$Q_{rej} = 318 C_T \text{ Btu/hr-ft}^2 \quad (\text{Eq. 1a})$$

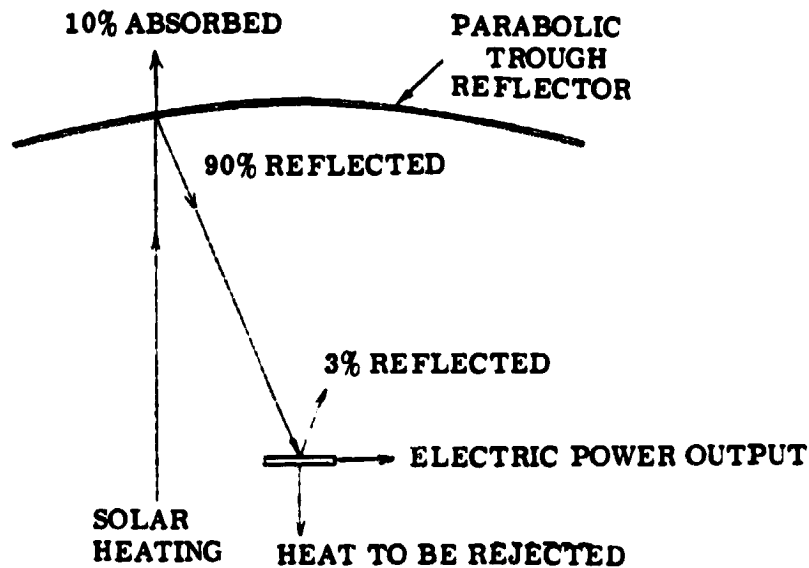


Figure 2-40. Spacecraft Thermal Model for Pumped Coolant System.

2.2.4.1.2 Coolant-to-Solar-Cell  $\Delta$  Temperatures. The portion of the concentrated solar energy absorbed by the solar cells which must be removed by the cooling system will conduct through the cell substrate and tubing wall and be transferred across the fluid boundary layer (see Figure 2-41).

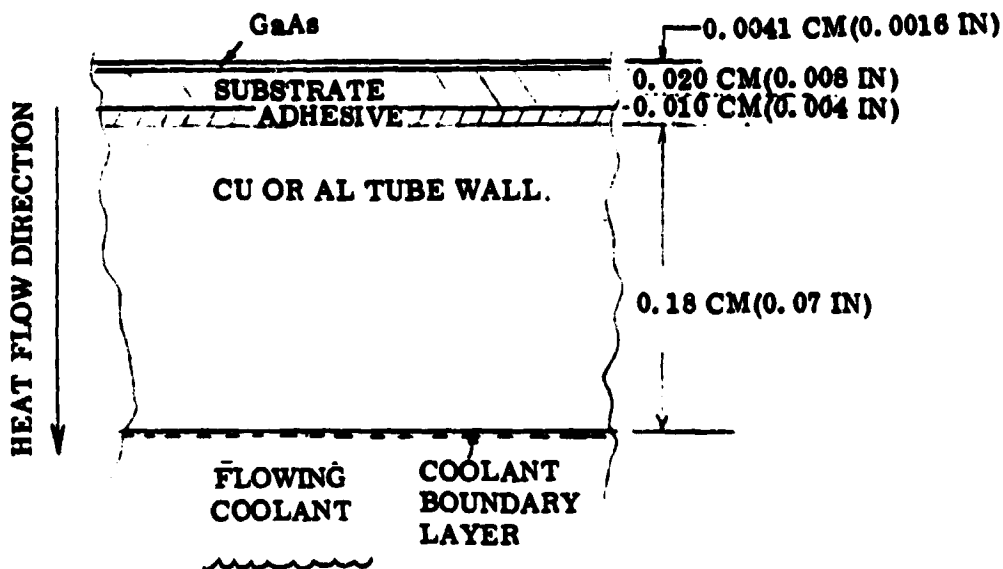


Figure 2-41. Solar Cell/Coolant Tube Wall/Coolant Cross-Section.

Heating of the solar cells by concentrated solar energy will establish  $\Delta$  temperatures across the various layers of material according to the following:

SI Units,  $\Delta T$  in  $^{\circ}\text{C}$

Solar cell substrate	$\Delta T_{ss} = 0.204 \frac{C_r}{k}$	(Eq. 2)
Substrate adhesive	$\Delta T_{sa} = 0.107 C_r$	
Copper tube wall	$\Delta T_{tw} = 0.00516 C_r$	
Fluid boundary layer	$\Delta T_{bl} = 1003 \frac{C_r}{h}$	

English Units,  $\Delta T$  in  $^{\circ}\text{F}$

Solar cell substrate	$\Delta T = 0.212 \frac{C_r}{k}$	(Eq. 2a)
Substrate adhesive	$\Delta T_{ss} = 0.192 C_r$	
Copper tube wall	$\Delta T_{tw} = 0.00928 C_r$	
Fluid boundary layer	$\Delta T_{bl} = 318 \frac{C_r}{h}$	

where:  $k$  = substrate material thermal conductivity,  $\text{w/m}^{\circ}\text{C}$  ( $\text{Btu/hr-ft}^{\circ}\text{F}$ )

$h$  = coolant heat transfer coefficient,  $\text{w/m}^2\text{-}^{\circ}\text{C}$  ( $\text{Btu/hr-ft}^2\text{-}^{\circ}\text{F}$ )

The solar cells will reside at a temperature established by the coolant temperature plus the sum of the four  $\Delta$  temperatures given above. The total solar-cell-to-coolant temperature difference is seen to be proportional to the concentration ratio,  $C_r$ . A concentration ratio of 50:1 will be used here as an example for investigating cell temperatures.

Temperature difference across the boundary layer,  $\Delta T_{bl}$ , is seen above to be inversely proportional to the convective film heat transfer coefficient,  $h$ . The heat transfer coefficient for fully developed turbulent forced convection flow in a tube is given by the following equation:

$$h = 0.023 \frac{k}{d} \frac{\rho v d}{\mu}^{0.8} \frac{C_p \mu}{k}^{0.33} \quad (\text{Eq. 3})$$

where:  $h$  = heat transfer coefficient,  $\text{w/m}^2\text{-}^\circ\text{C}$  ( $\text{Btu/hr-ft}^2\text{-}^\circ\text{F}$ )  
 $k$  = coolant thermal conductivity,  $\text{w/m-}^\circ\text{C}$  ( $\text{Btu/hr-ft-}^\circ\text{F}$ )  
 $d$  = tube diameter, m (ft)  
 $v$  = coolant velocity, m/sec (ft/sec)  
 $\mu$  = coolant viscosity, kg/m-sec (lb/ft-sec)  
 $\rho$  = coolant density,  $\text{kg/m}^3$  ( $\text{lb/ft}^3$ )  
 $C_p$  = coolant specific heat, joule/kg- $^\circ\text{C}$  ( $\text{Btu/lb-}^\circ\text{F}$ )

For a given tube diameter and coolant, the heat transfer coefficient is related to velocity by

$$h = K v^{0.8} \quad (\text{Eq. 4})$$

Earlier studies conducted at Convair (Reference 12) compared fourteen fluids for heat transfer performance in pumped-coolant space-radiator systems. Water has by far the best performance, but because of its relatively high freezing temperature is generally unsuitable for space radiators. Coolants Freon-21 (DuPont) and FC-75 (Minnesota Mining and Manufacturing) have about the same heat transfer coefficient and are next to water in performance. However, Freon-21 has an excessively high vapor pressure at the temperature range foreseen in this application (e.g.  $12.1 \times 10^5 \text{ N/m}^2$  at  $93^\circ\text{C}$  or 175 psi at  $200^\circ\text{F}$ ). FC-75 therefore appears to be the most suitable coolant. Its vapor pressure is less than  $13.8 \times 10^4 \text{ N/m}^2$  at  $93^\circ\text{C}$  (20 psi at  $200^\circ\text{F}$ ).

Using the properties of FC-75 and assuming a 1.9 cm (3/4 in) tube diameter, Equation 3 gives the relationship between velocity and heat transfer coefficient seen in Figure 2-42.

In terms of heat flux, the  $\Delta$  temperature across the convective film is given by:

$$\Delta T = \frac{Q/A}{h} \quad (\text{Eq. 5})$$

where:  $Q/A$  = heat flux transferred into coolant,  $\text{w/m}^2$  ( $\text{Btu/hr-ft}^2$ )

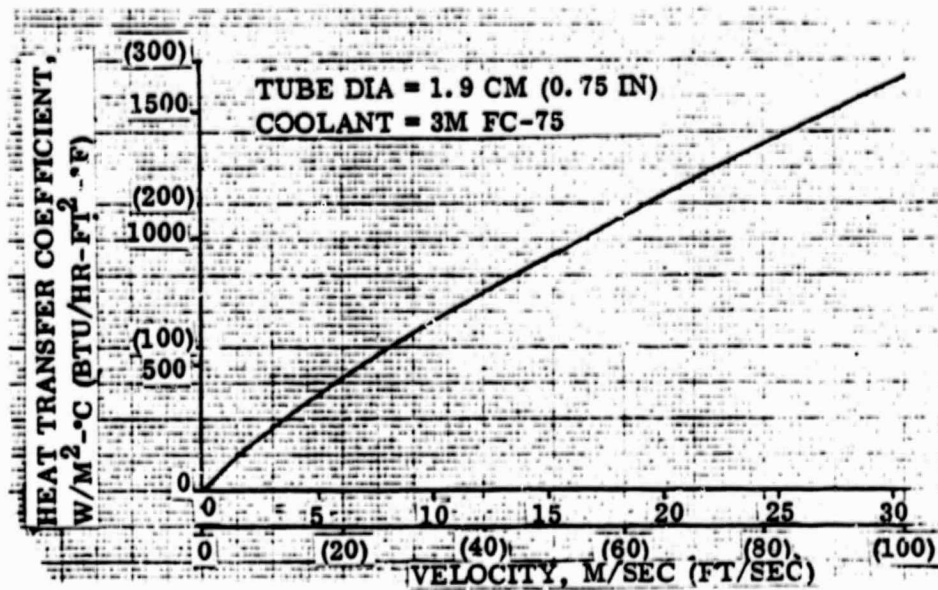


Figure 2-42. Heat Transfer Coefficient Versus Velocity for FC-75.

For a concentration ratio of 50, the heat flux to be removed is approximately  $50,200 \text{ w/m}^2$  ( $15,900 \text{ Btu/hr-ft}^2$ ). This assumes a 10% loss by absorption at the primary reflector, a 3% loss by reflection at the solar cells, and electrical energy developed by a 17% cell efficiency, all of which are removed before reaching the cell cooling system (Figure 2-40). The resulting film  $\Delta$  temperature is seen in Figure 2-43 as a function of heat transfer coefficient.

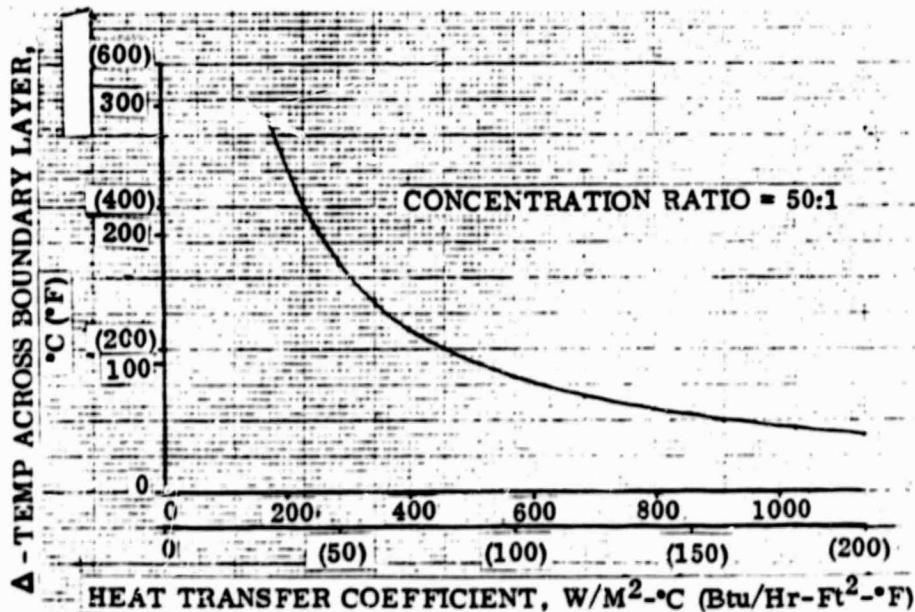


Figure 2-43. Temperature Difference Across Coolant Boundary Layer Versus Heat Transfer Coefficient.

From Figures 2-42 and 2-43, high heat transfer coefficients and correspondingly high velocities, 9.1 to 15 m/sec, (30 to 50 ft/sec) are seen to be required to bring the coolant boundary layer  $\Delta$  temperature down even to the 50-80°C (90-144°F) range. This is seen as a critical limitation with the pumped coolant approach to cooling solar cells in a concentrator system.

Since substrate material has not yet been defined for this analysis and candidate materials cover a range of  $k$  values, the potential cell substrate  $\Delta$  temperatures,  $\Delta T_{SS}$ , also cover a range of values. The spread of  $\Delta T_{SS}$  values shown in Figure 2-44 is representative of low- $k$  semiconductors and is seen to be low compared to predicted coolant film  $\Delta$  temperatures (typically over 55°C or 100°F). As an example, candidate substrate material  $\text{SiO}_2$  has a thermal conductivity of 2.1 w/m-°C (1.2 Btu/hr-ft-°F) which results in  $\Delta T_{SS} = 5^\circ\text{C}$  (9°F).

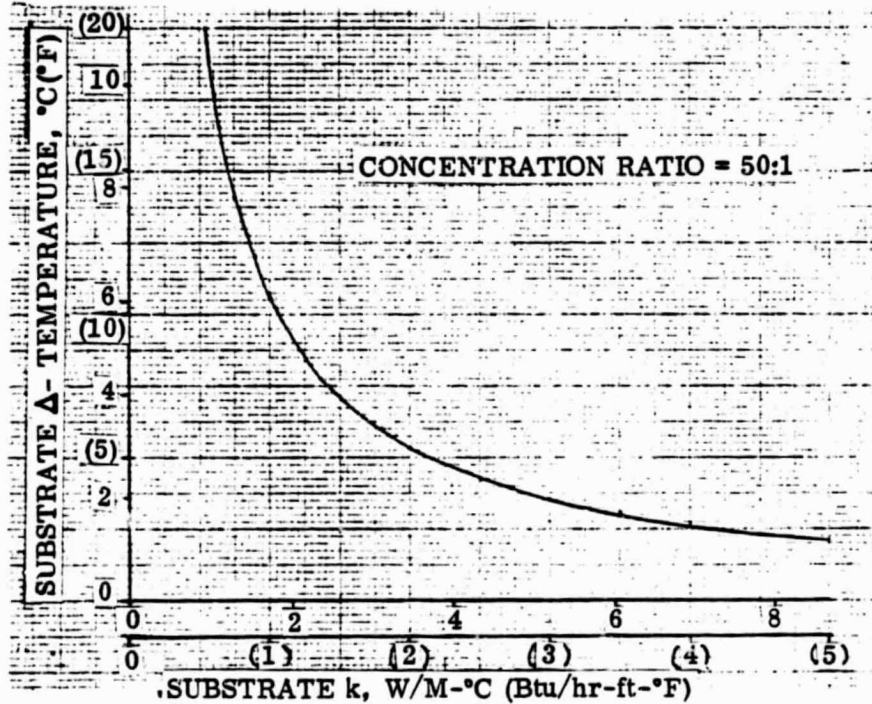


Figure 2-44. Solar Cell Substrate  $\Delta T$ s for Typical Low- $k$  Semiconductor.

The solar cell substrate can be bonded to the cooling tube using an Ablestick preform adhesive (Ableform 506) which has a thermal conductivity of approximately 0.80 w/m-°C (0.46 Btu/hr-ft-°F). Required thickness is approximately 0.01 cm (0.004 in). The resulting  $\Delta T_{SS} = 5.3^\circ\text{C}$  (9.6°F) at a 50:1 concentration ratio.

Copper tubing wall  $\Delta$  temperature is only 0.25°C (0.45°F) for a thickness of 0.18 cm (0.07 in) and a concentration ratio of 50:1. Thus, tubing wall  $\Delta T$ s can be ignored in solar cell temperature predictions.

The above discussion has shown that the coolant boundary layer  $\Delta T$  makes up nearly all the coolant-to-solar-cell  $\Delta T$ . It has also shown that the overall  $\Delta T$  is proportional to concentration ratio,  $C_r$ . Analysis to size the radiators required to reject the heat picked up by the fluid in cooling the solar cells appears later in this report.

**2.2.4.2 Heat Removal By Heat Pipes.** Heat pipe use in a multimegawatt space power system is generally limited to applications where transport distances are considerably less than the major dimensions of the spacecraft. A representative solar concentrator concept well suited to heat pipe use is that shown in Figure 2-45. A version of  $\mu$  was, unknown the author at a much later date first suggested in Reference 13.

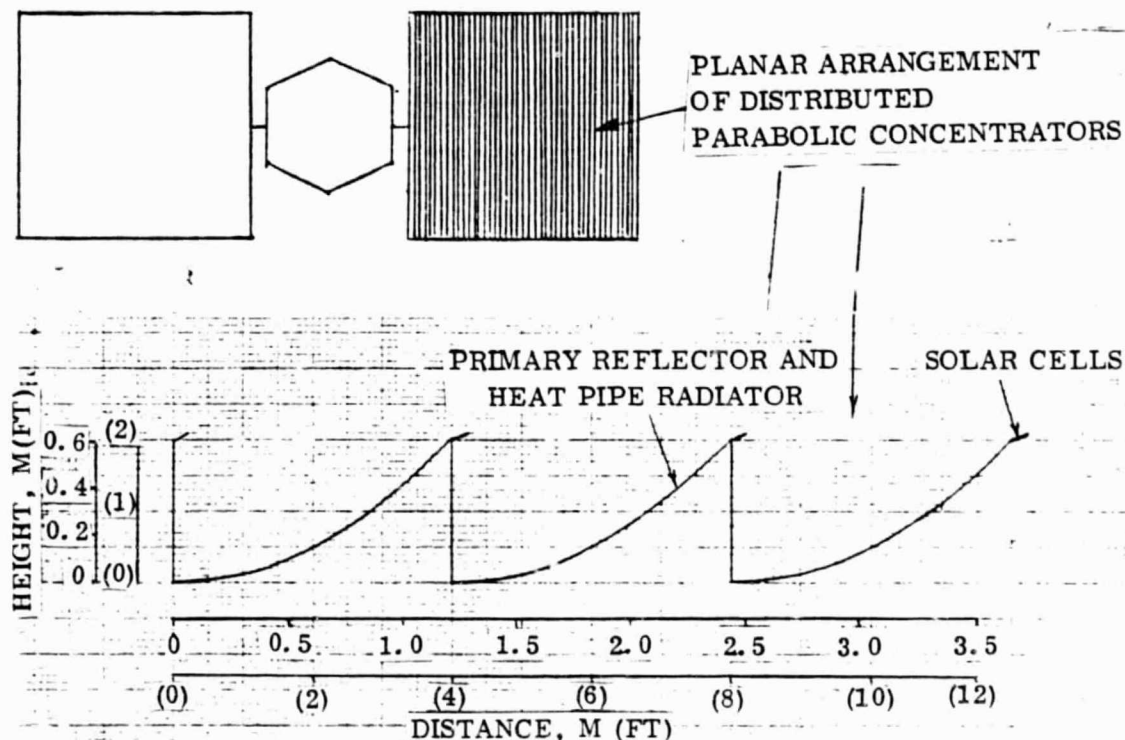


Figure 2-45. Solar Concentrator Concept Suited to Heat Pipe Use.

The array consists of a number of small concentrating parabolic reflectors, 0.6 m x 1.2 m (2 ft x 4 ft) in cross-section, arranged in a plane. The primary reflector acts as a heat pipe radiator for the solar cells on the adjacent concentrator. For a 50:1 concentrator, the solar cell strip is approximately 2.5 cm (one inch) wide. The assumed heat pipe arrangement for removing heat from the cells and distributing it to the heat pipe radiator is that shown in Figure 2-46. The heat pipe cross-section is representative only. Other designs, such as a wide heat pipe saddle, are possible and could result in a lighter weight. The following sections discuss

heat transport limitations, wick design, fluid selection, thermal modeling, and solar cell-to-radiator temperature drops for this heat pipe application.

**2.2.4.2.1 Heat Transport Limitations.** Four limiting conditions have been identified for heat pipe performance (Reference 14). That is, the heat pipe will continue to operate under increasing heat loads until one of the following conditions occurs: sonic limitation, entrainment limitation, wicking limitation, or boiling limitation. The sonic limitation occurs when the working fluid vapor flowing to the condenser section reaches sonic velocity. The entrainment limitation occurs with excessively high dynamic vapor pressure. In this case, some of the liquid in the wick-return system is picked up and entrained in the vapor, which is flowing in the opposite direction. Wicking limitation is reached when the pressure drop due to resistance of liquid and vapor flows balances the capillary pumping pressure. Boiling limitation occurs when the heat flux into the evaporator section is great enough to cause nucleate boiling (bubbles), which interferes with the liquid return.

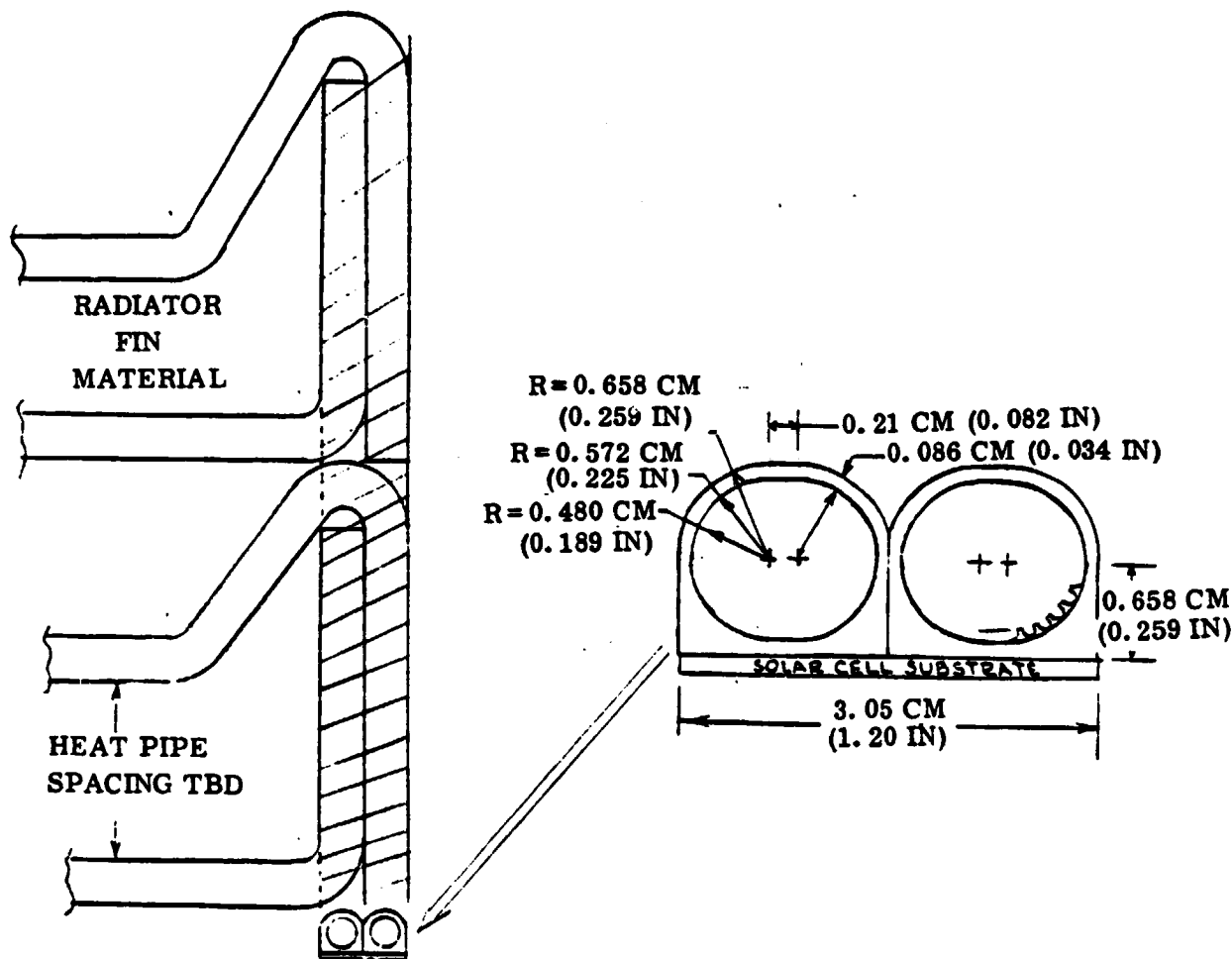


Figure 2-46. Heat Pipe Arrangement Assumed for Analysis.

For this application, the boiling limitation is the most likely of the four to be encountered because of the small solar cell (evaporator) area. The analysis, therefore, investigated the maximum flux the evaporator can accommodate without boiling, and the effects wicking design and fluid selection have on this max flux. The wicking limitation is also a potential limiting condition, but was not analyzed in this study.

Reference 14 has developed in equation for boiling limitation maximum heat rate into the evaporator section, and this equation is given below:

$$Q_{\max} = \frac{2T_g \sigma [\pi K_e Z_e (r_i + r_g)]}{h_{fg} \rho_g r_b (r_i - r_g) J} \quad (\text{Eq. 6})$$

where:  $Q_{\max}$  = max heat rate into evaporator, watts (Btu/hr)

$T_g$  = vapor temperature, °K (°R)

$\sigma$  = liquid surface tension, Kg/m (lb/ft)

$K_e$  = effective radial thermal conductivity of the liquid filled wick, w/m-°K (Btu/hr-ft-°F)

$Z_e$  = evaporator length, m (ft)

$r_i$  = wick outer radius, m (ft)

$r_g$  = wick inner radius, m (ft)

$h_{fg}$  = heat of vaporization of the working fluid joule/Kg (Btu/lb)

$\rho_g$  = vapor density, Kg/m<sup>3</sup> (lb/ft<sup>3</sup>)

$r_b$  = radius of wick capillary cavity where bubble originates, ft  
(taken to be 0.025 cm (0.01 inch) =  $2.5 \times 10^{-4}$  m ( $8.33 \times 10^{-4}$  ft))

$J$  = conversion factor of 0.102 m - Kg/joule (778 ft-lb/Btu) for correct units

2.2.4.2.2 Wick Configuration. The effective radial thermal conductivity of the fluid-filled wick,  $K_e$ , is strongly dependent on the wick configuration. Equation 7 gives effective thermal conductivity for parallel paths of fluid and wick material in an axial groove heat pipe.

$$K_e = \epsilon K_f + (1 - \epsilon) K_w \quad (\text{Eq. 7})$$

where:  $K_f$  = liquid thermal conductivity, w/m-°K (Btu/hr-ft-°F)

$K_w$  = wick material thermal conductivity, w/m-°K (Btu/hr-ft-°F)

$\epsilon$  = volume fraction of the liquid, dimensionless

Equation 8 gives effective thermal conductivity for distributed cylinders, arranged to form a screen, surrounded by the fluid.

$$K_e = \frac{K_f [K_f + K_w - (1 - \epsilon) (K_f - K_w)]}{[K_f + K_w + (1 + \epsilon) (K_f - K_w)]} \quad (\text{Eq. 8})$$

Effective thermal conductivities of 59 and 5.9 w/m-°K (40 and 3.4 Btu/hr-ft-°F) were calculated for axial groove and screen aluminum/water heat pipes, respectively. Because of the significantly higher conductivity, only axial groove heat pipes were considered from this point on.

**2.2.4.2.3 Fluid Selection.** A number of potential heat pipe fluids were investigated and eliminated. Water freezes at too high a temperature. Methane liquid surface tension approaches zero at -84°C (-120°F) and is only usable at temperatures below this.

Ammonia has a vapor pressure of  $13.8 \times 10^5 \text{ N/m}^2$  (200 psi) at 38°C (100°F), which is excessively high. The Minnesota Mining and Manufacturing fluorocarbons FC-43, FC-75, and FC-78 have acceptably low vapor pressures and freezing temperatures. They were compared for boiling limitation performance; i.e., for maximum evaporator heat rate without boiling.

Equation 6 was used to calculate boiling limit maximum heat rate (which was then converted to heat flux and equivalent suns). At a gas temperature of 66°C (150°F), the fluids FC-43, FC-75, and FC-78 were found to accommodate heating equivalent to 47.6, 8.1, and 3.6 suns. For a 50:1 concentration ratio and typical system losses and efficiency, the heat pipe is required to remove heating approximately equal to 31 suns. FC-43 was, therefore, selected as a suitable working fluid.

To determine how warm the evaporator temperature can be allowed to operate, Equation 6 was also used to determine FC-43 boiling limit heating at 100°C (212°F) and 150°C (302°F). Maximum fluxes corresponding to 38 suns (at 100°C) and 25 suns (at 150°C) were calculated. The nature of the working fluid (FC-43) properties causes the allowable heat flux entering the evaporator to decrease with increasing temperature. A concentrated solar flux of 31 suns could theoretically be accommodated at a heat pipe evaporator temperature of 127°C (260°F). However, because of the uncertainty of  $r_b$  (radius where bubble originates) in Equation 6 and for a margin of safety, 100°C (212°F) will be taken as the maximum allowable heat pipe evaporator temperature for this analysis.

**2.2.4.2.4 Solar Cell-to-Heat Pipe Temperature Drops.** Maximum operating temperature of the solar cell is set by the maximum allowable evaporator temperature (100°C) plus the cell-to-heat pipe temperature drops. Note that the solar cell operates at a greater efficiency at lower temperatures, but that this requires thicker radiation fin material between heat pipes and/or closer heat pipe spacing, both of which increase weight. Radiator fin sizing and heat pipe spacing are covered in Subsection 2.3. The design point for this analysis is based on the maximum allowable evaporator temperature which results in the lightest weight per unit aperture area.

The  $\Delta T$  across the cell substrate is identical to that for the pumped coolant system described in Subsection 2.2.4.1. Values are typically 1 to 10°C (2 to 18°F), depending on the thermal conductivity of the substrate material (Figure 2-44). A cell substrate  $\Delta T$  of 5°C (9°F) is taken to be a typical value for this example. Similarly, the  $\Delta T$  across the cell adhesive is also identical to that for the pumped coolant system. Bond line  $\Delta T$  was shown to be 5.3°C (9.6°F) for an Ablestick preform adhesive "Ableform 506."

Radial temperature drop across the liquid filled evaporator wick is given by the following equation:

$$T_e - T_g = Q (r_i - r_g) / [\pi K_e Z_e (r_i + r_g)] \quad (\text{Eq. 9})$$

where:  $T_e$  = temperature of heat pipe wall at evaporator, °C (°F)

$T_g$  = temperature of fluid vapor at evaporator, °C (°F)

$Q$  = heat rate into the evaporator, watts (Btu/hr)

$r_i$  = inside radius of heat pipe wall = outside radius of wick, m (ft)

$r_g$  = radius of gas passageway = inside radius of wick, m (ft)

$K_e$  = effective thermal conductivity of wick, w/m-°C (Btu/hr-ft-°F)

$Z_e$  = length of evaporator, m (ft)

At a heat flux into the heat pipe evaporator of approximately 30 suns (for  $C_r = 50:1$ ), the above equation gives a  $\Delta$  temperature across a typical axial groove wick of less than 1°C (2°F). Note that this  $\Delta T$  compares to the 50-80°C (90-144°F)  $\Delta T$  across a pumped coolant boundary layer as described in Subsection 2.2.4.1.

Maximum allowable cell operating temperature based on the heat pipe evaporator boiling limitation is therefore  $100 + 5 + 5 + 1 = 111^\circ\text{C}$  (232°F).

The foregoing analysis indicates that it is possible to conceive of attainable designs — albeit massive ones — which could be developed into modular concentrating systems.

During the Task III modularity studies, these approaches were refined further in an effort to minimize mass and cost.

**2.2.5 OPERATING OPTIONS.** During Task I, the preliminary power system requirements for the 10-megawatt radar and 2.5 MW Space Construction Facility were synthesized. These preliminary requirements assumed that ion engines were utilized to accomplish GEO injection of the 10-MW Radar and LEO stationkeeping of the Space Construction Facility. During Task II, these requirements were synthesized more accurately, based on the data generated for array specific powers, energy storage specific energies, and based on possible power system topologies and power system to ion engine interfaces. These calculations continued to support the use of ion engines in both configurations, as described below.

**2.2.5.1 Ion Engine GEO Orbital Transfer and LEO Orbital Stationkeeping.** Because by ground rules, this study concerned itself with multimegawatt electrical power systems, the natural first choice for a system to provide the thrust for LEO to GEO transfer and LEO stationkeep is an electrical propulsion system. Both ion engine and MPD thrusters could have been considered, but, since the potential efficiency of ion engine systems appears to be greater (Reference 15), they were used as a study baseline. Later trades should be conducted to establish the quantified benefits and liabilities of an MPD approach. However, with ISPs of 5,000 to 10,000 and efficiencies of 50%, even MPD systems seem to be beneficial compared to chemical propulsion, as discussed in the following section.

**2.2.5.2 Ion Engine Projections.** The projections of argon electrical ion engine propulsion technology have been described by Byers et al. (References 15 and 17). In this study, their equations and results were used to develop the expected spacecraft performance for the two study missions. Particular results that affected the study were:

- a. Argon engines that have a diameter of 50 cm, efficiency of 0.75, ISP of 5,000 at a net beam voltage of 900 VDC ( $V_B$ ) appear feasible, and were used in system configuration development.
- b. Beam and discharge voltages were regulated by the receiving AC power supply for the AC system, or by the DC regulator for the DC system.
- c. Thruster and gimbal mass was assumed to be 27 kg based on Figure 4 of Reference 6.

**2.2.5.3 GEO Electrical Injection Calculations.** Based on these projections, calculations were then made of the Argon propellants mass, thruster quantity, form, and cost of propellants transportation, and mass for the 10-MW space radar GEO orbit injection; total system mass was 141,000 kg, as shown in Table 2-6, which lists the breakdown of these mass properties.

**2.2.5.4 Chemical Injection.** A calculation of the mass of propellants required to inject the Space Radar into GEO orbit using chemical propulsion was also made. At ISPs of 450, the indicated total system mass would be about 443,000 kg, using a tank engine and electronics mass fraction of 0.12. Table 2-7 summarizes this data.

The chemical system orbital trajectory was based on a nine-burn injection with a 25-hour coast phase, as was developed in a study of low thrust OTV concepts for GEO injection (Reference 18).

For both the electrical and chemical systems, the cost to GEO orbit was also calculated, including the cost of money for the orbital transfer time, assuming a \$1,000 M spacecraft investment, \$1,000/kg shuttle transportation cost, and 15% interest rate.

**Table 2-6. Mass Properties for the 10 Megawatt Radar — Electrical Ion Engine Propulsion Injection with an AC Power Management System.**

10 Megawatt Solar Array — Small, modular, low-light-loss concentrator	55,000
Radar Membrane Array — Orientation drive and electronics	7,000
Power Management System	52,000
Argon Ion Engines and Gimbals, at a 5,000 ISP, $V_B = 900$ VDC, 50 cm diameter, 108 thrusters @ 27 Kg each	3,000
Storage/Tankage/Structure/Miscellaneous	8,000
Subtotal	125,000
Argon Propellant Mass	16,000
	141,000
Trip time	
30 days with continuous thrust, more likely 60 days with intermittent thrusting and extra velocity to be gained.	
Total Cost to Orbit plus Money Cost	≈ \$200 M

**Table 2-7. Mass Properties for the 10 Megawatt Radar — Chemical Propulsion Injection.**

10 Megawatt Solar Array — Small, modular, low-light-loss concentrator	55,000 Kg
Radar Membrane Array — Orientation drive and electronics	7,000 Kg
AC Power Management System or DC/DC Power Management	40,000 Kg
Emergency Storage/Electronics	2,000 Kg
Electronics, Engine/Tank Mass at 0.12 Mass Fraction	36,000 Kg
Subtotal	140,000 Kg
Propellant Mass at 450 ISP (Hydrogen/Oxygen, 1990s projection)	303,000 Kg
Total	443,000 Kg
Trip Time	6 days
Total Cost to Orbit plus Money Cost	\$440 M

The data shown in the tables clearly indicates the benefits of electrical propulsion for the 10-MW Radar Mission.

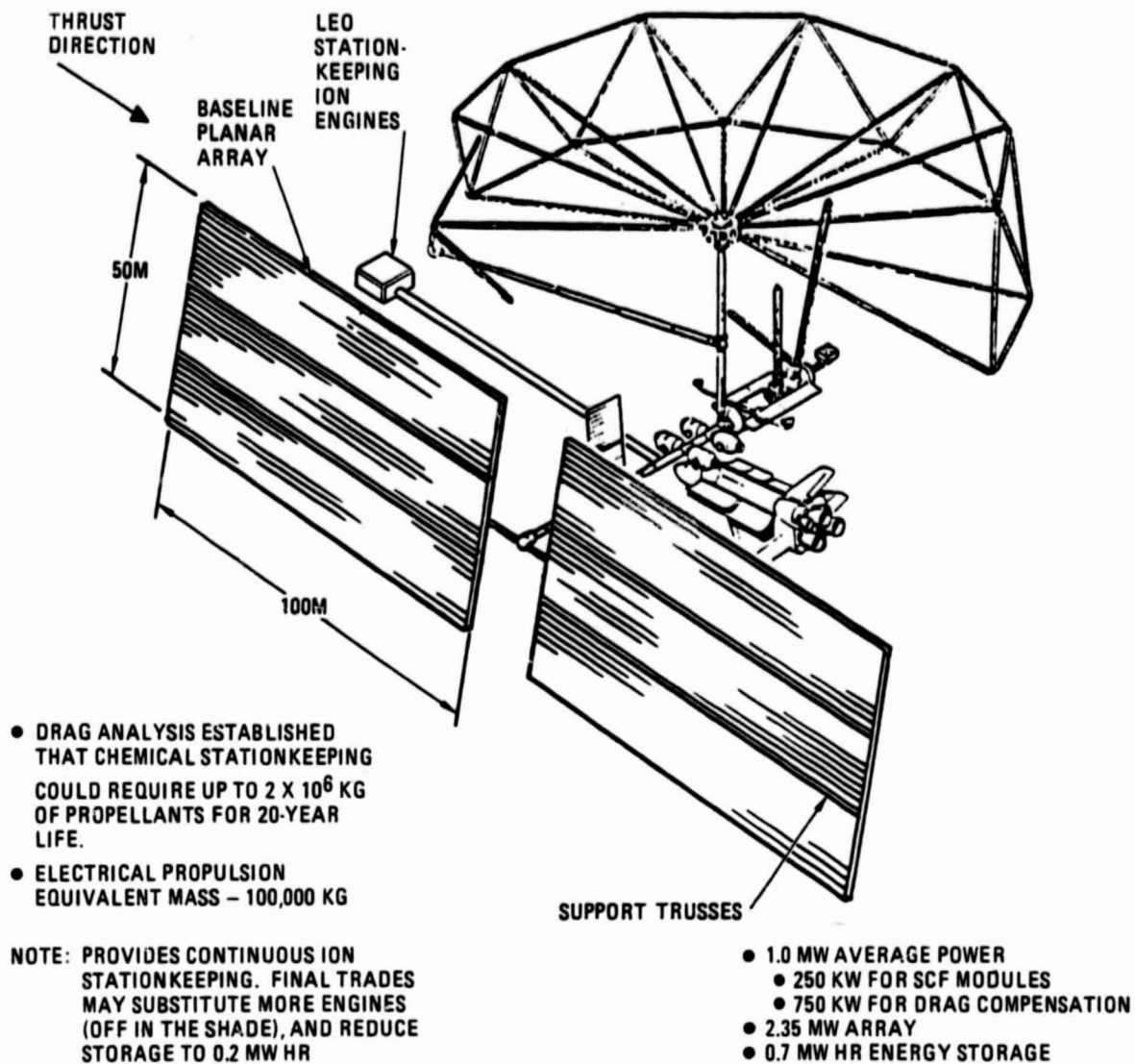
**2.2.5.5 LEO Space Construction Facility.** The Space Construction Facility requires engines to maintain it in low earth orbit against the drag forces caused by the reaction between the upper atmosphere and the large planar arrays, which it would be fabricating and assembling in space. To minimize gravity gradient effects, the large space structure under construction would probably be assembled outward from the bottom of the spacecraft (towards the earth). Since the majority of the mass of the system would come from the array under construction, crew quarters, and construction materials to counteract the drag forces should be located where they can thrust the spacecraft away from the earth's horizontal plane. By locating them on two truss frames as shown in Figure 2-47, the thrust vector can be kept along the center of gravity of the composite system of arrays and spacecraft modular components. Because these components comprise the major mass, it is assumed that, for this facility, if electrical propulsion stationkeeping is utilized, all the engine power will transverse through the rotary joint. Based on this conceptual design, calculations of the benefits and liabilities of electrical and chemical stationkeeping were made.

**2.2.5.6 Stationkeeping for the Space Construction Facility using Chemical or Electrical Stationkeeping Engines.** As discussed in Subsection 2.1, large solar arrays in the megawatt class will have a significant amount of drag that could cause their premature reentry before they have been transported out of low earth orbit to GEO synchronous orbit. To provide a stationkeeping acceleration, either chemical or electrical propulsion could be employed. Calculations were made of the amount of propellants and the cost of transporting the propellants to LEO using the shuttle for both chemical and electrical propulsion systems. The mass properties of the combined Space Construction Facility and 10-MW radar given in Table 2-6 were used to compute both the drag of the combined system and the propellant mass and transportation cost. The velocity loss caused by drag was decreased to 0.2 meter/sec/orbit because of the increased total mass of the entire system.

**2.2.5.7 Chemical Propulsion Versus Electrical Propulsion.** For the chemical system, a hydrazine ISP of 235 was assumed to be the maximum possible value that might be obtained. Tank and engine mass fractions of 0.12 were again used.

**2.2.5.8 Electrical Propulsion.** For electrical propulsion, the characteristics of the argon ion engine system were assumed to be identical to those described in Subsection 2.2.5.2, namely:

- a. Argon engines that have a diameter of 50 cm, efficiency of 0.75, ISP of 5,000 at a net beam voltage of 900 VDC ( $V_B$ ) appears feasible and were used in system configuration development.
- b. Beam and discharge voltages were regulated by the receiving AC power supply for the AC system or by a DC regulator for the DC system.
- c. Thruster and gimbal mass characteristics can be predicted from Figure of Reference 16.



264.770-2

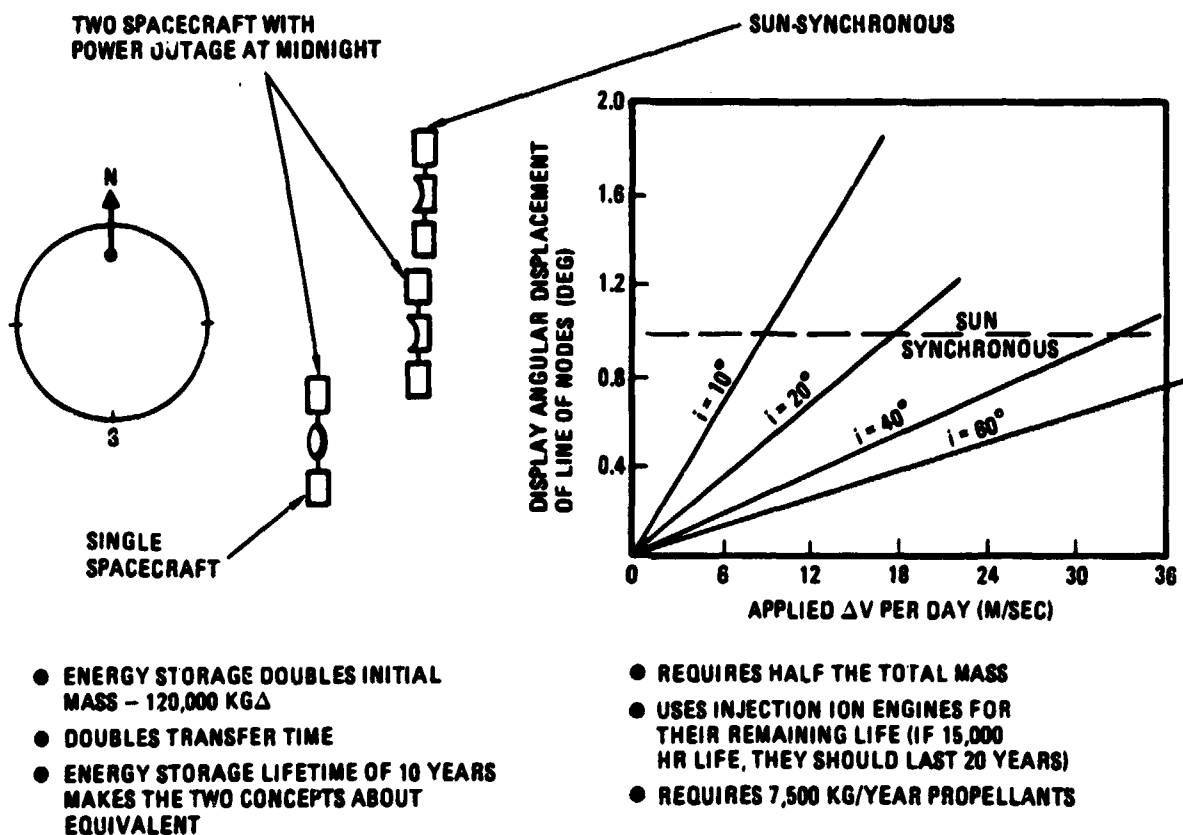
Figure 2-47. LEO Mission Concept Space Construction Facility.

Based on these projections and estimates, the propellant masses and transportation costs at \$1,000/kg shown in Table 2-7 were calculated, projecting ion engine system costs of \$13,500/kg for electrical systems (Reference 19) and hydrazine engine costs of \$12,000 per 6-pound thruster.

The conclusions reached from these updated calculations were that ion engine propulsion paid for itself in about 6 months and thereafter was less costly. Therefore, the power system structuring was accomplished using ion engine electrical propulsion requirements for both missions.

**2.2.6 GEOSYNCHRONOUS OPERATIONAL MODES.** Figure 2-48 shows the three possible geosynchronous operational modes. One mode is the normal mode used by geosynchronous satellites today. In this mode, the satellite rotates in the equatorial plane of the earth. A second possible mode is to drive the satellite with the ion engine systems so the satellite itself maintains sun synchronism. The effectiveness of this approach depends on the ultimate ISP of the ion engine system developed. For a system with an ISP of 3000, 15,000 kilograms per year of propellants would be required. However, if ISPs can be increased, perhaps this propellant usage would go down, and the sun-synchronous approach becomes more beneficial. Note that in this sun-synchronous mode, the satellite is actually inclined enough from the equatorial plane to avoid the shadow of the earth. The third operational mode involves simply the spaced apart placement of the two satellites, and the acceptance of the midnight power outage during the time interval when utilization on the earth has become significantly less.

**2.2.7 OPERATING OPTIONS - PLANAR SILICON ARRAYS.** There are several possible operating options that are reasonable alternatives to consider for the LEO and GEO spacecraft.



264.770-3

Figure 2-48. Three Geosynchronous Operational Modes are Feasible.

One of these involves the servicing of the spacecraft at approximately 4-year intervals to add modules to the photovoltaic arrays and to the energy storage systems to supplement degraded arrays/batteries. The advantage of this approach is that the cost of the supplemental hardware would be incurred later in the life cycle, and the higher cost of oversized hardware avoided. In addition, the added hardware would start its life cycle at peak efficiency, rather than in a degraded condition. Therefore, Planar silicon array costs were based on this approach.

Since the orbital injection degradation of the silicon arrays would require oversizing them by 50%, the operating option selected was to first inject a 10-MW radar with BOL LEO capability of about 20-MW, then, at 4-year intervals, maintain the array generation capability with orbital transfer vehicle supplied supplemental modules. No attempt was made to optimize this interval and its coverslide interaction. Later studies, with more accurate costing, could accomplish this analysis.

**2.2.8 POWER GENERATION SYNTHESIS AND EVALUATION.** The last subtask for Task II involved the analysis of the various component technologies for the three concept configurations (Planar Array, Large Trough, and Modular Trough).

**2.2.8.1 Planar Array Component Technologies.** The planar array baseline uses silicon solar cells combined with a kapton blanket stretched between truss members with a 15-meter spacing between members. The baseline array assumes that the 18% efficient cells at Air Mass One (AM1) described in recent laboratory news releases can be qualified and upgraded to be 16 to 17% efficient in space at IOC (36°C GEO and 60°C LEO) (see Silicon data sheet in Appendix A). The launch packaging of the baseline system appears to be accomplishable in a volumetrically efficient manner since the trusses would be fabricated from rolls and spools of material that have relatively high mass densities. For example, the estimated density for cap material is approximately 6.06 lb/in<sup>3</sup>, while the ideal shuttle density is 0.003 lb/in<sup>3</sup>. Likewise, the estimated density of rolls of solar blankets would be on the order of 0.03 lb/in<sup>3</sup>. The estimated number of flights to orbit planar arrays can then be based on the shuttle cargo payload bay mass capability. The 15 meter truss spacing of the planar array was established for two reasons; they are:

- a. Reasonable maximum for the width of a roll of solar cell blankets when packaged in the shuttle, compared to the 17-meter length of the cargo bay.
- b. Calculations of the g-level capability of a 150-meter truss when loaded with the solar blanket shows that the torsional cap buckling load capability of 600 lb was not exceeded. (The yield point is 900 lb, but a safety factor of 1.5 was used). To allow the 0.005g loads required when thicker and heavier solar cells are used, the cap thickness of the baseline space-fabricated beam was changed from 0.76 mm (0.030 in.) to 0.93 mm (0.036 in.) and truss height from 1.18M (3.87 ft) to 1.62m (5.31 ft). The beam mass per unit length increased from 0.87 kg/m<sup>2</sup> to 1.15 kg/m<sup>2</sup> for planar arrays. For concentrators with even heavier mass per unit area, a truss mass of 3.5 kg/m was used.

The study did not attempt to particularly optimize the thickness of the coverslides to be employed versus cost versus radiation degradation over time. The rationale was simply that these factors will depend on economic factors prevailing at the time of the decision, such as discounted rates of return, cost of money, and cost of the ion engines. Instead, a GEO baseline with 0.15mm coverslides was used for comparison purposes. This represents the transit time from LEO to GEO and was based on using the full 10-megawatt output capability of the array to drive the 104 ion engines, but only with a duty cycle of 10% of the orbital time, i.e., the trip time used by Byers, et.al., in Reference 17 was increased one order of magnitude, to calculate the proton radiation exposure that was then averaged, based on the data from Table 2-8 (Reference 20) to be  $2 \times 10^{16}$  equivalent 1 MEV electrons per year. This dosage results in the efficiency chain loss of about 58%, as shown in Figures 2-49 and 2-50. The reader is cautioned that this estimate may be somewhat pessimistic, later trajectory studies may decrease exposure time. It could also be optimistic, if ISPs 5000 seconds are not achieved. Nonetheless, such a severe degradation would make today's silicon technology less attractive. On the other hand, for the LEO mission, without this exposure, the silicon blankets are significantly more attractive.

**2.2.8.1.1 Cost of the Baseline Planar Array.** The cost of the baseline planar array was estimated using conservative factors. The intent was to consider the alternative approaches and evaluate them against a baseline whose cost attainability is not in question.

Today's space solar arrays typically cost \$300 to \$500 per watt. Costing studies of the arrays reveal these costs are split roughly 50-50 between the cost of the solar cells themselves and the cost of the cover slides, blanket, module assembly, and assembly and test. The solar cells, made of single crystal silicon, are currently becoming available terrestrially at \$8 to \$14 per watt. Even when the cost of space requirements (such as weldability, wraparound contacts and more stringent quality) are added, the cost should be \$20 to \$50 per watt for reasonable volume, therefore, an optimistic \$20 per watt will be used for the cell. This cost will be doubled to include the cost of cell assembly on the blanket. Total cost will be raised to \$40 per watt.

**2.2.8.1.2 Alternative Planar Array Configurations.** Several alternate planar array configurations were considered in addition to the baseline:

- a. Lower efficiency, low-cost silicon approaches
- b. Planar and CR=2 Gallium Arsenide configurations
- c. Encapsulated blanket approaches
- d. Honeycomb panel arrays
- e. Multibarred planar CR=2 arrays

Table 2-8. Annual Equivalent 1 MEV Electron Fluence for Voc and Pmax Due to Trapped Protons, Circular Orbits, Inclination 0 Degree, Infinite Backshielding Assumed from Reference 20.

EQUIV. 1 MEV ELECTRON FLUENCE FOR VOC AND Pmax - CIRCULAR ORBIT, IMC = 0 DEGREE.  
DUE TO GEOM/C TRAPPED PROTONS. REF. APS. AP6, AND AP7.

ALTITUDE		O.	SHIELD THICKNESS, GM/CM <sup>2</sup> (CM)		1.12E-01	1.60E-01	3.39E-01
(M.N.)	(KMI)		5.90E-03	6.71E-02			
		(2.34E-3)	(1.64E-3)	(1.32E-2)	(3.05E-2)	(1.50E+10)	(1.40E+10)
3.00E+02	5.56E+02	0.53E+11	6.69E+10	2.40E+10	1.91E+10	6.00E+12	5.37E+12
4.50E+02	8.34E+02	4.47E+14	4.00E+13	1.55E+13	9.91E+12	6.00E+12	5.37E+12
6.00E+02	1.11E+03	4.77E+15	4.29E+14	1.76E+14	1.01E+14	6.49E+13	4.70E+13
8.00E+02	1.40E+03	3.75E+16	3.32E+15	1.41E+15	7.34E+14	4.29E+14	2.93E+14
1.00E+03	1.69E+03	1.00E+17	1.17E+16	5.00E+15	2.40E+15	1.39E+15	8.03E+14
1.25E+03	2.32E+03	3.03E+17	3.47E+16	1.51E+16	6.62E+15	3.30E+15	2.00E+15
1.50E+03	2.70E+03	6.90E+17	8.20E+16	3.56E+16	1.30E+16	6.23E+15	3.54E+15
1.75E+03	3.24E+03	1.45E+18	1.82E+17	7.70E+16	2.04E+16	1.60E+16	5.72E+15
2.00E+03	3.71E+03	2.67E+18	3.22E+17	1.22E+17	4.49E+16	2.21E+16	8.40E+15
2.25E+03	4.17E+03	4.03E+18	4.72E+17	2.13E+17	6.23E+16	2.21E+16	1.03E+16
2.50E+03	4.63E+03	4.93E+18	6.32E+17	2.94E+17	8.90E+16	2.33E+16	1.06E+16
2.75E+03	5.10E+03	5.24E+18	8.12E+17	2.73E+17	7.04E+16	2.23E+16	9.01E+15
3.00E+03	5.56E+03	5.01E+18	1.04E+18	2.64E+17	6.91E+16	1.99E+16	6.23E+15
3.50E+03	6.49E+03	8.52E+18	1.59E+18	1.90E+17	4.93E+16	1.91E+16	6.06E+15
4.00E+03	7.41E+03	6.73E+19	2.74E+18	1.09E+17	2.87E+16	9.50E+15	4.30E+15
4.50E+03	8.34E+03	2.99E+20	4.10E+18	6.27E+16	1.56E+16	4.77E+15	2.09E+15
5.00E+03	9.26E+03	4.42E+20	5.21E+18	3.83E+16	7.43E+15	1.94E+15	7.34E+14
5.50E+03	1.02E+04	6.37E+20	2.99E+19	1.80E+16	3.40E+15	7.93E+14	2.77E+14
6.00E+03	1.11E+04	9.82E+20	1.97E+19	8.64E+15	1.60E+15	3.19E+14	1.04E+14
7.00E+03	1.30E+04	2.54E+21	1.10E+19	4.60E+15	2.44E+14	4.70E+13	1.47E+13
8.00E+03	1.48E+04	3.30E+21	4.60E+17	3.31E+14	4.31E+13	7.90E+12	2.31E+12
9.00E+03	1.67E+04	5.42E+21	1.52E+15	3.51E+13	4.52E+12	7.01E+11	2.13E+11
1.00E+04	1.85E+04	5.44E+21	4.13E+14	3.54E+12	4.32E+11	7.19E+10	1.90E+10
1.10E+04	2.04E+04	1.95E+22	1.79E+14	1.79E+12	5.62E+06	0.	0.
1.20E+04	2.22E+04	6.94E+22	1.79E+15	1.19E+12	5.05E+05	0.	0.
1.30E+04	2.41E+04	1.30E+24	1.57E+14	1.14E+10	0.	0.	0.
1.40E+04	2.59E+04	8.24E+24	1.64E+13	0.	0.	0.	0.
1.50E+04	2.78E+04	3.47E+25	9.58E+12	0.	0.	0.	0.
1.60E+04	2.96E+04	3.67E+25	4.50E+12	0.	0.	0.	0.
1.70E+04	3.15E+04	2.99E+25	9.59E+06	0.	0.	0.	0.
1.80E+04	3.34E+04	1.50E+25	7.55E+12	0.	0.	0.	0.

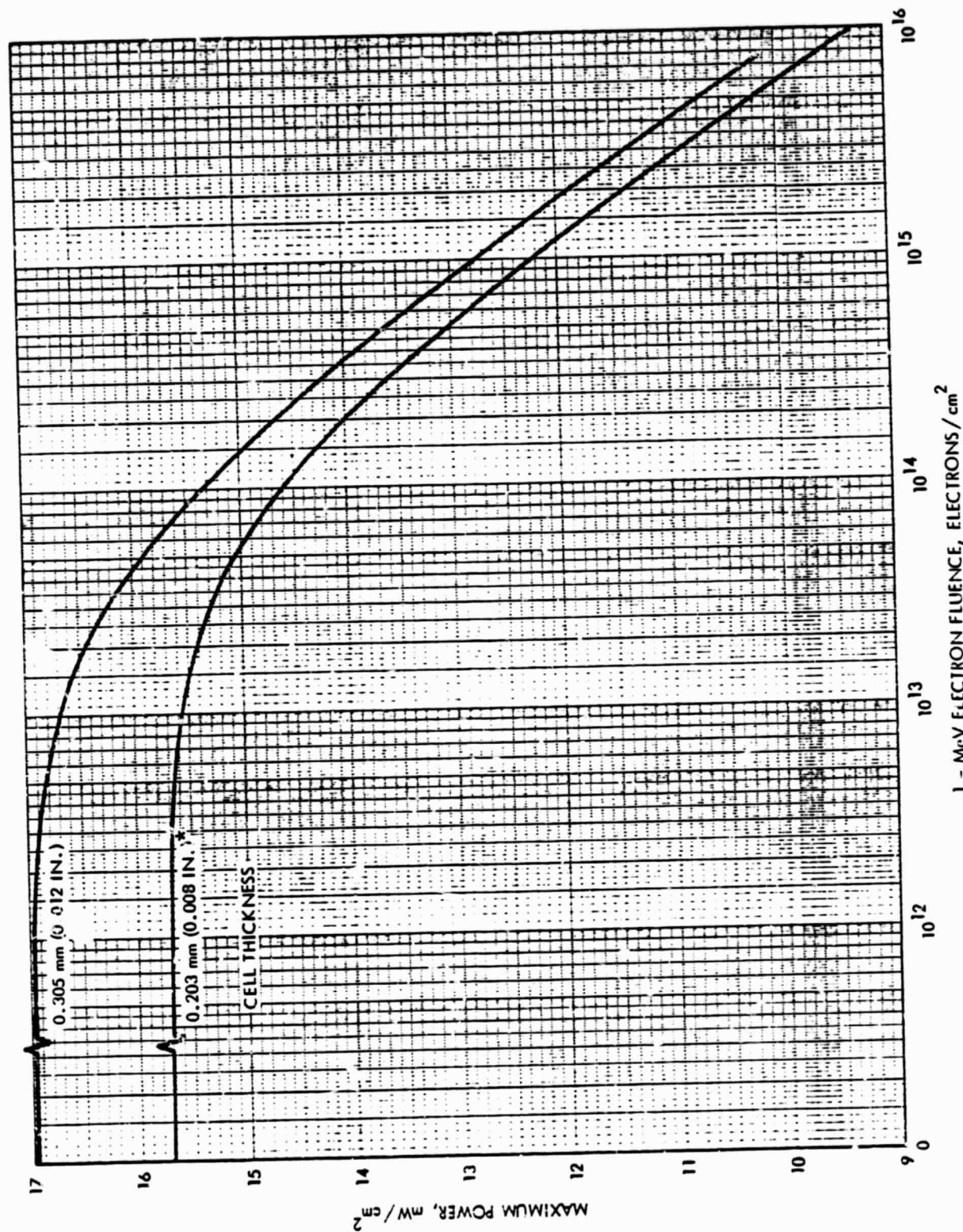


Figure 2-49. Maximum Power Versus 1 MeV Electron Fluence for 2 Ohm-cm n/p Textured Silicon Cells. At 135.3 MW/cm<sup>2</sup> AMO Illumination, 30°C from Reference 20.

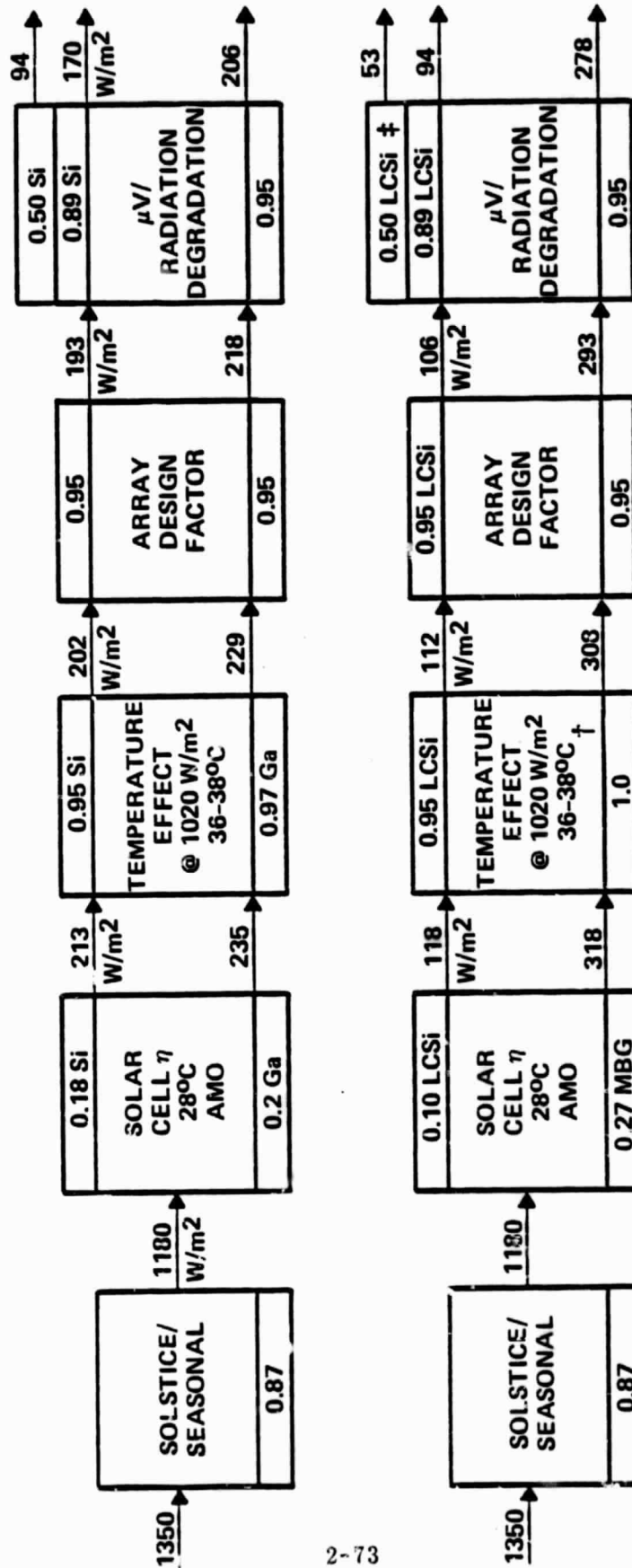


Figure 2-50. Efficiency Chains GEO Planar Array.

The alternatives were scoped to provide a selection of possible configurations from the baseline up to relatively higher risk options. Some are theoretical only (multi-bandgap cells for example) and have not been demonstrated yet in the laboratory.

**2.2.8.1.3 Advanced Silicon Technologies.** The DOE/JPL Low Cost Solar Array Program is developing silicon solar cell technology in several areas applicable to space usage. Ribbon cells, using EFG or dendritic wets promise lower cost. So do amorphous cells. These processes, as they will exist in 1990s, initially produce either single crystal, polycrystalline, or amorphous wafers. With laser techniques, the polycrystalline and amorphous wafers may be annealable into single crystal surfaces. Since the 1985, DOE goals specify initiatives across the entire scope of this activity. This study assumes that the technology and cost of silicon cells will, by 1990, be driven to the point where the manufacture of cells can be accomplished for \$0.5/watt, plus space requirements and standards, that would raise the price to \$5-\$20/watt.

**Transportation Costs for Advanced Silicon Cells.** The silicon technologies considered included alternatives that assumed that terrestrial laser annealing of cells will accomplish what will be alternatives in which the cells remain polycrystalline and amorphous. The baseline array area would be increased to accommodate the lower efficiency cells. Less obvious is the effect of radiation on the life of such systems and how they could be "space qualified."

For purposes of this study, the assumption is made that "space qualification" will introduce cost of \$35/watt for the cells, just as in the case of the baseline and that the baseline and that the savings in cell cost of \$15/watt are offset by extra transportation costs of \$5/watt and extra assembly and test costs of \$20/m<sup>2</sup> (the array is twice as large).

The conclusion is that the decreased efficiency that would require increased flights and increased assembly costs will always cost more totally than the cell cost savings. Note that this conclusion is only valid for lower efficiency cells. If laser annealed or largely single crystal ribbons can be fabricated, the distinction is lost, and these approaches should then be "spaced qualified".

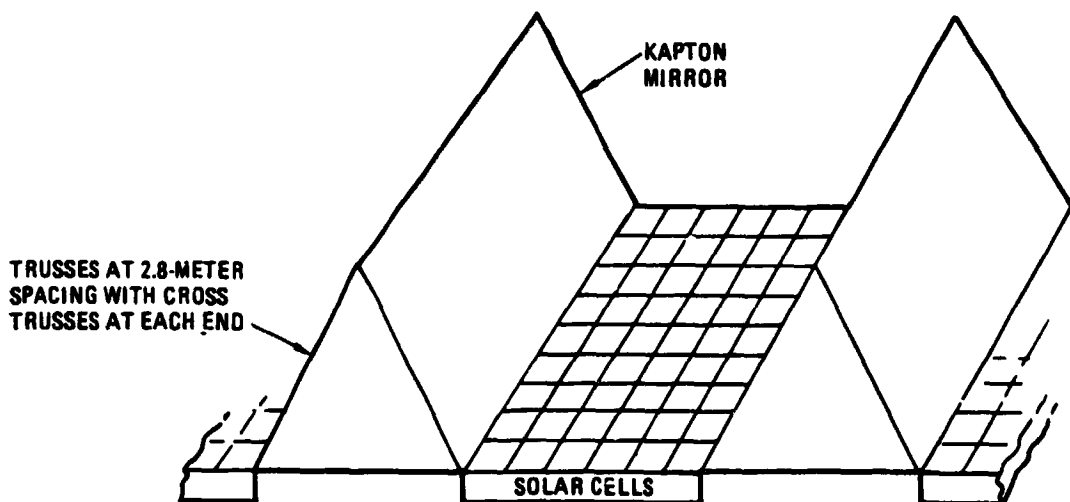
**2.2.8.1.4 Single Bandgap Gallium Arsenide.** By the 1990s, single bandgap GaAs cells with efficiencies of 16% (air mass zero, 125°C) could reduce the area requirements of the planar array blanket about 45%.

Since Gallium Arsenide density using 50- $\mu$ m cells adds 16% to the specific array mass, an extra 7% penalty is paid. This penalty is made up by the improved radiation performance of the Gallium Arsenide, which is assumed to be self annealing, or reannealable using heating circuits and, therefore, does not exhibit the approximately 6-7% loss caused by the 5-year radiation flux that degrades the silicon. (The 6-7% assumed silicon array supplements at 5-year intervals as discussed in the operating options section).

**Gallium Arsenide Planar Array Mass.** The Gallium Arsenide planar array mass has been estimated based on the same blanket and truss concept used for the silicon planar arrays. The cells themselves have a higher mass (129%) due to the  $5.3 \text{ gm/cm}^3$  density of Gallium Arsenide, however, the cover slides are thinner, because self annealing of the  $\text{GaAs}$  is assumed. The array design factor was also assumed to be 0.95; it accounts for intercell spacing for thermal expansion.

**2.2.8.1.5 Low Concentration Ratio Gallium Arsenide Concentrators.** A Gallium Arsenide concentration system with a concentration ratio of about two as proposed for one of the SPS prototype concepts is a viable planar type option. The mass of the system is slightly lower than the planar array mass, since the extra mass of trusses required to position the mylar mirrors is offset by the reduced blanket mass of one half of the number of solar cells. This discussion assumes that the geometry of the array is as shown in Figure 2-51. Array design factor was assumed to be 0.9; the additional 0.05 is caused by temperature mismatch power loss. Low radiation degradation is assumed (0.98), due to the self annealing characteristic of the Gallium Arsenide at  $125^\circ\text{C}$  or at a slightly higher temperature with electronic annealing.

The first order analysis of the area required for Gallium Arsenide arrays indicates blanket areas of 47,000 and 23,500  $\text{m}^2$  for CRs of 1 and 1.9 respectively. Because Gallium cost \$40/watt for 10 times the price of silicon, cells cost of \$20 to \$40/watt seems more reasonable for the 1-10 megawatt systems. This price accounts for the extra costs associated with space qualification and the yield loss. To keep the comparison with silicon consistent, \$4,000/ $\text{m}^2$  is used for blanket assembly and test cost.



264.770-4

Figure 2-51. CR=2 Geometry.

**2.2.8.1.6 Planar Multi-Bandgap Arrays.** Planar multi-bandgap arrays are configurable with the hypothetical multi-bandgap cells being investigated at Hughes Research, Varian, and several universities. Two alternates were considered; a variation of the baseline planar array and a low concentration (CR=2) linear trough similar to the SPS Gallium Arsenide alternate. The first order analysis of the configurations assumed that the planar array would operate at approximately 36°C in GEO and 60°C in LEO and the linear trough at approximately 125°C in both orbits. The cells were assumed to be stacked with a series  $V_{mp}$  at 28°C AM0 of 1.1 + 0.8 + 0.5 VDC. The temperature coefficient for the three series cells was included in the calculations provided by Varian Associates. (See Appendix C).

The radiation environment was assumed to cause insignificant degradation; circuitry being provided will self anneal briefly when the array has degraded 2 to 3%. Cover slide density was a low  $5.6 \times 10^{-3}$  gm/cm<sup>2</sup> ( $2.6 \times 10^{-3}$  gm/cm<sup>3</sup>).

With these assumptions, first order calculations for the GEO planar array would require 36,000 m<sup>2</sup> of area and have a mass of 61,200 kg. The cost of manufacturing multi-bandgap cells was assumed higher than silicon or Gallium Arsenide because of the many process steps – and insensitive to quantity reductions, which normally would occur because of increased yield. A value of \$100/watt will remain appropriate. Thus, cost benefits do not appear to be likely for this technology; the drivers and benefits will more likely come from the fact that gain in performance may benefit SEPS or FETS type missions if a lower thickness cell can eventually be made.

**2.2.9 LARGE PARABOLIC TROUGHS.** Task II evaluated large parabolic trough concentrators to see whether economies of scale could provide significant benefits. Figure 2-52 shows the configuration evaluated. Cross-members run the length of the trough to support aluminized Mylar which reflects incident insolation onto the solar cells which lie along the focal line of the trough. Radiators on both the far and near side radiate waste heat from the solar cells. The solar cells themselves were actively cooled using fluid cooling loops. The basic problem associated with the configuration turned out to be the mass of the radiators (refer to Subsection 2.2.12, Figure 2-64). Because of the requirements for micrometeoroid protection, they were large and relatively massive compared to concentrating and planar array approaches with smaller cell sizes apertures.

**2.2.9.1 Hybrid Approaches.** In an effort to try to establish whether reduced radiator size could be achieved, two configurations were evaluated that used the waste heat provided by the cooling system to drive Rankine turbine systems. Figure 2-53 is a graph of data provided by the Sunstrand Corporation for the upscaling of their "KIPS" Rankine Combined Rotating Unit Mass. This unit includes the Turbine, Generator, and Condenser. From the data asymptote, a specific mass of 7 kg/kW was obtained and used for the hybrid system calculations. The first hybrid provided solar cells on the primary target area as part

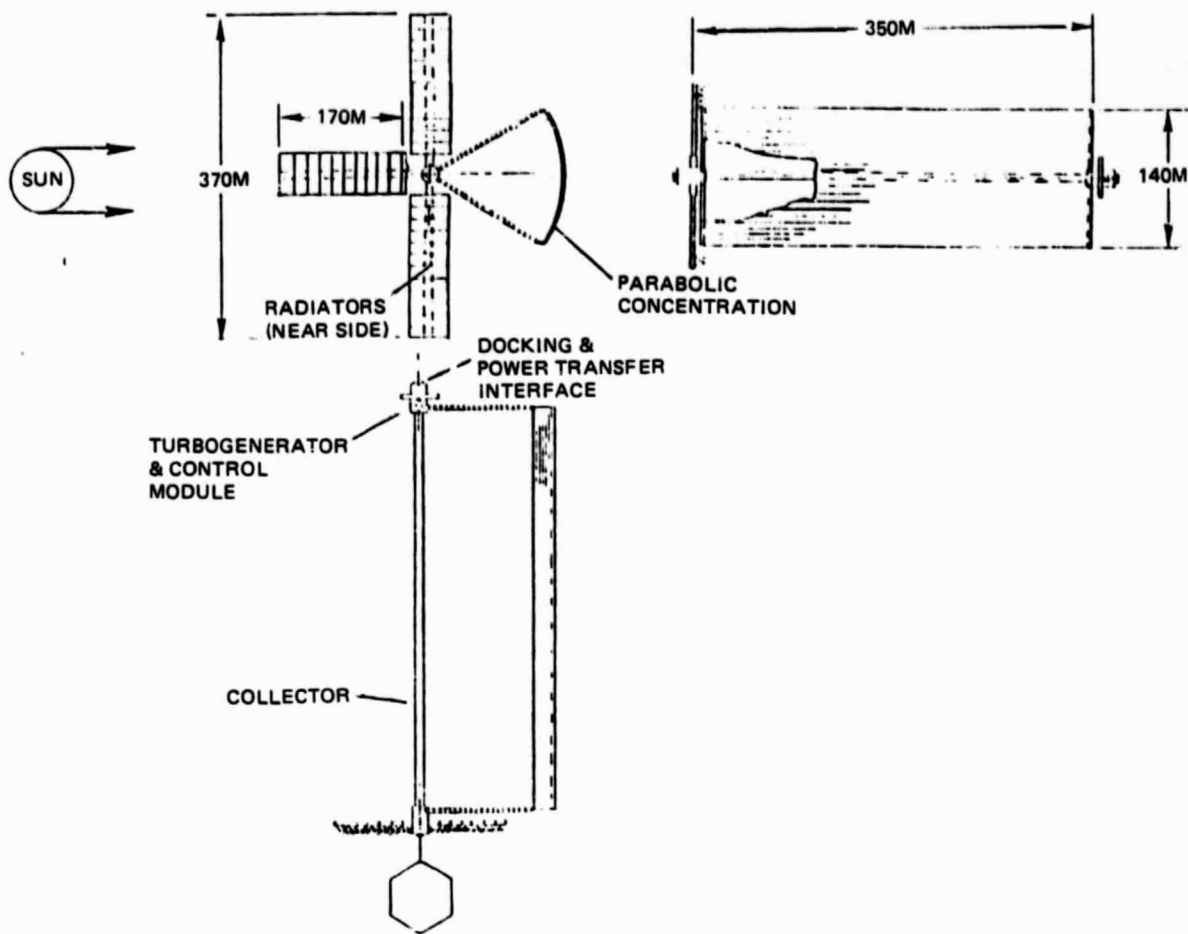


Figure 2-52. Parabolic Trough Collector.

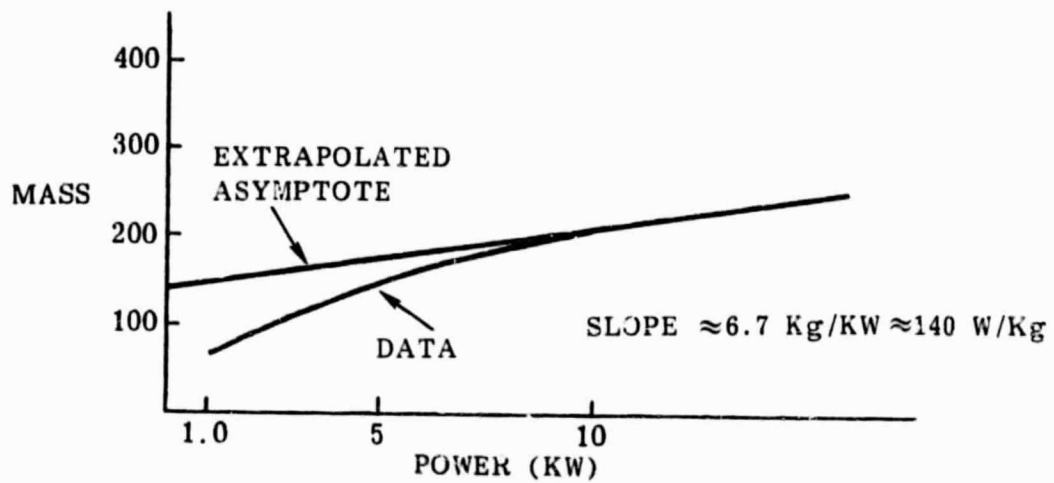


Figure 2-53. Mass Extrapolation — Rankine Cycle Turbine-Generator.

of the Mylar blanket. The solar cells themselves reflected waste heat because of blue-red filters on their front surface, and in this way the portion of the solar spectrum unused by the solar cells could provide heat to the turbine system (see Figure 2-54 and Table 2-9). This heat was collected along the focal line of the parabola. In the second configuration, the mirror itself remained aluminized Mylar (see Figures 2-55 and 2-56). Cells at the secondary focal line simply absorbed the entire spectrum, and an attempt was made to use the waste heat by driving a Rankine turbine. In both cases, the amount of radiator area required to radiate the waste heat, and its mass, offset the gains provided by the Rankine system turbine.

**2.2.9.2 Paraboloids of Revolution.** The fourth large-scale configuration considered utilized a paraboloid of revolution to focus energy in three dimensions on the focus of the mirror system. It is shown in Figure 2-57. The system uses the thermophotovoltaic approach developed by Stanford University. The energy illuminates a 2,100° Kelvin absorber that then reradiates energy at its black body temperature to a surrounding group of silicon solar cells. Because the energy of illumination peaks near the bandgap of the silicon cells, the system may have very high efficiencies, when it is compared with normal silicon cells up-radiated with the normal solar spectrum. Nonetheless, there is considerable waste heat required to be dissipated from the silicon cells during the operation of the system, and this makes for large massive radiators just as in the case of the parabolic trough concentrators. In addition, the 2,100° Kelvin illuminator has some concerns associated with its life. This is because the tungsten absorber element involved has a lifetime that has been estimated by various researchers at from 7-10 years (Reference 21). Another concern is whether the pointing angle error might cause destruction of the truss assembly holding the illuminator and cell assembly. The problem is that this significant amount of energy might actually cause the supports to melt. This is not true of other concentrating configurations considered, because the concentration ratio is not as high as the concentration ratio of about 2,000 required for the large thermophotovoltaic concentrator. Figure 2-58 shows the efficiency chain projected for the thermophotovoltaic concentrator. Notice that the specific power is relatively high, but that ultimate costs will probably be affected by the significantly higher risk.

**2.2.10 MODULAR TROUGH CONCENTRATORS.** The most effective approach developed during Tasks II and III was a small, low-light-loss parabolic louver concentrator. As defined during Task III, this approach used a series of parabolic louvers to reflect sunlight to a single-band, dual-band, or multi-bandgap cell configuration (Figure 2-59). The benefits of this concept over others considered were:

- a. The concentration ratio of between 30 and 100 permitted a reduction in total solar cell area and its attendant cost reduction, while at the same time enabling a cell operating temperature of between 90 and 100°C, with a reasonable specific power (250 W/kg) when constructed from mirror whose thickness is between 0.25 and 0.5 mm (10 to 20 mils).

PRIMARY BLANKET WITH SOLAR CELLS,  
REFLECTING TO SECONDARY ABSORBER

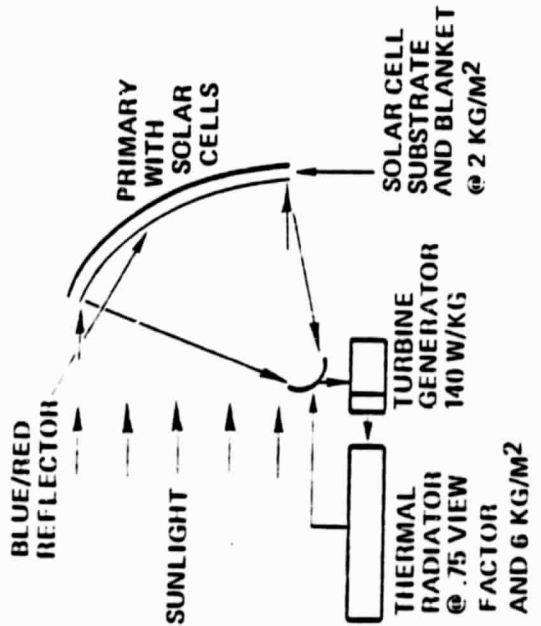
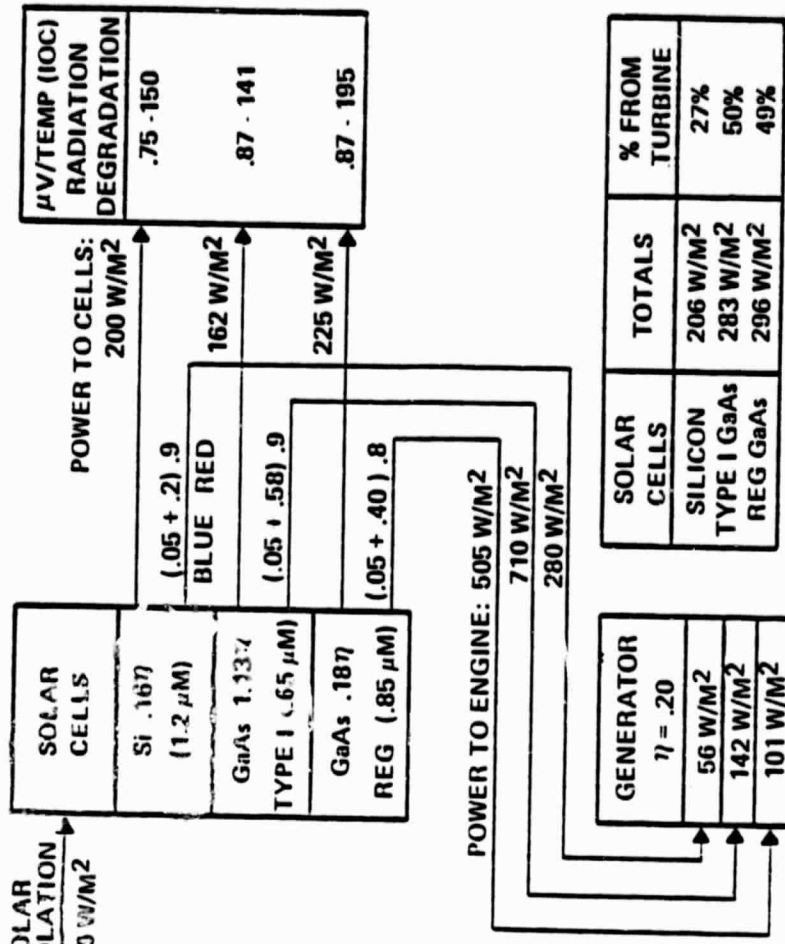


Figure 2-54. Hybrid Concentrator - Efficiency Chain.

Table 2-9. Mass Properties, Hybrid Concentrator.

HEAT ENGINE AT SECONDARY, CELL/RED  
SPECTRUM MIRRORS ON PRIMARY

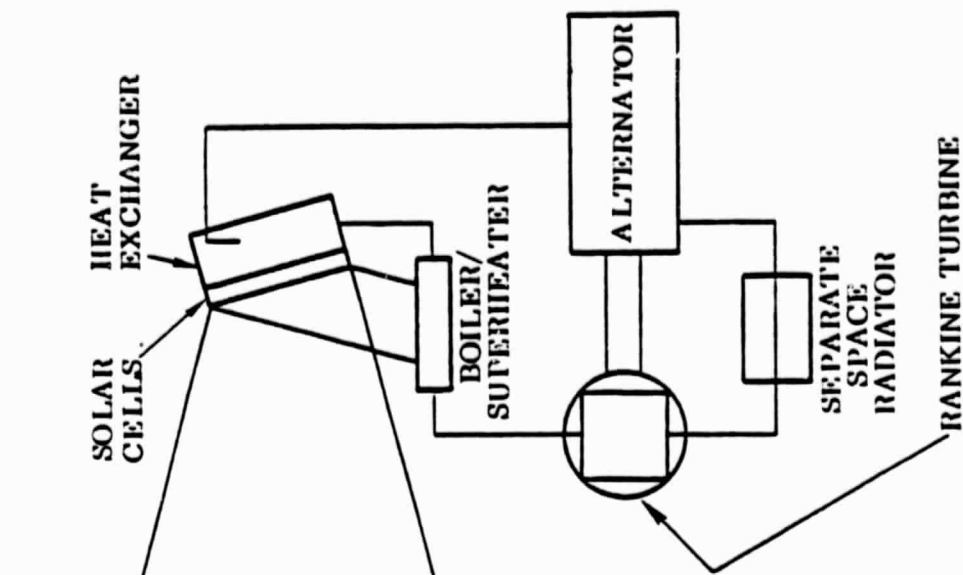
SOLAR CELL TYPE	POWER PER UNIT AREA (W/M <sup>2</sup> )	APERTURE AREA REQUIRED (M <sup>2</sup> )	RADIATOR AREA @ 850 W/M <sup>2</sup> * (M <sup>2</sup> )	REMAINING APERTURE FOR CELLS ONLY	RADIATOR MASS @ 5 Kg/M <sup>2</sup> ** (Kg)	APERTURE MASS @ 2 Kg/M <sup>2</sup> †	TURBINE MASS @ 7 Kg/KW Kg	TOTAL MASS Kg	SPECIFIC POWER W/Kg
2.5 MW									
SILICON	206	12,000	2,800	12,100	14,000	24,200	4,350	42,500	59
TYPE I GaAs	283	8,800	5,900	8,800	29,400	17,600	8,800	55,800	45
GaAs	296	8,500	4,000	8,500	20,000	17,000	5,900	42,900	59

LOW SPECIFIC POWERS COMPARED TO MULTIBAND SYSTEMS

\*A THERMODYNAMIC RADIATOR VIEW FACTOR OF .75 ASSUMED

\*\*RADIATOR/MIRROR AND/OR BLANKET

† FOR CELLS ONLY



WITH CELLS AT SECONDARY FOCUS

KAPTON SILVERED MIRROR

SOLAR CELL TYPE I	AREA & MASS OF MIRROR	RADIATOR AREA AND MASS	TOTAL MASS	SPECIFIC POWER
GaAs	8,400 M <sup>2</sup>	8,500 M <sup>2</sup>	50,900 KG	49 W/KG
	8,400 KG	42,500 KG		
GaAs .85	9,000 M <sup>2</sup>	9,300 M <sup>2</sup>	55,300 KG	44 W/KG
	9,000 KG	46,300 KG		
Si	10,000 M <sup>2</sup>	10,700 M <sup>2</sup>	63,500 KG	39 W/KG
	10,000 KG	53,500 KG		

FOR 2.5 MW SPACE CONSTRUCTION FACILITY - CONFIGURATION 2

Figure 2-55. Block Diagram and Mass Properties Hybrid Concentrator with Cells at Secondary Focus.

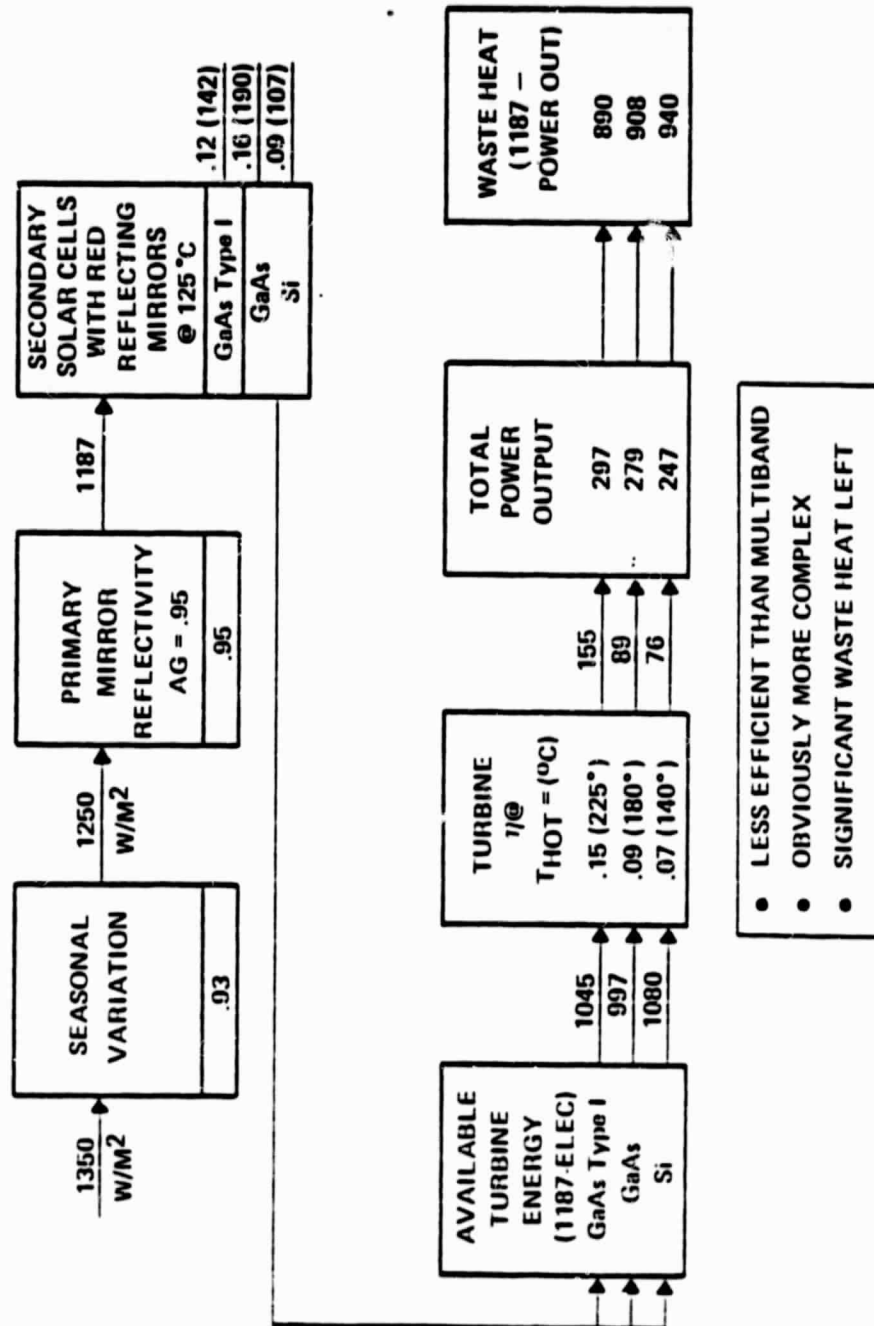


Figure 2-56. Efficiency Chain - Hybrid Concentrator with Cells at Secondary Focus.

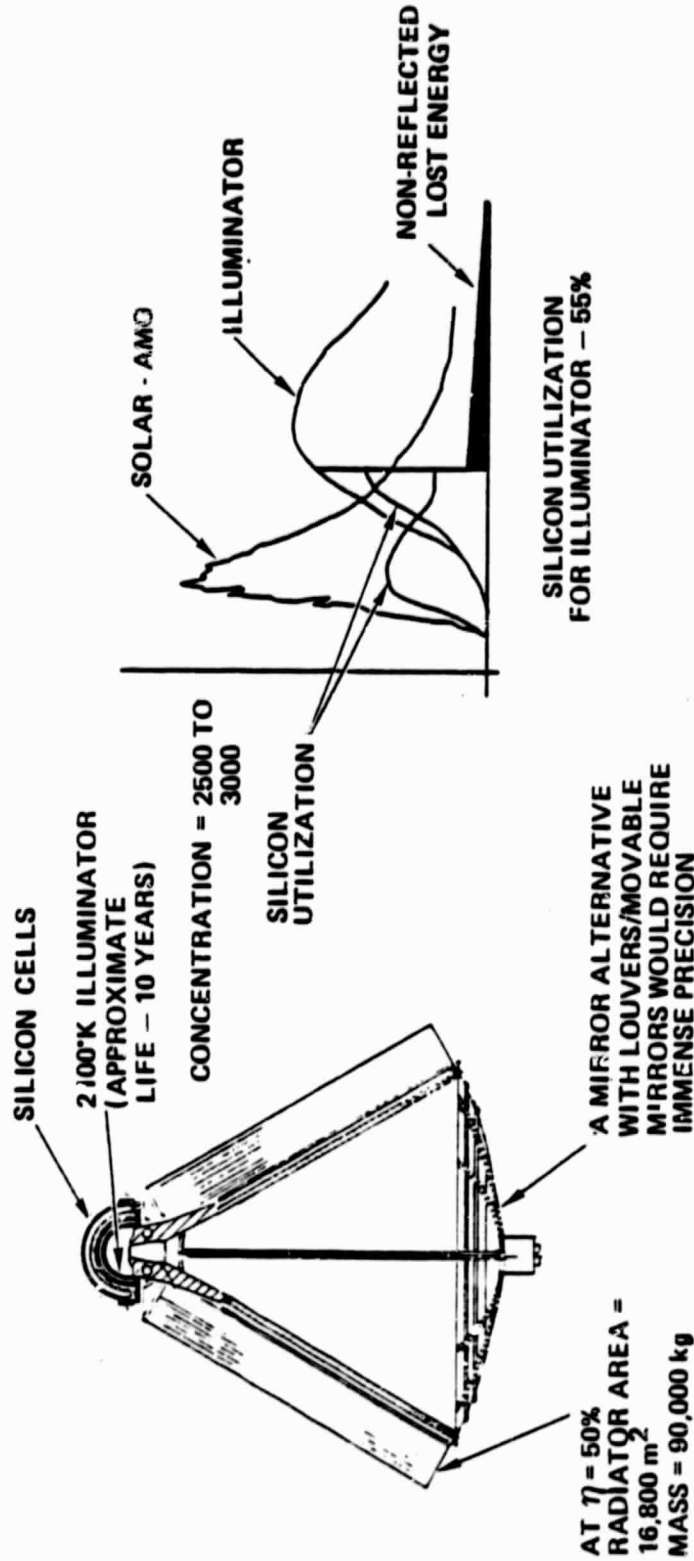


Figure 2-57. Advanced Goal (50% Efficient) Photovoltaic Array.

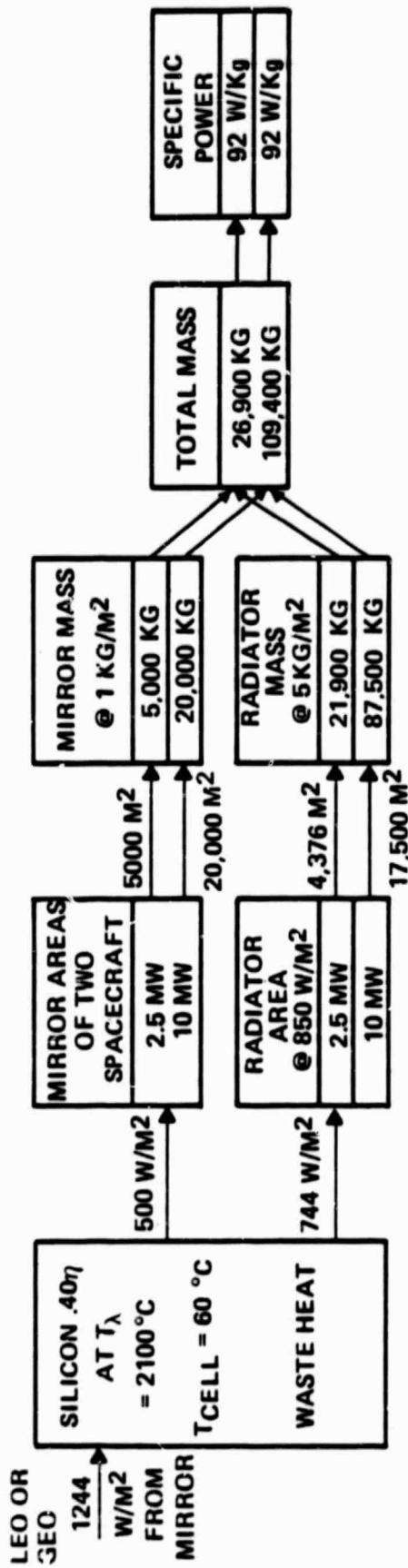


Figure 2-58. Thermophotovoltaic Efficiency Chain.

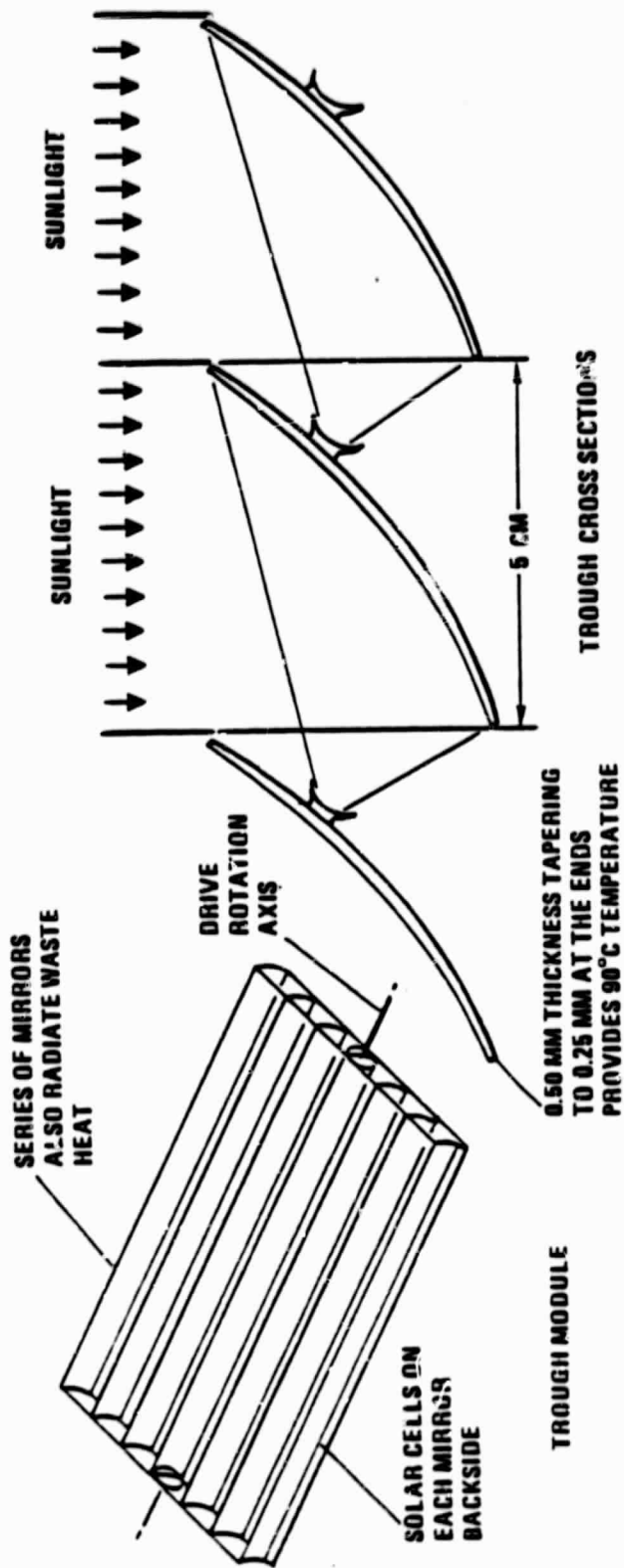


Figure 2-59. Small, Modular Trough Assembly.

- b. Geometrically, the system should show low aperture light loss. Since there are no Cassegrainian secondary reflectors, the aperture blockage and absorption losses in Cassegrainian designs are avoided. From a constructability viewpoint, the mirror radiator louvers are modularizable, can be assembled in space using a supporting truss structure, and are self supporting — less extra structure is required to hold them aligned.
- c. Inherent shielding from natural radiation. The 20-mil thick trough louver to which the solar cell substrate is attached, along with the substrate itself, should provide up to an average of between 0.75 and 1 mm (30 and 40 mils) shielding on the backside of each solar cell. The sides of the cells are shielded by the reflectors, which provide a minimum of 0.25 mm (10 mils) shielding. Coverslides could increase this front surface shielding.

The recommended mini-trough design has an additional benefit — one that involves how it is pointed to receive the solar insulations.

**2.2.10.1 Concentrator Pointing Strategies.** The geometrical design of a concentrating solar array must be compatible with the spacecraft orbital geometry and its overall relationship to the ecliptic plane and the direction of the sun. Since this geometry changes with the seasons, the approach to the overall design should be compatible with this seasonal change. Figure 2-60 shows the relationship of the sun to the earth during winter. For a spacecraft with a rotary solar array joint in GEO or LEO, three options are possible that could accommodate the geometrical variations, there are:

- a. Option 1 — A single rotary joint can be utilized, with its axis (the spacecraft pitch axis) oriented normal to the plane of the orbit. Then, as the spacecraft rotates, the array counter-rotation in the opposite direction just compensates for this, and the array remains facing the sun. Depending on the season, it will be from the direction of the sun by an angle of from 0 degrees (during the spring and autumn equinoxes) to up to 23.5 for GEO in July and December). In July and December, the tilt angle of 23.5 degrees causes the effective insolation incident upon the array plane to be decreased by  $\cos 23.5$  (8%). This loss is compensated for by the fact that problems associated with the other two strategies are avoided. The control and coordinate strategy of many three axis stabilized satellites launched today — specifically, FLTSATCOM, Intelsat V, RCA SATCOMS, Communication Technology Satellite, and European OTS, utilize this single rotary joint approach.
- b. Option 2 — The array can be designed with two gimbals and two rotary joints so that as the seasons change, the second compensates for the change in tilt angle. This strategy has obvious mass penalties, momentum interaction penalties, and reliability disadvantages (extra rotary joint).
- c. Option 3 — The spacecraft can be aligned so that its single rotary joint axis is aligned normal to the plane of the ecliptic.

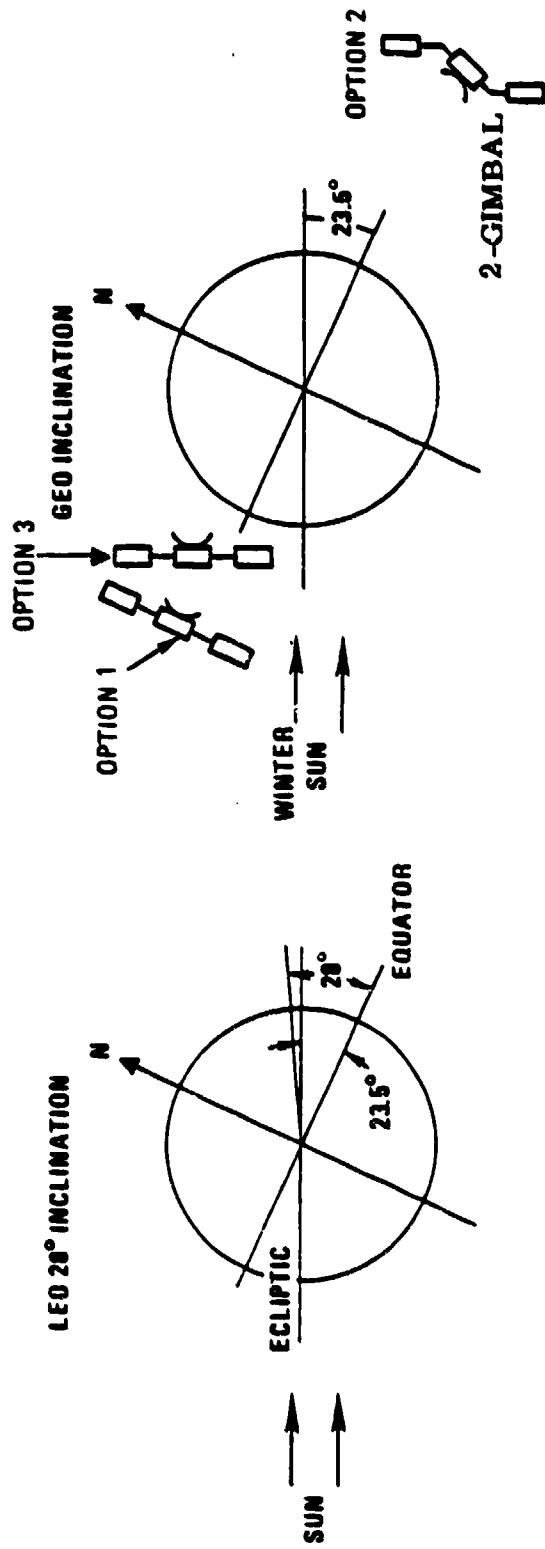


Figure 2-60. Orbital Geometry.

The penalties associated with this option are that one of the benefits of geosynchronous orbits is that the shifting antenna pointing over the orbit can be avoided. It is desirable to avoid extra antenna gimbals, and their momentum/angle interactions/rotary joints, etc. Further, this option requires that the total angular momentum vector must be adjusted so that it is normal to the plane of the orbit; therefore, extra momentum storage is required.

For LEO orbits inclined at 28 degrees, the same alternative strategies can be considered. Namely, they are:

- a. Two gimbals
- b. One gimbal, sun pointing
- c. One gimbal, earth pointing (see Figure 2-60)

The two gimbal systems have the same penalties at LEO that they have at GEO — extra mass and momentum interactions, which are desirable.

Of the single-gimbal systems, an earth-pointing spacecraft system has advantages, since gravity gradients remain constant, and, if the larger masses hang down from the array (toward the earth), the system is neutrally stabilized.

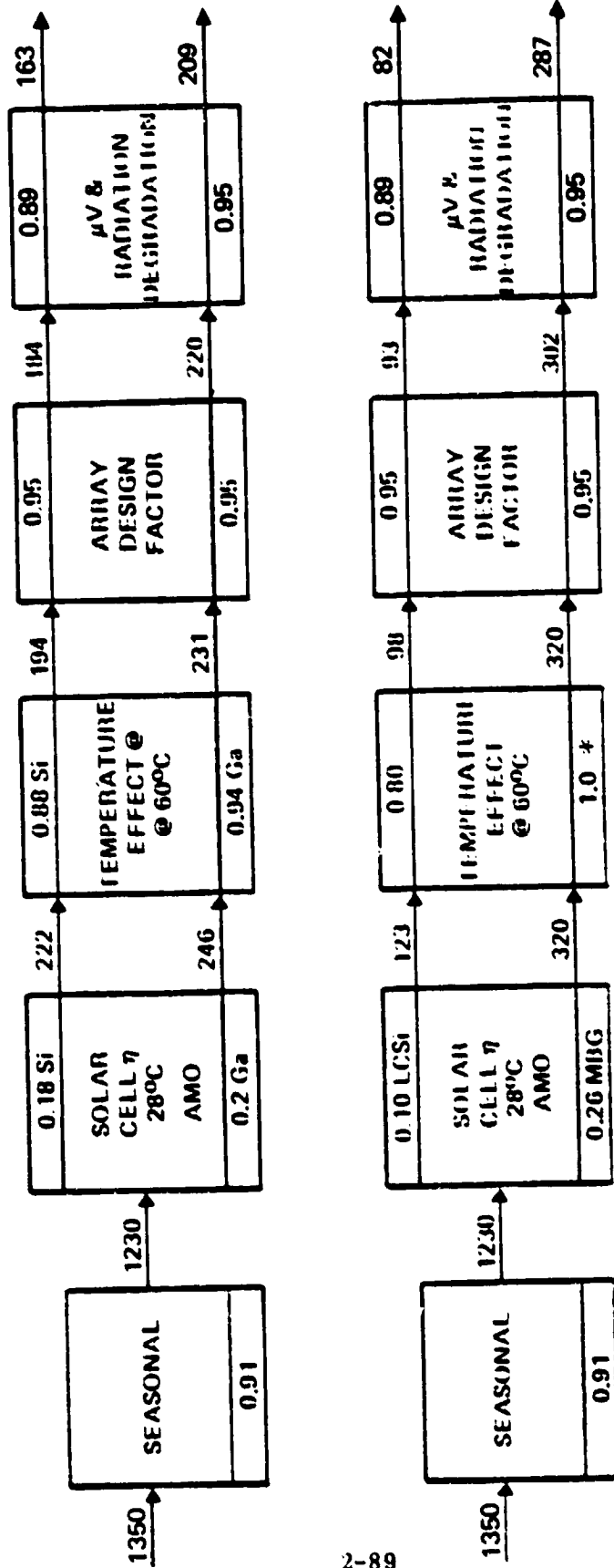
Since an infinite number of 28 degree inclinations are possible, the 28 degree inclination closest to the ecliptic should be considered first. This constrains the launch time but does not impact performance. It also suggests a 4.5 degree pointing angle (28-23.5 degrees) tolerance along the array axis is desirable.

Now, consider the mini-trough geometry. If the single rotary joint axis is aligned along the trough axis, as shown in Figure 2-59, and the axis of the rotary joint is aligned normal to the orbital plane, the rotary joint can keep the array properly pointed as the spacecraft orbits, even if the body of the spacecraft points toward the earth. The LEO  $\pm 4.5$ -degree pointing error and GEO  $\pm 23$ -degrees pointing error will cause the light to fall on different cells along the trough, with losses due to edge loss, defocusing, and non-normal (cosine) pointing. Since these should be less than 10%, the mini-trough accommodates these pointing errors with only one gimbal, without the extra mass of two gimbals and without constraining the spacecraft pointing. Both the GEO and LEO systems can work the same simple fashion utilized by today's single-gimbal axis spacecraft.

**2.2.11 EFFICIENCY CHAINS.** The efficiency chains shown in Figures 2-61 to 2-64 were developed to document the calculations for the preceding configurations.

They include seasonal variation caused by the cosine loss resulting from the orbital plane and by variation of insolation at aphelion, all efficiencies at the expected operating temperatures, and degradation and array design factors.

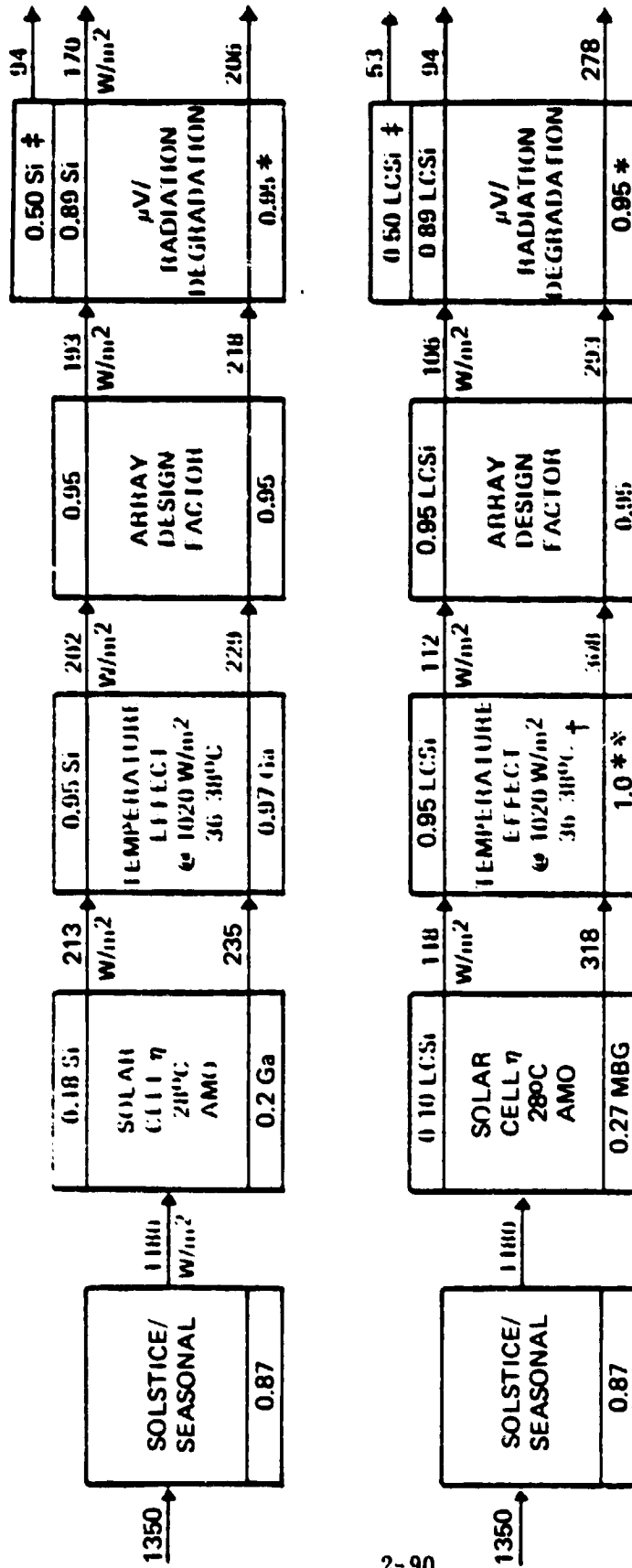
The chains indicate the expected result two-cell and multi-band configurations will out perform (have higher efficiencies) single-cell configurations, and calculations of truss, blanket heat radiator/mirror mass for the geometrics.



TOP - SILICON  
 TOP MIDDLE - GaAlAs  
 BOTTOM MIDDLE - "LOW COST" SILICON  
 BOTTOM - MULTIBANDGAP

Figure 2-61. Efficiency Chains - LEO Planar Array.

\* INCLUDED IN 0.26η



\* WITH ON ARRAY ANNEALING

\*\* INCLUDED IN 0.27 $\eta$

† BACK SURFACE REFLECTOR

‡ INCLUDES INJECTION DEGRADATION

Figure 2-62. Efficiency Chains - GEO Planar Array.

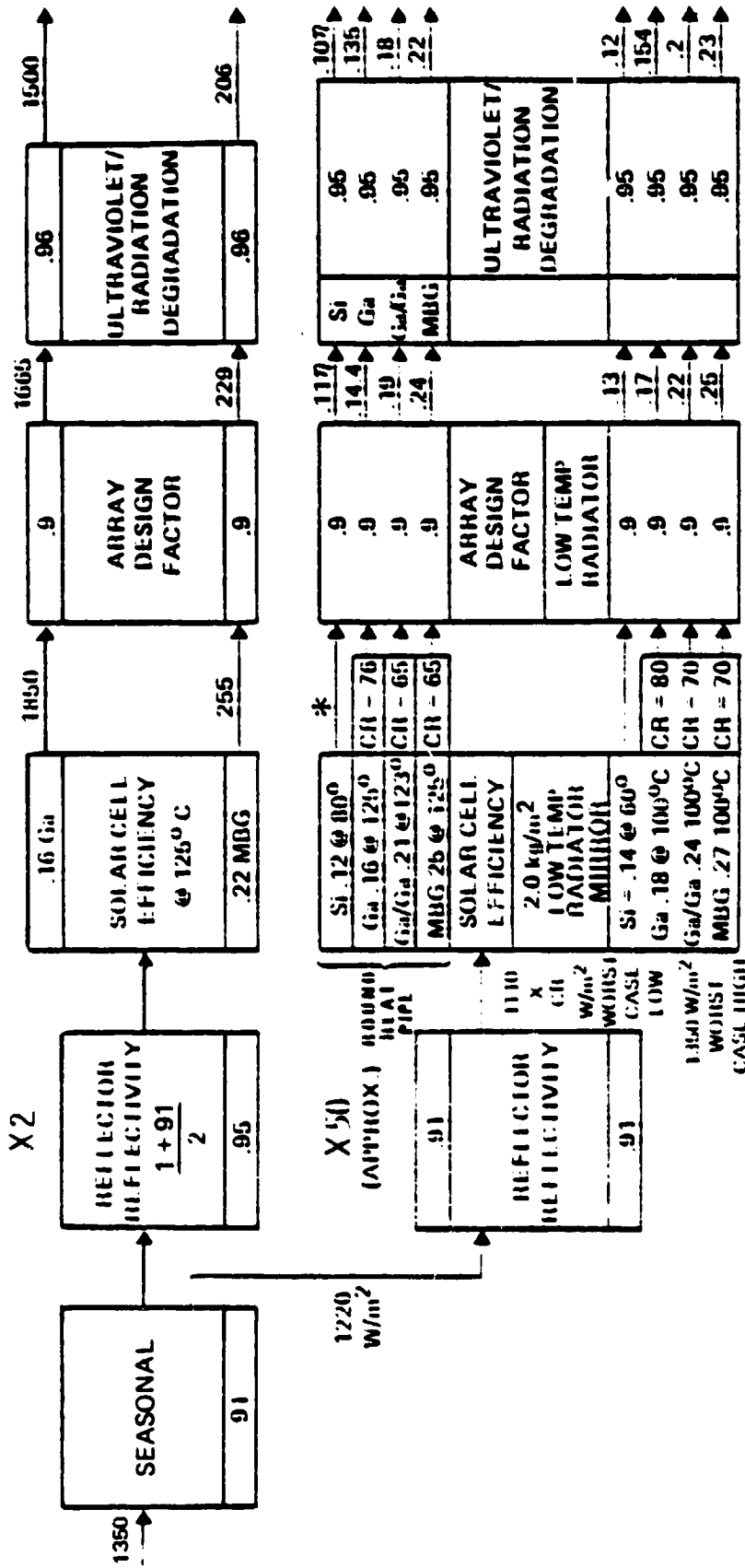
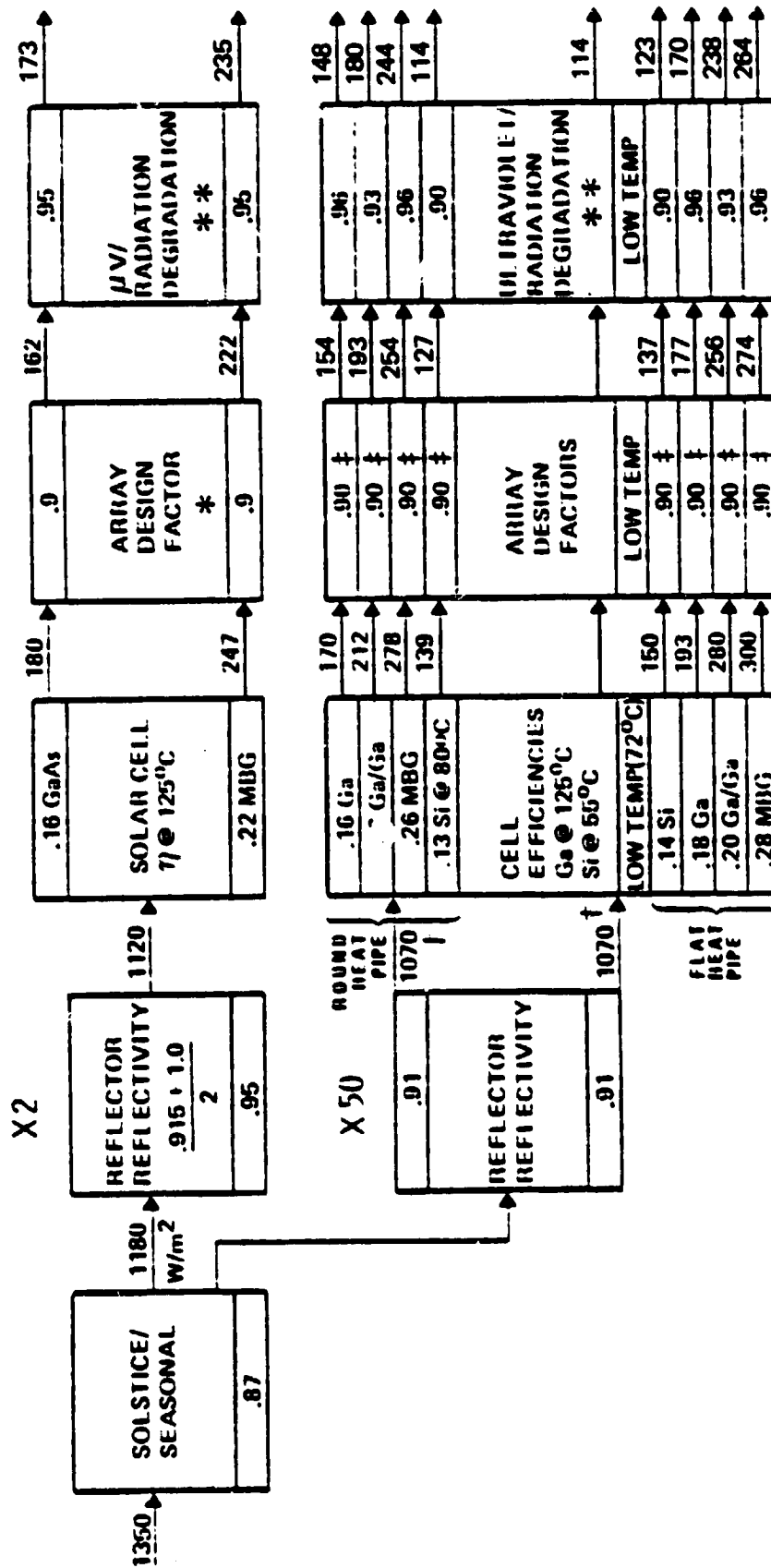


Figure 2-63. Efficiency Chain - LEO Concentrators.



\*\* MAY BE ACHIEVABLE  
 \*\* IN PLACE RE-ANNEALING  
 † DOES NOT INCLUDE CONCENTRATION  
 ‡ RATIO USED FOR APERTURE SIZING  
 † UNSUPPORTED ESTIMATES

Figure 2-64. Efficiency Chain - GEO Concentrators.

These charts indicate that the most attractive configurations for GEO radar are based on then Gallium Arsenide technology, followed by silicon planar arrays, followed by concentrators. Although concentrators were heavy for this Task II analysis, later modularity studies in Task III provided versions with almost the same mass as silicon for the GEO mission.

**2.2.12 MASS PROPERTIES.** Figures 2-65 to 2-68 show the results of geometrical analysis of the preceding configurations, and calculations of truss, blanket heat radiator/mirror mass for the geometrics.

**2.2.13 COSTS.** Figures 2-69 and 2-70 provide cost estimate data for the three power generation options. They show that the cost of concentrators is lowest. This is a significant driver when a new mission, such as the radar, is being developed. If cost can't be lowered then some of the benefits which the nations should be reaping from the space program will not be realized.

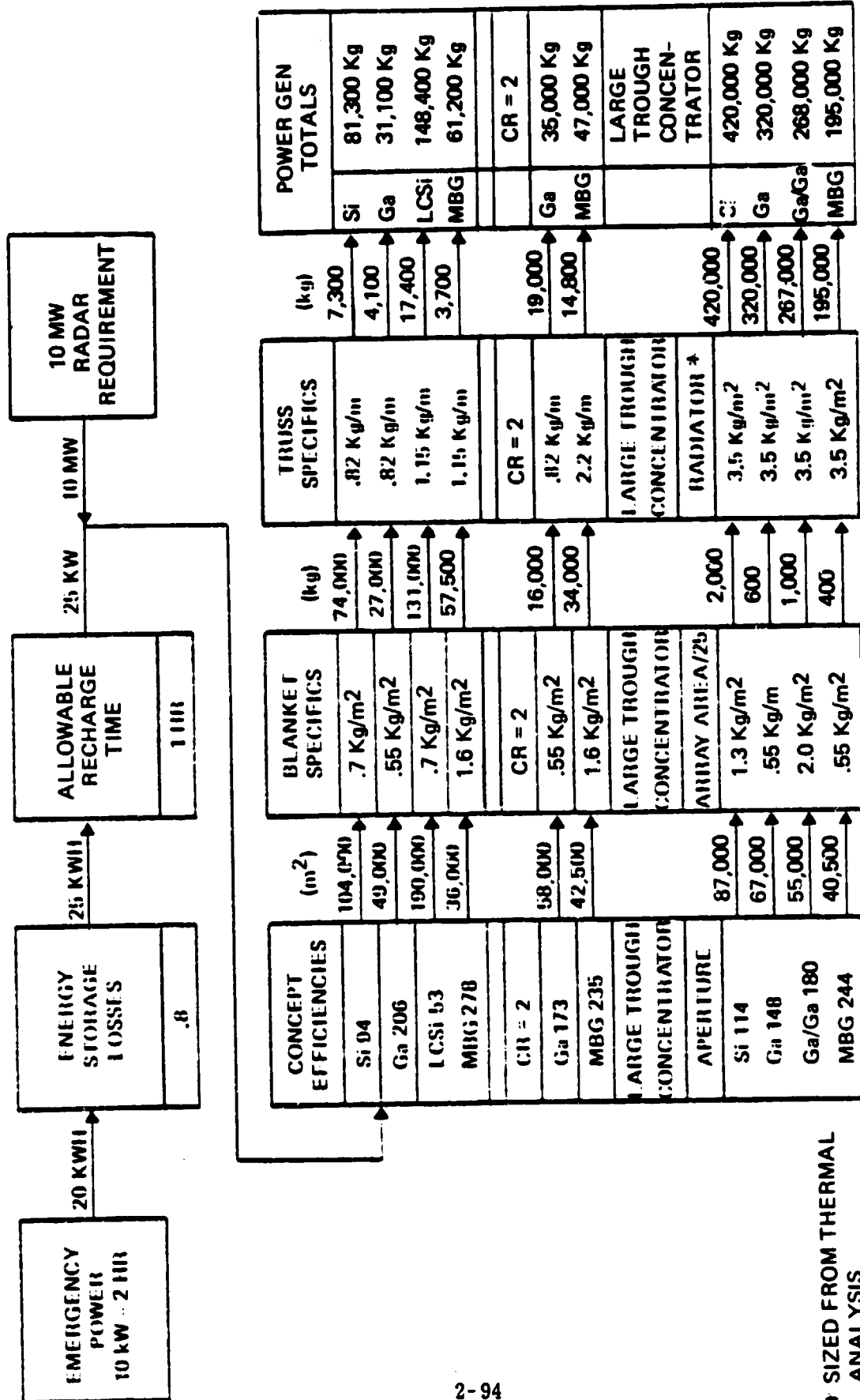
**2.2.14 ENERGY STORAGE.** Three types of energy storage components were considered as possible concepts for meeting the LEO SCF energy storage requirements - batteries, fuel cells, and flywheels (see Figure 2-71). Batteries with solid anode and cathode plate materials typically have limited cycle lives more suitable to higher orbits including GEO with fewer cycles, in LEO, they must be restocked at varying intervals. Fuel cells are less efficient, requiring more array area and larger radiators for waste heat rejection. Flywheels are efficient and very long life; however, their specific energy is limited because the energy stored cannot exceed the elastic limit of the material or catastrophic failure occurs. During Task II, the advantages of flywheels were significant enough to make them the initially recommended choice (Figure 2-72).

A review of this data, and consideration of the large penalties being paid for transportation to orbit, led to the decision to investigate other high energy density systems during tasks III & IV. They were:

- $Z_N BR_2$  systems
- LiMS systems - in particular Li FeS<sub>2</sub>
- Na S.

**2.2.15 10-MEGAWATT RADAR POWER SYSTEM SYNTHESIS.** The 10-megawatt radar system requires power conditioning for the ion engines which inject it into its GEO orbit and power conditioning on the radar array to convert the higher voltage power from the photovoltaic system to the voltages required by the radar module. Table 2-10 lists the components considered for use in the system. Two alternate component configurations were initially considered for the system. They were:

- a. An all DC system with power for the ion engine beam voltage and discharge currents provided by DC to DC regulators and radar power provided at the radar modules by a separate set of DC to DC converters.



\* SIZED FROM THERMAL ANALYSIS

Figure 2-65. 10-Megawatt Radar Sizing — Planar Arrays and Large Concentrators.

PLANAR ARRAY POWER REQUIRED	APERTURE	BLANKET SPECIFIC MASS	TRUSS MASS $L = 2\sqrt{AP/2}$	TOTAL MASS (kg)
Si 163 W/m <sup>2</sup>	15,300 m <sup>2</sup>	.5 kg/m <sup>2</sup>	7,700 kg	1,200 kg
Ga 209	11,950 m <sup>2</sup>	.7 kg/m <sup>2</sup>	8,400 kg	1,340 kg
LCSi 82	30,600 m <sup>2</sup>	1.2 kg/m <sup>2</sup>	36,600 kg	3,140 kg
MBG 287	8,700 m <sup>2</sup>	1.6 kg/m <sup>2</sup>	14,000 kg	1,060 kg
CR = 2		CR = 2		CR = 2
t = 125°C	15,500 m <sup>2</sup>	M = AP * X Spmv/2	5,400 kg	6,600 kg
Ga * 161 W/m <sup>2</sup>	11,300 m <sup>2</sup>	.7 kg/m <sup>2</sup>	8,400 kg	4,900 kg
MBG * 221 W/m <sup>2</sup>		1.6 kg/m <sup>2</sup>		

\* EQUIVALENT ONE SUN INSOLATION REQUIRED

Figure 2-66. LEO Planar Array Sizing & Mass.

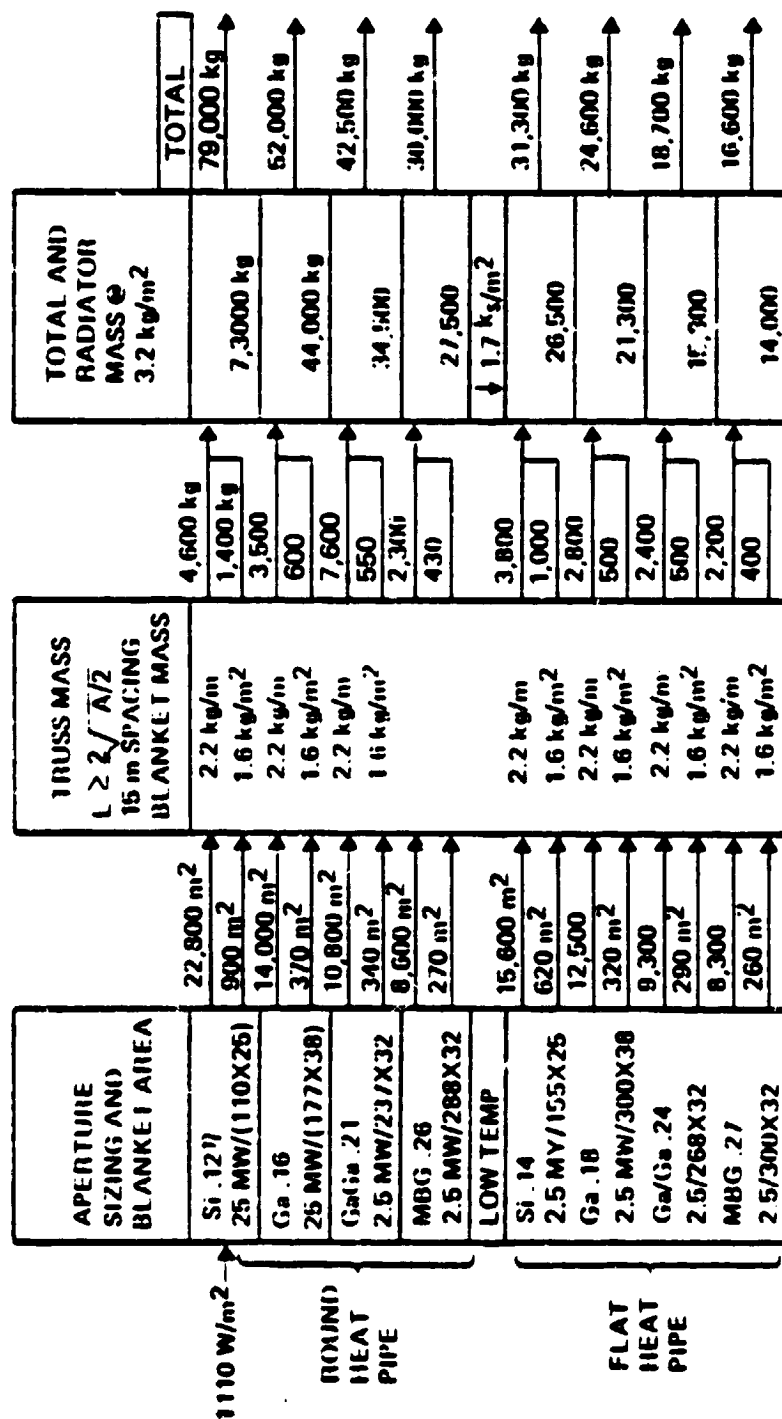
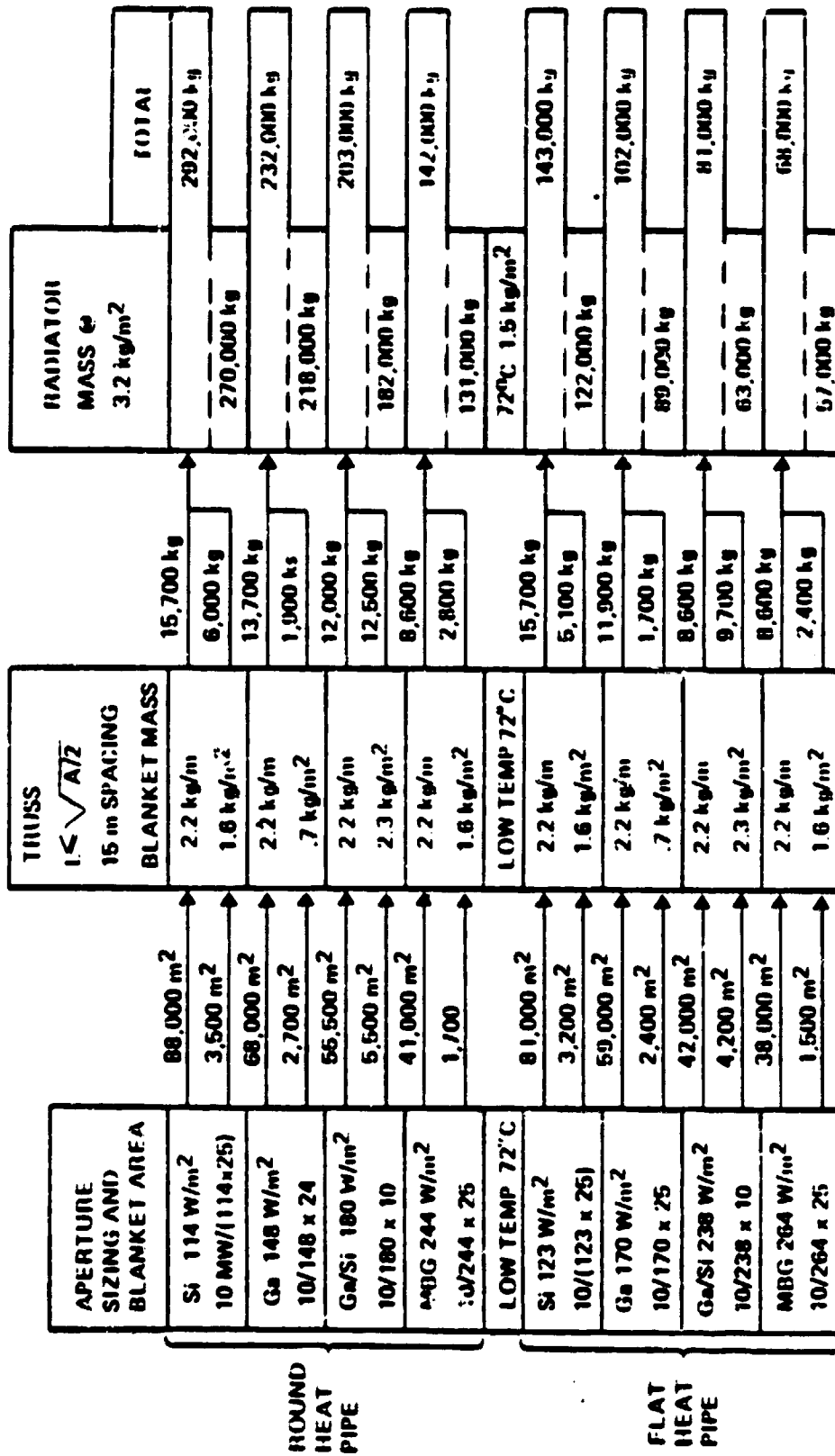


Figure 2-67. 2.5 Megawatt Sizing Modular Concentrator (CR=50).



MBG = MULTIBANDGAP

Figure 2-68. 10 Megawatt Sizing Modular Concentrator (CR=50).

	MASS OF POWER GENERATION SYSTEMS (kg)	AREA (m <sup>2</sup> )	COST (\$M)	COST TO ORBIT (\$M)	COST OF ROUTINE MAINTENANCE (RADIATION)	TOTAL
<u>PLANAR ARRAYS</u>						
GaAs	31,100	49,000	346	44	...	390
SILICON	81,300	104,000	515	125	\$30 M EVERY 5 YEARS	728
<u>MULTIBAND</u>						
	61,200	36,000	394	100		494
<u>LARGE TROUGH</u>						
	220,000	40,500	140	320		460
50% $\eta$	60,000-150,000	25,000	*			TBS
<u>SEMI-PARABOLIC TROUGH</u>						
	142,000	41,000	140	240		380
<u>ROUND HEAT PIPE MULTIBAND</u>						
2 BAND	203,000	55,500	170	320		490
<u>FLAT RADIATOR</u>						
2 BAND	91,000	42,000	160	120		280
MULTIBAND	68,000	38,000	140	100		240

3-SAFETY PROBLEMS,  
LIQUID COOLING

Figure 2-69. Comparison of Estimates for the Three Power Generation Options (10 MW Space Radar).

	MASS OF POWER GENERATION SYSTEMS (kg)	AREA (m <sup>2</sup> )	COST (\$M)	COST TO ORBIT (\$M)	COST OF ROUTINE MAINTENANCE	TOTAL COST (\$M)
<u>PLANAR ARRAYS</u>						
• SILICON	8,900	15,300	85	14	--	100
• GALLIUM AR ARSENIDE	9,700	11,950	85	15	--	100
• LC SILICON	39,790	30,600	140	60	--	200
• MBG	15,100	8,700	97	25	--	122
<u>LARGE CONCENTRATORS</u>						
LARGE TROUGH $\eta = 50\%$	55,000 25,000	10,000m <sup>2</sup> 5,000m <sup>2</sup>	35 30	85 40	?	120 70
<u>MODULAR CONCENTRATORS</u>						
BASELINE MBG	30,000	8,600m <sup>2</sup>	31	48	--	79
BASELINE 2 CELL, FLAT HEAT PIPE	42,500	10,800m <sup>2</sup>	60	64	--	124
MBG 2 CELL.	16,600 18,700	8,300m <sup>2</sup> 9,300m <sup>2</sup>	31 60	27 30	--	58 98

Figure 2-70. Cost Comparison - LEO Power Generation.

<u>TECHNOLOGY</u>	<u>CHARACTERISTICS</u>	<u>REMARKS</u>	<u>RISKS</u>
NICKEL-CADMIUM (ADVANCED)	20 W-hr/kg 100 kWh/m <sup>3</sup> 30,000 cycles @30% DOD	High confidence system with little room for improvement.	<b>LOW</b> Terrestrial impact of Cadmium.
NICKEL-HYDROGEN	30 W-hr/kg 50 kWh/m <sup>3</sup> 30,000 cycles @50% DOD	Superior to NiCd in some applications. Easy to control by pressure sensing.	<b>LOW</b> High pressure gas. Any puncture/tear causes immediate cell failure.
FUEL CELLS (W/ELECTROLYZER)	60 W-hr/kg 50 kWh/m <sup>3</sup> 60,000 hour life	Separate charge/discharge subsystems may be an advantage as may be alternative use of water, H <sub>2</sub> gas, and O <sub>2</sub> gas.	<b>MEDIUM</b> Low cost cells may not be able to retain high reliability, efficiency lifetime.
SILVER-ZINC	50 W-hr/kg 200 kWh/m <sup>3</sup> 500 cycles @40% DOD	Good charge retention, weight vs. poor cycle life. Calendar life < 2 years.	<b>LOW</b>
LITHIUM ADVANCED (LOW TEMP)	150 W-hr/kg 300 kWh/m <sup>3</sup> 300 cycles @75% DOD	Early stages of development. Improvements may be forthcoming.	<b>HIGH</b> Explosion is a consideration in L <sub>1</sub> batteries.
FLYWHEELS	40 W-hr/kg @2:1 speed red. Potentially unlimited cycle life.	Long life and alternate functions: CMG, AC-DC conversion.	<b>HIGH</b> Motor/Gen runaway and rotor failure.

Figure 2-71. Six Energy Storage Technologies were Considered.

## 1 MW CONSTRUCTION FACILITY

	MASS OF STORAGE BATTERIES (kg)	INITIAL COMPONENT COST (\$M)	TRANSPORT COST TO ORBIT (\$M)	O&M COST (REPLACEMENT) (\$M)	TOTAL COST FOR 20-YR LIFE (\$M)
NICKEL CADMIUM	35,000	3.5	42	140 (5-YR LIFE)	185
NiO FUEL HYDROGEN	23,000	1.4	27	60 (7-YR LIFE)	90
SILVER HYDROGEN	11,500	5.3	14	400 (1-YR LIFE)	420
H <sub>2</sub> O <sub>2</sub> FUEL CELL	19,200	4.8	23	45 (7-YR LIFE)	75
FLA WIFFI	15,400	3	18.5	5 (FULL LIFE)	25

Figure 2-72. Task II Comparison of Estimates for Alternative Storage Options.

Table 2-10. Power Management Major Components Considered

<u>COMPONENTS</u>	<u>CHARACTERISTICS</u>	<u>REMARKS</u>	<u>RISK</u>
ON ARRAY CONDITIONING	<ul style="list-style-type: none"> <li>SOLID-STATE SWITCHING</li> <li>VOLTAGE &amp; FREQUENCY CONTROL</li> <li>AC OR DC DIRECT OUTPUTS</li> </ul>	<ul style="list-style-type: none"> <li>ELIMINATES NEED FOR CONVERSION EQUIPMENT</li> <li>ELIMINATES NEED FOR VOLTAGE REGULATION EQUIPMENT</li> <li>CONTROLS COLLECTOR ECLIPSE TRANSIENTS</li> </ul>	MED MED
POWER BUS SWITCHING	<ul style="list-style-type: none"> <li>SOLID-STATE, 50-100 AMP</li> <li>NOMINAL VOLTAGE DROP OF 1.2V</li> <li>SPURIOUS TURN-ON PROTECTION</li> <li>FORCED TURN-OFF CIRCUITRY</li> </ul>	<ul style="list-style-type: none"> <li>REDUNDANT SWITCHES PER INTERCONNECT</li> <li>GREAT TECHNOLOGY POTENTIAL FOR DECREASING SWITCHING LOSSES</li> </ul>	MED
ROTARY TRANSFORMER	<ul style="list-style-type: none"> <li>HIGH AC FREQUENCY ( 20 KHZ)</li> <li>SINGLE PHASE</li> <li>EFFICIENT TRANSFER OF AC POWER ACROSS PIVOTING AXIS VS SOLID-STATE CONVERTER</li> </ul>	<ul style="list-style-type: none"> <li>MODULAR EXPANSION OF SYSTEM POWER CAPACITY ON SAME PIVOT AXIS</li> </ul>	MED
OPTICAL SLIP RINGS	<ul style="list-style-type: none"> <li>TRANSFERS CONTROL AND DATA SIGNALS</li> </ul>	<ul style="list-style-type: none"> <li>ASSEMBLY FITS ON SAME PIVOT AXIS AS ROTATING TRANSFORMERS</li> </ul>	LOW
POWER DISTRIBUTION NETWORK	<ul style="list-style-type: none"> <li>SOLID-STATE, HIGH-POWER SWITCHING</li> <li>SPURIOUS TURN-ON PROTECTION</li> <li>FORCED TURN-OFF CIRCUITRY</li> </ul>	<ul style="list-style-type: none"> <li>HIGH RELIABILITY REDUNDANT SWITCHING</li> <li>REDUNDANT BUSES</li> </ul>	LOW
POWER DISTRIBUTION BUSES	<ul style="list-style-type: none"> <li>MULTIPLE BUSES TO ALL PORTS</li> <li>TUBULAR BUS CONSTRUCTION</li> <li>HIGH VOLTAGE, HIGH FREQUENCY AC</li> </ul>	<ul style="list-style-type: none"> <li>REDUNDANT BUSES INCREASES RELIABILITY</li> <li>TUBULAR BUS INCREASES HEAT DISTRIBUTION &amp; PROVIDES STRUCTURAL STRENGTH AT NO COST IN WEIGHT</li> </ul>	LOW

Table 2-10. Power Management Major Components Considered (Continued)

<u>COMPONENT</u>	<u>CHARACTERISTICS</u>	<u>REMARKS</u>	<u>RISK</u>
BATTERY CHARGER	<ul style="list-style-type: none"> <li>SOLID STATE VOLTAGE SENSE &amp; SWITCHING</li> </ul>	<ul style="list-style-type: none"> <li>REDUNDANT SWITCHING SYSTEM</li> </ul>	LOW
AC/DC CONVERTER	<ul style="list-style-type: none"> <li>MULTIPLE HIGH FREQUENCY</li> </ul>	<ul style="list-style-type: none"> <li>HIGH FREQUENCY SIMPLIFIES FILTERING</li> <li>HIGH-RELIABILITY REDUNDANT SYSTEM</li> </ul>	LOW
DC/AC CONVERTER	<ul style="list-style-type: none"> <li>RESONANT SOLID STATE CONVERTERS</li> </ul>	<ul style="list-style-type: none"> <li>NO ADDITIONAL AC REGULATION REQUIRED</li> <li>HIGH-RELIABILITY REDUNDANT SYSTEM</li> </ul>	MED
AC/DC CYCLOINVERTER	<ul style="list-style-type: none"> <li>PROVIDES LOW FREQUENCY AC OUTPUTS FOR PAYLOADS</li> <li>SINGLE PHASE OR THREE-PHASE OUTPUTS</li> </ul>	<ul style="list-style-type: none"> <li>CAN PROVIDE AC FOR TERRESTRIAL TYPE USER EQUIPMENT</li> </ul>	MED
ADAPTIVE CONTROLLER	<ul style="list-style-type: none"> <li>AUTOMATIC CONTINGENCY ACTION</li> <li>AUTOMATIC PRIORITY PLANNING</li> <li>EMERGENCY COMMAND PRIORITY OVER-RIDE</li> <li>REDUNDANT VOTING PROCESSORS</li> <li>LOAD DISTRIBUTION PLANNING</li> </ul>	<ul style="list-style-type: none"> <li>SYSTEM EXPANSION PROGRAMMABLE</li> <li>PROGRAMMABLE TO SUPPORT OTHER PROCESSING FUNCTIONS DURING FAILURES IN ATTITUDES OR ENVIRONMENTAL CONTROL SYSTEMS</li> </ul>	MED

- b. A split inverter AC system with one set of DC/AC drivers that delivered AC to receivers at the radar low voltage system and with on array regulators for the ion engines.

In a split AC system, described in Reference 22, the entire power system is designed as a single, distributed resonant converter. A multimodule unidirectional, four-quadrant converter driving a resonant circuit, including the source and load transformers and power transmission buses, converts DC into high frequency AC (like the usual front half of any resonant DC-DC converter). Unidirectional, four-quadrant converter modules are transformer-coupled to the transmission system at the load end to provide the loads with either DC or any frequency and format AC, depending on their individual requirements. (This end is equivalent to the load-end half of a DC-DC converter.) A typical multiple-driver, multiple-receiver system is shown in Figure 2-73.

Notice that the rotary transformer not only provides frictionless power transfer across the array rotary joint but also serves as the load inductance of the AC resonant converter. Rotary transformer efficiencies of 0.98 were projected, although data was sparse. For example, air gap losses for alternators are only briefly mentioned in standard textbooks. Apparently they were ignored quantitatively because they were not significant compared to other losses.

Review of these configurations revealed several alternate topologies which would be considered as a part of modularization activities during the next study phase. They were:

- a. Consideration of the topology of Figure 2-74 for the AC system. In this topology, a single set of AC drivers drives both the ion engine regulators and the radar power supply modules for the 10-megawatt radar. Advantages appeared to be lower mass for the ion engine power conditioning portion of the circuitry.
- b. Consideration of wing topology modularity levels compatible with on-array electrical annealing of solar cells and with lowest possible mass and cost.
- c. Consideration of alternate array and transmission voltage levels. Higher array voltages (900V) will minimize transmission losses and may permit increased ion engine specific impulse, thus reducing propellant mass; but they are also less safe, susceptible to arcing, and, for the DC system, they increase LEO plasma losses. Of these issues, lethality is certainly one to be considered carefully; it is also difficult to evaluate. For this study, it was decided to consider both higher and lower distribution/array voltages, and estimate the increased mass cost of lower voltage approaches, along with the higher voltage alternate topologies. This task was accomplished in Task III.

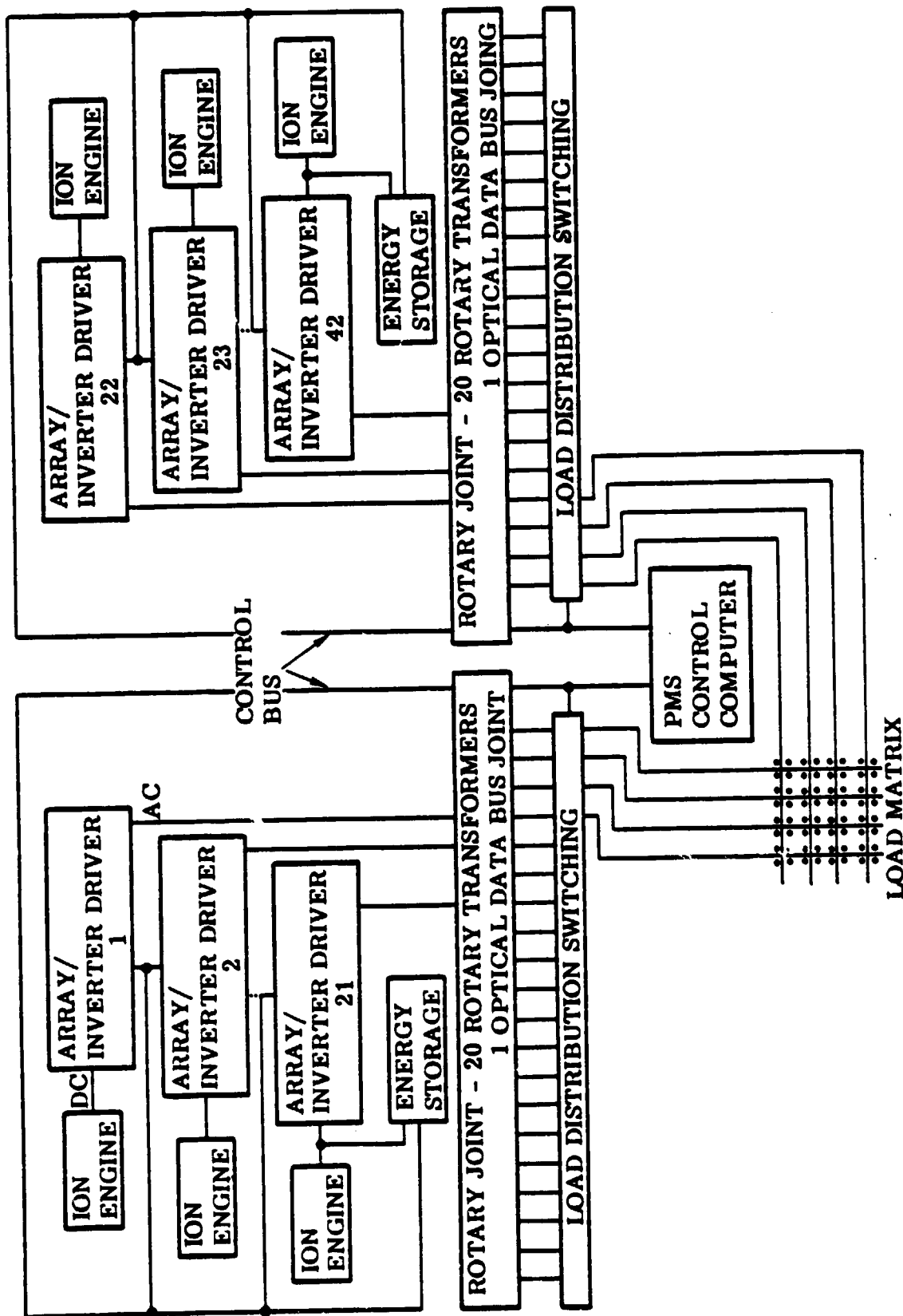


Figure 2-73. Typical Multi-Driver, Multi-Receiver System.

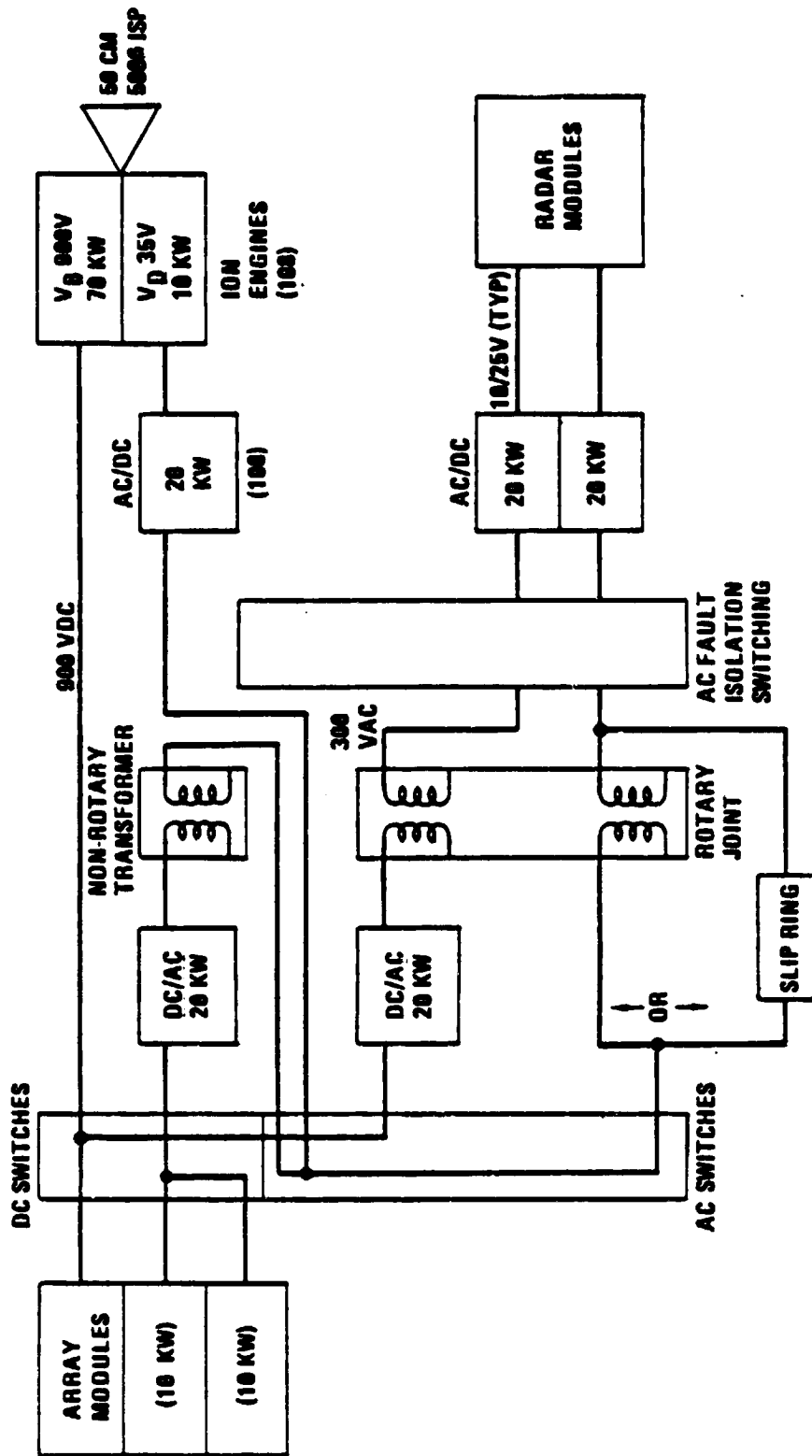


Figure 2-74. Hybrid Power Management and Control Block Diagram - GEO Radar System.

## 2.3 TECHNOLOGY GOALS — SENSITIVITY TRADES AND ANALYSES

Figure 2-75 shows how technology goals and benefits were developed.

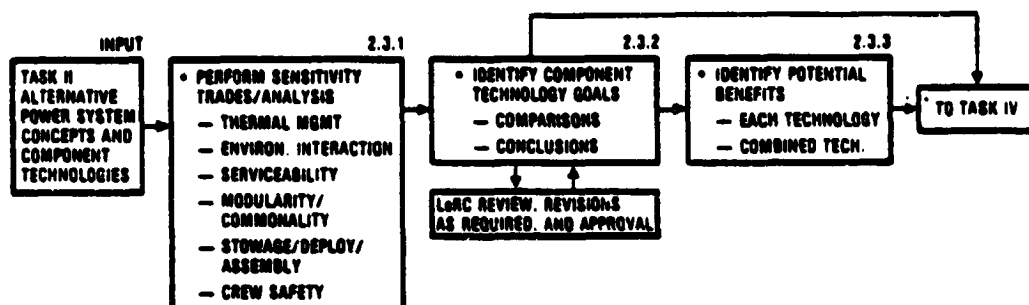


Figure 2-75. Technology Goals.

Trades and sensitivity studies conducted to optimize the various concepts considered in the evaluation included: Thermal management; environmental interactions; constructability, storage, and assembly on orbit; safety; and modularity.

**2.3.1 THERMAL MANAGEMENT.** The power generation, energy storage, and power management and control systems are all affected by the approach taken to their thermal management.

**2.3.1.1 Thermal Management for the Power Generation System.** The power generation options considered included planer arrays and concentrators as previously discussed. For the planer array cases, the study projected that no significant changes would be made in lowering the temperature of planer arrays beyond that experienced by today's planer arrays and initially projected during Task II. In particular, it was projected that the average emmissivity might run around 0.7 (0.9 for the back surface and 0.4 for the front surface). As a result, the LEO array temperature is expected to be approximately 60°C while the array is operating in the sunlight, and the GEO temperature should average around 30°C during insolation periods.

**2.3.1.2 Thermal Management System Sizing for Large Concentrators.** Solar cell thermal management systems identified in Subsection 2.2 were analyzed to determine pumped coolant radiator size, heat pipe spacing, and heat pipe radiator skin thickness. The following sections shown the extremely large pumped coolant radiator sizes required, and describe the thermal and weight effects of varying pipe spacing and skin thicknesses of the heat pipe system.

**2.3.1.2.1 Pumped Coolant Radiator Sizing.** A method for sizing pumped coolant space radiators was developed at Convair in an earlier study (Reference 23). The equations giving heat rejection per unit radiator area as a function of inlet, outlet, and environmental sink temperature is given below:

$$Q/A = \frac{2\sigma\eta_f\epsilon T_s^3 (T_i - T_o)}{\tan^{-1}\left(\frac{T_o}{T_s}\right) - \tan^{-1}\left(\frac{T_i}{T_s}\right) + \frac{1}{2} \ln \left[ \frac{(T_i - T_s)(T_o + T_s)}{(T_i + T_s)(T_o - T_s)} \right]} \quad (\text{Eq. 10})$$

where

- $Q/A$  = heat rejection flux, watts/m<sup>2</sup> (Btu/hr-ft<sup>2</sup>)
- $\sigma$  = Stefan-Boltzman constant, watts/m<sup>2</sup> - °K<sup>4</sup> (Btu/hr-ft<sup>2</sup>-°R<sup>4</sup>)
- $\eta_f$  = radiator fin efficiency = actual heat rejection/heat rejection if the entire radiator fin temperature were that of the coolant at the fin base = .90
- $\epsilon$  = radiator surface emittance = .85
- $T_s$  = sink temperature, °K (°R)
- $T_i$  = inlet temperature, °K (°R)
- $T_o$  = outlet temperature, °K (°R)

Calculations to determine (a) the coolant temperature rise as it passes across the solar cells, and (b) radiator sink temperature for low-earth and geosynchronous orbits (LEO and GEO), are required before proceeding with the radiator sizing equation.

- a. Coolant Temperature Rise - Coolant temperature increase is given by the absorbed heat rate divided by the product of coolant mass flow rate (per unit area of solar cells) times specific heat:

$$\Delta T = \frac{Q/A}{\dot{w}C_p} \quad (\text{Eq. 11})$$

For a given velocity, the mass flow rate per unit area of solar cell will vary with passage depth. Calculated fluid temperature rise is shown in Figure 2-76. Coolant temperature rise is seen to be very small compared to the temperature difference across the boundary layer. A temperature rise of 5.6°C (10°F) will be used in the radiator sizing calculations.

ORIGINAL PAGE IS  
OF POOR QUALITY

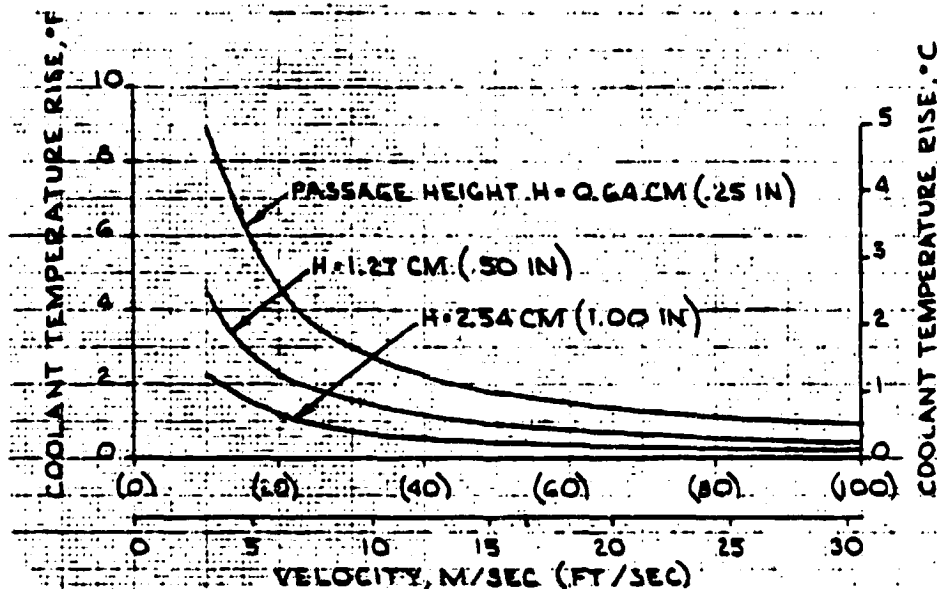


Figure 2-76. Variation of Coolant Temperature Rise with Passage Height and Velocity.

- b. Sink Temperature - Radiator environmental sink temperature is the temperature the radiator would come to with no heat load on the fluid. Skin temperatures  $-59^{\circ}\text{C}$  ( $-74^{\circ}\text{F}$ ) for LEO and  $-110^{\circ}\text{C}$  ( $-167^{\circ}\text{F}$ ) for GEO were calculated, using the configuration of Figure 2-26 and the orbital average space heating, view factor, and surface property assumptions of Table 2-11.
- c. Radiator Sizing - Equation 10 was used to calculate four heat rejection flux cases (two cell temperatures and two coolant velocities) at LEO and the same four cases at GEO. The two solar cell temperatures analyzed are  $200^{\circ}\text{C}$  ( $392^{\circ}\text{F}$ ) and  $125^{\circ}\text{C}$  ( $257^{\circ}\text{F}$ ). The two coolant velocities are 3 and 15 m/sec (10 and 50 ft/sec) with corresponding coolant boundary layer  $\Delta$  temperatures of  $193^{\circ}\text{C}$  ( $348^{\circ}\text{F}$ ) and  $53^{\circ}\text{C}$  ( $93^{\circ}\text{F}$ ). These assumptions result in coolant temperatures (radiator inlet temperatures) of  $7^{\circ}\text{C}$  ( $44^{\circ}\text{F}$ ) and  $147^{\circ}\text{C}$  ( $296^{\circ}\text{F}$ ) for  $200^{\circ}\text{C}$  solar cells and  $-68^{\circ}\text{C}$  ( $91^{\circ}\text{F}$ ) and  $72^{\circ}\text{C}$  ( $161^{\circ}\text{F}$ ) for  $125^{\circ}\text{C}$  solar cells. Calculated heat rejection fluxes are summarized in Table 2-12. The highest (best) heat rejection flux occurs at GEO (lower sink temperature) for the case of the highest coolant temperature ( $200^{\circ}\text{C}$  cell and velocity = 15 m/sec).

Table 2-11. Assumptions for Calculating Radiator Sink Temperatures.

---

Solar heat flux = $1350 \text{ w/m}^2$ ( $429 \text{ Btu/hr-ft}^2$ )
Earth thermal heat flux = $237 \text{ w/m}^2$ ( $75 \text{ Btu/hr-ft}^2$ )
Radiator direct solar heating (LEO and GEO) = zero
Primary reflector earth heating during GEO = zero
Primary reflector (both sides) view to earth during LEO, $F = .40$
Radiator (one side) view to primary reflector, $F = .35$
Radiator (both sides) view to earth during LEO, $F = .40$
Primary reflector front surface:
Solar absorptance, $\alpha_s = .19$
Emittance, $\epsilon = .75$
Primary reflector back surface:
Emittance, $\epsilon = .85$

---

Table 2-12. Summary of Radiator Heat Rejection Fluxes,  $\text{W/m}^2$  ( $\text{Btu/hr-ft}^2$ ).

---

	LEO		GEO	
	Cell Temp = $200^\circ\text{C}$	Cell Temp = $125^\circ\text{C}$	Cell Temp = $200^\circ\text{C}$	Cell Temp = $125^\circ\text{C}$
Velocity = 3 m/sec	164 (52.1)	N/A*	226 (71.6)	42 (13.3)
Velocity = 15 m/sec	1224 (388)	503 (159.5)	1278 (405)	565 (179.2)

---

\* Radiator inlet and outlet temps are below sink temp.

---

To determine required radiator area, a 10-megawatt power output system was assumed. Cell efficiency dependence on temperature was assumed to follow the equation shown below:

$$\eta = .17 - .002 \times .17 (T - 28^\circ\text{C}) \quad (\text{Eq. 12})$$

where:  $T$  = cell temperature,  $^\circ\text{C}$

Calculated required heat rejection rates are  $7.91 \times 10^7$  watts ( $2.70 \times 10^8$  Btu/hr) for  $200^\circ\text{C}$  cells and  $6.27 \times 10^7$  watts ( $2.14 \times 10^8$  Btu/hr) for  $125^\circ\text{C}$  cells. Required radiator areas are shown in Table 2-13. Note that both sides of the radiator would be used to achieve the areas shown. The areas are all so great that none of the cases investigated appears practical.

Table 2-13. Summary of Required Radiator Areas,  $m^2$  ( $ft^2$ ).

	Cell Temp = 200°C	Cell Temp = 126°C	Cell Temp = 200°C	Cell Temp = 125°C
Velocity = 3 m/sec	$4.81 \times 10^5$ ( $5.18 \times 10^6$ )	N/A	$3.51 \times 10^5$ ( $3.78 \times 10^6$ )	$1.51 \times 10^6$ ( $1.62 \times 10^7$ )
Velocity = 15 m/sec	$6.47 \times 10^4$ ( $6.96 \times 10^5$ )	$1.24 \times 10^5$ ( $1.34 \times 10^6$ )	$6.19 \times 10^4$ ( $6.66 \times 10^5$ )	$6.19 \times 10^5$ ( $66.6 \times 10^6$ )

2.3.1.2.2 Heat Pipe Spacing and Fin Thickness Sizing. Heat pipe spacing and radiator fin thickness sizing are analyzed in this section for the spacecraft configuration shown in Figure 2-45 and heat pipe arrangement shown in Figure 2-46. The spacecraft thermal model employed to determine the heat load on the radiator is shown in Figure 2-77.

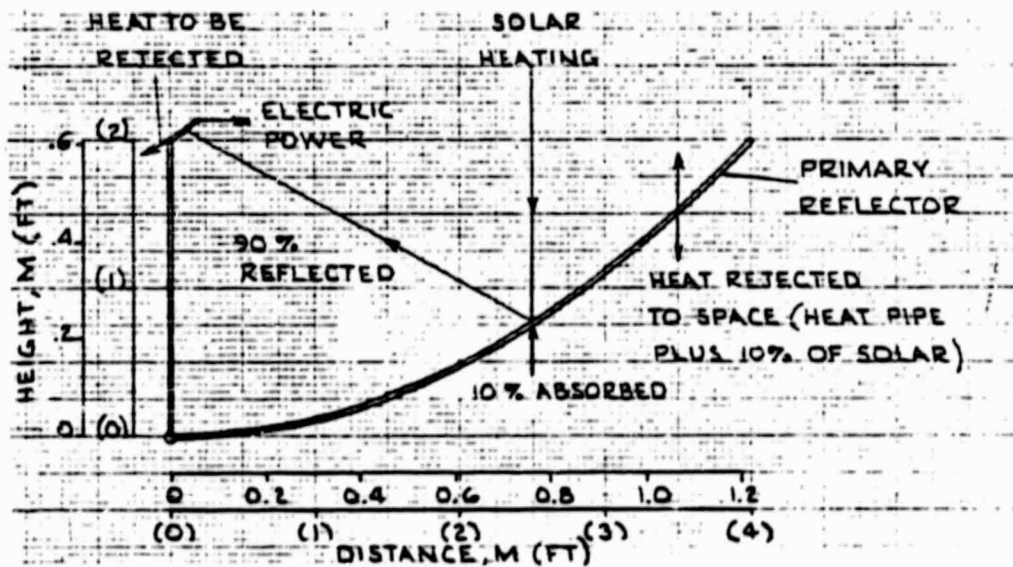


Figure 2-77. Spacecraft Thermal Model for Heat Pipe System.

The primary reflector will radiate to space all the heat conducted down the heat pipes from the adjacent concentrator plus the absorbed part of direct solar irradiation (assumed to be 10%).

A major objective of this analysis is to define a heat rejection/primary reflector system which is weight/cost effective with planar arrays. The weight per unit aperture area of the concept shown in Figure 2-46 is presented in Figure 2-78 as a function of aluminum sheet primary reflector thickness and heat pipe spacing.

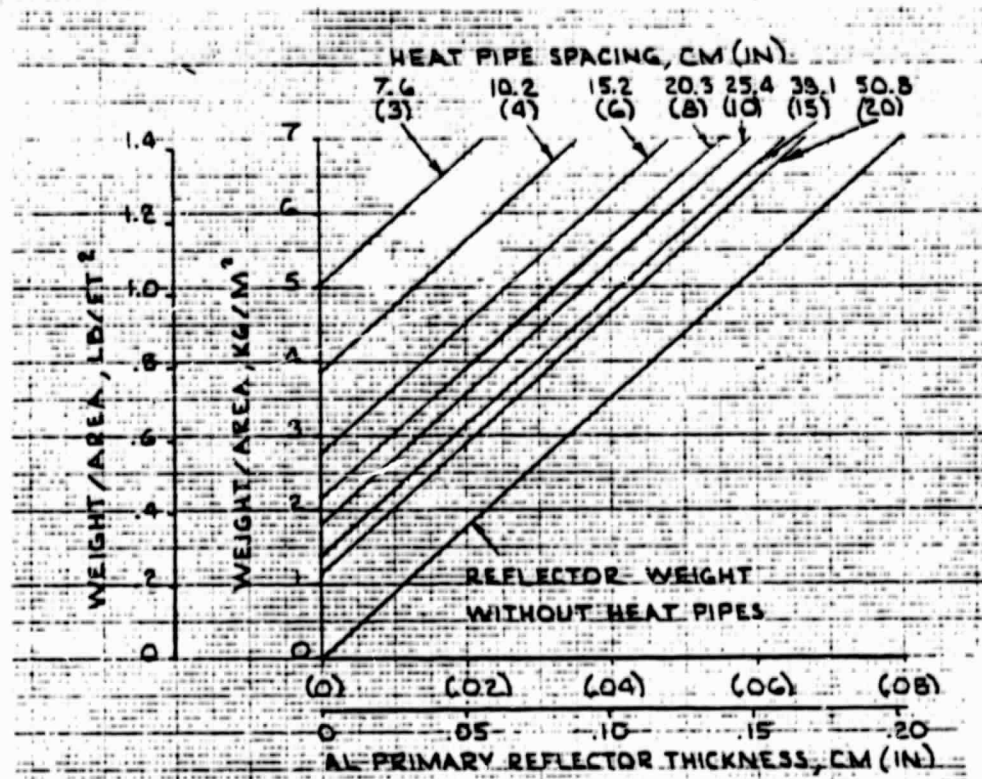


Figure 2-78. Weight/Aperture Area as a Function of Sheet Reflector Thickness and Heat Pipe Spacing.

The heat pipe cross-section is similar to that of existing heat pipes tested at Convair (Reference 12) and, as noted earlier, may not be the lightest weight design. A system weighing in the range of 2 to 3 Kg/m<sup>2</sup> is sought.

The thermal effect of spreading out the heat pipes is twofold. First, the heat load per pipe increases. With the arrangement shown in Figure 2-46, the evaporator area for heat transfer to the heat pipe increases with greater spacing, so the heat flux with respect to the boiling limitation is not affected. However, the greater heat load per pipe does affect performance with respect to the wicking limitation, and this should be analyzed in any future studies. The second thermal effect of spreading out the heat pipes is an increase in heat pipe temperature caused by the reduction in fin efficiency of the primary reflector. The distributed temperature in the fin (primary reflector) will attain a high enough level to radiate away all of the heat carried by the heat pipe. The less the fin efficiency, the greater is the temperature "sag" in the fin material.

Heat pipe spacing of 10 to 25 cm (4 to 10 inches) were thermally analyzed. Temperature distribution in primary reflectors of .025 and .05 cm (.01 and .02 inches) thickness were determined using the Convair Radiation/Convection Fin computer program P5399 (Reference 24). Example temperature distributions are illustrated in Figure 2-79. Greater spacing causes the heat pipe (fin root) temperature to increase. It was determined in Subsection 2.2 that a heat pipe temperature of approximately 100°C (212°F) was the maximum allowable without surpassing the

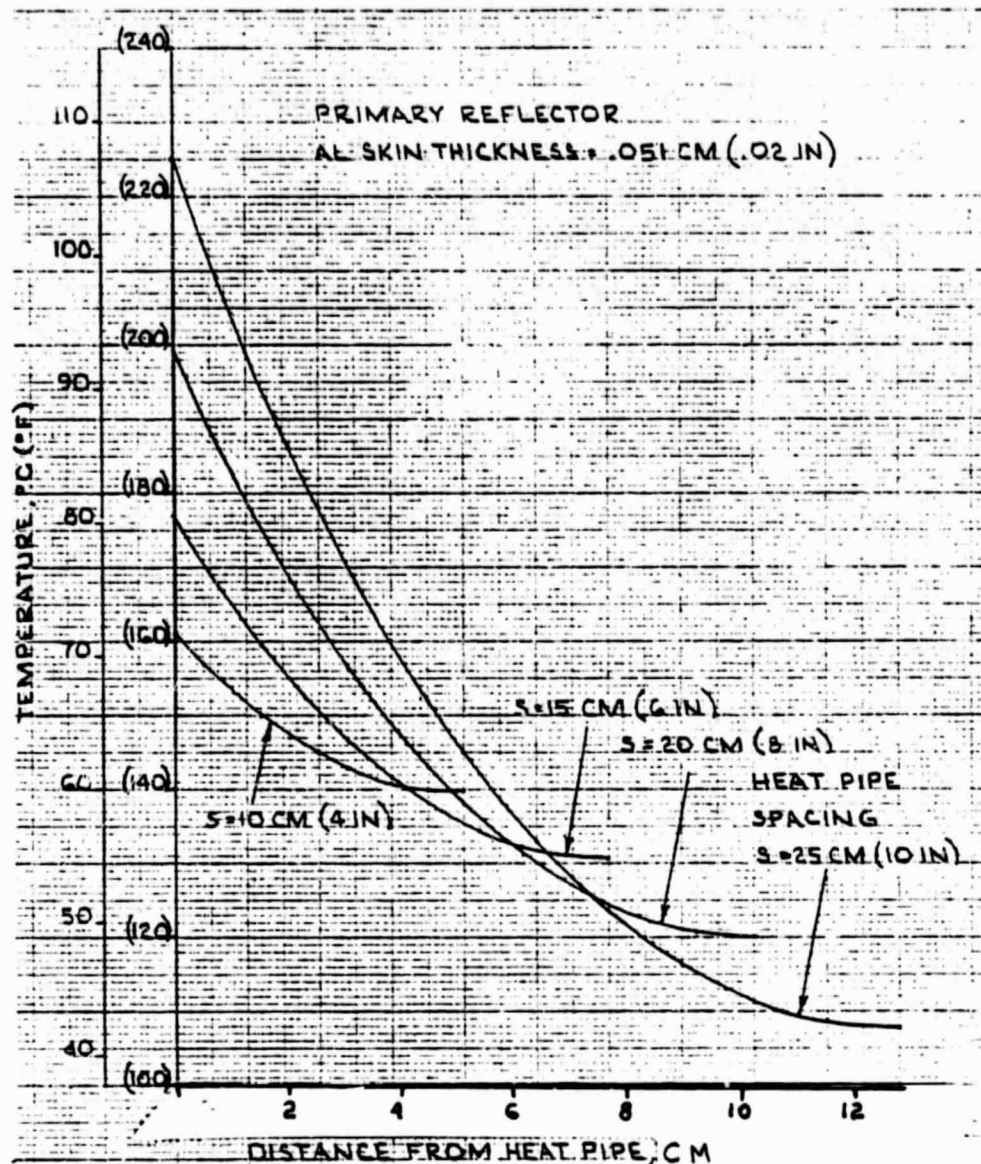


Figure 2-79. Primary Reflector Temperature Distribution as a Function of Heat Pipe Spacing.

boiling limitation at the evaporator. Figure 2-80 summarizes heat pipe (fin root) temperatures for the cases analyzed. The two points indicated by footnotes in the figure are both under the maximum allowable temperature. Primary reflector/heat pipe weights at these design points are 3.6 and 4.0 kg/m<sup>2</sup>.

**2.3.1.3 Small Modular Concentrators.** The thermal management of the small modular concentrators described in Subsection 2.2 was conducted using some of the same assumptions that had been made for planer arrays, namely, that the back surface of the concentrators would be painted black and have high emmissivity -- 0.90 to 0.95. The front surface could use a reflective aluminum or silver finish overcoated with multilayer quarter-wavelength silicon of SiO<sub>x</sub> type material.

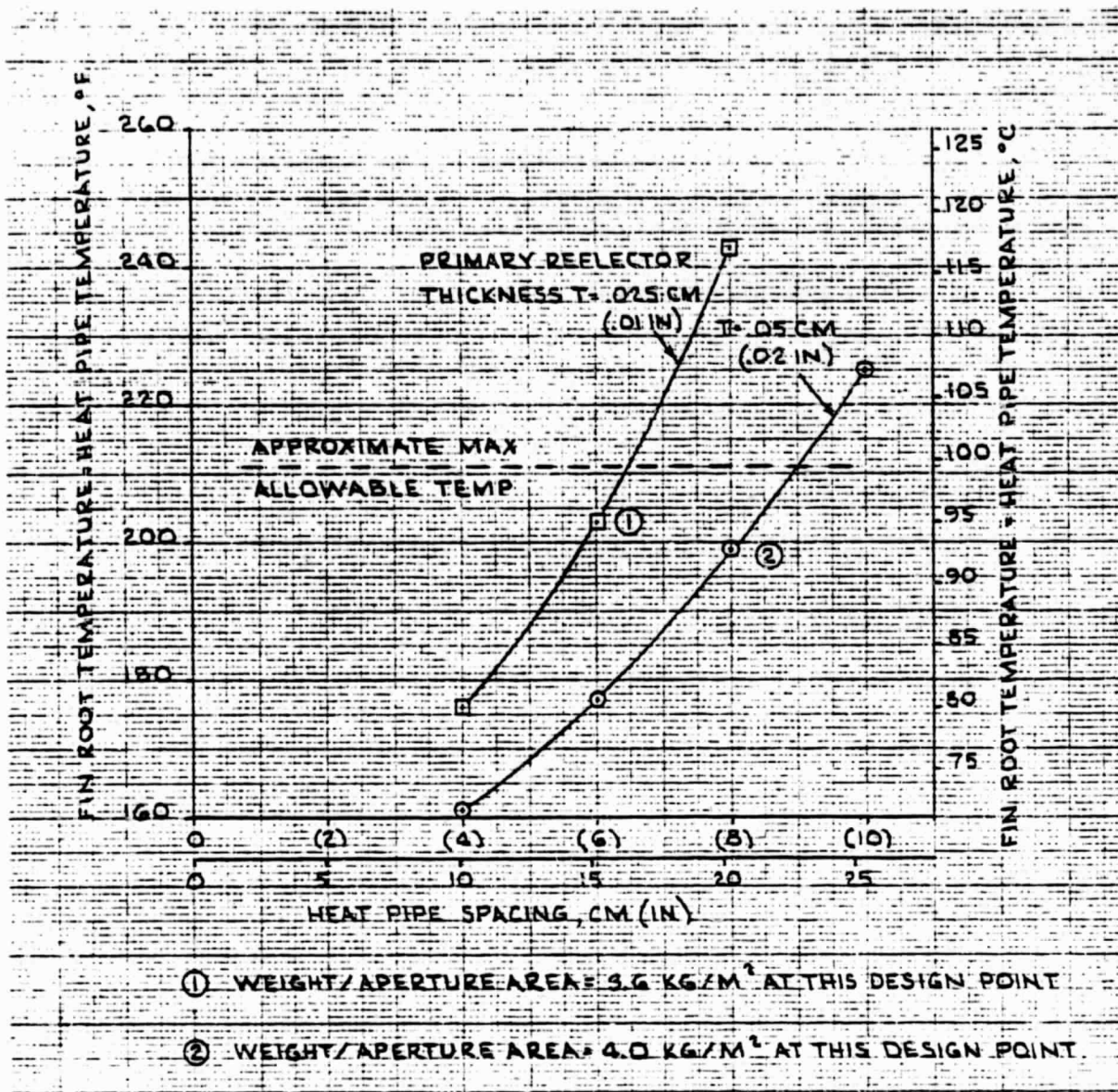


Figure 2-80. Heat Pipe Temperature as a Function of Heat Pipe Spacing and Reflector Thickness.

These overcoats could tune the front surface so that it provided a highly reflective surface in the visible range usable by the solar cell, and a highly emissive ( $E = .65$  infrared surface). These type surfaces would be preferred to a more cost-effective teflon overcoating, because they can be made conductive by adding indium oxide surface layers in addition to the silicon dioxide layers. View factors to space are somewhat less for the small modular concentrators than for planar arrays because of geometrical shielding by the reflector sides.

The two competing small concentrator configurations each partially block their own cooling black body radiation to deep space. The scope of this study did not permit a detailed analysis of this blockage. The two configurations can be compared cursorily with the following results. Both the small semiparabolic trough

and the eggcrate geometries block about 35% of the radiated energy. Figure 2-81 shows an estimate (made using a protractor) of three representative points and their approximate blockage. The blockage for the eggcrate could be reduced by eliminating the light cone, but then the design would become more pointing angle sensitive. Light prisms added to the trough design, on the other hand, do not appear to cause significant blockage.

Thermal gradients of between 10 and 20 degrees centigrade from the cell proper to the radiator extreme edge were calculated. The Stephen Boltzman equation was used to calculate the temperature; which ran from 90 to 100 degrees centigrade.

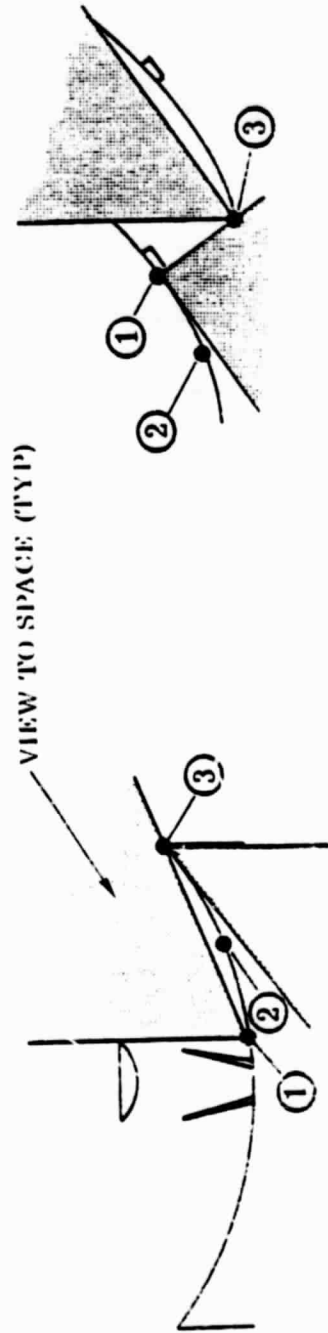
**2.3.1.4 Energy Storage Components.** The thermal management of the energy storage components was also assumed to be done passively for components mounted on the array. In previous studies accomplished for NASA, the modularity of these components had been driven up to achieve higher reliability. In this specific case, modularity levels for the energy storage component have been established to be approximately 10 to 25 kilowatt hours. At this level, passive thin-fin cooling is possible for the component, as long as view factors are not restricted unduly. It was projected that this could be accomplished. The density of the radiators involved would be approximately 3 kilograms per square meter. The thermal management of the power generation and control system was also assumed to be done passively since these components would be modularized at the 25 kw level, and (since they are highly efficient) very small amounts of power are radiated into space and wasted.

**2.3.2 ENVIRONMENTAL INTERACTIONS.** The GEO Radar Illuminator and the LEO Space Construction Facility must be designed to survive the natural environments that they will encounter on station. Since the radar will be assembled at LEO and transitioned by GEO, it must also survive the injection environment. Environment factors include:

- a. Natural Radiation
- b. Micro Meteoroid Particles
- c. Space Plasma and its losses/arcing susceptibility
- d. Injection, stationkeeping, and docking G loads and vibration loads.

The environments can affect power generation, energy storage, systems, and Power Management Systems.

**2.3.2.1 Power Generation — Environmental Effects.** The degradation of solar cells as a result of exposure to natural electron and proton radiation has been described in the literature and is well understood, although more completely for silicon than for Gallium Arsenide. This study projects that silicon planar array degradation will not be significantly decreased by efforts now underway to identify and remove the causes of the imperfections which made silicon susceptible. The judgement was based on current literature (Reference 20) and, of course, is



① NEAR CELL BLOCKAGE	BACK SIDE FRONT SIDE AVG	50% 30% 40%
② MID RADIATOR BLOCKAGE	BACK SIDE FRONT SIDE AVG	50% 25% 37%
③ FAR-OUT BLOCKAGE	BACK SIDE FRONT SIDE AVG	10% 60% 35%

① NEAR CELL BLOCKAGE	BACK SIDE FRONT SIDE AVG	0 70% 35%
② MID RADIATOR BLOCKAGE	BACK SIDE FRONT SIDE AVG	20% 50% 35%
③ FAR-OUT BLOCKAGE	BACK SIDE FRONT SIDE AVG	80% 30% 55%

Figure 2-81. Radiator Heat Rejection View Factor Blockages for Two Representative Small Concentrators.

susceptible to a technology breakthrough. It is in keeping with the philosophy and ground rules of the study, which were: do not postulate the existence of any components or processes which had not been demonstrated, in principle, in the laboratory. In this regard, the more pessimistic view of silicon contrasts to the more optimistic view maintained for Gallium Aluminum Arsenide single-band cell annealing—which has some supporting data (References 25 and 26).

Given the above projection for silicon, the environmental radiation effects on silicon blankets were then calculated based on Reference 8 projections, and they were included in the efficiency projections made for silicon.

For the LEO Space Construction Facility, the effects of trapped particle radiation are small, since the 225 mile orbit is low. However, for the 20-year lifetime, there is a significant probability of a 1972 type solar flare occurring once per decade. This dosage could be as high as  $4 \times 10^{10}$  protons or  $1.2 \times 10^{14}$  1 MEV equivalency—this dosage then causing a 9% drop in output (Reference 27). Combined with a 2% drop in adhesive darkness; the overall loss could be 11% every 10 years (Figure 2-82).

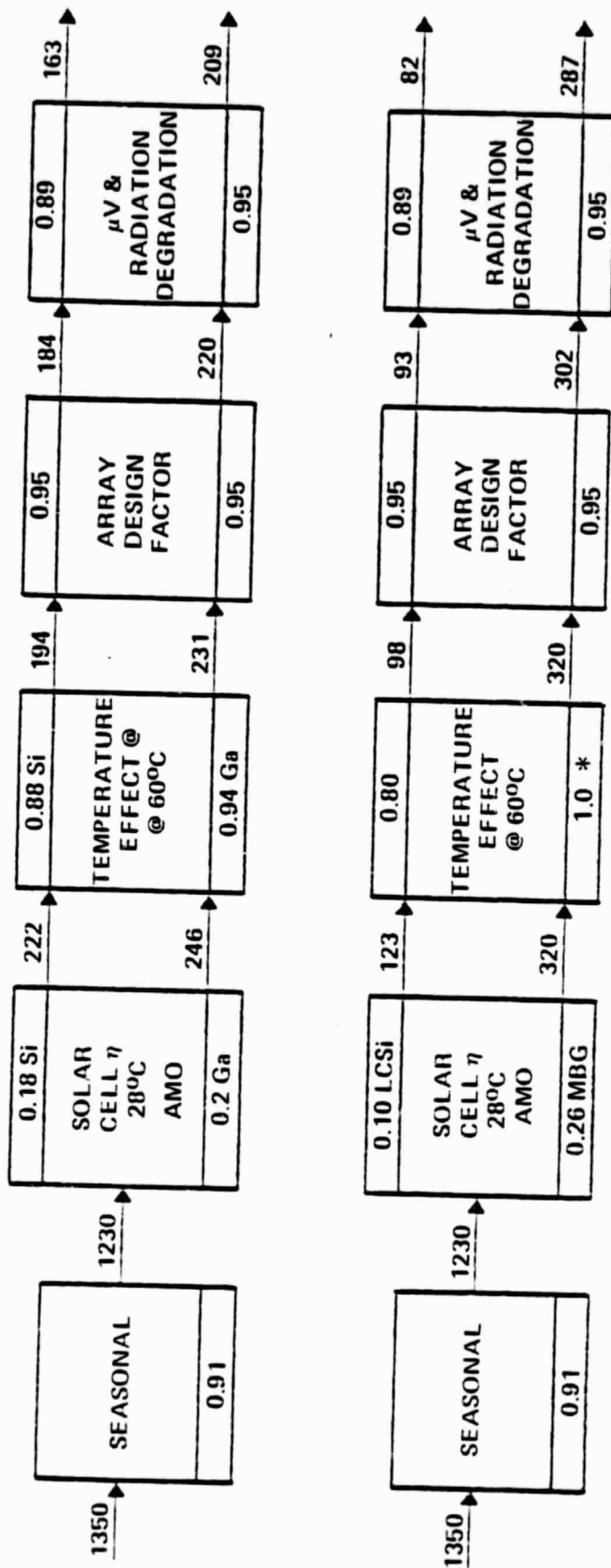
For the GEO Radar Illuminator, the same flare activity and the higher trapped electron fluence combine to require additional silicon array modules added every five years. Also, as discussed under operating options, the LEO to GEO injection causes severe degradation if slower electric propulsion is used.

**2.3.2.1.1 Radiation Effects on Gallium Arsenide.** In contrast to Silicon Planar Arrays, this study projects that Gallium Arsenide cells will be designed with the capability of being re-annealed to effect significant recoveries from radiation degradation, including that resulting from solar flares, should they occur.

The currently proposed schemes for accomplishing this involve scanning the array with laser pulses (complex and possibly hazardous) or operating a concentrated array at a temperature high enough to result in continuous annealing (accompanied by a continuous reduction of conversion efficiency).

This study assumes the array has on-array regulation and array modularization with accompanying switching. In these cases, it is possible to direct a large current through the photovoltaic cells by applying a voltage in excess of the open-circuit voltage. This technique could be used to periodically heat segments of the array to an annealing temperature by drawing current from other array segments and dissipating it in the cells internal resistances. Accordingly — Gallium Arsenide Planar arrays were assumed to be electrically re-annealable — with recovery from 90% of radiation degradation.

**2.3.2.1.2 Radiation Effects on Concentrators.** The development of concentrators offers some significant potential benefits as far as radiation damage is concerned. These occur because the solar cells area is small compared to the mirror area, and therefore, thicker glass coverslips can be utilized to the front surface of they all. In the cases of the mini parabolic trough and mini cassegrainian



TOP - SILICON  
 TOP MIDDLE - GaAs  
 BOTTOM MIDDLE - "LOW COST" SILICON  
 BOTTOM - MULTIBANDGAP

\* INCLUDED IN 0.26 $\eta$

Figure 2-82. Efficiency Chains LEO Planar Array.

geometries, the cells are also protected by some thickness of mirror as well. The back surface of the cell is also protected by a thicker substrate/radiator surface. The net effect should be two orders of magnitude reduction in flux with a 5% power reduction over the 20-year lifetime, when the decreased dosage is combined with electrical annealing.

When these effects are combined with the potential for on-array annealing of the Gallium Arsenide cells, utilized - concentrators show significant benefits.

**2.3.2.1.3 Micro-Meteoroid Environmental Interaction.** The effects of micro-meteoroids on Solar Array performance appear to be small, certainly smaller than radiation effects. This conclusion is based on the observed small amount of degradation which occurs in LEO. Other workers share this view, (Reference 28). On the other hand, the size and life of the solar arrays for multimegawatt systems will increase by three to four orders of magnitude over 1970 systems, and there is a significant likelihood of collisions with particles large enough to penetrate the thin cover slides of Planar Arrays and perhaps fracture the cell. A cursory analysis, based on collision dynamics equations described in Appendix A of this report and on the meteoroid statistics in NASA SP-8013, suggests that up to  $8 \times 10^7$  collisions capable of coverslide penetration could occur over the 20 year life. Further evaluation is required in this area, should concentrators not be developed.

**2.3.2.1.4 Micro-Meteoroid Effects on Concentrator Mirrors.** Since the publication of NASA SP-8013, and experiment was conducted by NASA on the SERT II spacecraft in Polar Orbit (Reference 29). The temperature of highly polished aluminum was observed over a 5 year period, and found to vary insignificantly. Previous laboratory bombardment with particles in the  $10^{-11}$  gm mass range had indicated variation in thermal  $\alpha/\epsilon$  under bombardment, the lack of temperature change over the 5 year orbit is interpreted to mean that micro-meteoroid damage is not appreciable. As a result, concentrator mirror performance should be projected to show only minor mirror degradation over the 20 year life. A degradation value of 10 percent was used for the efficiency calculations.

It should also be observed that because the cell area is only 1 to 3 per cell of the aperture (mirror) area, the incidence of cell damage from larger meteoroids should be one to three orders of magnitude less if the meteoroid environmental specific is later increased back to the levels of NASA SP-8013.

**2.3.2.1.5 Plasma Interactions.** A body of literature exists which indicates that the space plasma interacts with the power generation and management system in several ways. They are:

- a. The plasma at GEO may indicate charge buildup on dielectric surfaces, and these may later discharge causing power system failures, and noise which adversely affects satellite performance. (Reference 30.)

- b. The arrays may collect electrons and ions from the plasma, a shunting loss as far as the array is concerned. (Reference 30.)
- c. The plasma might support arcs from high voltage solar cell conductors to ground.

**2.3.2.1.6 Dielectric Chargeup and Discharge.** Data now exists which confirms charge buildup phenomena on dielectric surfaces. Based on this data, it is projected that the best static discharge prevention approach for dielectric surfaces will be to conductively coat the surfaces to keep them close to ground potential, or at least close to the potential of their adjoining cell conductors, so that there is a relatively low impedance to ground. Any surface not inherently conductive would be coated or painted to make it conductive. As discussed previously, this is the reason for utilizing indium oxide overcoat on the reflector front surface and radiator surfaces evaluated by this study. Conductive coatings and paints or anodized aluminum surfaces should be employed.

**2.3.2.1.7 Plasma Losses.** As array voltages become higher, it is expected that losses caused by plasma short circuiting of the array will increase, because plasma electrons will be captured. cursory studies for particular geometries were conducted for past power system studies (Reference 30). They indicated some loss for the two particular geometries considered. The losses are a function of array voltage lower voltages (100-200 Vdc) minimize plasma losses and higher voltages (900-1000) make them large and significant (5-10%), but not insurmountable.

The accurate prediction of these losses requires the use of software now under development by NASA, and even then is very dependent on the geometry of the spacecraft and the detailed array voltage distribution strategy. Eventually, this entire problem should be attacked and solved for spacecraft over several power ranges such as 10-100 KW, 100-1 mW, and 1-10 MW, and with several potential likely mission configurations. The investigation should also consider alternate insulation voltage partitioning strategies, and their possible negation by micro-meteoroids, with subsequent increased arcing probability.

- a. **Planar Arrays - Plasma Concepts Summarized.** For the planar array, the front surface of the cells is at the potential defined by the cells. If the back surface is slightly conductive (an indium oxide overcoat or black paint with a sheet resistance of  $1 \text{ k}\Omega/\square$ ) and if the paint is in contact with the cell conductors intermittently, the paint will represent a high impedance shunt across the cells. It should keep the array blanket from becoming charged and, at the same time, limit arcing and limit the shunt losses to 1% or less of the system output. Because the blanket is non-conducting, the initiation of arcing to the structure from the cell conductors requires a large voltage gradient, since the back surface is some distance from the truss supports. Therefore, it is projected that planar array can support the high voltage concept of this study, albeit with some plasma and conductive surface shunting losses.

- b. Mini-Concentrators — Plasma Concepts Summarized. The min-concentrator can also be designed using many of these same concepts. The reflectors/louvers can be insulated from the truss structure just as the planar array blanket is, so that they are close to the potential of the cells. If this approach works to prevent chargeup/discharge phenomena for planar arrays, it should work for the mini-concentrator as well.

Arcing from the solar cell conductors to the reflectors could conceivably short out sections of the array, except that by holding the voltages of the troughs to close to the solar cell values, the arcing should be no more likely than it is for today's honeycomb-backed arrays operating at the same voltages. Therefore, it is projected that mini-concentrators should be able to use high distribution voltages (using series-connected louvers) also with some plasma loss.

- 2.3.2.1.8 Launch Environmental Effects. The launch environment will affect the power generation approach, (either planar arrays or concentrators) the energy storage system components, and the power management component.

The frame modules used to package and align the miniature troughs of the concentrator system are shown in Figure 2-12. The 1.5-meter-long troughs should have quite a low natural frequency: excitation of the significant bending modes will probably come mostly from acoustic energy and should be handled easily by the structure. A greater potential source of interaction would be linear acceleration from the shuttle engines. If it were normal to the plane of the trough, it could be a problem. However, by packaging the array so that the troughs run longitudinally along the length (X-axis) of the shuttle cargo bay, the effect and interaction of this load is minimized. This packaging approach is viable, as long as it is included in cargo container baseline designs as they emerge.

Planar array blankets can be rolled or folded so that they become a compact mass during launch phase. This compaction should permit them to also tolerate the launch environment without penalties imposed on their design.

As discussed in the section on storability, the launch environment should also be well tolerated by Energy storage, power management, and beam builder components and robotic machines.

- 2.3.2.2 Energy Storage and Power Management Components. The potential energy storage candidates, batteries, flywheels, fuel cells, and power electronics components are not known to be sensitive to the natural particular radiation environment, or to plasma interactions, assuming the operating and power distribution voltages are selected so that losses are not excessive. Of course, their solid state control devices, if not shielded, may suffer some degradation, but good packaging should make these effects negligible.

Micro-meteoroids are another concern. The Fuel Cells, Electrolysis Storage System, with its reactant tanks and gasses under pressure, could leak from one puncture if not protected. In fact, this study penalized the original suppliers projected mass estimates, so that extra shielding mass was included.

Flywheels and batteries were not penalized. Instead, it was assumed that their casing and mechanical parts would not be as adversely affected, since cross actions are smaller and they are modular. All energy storage options were assumed to be capable of being designed to withstand the launch environment of the shuttle; in particular, sodium sulphur batteries can be launched frozen.

The solid state component of the power management and control system should also be protected by careful packaging design, which will place them inside of thickness of their own and adjacent structural components, so that degradation caused by radiation and micro-meteoroids is minimized.

**2.3.3 STORAGE, DEVELOPMENT AND ASSEMBLY.** The three types of miniature concentrator were all evaluated for their constructibility attributes, benefits, and efficiencies. The minitrough configuration has a line of solar cells which is easy to assemble using automatic machinery. The cells can be easily assembled, wiring to them can be easily accomplished, and an entire trough can be fabricated in one easy step. On the other hand, the other two square configurations may require hand wiring to interconnect the solar cells. Even if automated, the complexity of automation appears to be greater, since the sides of the "eggcrates" block the easy installation of wiring on the front side. Back-side wiring would require accesses to the cell through holes in the radiator, or separate mirror/radiator structures, a potential weight penalty.

Fabrication of the Planar Array blankets, with Silicon or Gallium Arsenide cells is under development for arrays such as the SEPS system and poses no particular technology problem.

Likewise, storage of small modular concentrators and planar arrays, with their reasonably high densities, should pose no known problems. On orbit, fabrication of the arrays would make use of beams fabricated using the beam builder, while the attached space crane (a part of the space construction facility) would maneuver the beams into position, and either the crane or a robotic machine would place the array modules in their desired final position. The truss itself has dimension which can accommodate manned maneuvering, if the danger to the astronaut from meteoroids can be reduced to an acceptable level.

Installation of Power Management and Energy Storage components could also be done robotically (by a robot maneuvering along and inside the beams) or manually.

**2.3.4 SAFETY.** If the arrays and power system are to be designed to be modularly interconnected to provide 900-1000 volts, then the entire spacecraft under test will require safety caging or more elaborate safeguards to assure lethality risk is minimized. This issue will require careful consideration prior to the final

design decision of array voltage. In each case the benefit of the mass saved and corresponding transportation cost savings must be weighed against this risk.

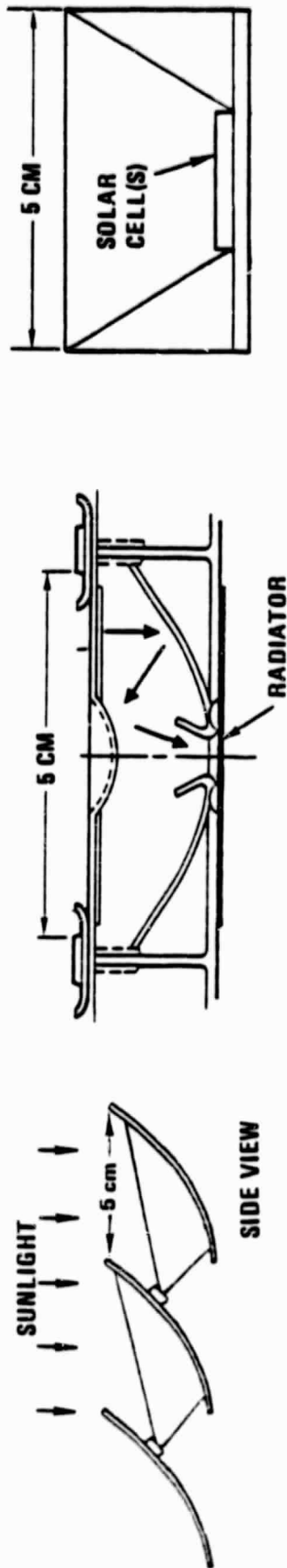
### 2.3.5 MODULARITY AND BENEFITS ANALYSIS.

2.3.5.1 Power Generation - Mini-Concentrators Modularity. Modularity studies for three concentrator geometries were conducted in this portion of the study. The three types of concentrators were the minitrough, the mini-Cassegrainian dish, and a minitruncated pyramid (see Figure 2-83). The minicassegrain configuration and minipyramid concentrator both utilized a 5 cm<sup>2</sup> aperture. The geometrical performance of the three concentrators considered is presented in the tabular data, which shows that both the minitrough and minipyramid have a fairly significant advantage in the amount of light received over the minicassegrain system. The advantage comes about because the Cassegrainian secondary reflector reflects aperture light (which, in the other configuration, would pass through to the solar cells) while also absorbing aperture insolation.

Table 2-14 shows the beginning of life performance for the three different mini-concentrators with three different cell types. The table also shows the effect of performance of having the mini-concentrators misaligned from the insolation vector when only one gimbal is utilized. Here the advantages of the minitrough become more evident to the reader. For all but one of the LEO and GEO configurations and all of the three cell types, the minitrough provides greater output power.\* Table 2-15 summarizes the performance of the small concentrators after their masses and the masses of their supporting hardware are estimated for the various cell configurations. The one gimbal minitrough appears to be the least massive system.

Finally, cost estimates were made for all the configurations studied. Tables 2-16 and 2-17 shows this data. The cost effectiveness of the minitrough configurations then becomes evident, it projects the lowest cost.

2.3.5.2 Energy Storage - Flywheels and Batteries. When the sensitivity trades and benefits analysis of the energy storage alternatives were completed, two technologies appeared to offer significant benefits, Flywheels and sodium sulfur batteries (see Figure 2-84). The other two high energy systems, ZnBr<sub>2</sub> and LiMS, were not as attractive because of their lower specific energy. ZnBr<sub>2</sub> also requires pumps and fluid loops, and appears to be less efficient and less capable than the NaS alternative recommended. The LiMS approach does not have active loops but also has probable penalties due to low efficiency. Both of these systems have a solid plate electrode, which is perhaps more vulnerable to life cycling degradation than the liquid NaS system.



ITEM	MINI-TROUGH	MINI-CASSEGRAIN	MINI-PYRAMID
APHELION INSOLATION	1310 W/M <sup>2</sup>	1310 W/M <sup>2</sup>	1310 W/M <sup>2</sup>
SECONDARY BLOCKAGE	NONE	(-10%)	NONE
MODULE FRAME LOSS	(-2%)	(-2%)	NONE
PRIMARY ABSORPTION	(-8%)	(-8%)	NONE
SECONDARY ABSORPTION	NONE	(-8%)	NONE
LIGHT CONE LOSS	(-4%)	(-4%)	(10%)
ENERGY AVAILABLE AT CELL	1134	948	1179
ARRAY WING CONCEPT			
2 GIMBAL - NORMAL $\angle$	NONE	NONE	NONE
1 GIMBAL			
LEO 5° $\angle$	(-1%)	0	(-10%)
GEO 23° $\angle$	(11%)	0	(-50%)
END OF LIFE			
NORMAL	-15%	-25%	-8%
LEO	-15%	0	-8%
GEO	-15%	0	-8%
	963	711	1084
	953	0	976
	857	0	543
	1010	0	590
	1122	0	1061
	1134	948	1179

Figure 2-83. Geometrical Performance - 3 Mini-Concentrators.

Table 2-14. BOL Performance — Three Mini-Concentrators.

ITEM	MINI-TROUGH	MINI-CASSEGRAINIAN	MINI-PYRAMID
<b>G<sub>A</sub>A<sub>S</sub> SINGLE CELLS (16% <math>\eta</math> AT 80°C)</b>			
TWO GIMBAL NORMAL $\angle$	181 W/M <sup>2</sup>	152 W/M <sup>2</sup>	203 W/M <sup>3</sup>
ONE GIMBAL			
LEO 5° $\angle$	180	0	182
GEO 23° $\angle$	161	0	182
<b>TWO CELL (SANDWICH OR SPLIT SPECTRUM)</b> $\eta_1 G_A A_S = 15, 6; \eta_2 G_A A_S = 8$			
TWO GIMBAL NORMAL	260	218*	292*
ONE GIMBAL			
LEO 5° $\angle$	258	0	262
GEO 23° $\angle$	232	0	146
<b>MULTIBAND GAP — <math>\eta = 28\%</math>; CR = 5</b>			
TWO GIMBAL NORMAL	318	265	356
ONE GIMBAL			
LEO 5° $\angle$	314	0	320
GEO 23° $\angle$	282	0	178

\* SANDWICH ONLY

Table 2-15. Final Trades Support the Minitrough.

ITEM	MINI-TROUGH	MINI-CASSEGRAIN	MINI-PYRAMID
<b>CELL AREA AS A PERCENTAGE OF APERTURE AREA</b>	CR = 50 2%	CR = 50 - 125 1 - 2%	CR = 5 20%
<b>CELL COST — \$/WATT</b>			
ONE CELL (1985)	50 \$/W	50 \$/W	\$500/W
TWO CELLS (1985)	100 \$/W	100 \$/W	\$1000/W
MULTIBAND GAP (1990s)	10 \$/W	10 \$/W	\$100/W
<b>SECOND GIMBAL MASS WITH ATTITUDE CONTROL AND EXTRA STRUCTURE</b>			
10 MW RADAR	10,000 Kg	10,000 Kg	10,000 Kg
2.5 MW SCF	2,500 Kg	2,500 Kg	12,500 Kg

The thermal analysis of radiator sizing for the alternatives, conducted during this phase of the program, was based on the estimated waste heat radiation required, and on the use of heat pipes/radiators/non-fluid/non-pump components which are located directly adjacent to the energy storage modules radiator. Mass estimates were based on 3.2 Kg/M<sup>2</sup>, and on the Stefan Boltzman equation for the rejections temperatures specified in Table 2-18.

Table 2-16. Cost Comparison LEO Power Generation.

## 2.5 MW SPACE CONSTRUCTION FACILITY

	MASS OF POWER GENERATION SYSTEMS (kg)	AREA (M <sup>2</sup> )	CELL AREA (M <sup>2</sup> )	COST (\$M)	COST TO ORBIT (\$M)	COST OF ROUTINE MAINTENANCE	TOTAL COST (\$M)
PLANAR ARRAYS							
o SILICON	8,900	15,300	15,300	139	12	\$15M IN 10 YEARS	168
o GALLIUM ARSENSIDE	9,700	11,950	11,950	215	13	10 YEARS	230
o I.C. SILICON	39,790	30,600	30,600	194	52	\$15M IN 10 YEARS	267
o MGB**	15,100	10,300	10,300	295	20	10 YEARS	320
LARGE TROUGH							
MULTIBAND GAP**	55,000	10,000	200	135	85	\$10M 5 YEARS	230
RANKINE HYBRID	50,900	8,400	170	100	66	\$10M 5 YEARS	196
LARGE SPHERICAL THERMO PHOTOVOLTAIC*	26,900	5,000	500	50	35	\$25M 5 YEARS	160
SMALL MODULAR CONCENTRATORS							
TRUNDATED PYRAMID TWO CELL	40,700	10,200	2,000	60	52	-	112
MULTIBAND GAP**	34,000	8,600	1,700	44	44	-	88
MINI CASSEGRAIN TWO CELL	48,400	13,200	132	42	63	-	105
MULTIBAND GAP**	40,300	11,100	111	32	53	-	85
MINI TROUGH TWO CELL	22,100	11,500	230-600	40	29	-	69
MULTIBAND GAP**	18,200	9,300	230	40	24	-	64

\*SAFETY PROBLEMS LIQUID COOLING HIGH RISK.

\*\*HIGH RISK TECHNICAL BREAKTHROUGH REQUIRED.

Table 2-17. 10 MW GEO Radar Mass and Cost Estimates.

	MASS OF POWER GENERATION SYSTEMS (kg)	AREA (m <sup>2</sup> )	SOLAR CELL AREA (m <sup>2</sup> )	COST (\$M)	COST TO LOW EARTH ORBIT (\$M)	COST OF ROUTINE MAINTENANCE (RADIATION)	LIFE CYCLE TOTAL (\$M)
PLANAR ARRAYS							
GaAs	31,100	49,000	49,000	423	40	SMALL	473
SILICON	81,300	104,000	104,000	348	105	\$30M EVERY 5 YEARS	453
MULTIBAND GAP**	61,200	36,000	36,200	585	80	SMALL	665
LARGE TROUGH							
MULTIBAND GAP**	220,000	40,500		298	286	SMALL	584
RANKINE HYBRID <sup>1</sup>	DATA NOT GENERATED	ELIMINATED BECAUSE OF LEO SCF CALCULATIONS					
LARGE SPHERICAL THERMO- PHOTOVOLTAIC	109,000	20,000	1,000	200	142	\$342 5-10 YRS	684
SMALL MODULAR CONCENTRATORS							
TRUNCATED PYRAMID							
TWO CELL	160,000	40,800	8,200	180	210	SMALL	390
MULTIBAND GAP**	136,000	34,000	6,800	150	172	SMALL	322
MINI CASSEGRAIN							
TWO CELL	192,900	53,000	530	90	250	SMALL	340
MULTIBAND GAP**	160,000	44,500	440	80	210	SMALL	290
MINI TROUGH							
TWO CELL	101,000	51,000	1,020/ 2,400	90	132	SMALL	222
MULTIBAND GAP**	79,500	41,500	830	100	103	SMALL	203

\*\*HIGH RISK -  
REQUIRES TECHNOLOGY  
BREAKTHROUGH

Table 2-18. Costs and Benefits of Alternative Energy Storage Options.  
 (2.5 MW SPACE CONSTRUCTION FACILITY)  
 700 KW HR STORAGE (25% RESERVE CAPACITY)

Option	Energy Storage Option					Storage Radiator Impact		
	Initial Mass (kg)	Initial Component Cost (\$M)	Initial Transportation Cost (\$M)	20 Year Replacement Cost (\$M)	Projected Life (Yr/DoD)	Mass (kg)	Radiator Component/Transportation Cost (\$M)	Rej. Temp. (°C)
Nickel Cadmium	35,000	6.3	45.5	155.4	5/35%	800	0.65 1.05 } 1.7	-5
Present Sodium Sulfur	7,000	10.5	9.1	372.4	1	30	.1 .04 } .14	340
Long Life (5 Yr.) Sodium Sulfur	7,000	10.5	9.1	58.5	5/35%	30	.1 .04 } .14	340
Nickel Hydrogen	23,000	13.9	30.0	87.8	7/35%	525	0.5 0.65 } 1.15	10
Silver Hydrogen	14,000	19.5	18.2	722.0	1/40%	650	0.55 0.85 } 1.4	10
H <sub>2</sub> O <sub>2</sub> Fuel Cell	11,500	71.5	15.0	103.8*	7*/75%	1525	0.9 2.0 } 2.9	90
Flywheels	17,500	18.6	23.0	5.0	20/75%	200	0.3 0.45 } 0.75	60

Option	Expected Efficiency	Incremental Array Impact			Total System		Total System	
		Size (kW)	Cost (\$M)	Mass @ 100 W/kg	Initial Cost (\$M)	Initial Mass (kg)	L.C. Cost	L.C. Mass
Nickel Cadmium	0.8	820	41.2	8,200	95	44,000	250	150,000
Present Sodium Sulfur	0.8	820	41.2	8,200	60	15,000	430	148,000
Long Life (5 Yr.) Sodium Sulfur	0.8	820	41.2	8,200	60	15,000	120	36,000
Nickel Hydrogen	0.83	790	39.5	7,200	80	31,000	170	77,000
Silver Hydrogen	0.8	820	41.2	8,200	80	23,000	800	289,000
H <sub>2</sub> O <sub>2</sub> Fuel Cell	0.5	1320	66.0	13,200	160	26,000	260	40,000
Flywheels	0.85	780	39.0	7,800	85	25,500	90	25,500

NOTE:  
 Life cycle costs and mass are for 20 year life.

\* Assumes 60% replacement of component (cost and weight) per 7 years.

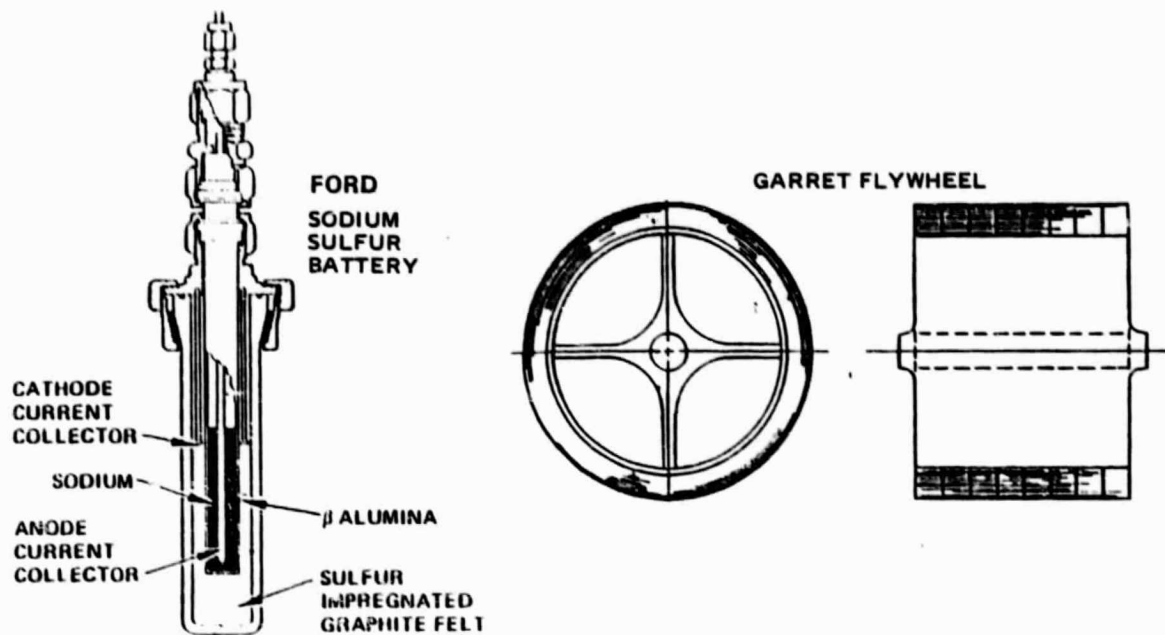


Figure 2-84. Energy Storage - Flywheels and Sodium Sulfur Batteries Could Support 30,000 - 120,000 LEO Cycles over 20-Year Life

During earlier studies of electronics modularity (Reference 31), the recommended level of modularity for advance power system components was between 8-20 modules. This recommendation is based on the conclusions that:

- a. Low levels of modularity (from 2 or 3 up to 6 or 7) cost and weigh more, since the total system capability is significantly over-designed. For example, for a prime/backup 2-module configuration, the backup weighs and costs as much as the prime.
- b. Very high levels of modularity (100 plus 1 spare) are complex and require complex control, which itself may defeat the intended redundancy, and are therefore, more excessive and expensive than lower levels.

At the recommended modularity level of around 10, the cost and mass of spare modules is only 10% or so of the total cost, and the system should be manageable. Based on this approach, the modularity of the Flywheels was established by partitioning the storage requirement into approximately 10 modules on the two array wirings, so that acceptable cost and reliability would result. At this modularity level, each module would have an energy storage of 75 KWHR. For multiple rim flywheels made from Kevlar<sup>R</sup> 49 (Reference 32 and Figure 2-84), the diameter of each flywheel was calculated to be slightly under 2 meters. This sizing is then compatible with shuttle payload bay geometry.

Sodium Sulfur modularity sizing was based on preliminary sizing done by Hughes under study to the Air Force (Reference 33). Again, a 25 KWHR modularity is feasible, three in parallel would provide a 75 KWHR module.

**2.3.5.3 Power Management System Modularity.** The Power Management and Control System Preliminary Concepts developed during Task II of this contract were inherently modular initially conceived. During this portion of the task several modularity alternatives were examined to estimate their potential benefits. They were:

- a. A hybrid approach with DC ion engine beam power supplied directly from the photovoltaic array modules, and with DC/AC/DC converters for discharge power and user power. The Space Radar Illuminator Block Diagram was shown in Subsection 2.2, Figure 2-73. The Space Construction Facility Block Diagram is shown in Figure 2-85.
- b. An all AC system, with AC-AC-DC converter modules for the ion engine beam supply, using 10 or 20 KW modules compatible with the 50 CM 5000 ISP ion engines.
- c. A variation of this all AC system, with larger 250 KW modules. This level of modularity could save some mass and cost, since complexity might be decreased or fewer spares required.

The results of this analysis activity were that the first approach with the 900 Vdc beam power supplied on array appears to be more attractive than the others, from a mass and cost standpoint.

It should be emphasized that the safety issue associated with 900 Vdc power distribution and array voltages must be resolved satisfactorily, and that the ion engines themselves must be able to accept delta regulation of the beam voltage (switched banks of solar cells) with a step size of approx. 10-20 volts.

As described in Subsection 2.2, the Task II system synthesis considered AC and DC power distribution and power components approaches. The AC distribution voltage was set at 1,000 Vac, the DC one at 750 volts based on a previous power management study activity (Reference 34). During Task III, the AC and DC approaches developed in Task II were amended to minimize system mass while at the same time providing a safe, maintainable system. Alternate voltages were considered.

A review of future ion engine concepts (Reference 35), indicates that the ion engine Screen Beam Supply consumes approximately 75% of the power delivered to the engine. During Task III, configurations for both the AC and DC system were considered which provide beam power directly from the solar array. Specifically, calculations of the argon ion engine beam voltage  $V_B$ , using the equations developed in Reference 9, showed that for a 50 cm, argon 5,000  $I_{sp}$  engine,  $V_B$  was 900 Vdc. In Reference 36, it was shown that this power is used as the engine screen supply,

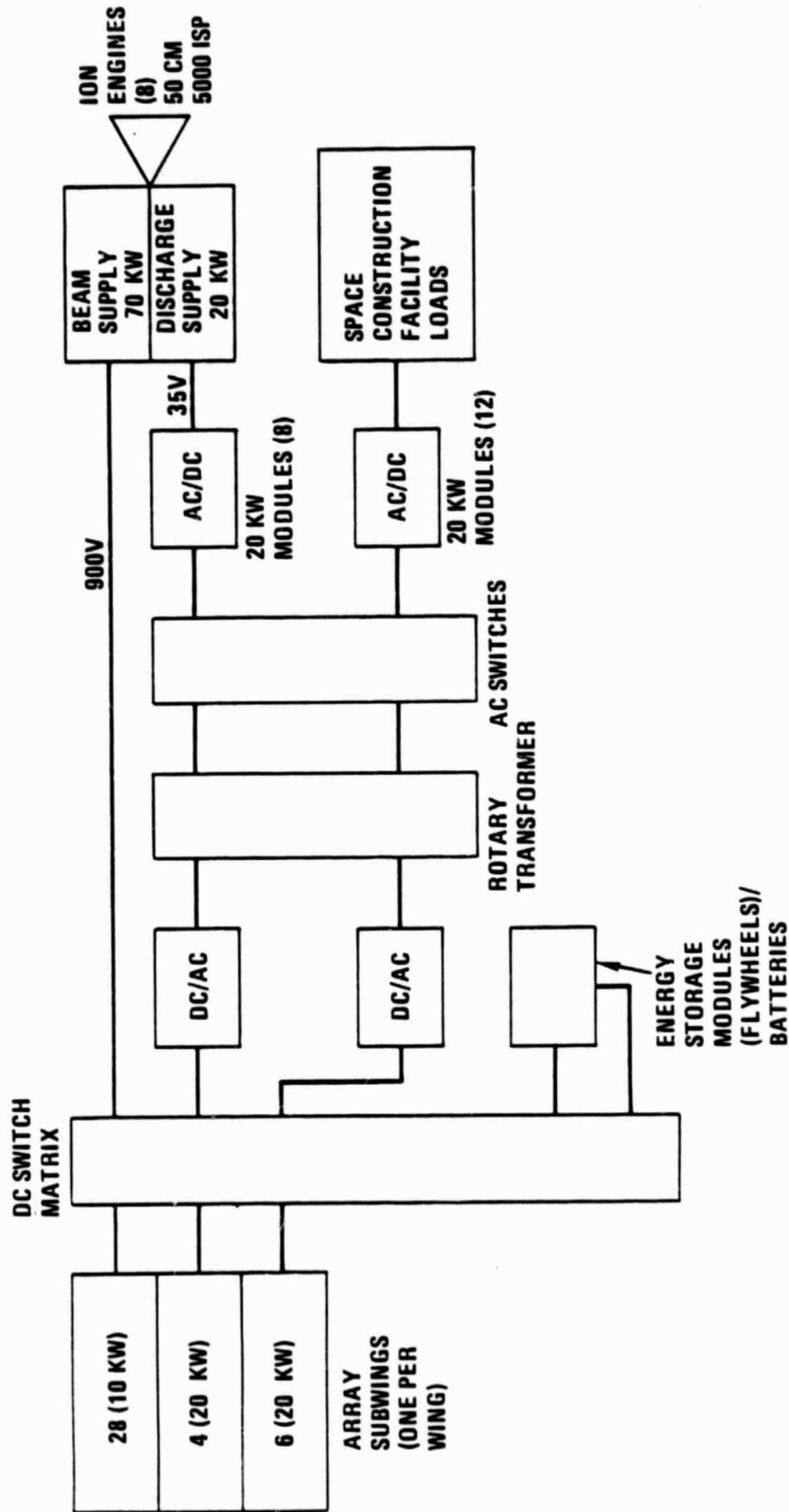


Figure 2-85. Hybrid Power Management and Control Block Diagram — LEO SCF System.

and must be isolated and, for the 30 cm Mercury engine, regulated to  $\pm 3\%$ . For this study, it was assumed that:

- a. Beam current varies linearly with  $V_B$ : therefore, variations in array voltage and current drive capability vary engine  $I_{sp}$  and do not adversely affect ion engine performance, or, at the worst, require additional ion engine control strategies. This implies that the 3% requirement can be met by switching in-array voltage modules of about 2.5% of the desired beam voltage. A group of four modules would provide 10% control.
- b. The solar cells on the photovoltaic array will be isolated and therefore can easily be connected to ion engine cathode and neutralizer cathodes without adverse effects on ion engine performance.
- c. Plasma interaction with the ion engine screen supply beam voltage will be acceptable, i.e., +DC from the array should directly provide the net accelerating voltage of +900 Vdc for the ion engines without significant arcing or losses. The solar cell array should probably have the potential characteristics shown in Figure 2-86. With these characteristics, the gradients on the array do not have step functions but are as continuous as possible, minimizing arcing potential.

In Reference 22, Appendix 2, a postulated plasma potential for an insulated array was developed. It was noted that arcing probability was a function of geometry, array voltage, and dynamic plasma interactions. Analysis of the geometries of the arrays and plasmas dynamics for the multiple power systems and array configurations considered was outside of study scope. However, it should be noted that a 900 V array gradient has a higher arcing risk because of increased potential gradients between the concentrator mirrors and solar cells and this may require acceptance of a lower voltage system with its mass penalties.

Based on these assumptions, the remaining studies of optimum transmission voltage, modularity levels, and safety were then carried out.

2.3.5.3.1 Safe and Minimum Loss Distribution Voltage. Three possible distribution voltage ranges were considered. A 900 Vdc level satisfies the need for a level compatible with the 5000 sec.  $I_{sp}$  argon ion engine screen supply. It also reduced resistance transmission line losses. It raises safety questions; special conduits may be required. Very low voltages (30 volts) would permit simple DC regulators for such requirements as the ion engine discharge supply but have excessively high resistance losses. For example, the mass penalty of the optimal transmission line at 30 Vdc was calculated for the 10 megawatt radar to be 30,000 Kg for the discharge supply alone. This is too large to be viable. A medium voltage range between 250-350 volts appears to represent a middle ground.

ORIGINAL PAGE IS  
OF POOR QUALITY

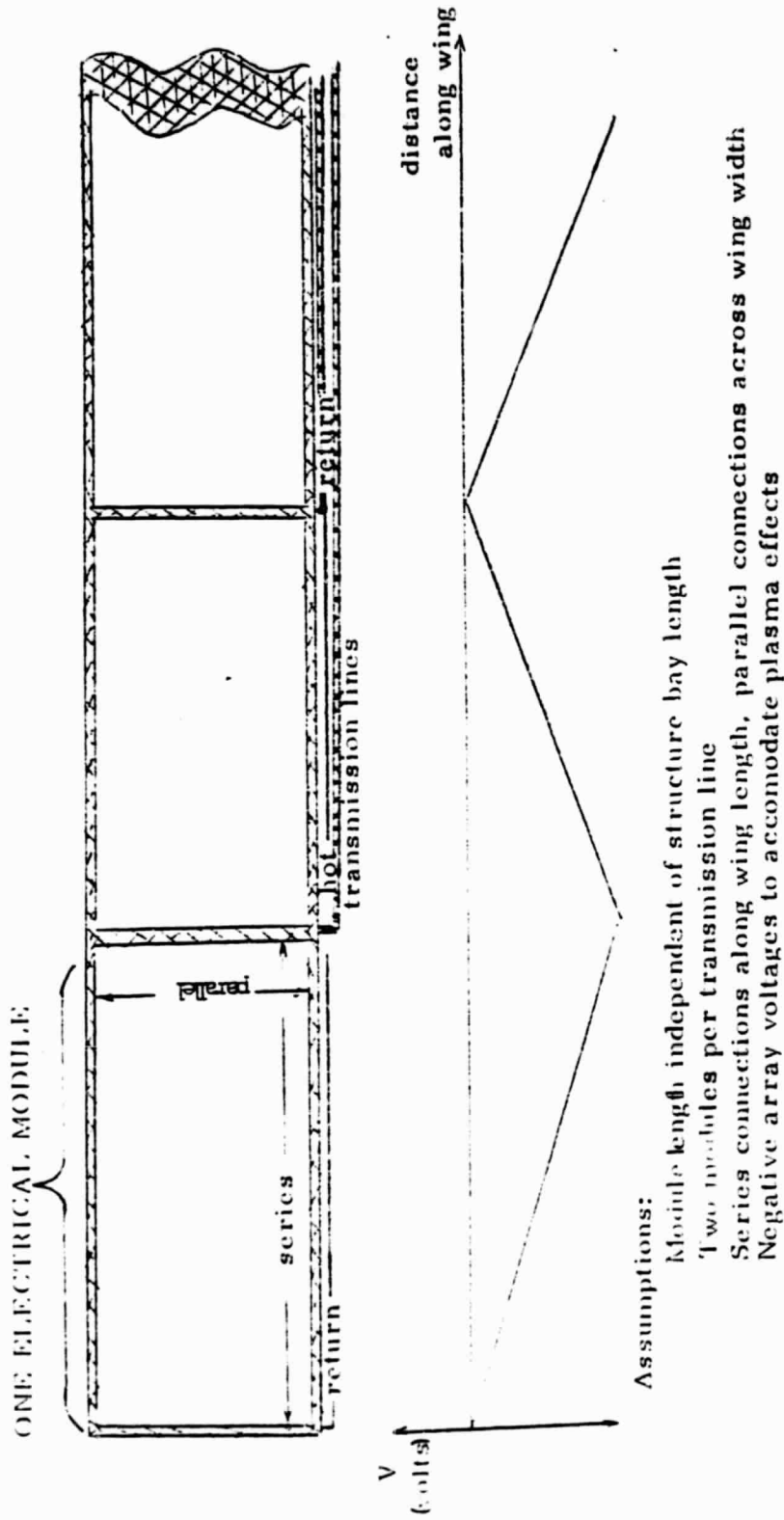


Figure 2-86. Suggested Potential Distribution.

Therefore, the range of voltage levels considered for array power collection and power distribution purposes were 300 and 900 Vdc and 300 and 900 Vac. The 300 volt DC and AC levels are presumed to be nonlethal when shrouded with "Romex" type protective sheath, have a low arc probability, and minimize plasma losses. However, they increase transmission line mass.

The 900 volt level is presumed lethal and requires a conduit. This conclusion is one of the most judgemental in the study. If astronauts wear insulating and indestructible gloves and if it could be concluded that no safety hazard exists because of the high voltage, since lethality is shown to be more a function of current than voltage, then lethal current flow would not be possible through these gloves and the benefits of higher voltage would be increased. However, after due consideration, it was decided that it is necessary that DC and AC systems in the 1 kV range of interest compatible with the 5000 sec. argon engine  $I_{sp}$  require conduit shielding; therefore, the mass of that conduiting around the transmission lines was added to the trade between the high and low voltage approaches.

In developing the mass properties of the two systems, both 1 kv systems (ac and dc) were penalized by adding the mass of conduit to the total system weight. The dc configuration used 2-inch-diameter conduit, 0.1-inch thick. The ac system, because of the hollow 2-inch-diameter center conductor, used 4-inch-diameter conduit.

Mass of the conduit for the dc systems is approximately the same as the mass which the return would have if the system did not employ a conduit. Specifically, each of the 108-Radar ion engines required 8 kg of center conductor and 8 kg of conduit, a total of about 1728 kg. For an ac system, the conduit mass with twice the diameter was four times as large, a penalty of about 2800 kg.

In this study, the mechanical configurations and geometry of the 2.5 mw space construction facility and 10 mw radar were developed as part of Task II. The geometry of the SCF was assumed to be identical to the geometry of the Space Platform studied in Reference 14, except for increased array sizing and its resultant path length increase. The geometry of the radar was developed to provide symmetrical spacecraft mass distribution and symmetrical rotations of array wings as the spacecraft rotates around the earth. Transmission cable lengths of 100 and 100 meters compatible with these geometries were then used to calculate losses.

2.3.5.3.2 PMS Modularity Levels for the Two Spacecraft. The 10 megawatt radar and the one megawatt average power (2.5 mw array) space construction facility both would utilize modularized power management systems. The modularity provides redundancy in the event of a failure and allows the power management system to better match the ion engine power requirements. For example, the 50 cm diameter argon ion engine thrusters require a 20.2 kW discharge supply for an  $I_{sp}$  of 5000. A module size of 20 kW can interface with the one engine and meet this need. In presenting the final power management masses, the module size was therefore used.

Calculations of the penalties of this sizing, compared to "optimal" sizing, indicate insignificant differences for the SCF facility. The 10 mw radar also was only slightly affected by this choice, at least for modules in this power range.

For these calculations, the characteristics of these modules, the DC regulators, the DC/DC, DC/AC, AC/DC converters were predicted from specific weight vs. power curves based on data developed for NASA on Contract NAS3-21757 (Reference 14). For the AC system calculations, rotary transformers mass is included in the primary drive module mass. The cost analysis was also based on the equation relating cost and mass developed in that study.

$$\text{COST} = 0.005 (\text{MASS}/2.2)^{0.921}$$

where cost is in millions of dollars and M = mass in kg.

A learning curve equation was used to estimate total cost.

$$\text{TOTAL COST} = \text{MODULE COST} (0.6 \times 0.85^{\text{NUMMOD}} + 0.4 \times \text{NUMMOD})$$

where NUMMOD = the number of modules

The modularity of the system was allowed to vary in two ways. First, the two solar panel wings were assumed to be modularizable at a level of from one to 10, and then each subwing is assumed to modularize at a level of from one to 10.

As previously discussed, alternative voltage levels were also considered, Fortran programs were then used to calculate the system masses and costs for the various alternate configurations.

**2.3.5.3.3 Conclusions - PMS Modularity.** The net effect of all these considerations was to make this AC system and the DC system have almost identical masses for the new configurations. See Table 2-19. It also shows the additional weight of several alternative topologies. (See Figure 2-87.) If an all AC system is used on the LEO SCF, the added regulator mass for, Beam regulators is about 2600 Kg, so is the mass of beam DC regulators for the DC system. The Radar column also shows similar deltas for Radar Alternative. The other two options are an all DC system with DC-DC converter for Ion Discharge supply does add some mass to the Radar, because of the duplicated DC to AC regulator section. Because the masses are approximately the same, the eventual selection process is likely to concern itself with other considerations. These include those discussed previously—namely, the ability to design DC overload protection circuitry which will not either fail to provide protection or require excessive mass, and the ability to be able to ever close the high power, high voltage DC components gap.

For the AC version of the SCF PMS, AC drivers provide AC to the facility and ion engine AC/DC supplies. For the DC version, DC-to-DC converters provide this function. DC distribution was at 900 Vdc, AC at 300 volts AC. DC required safety conduiting; AC did not.

Table 2-19. Comparison of Alternative Power Management Options

TOPOLOGY	LEO SPACE CONSTRUCTION FACILITY	GEO 10 MW SPACE RADAR
HYBRID AC-DC		
SPLIT INVERTER MASS*	1770 Kg	43,200 Kg
NO. OF MODULES/SUBWINGS	10 + 1 SPARE	27 + 2 SPARES
NO. OF SUBWINGS/WING	1	9
NO. OF WINGS	2	2
P.M. MODULE SIZE(S)	20 KW	20 KW
ARRAY MODULE SIZE	10 KW	10 KW
MASS OF TRANSMISSION LINES	60 Kg	2040
ARRAY MASS FOR LINE LOSSES	30	2410
TOTAL MASS	1860 Kg	47,650 Kg
OTHER ALTERNATIVES	IMPACT ON SYSTEM MASS	IMPACT ON SYSTEM MASS
1. ALL AC (900 VAC) WITH ION BEAM CONVERTERS	+ Δ 2600	+ Δ 14,500 Kg
2. ALL DC (900 VDC) WITH DISCHARGE CONVERTERS ONLY	SMALL DELTA	+ Δ 4,100 Kg
3. ALL DC WITH BEAM CONVERTERS	+ Δ 2600	+ Δ 29,000 Kg
4. WITH 250 KW MODULE SIZE AND MULTIPLE LOADS	NOT APPLICABLE	- Δ 500 Kg
* SPLIT INVERTER MASS INCLUDES ARRAY MASS FOR INVERTER LOSSES AND ARRAY SWITCHING.		

- ALL AC SYSTEM - 300 VAC DISTRIBUTION**
- EXTRA CONVERTERS FOR ION ENGINE BEAM SUPPLY ADD 14,500 KG
  - FALL BACK IF DC FAULT ISOLATION FAILS
- AC SYSTEM WITH 40 LARGER 250 KW MODULES FOR RADAR/DISCHARGE**
- REQUIRES MULTIPLE (12) LOADS/MODULE
  - SAVES 500 KG BUT MULTIPLE LOADS ON EACH MODULE DEGRADE REDUNDANCY

- ALL DC SYSTEM WITH ON ARRAY REGULATION**
- EXTRA HALF-CONVERTERS FOR ION ENGINE DISCHARGE SUPPLY
  - ADD 4100 KG
- ALL DC SYSTEM WITH DC CONVERTERS FOR ION DISCHARGE AND BEAM SUPPLIES**
- ADD 4100 KG + 29,000 KG

- MASS USING + 35 VDC DISTRIBUTION ADDS APPROXIMATELY 12,000 KG**
- 900 VAC DISTRIBUTION TO DISCHARGE SUPPLIES AND RADAR**
- ADDS 6200 KG FOR SOLID SHIELD
- 300 VDC DISTRIBUTION ADDS 3000 KG**

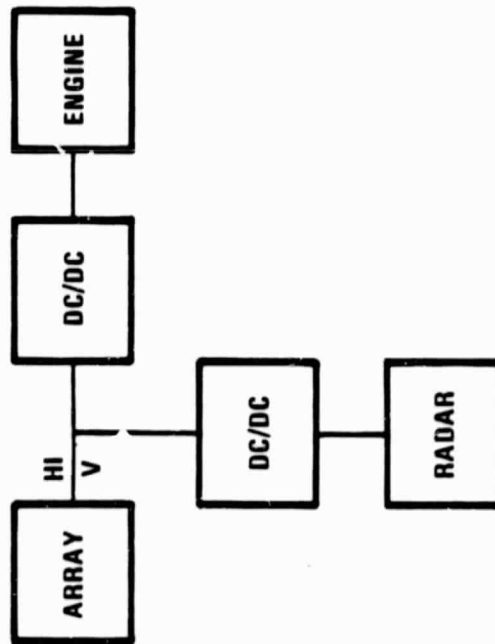
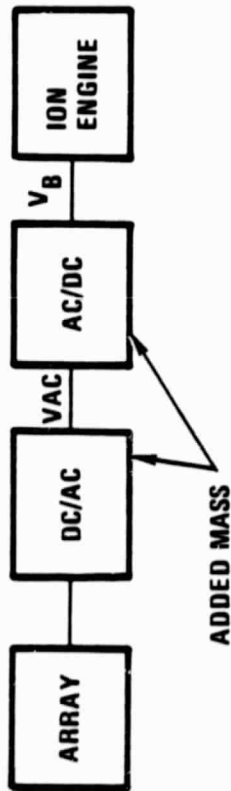


Figure 2-87. GEO Mission - Radar Power Management and Control Approaches.

## 2.4 TECHNOLOGY RECOMMENDATIONS

This part of the study was performed as shown in Figure 2-88.

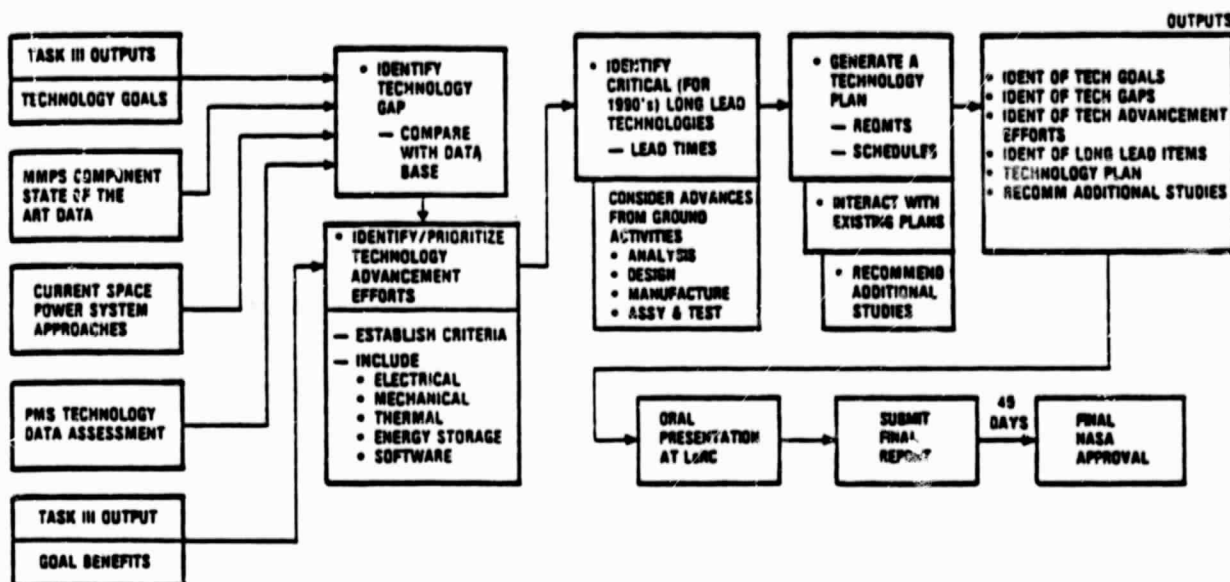


Figure 2-88. Technology Recommendations

**2.4.1 POWER GENERATION TECHNOLOGY GAP IDENTIFICATION.** The technology gaps in Photovoltaic power generation whose closure will provide significant technology benefits are listed in Table 2-20, beginning on Page 2-140. Specific recommendations are being made to close a gap in robotic beam builder development. The remaining needed technology activities associated with multiband gap cells and low light loss modular concentrator development are expected to be closed for lower power systems in the 1980s. Of course, should this expected development not occur as planned, backup plans for 2 cell modular low loss concentrators should be implemented.

**2.4.1.1 Power Management and Control.** As discussed in Section 2.3.3, NASA's on-going AC power management technology program, coupled with the technology goals recommended in Reference 14, cover the required multimegawatt technology gaps uncovered by this study. Two areas still require additional attention. Present concepts for a 25 KW axially-wound rotary joint are not viewed as maintainable. Therefore, a technology gap exists in this area for manual/maintainable spacecraft such as the radar and SCF missions. This assumes that the gaps which Ref. 14 recommended closing are indeed closed in accordance with the recommendations of that study.

The second gap involves switching components capable of switching the high power AC and DC power modules.

**2.4.1.2 Energy Storage.** For LEO applications like the Space Construction Facility, the high specific energy of Sodium Sulfur and the long life of flywheels make both technologies attractive. The Air Force is studying the development of Sodium Sulfur systems, but corrosion of the present steel containers limits life. There exists a technology gap which should be addressed - the testing of cells utilizing protective chromium, molybdenum, or rutile titanium dioxide coatings.

For LEO applications like the Space Construction Facility, the mass, cost, reliability, and life advantages of flywheel energy storage elements were developed in Task III, laboratory data on motor generators, and analysis of magnetic bearings all appear to offer potential advantages and benefits of enough significance to warrant development for space applications. The last activity in this area (Ref. 21) appears to have been completed in 1974, with no ongoing effort now taking place. This study recommends that this gap be closed for multimegawatt systems. It further recommends study at lower system power levels, since the results will probably downscale to systems below one MW.

**2.4.2 TECHNOLOGY REQUIREMENTS DEFINITION.** The technologies requirements crucial to enabling multimegawatt space power systems have been identified and documented in a format which provides the information required to prepare a technology plan to enable Multimegawatt Space Power Systems in the 1990s. Appendix B of the final report provides the data for NASA planning purposes.

**2.4.3 CRITICAL LONG LEAD TECHNOLOGY IDENTIFICATION.** The long lead items identified in this study were for power generation:

- a. The low loss concentrator - which should begin development now for use in lower power systems.
- b. Multi-bandgap cell technology for concentrators, now underway with planned availability for environmental, life, and automated assembly development in the next five years.
- c. The robotic beam builder - which requires some seven years to first flight and another three to achieve operational status in space.
- d. Backup two-cell concentrators.

Appendix B summarizes the expected plans/lead times which should occur if development is to proceed to meet 1990s availability.

For power management, the plan for the rotary transformer development, along with the list of required technologies being developed for lower power levels is given in Appendix B.

The plan for primary Sodium Sulfur battery and flywheel and energy storage approaches is given in Appendix B. This development should also be considered for lower earth orbit missions in the 50-900 KW class.

Table 2-20. Technology Gap Identification.

## MULTIBANDGAP CELL PLANAR ARRAYS

Description of Gap	Technical Approach to Gap Closure	Will Gap readily close without special Multimegawatt planning?		Benefit of Closure	Will this study plan a Gap closure and justification for this plan?	Justification
		Yes - if the basic technical	No			
Multi-bandgap cells for Planar Arrays 300 $\mu\text{m}$ thick, weldable	Continued analysis, fabrication, and test of Multi-bandgap cell approaches.	Yes - if the basic technical	No	Small - these cells are too massive for planar array usage - and 50 $\mu\text{m}$ thickness will have low yields - with prohibitive costs.	No	These cells should be used in concentrators where their mass is much less significant.
<ul style="list-style-type: none"> <li>● Robotic Truss Beam Builder</li> </ul>	Beam Builder development	No	No	Low mass trusses (1 kg/m)	Yes	Beam Builder will be useful for both planar arrays and concentrators.
<ul style="list-style-type: none"> <li>● Robotic Blanket Module positioning and tensioning machine.</li> </ul>	Blanket Installer development	No	No	Enables Large Planar Array Construction	No	Benefits of concentrator greater.

Table 2-20. Technology Gap Identification (cont)

MODULAR CONCENTRATOR DESIGN

Description of Gap	Technical Approach to Gap Closure	Will Gap readily close without special Multimegawatt planning	Benefit of Closure		Will this study plan a Gap closure and justification for this plan	
			Benefit of Closure	Benefit of Closure	Plan?	Justification
<ul style="list-style-type: none"> <li>Optimized geometry for low light loss and low temperature combined with high specific power.</li> </ul>	Conduct a computerized optimization with all requirements specified.	Yes	For Multimegawatt Systems, solar cell areas and their associated costs are minimized by modular concentrators.	Lower power technology planning should develop these concepts in the 1980s but recommended to ensure this occurs.	Yes	Lower power technology planning should develop these concepts in the 1980s but recommended to ensure this occurs.
<ul style="list-style-type: none"> <li>Robotic Truss Beam Builder</li> </ul>	Beam Builder development	No	Low Mass Trusses	Beam Builder will not be required for lower power, deployable truss satellites; therefore, it is recommended for this system.	Yes	Beam Builder will not be required for lower power, deployable truss satellites; therefore, it is recommended for this system.
<ul style="list-style-type: none"> <li>Ground Manufacturing Process Development - Concentrator Modules</li> </ul>	Automatic Layout/Fabrication and coating of mechanical modules.	Yes	For Multimegawatt Systems, solar cell areas and their associated costs are minimized by modular concentrators.	Lower power technology planning should develop these concepts in the 1980s but recommended to ensure this occurs.		Lower power technology planning should develop these concepts in the 1980s but recommended to ensure this occurs.

Table 2-20. Technology Gap Identification (cont)

## GALLIUM ARSENIDE PLANAR ARRAYS

Description of Gap	Technical Approach to Gap Closure	Will Gap readily close without special Multimegawatt planning	Benefit of Closure	Will this study plan a Gap closure and justification for this plan	
				Plan?	Justification
<ul style="list-style-type: none"> <li>Weldable 50 <math>\mu\text{m}</math> Gallium Arsenide Cell Development</li> </ul>	Material deposition and welding process development	Yes - if the technical problem can be solved	<p>20-year life achievable</p> <p>Some low mass missions enabled (Fast Electric Transfer Mission)</p>	No	Earlier activity should close this gap.
<ul style="list-style-type: none"> <li>Robotic Truss Beam Builder</li> </ul>	Beam Builder development	No	Enables Multi-megawatt power	Yes	Since the Beam Builder may not be required for the lower power satellites, it must be planned here for these large systems.
<ul style="list-style-type: none"> <li>Robotic Blanket Module Positioning and Tensioning Machine</li> </ul>	Blanket Installer development	No	Enables Large Planar Array Construction	No	Benefits of concentrator greater. Tug blankets would be deployed under astronaut control.

Table 2-20. Technology Gap Identification (cont)

SILICON PLANAR ARRAYS  
SPACE QUALITY AND "LOW COST" QUALITY

Description of Gap	Technical Approach to Gap Closure	Will Gap readily close without special Multimegawatt planning	Will this study plan a Gap closure and justification for this plan	
			Benefit of Closure	Plan? Justification
<ul style="list-style-type: none"> <li>Annealable silicon cell development.</li> </ul>	Defect removal to permit an array annealing.	Yes - if the technical problem can be solved.	20-year life achievable with on-array annealing.	No Cost benefits of concentrators, even with defect removal, are greater.
<ul style="list-style-type: none"> <li>Weldable 50 <math>\mu\text{m}</math> silicon cell development.</li> </ul>	Material deposition and welding process development.	Yes - "	20-year life achievable.	No "
<ul style="list-style-type: none"> <li>Robotic Truss Beam Builder</li> </ul>	Beam builder development.	No	Low mass trusses	Yes Beam builder will not be required for lower power, deployable truss satellites. Useful for concentrators.
<ul style="list-style-type: none"> <li>Robotic Blanket Module positioning and tensioning machine.</li> </ul>	Blanket installer development.	No	Enables Large Planar Array Construction	No Cost benefits of concentrator greater.

Table 2-20. Technology Gap Identification (cont)

MODULAR THERMOPHOTOVOLTAIC CONCENTRATORS

Description of Gap	Technical Approach to Gap Closure	Will Gap readily close without special Multimegawatt planning		Will this study plan a Gap closure and justification for this plan	
		Benefit of Closure	Plan?	Justification	
Thermophotovoltaic Concentrators are in their initial conceptual design phase. Many unanswered questions remain.	Conduct and document studies which evaluate total overall system losses with an analytical model of system geometry and thermal properties.	No	No	The existing performance prediction for thermophotovoltaic systems is very optimistic. However, even if the real systems could hold losses to an optimistic 70%, limited receiver life would be a problem.	The life limitation is too great a constraint.

Table 2-20. Technology Gap Identification (cont)

## MULTIBANDGAP CELL PLANAR ARRAYS

Description of Gap	Technical Approach to Gap Closure	Will Gap readily close without special Multimegawatt planning	Will this study plan a Gap closure and justification for this plan	
			Benefit of Closure	Plan? Justification
Multibandgap cells for Planar Arrays 300 $\mu\text{m}$ thick, weldable	Continued analysis, fabrication, and test of Multibandgap cell approaches	Yes - if the basic technical problem with the tunnel current can be solved.	Small - these cells are too massive for planar array usage - and 50 $\mu\text{m}$ thickness will have low yields - with prohibitive costs.	No These cells should be used in concentrators where their mass is much less of a factor.
● Robotic Truss Beam Builder	Beam Builder development	No	Low mass trusses	Yes Useful for concentrators. Beam Builder will not be required for lower power, deployable truss satellites.
● Robotic Blanket Module positioning and tensioning machine.	Blanket Installer development	No	Enables Large Planar Array Construction	No Benefits of concentrator greater.

Table 2-20. Technology Gap Identification (cont)  
LARGE APERTURE PARABOLIC CONCENTRATORS

Description of Gap	Technical Approach to Gap Closure	Will Gap readily close without special Multimegawatt planning	Benefit of Closure	Will this study plan a Gap closure and justification for this plan	
				Plan?	Justification
Accomplish further conceptual studies of Large Parabolic Concentrator for High Concentration Systems, with Pure Photovoltaics or Hybrid Photovoltaic/Rankine Combined Rotating Unit Power Generation Systems.	Further studies to establish life limits of Turbines, true meteroid reliability values for contained liquid and gas portions of the system.	No	Although the system might be as efficient as small modular photovoltaic concentrators, they are much more complex and massive. They are also not as testable terrestrially. Their rotating unit angular momentum also would require unaccepted control.	No	The liabilities of Large Concentrators outweigh their benefits. They are: 1. Costly. 2. Massive. 3. Not terrestrially testable. 4. Concentration limited. They might: Obscure the cell/mirror surfaces as they leak dust if they used advanced radiators concepts such as the vapor drop radiator.

Table 2-20. Technology Gap Identification (cont)

SODJUM SULFUR BATTERY

Description of Gap	Technical Approach to Gap Closure	Will Gap readily close without special Multimegawatt planning		Will this study plan a Gap closure and justification for this plan	
		Benefit of Closure	Benefit of Closure	Plan?	Justification
Sodium Sulfur Batteries have the potential for 100 or more Wt-hrs/Kg, if the crucial container corrosion problems can be solved.	Use of rutile titanium dioxide, molybdenum, or chromium platings.	Yes	High cycle life, high specific energy, energy storage systems.	Yes	Although activity is under way, it needs more emphasis to assure its eventual success.

Table 2-20. Technology Gap Identification (cont)  
HIGH SPECIFIC ENERGY FLYWHEEL

Description of Gap	Technical Approach to Gap Closure	Will Gap readily close without special Multimegawatt planning	Will this study plan a Gap closure and justification for this plan	
			Benefit of Closure	Plan? Justification
Inertial Energy Storage System with a specific energy of 40 Wt-Hr/Kg which combines the functions of Energy Storage, Solar Array Wing Attitude Control, and Wing Binding Mode Damping	Use of two counter-rotating Dual Rim Kevlar 49 or 29 wheels, with a 1 Hz frequency response. The approach should also provide added safety/immunity to catastrophic failure.	No - Lower power systems tend to have shorter lives, making the benefits less significant.	Yes	Benefits significant. Closure should be accomplished.

Table 2-20. Technology Gap Identification (cont)

## HYBRID POWER DISTRIBUTION

Description of Gap	Technical Approach to Gap Closure	Will Gap readily close without special Multimegawatt planning	Benefit of Closure	Will this study plan a Gap closure and justification for this plan	
				Plan?	Justification
Three Phase 250 VAC Power Distribution and Switching Sys. with 25 KW module sizes and "ROMEX" overshield.	Development of 25 KW split AC power system.	Yes	Safe 5000 ISP ARGON ION Engine 900V beam voltage enabled. Solid-state fault detection and isolation system enabled for low fault risk.	No	Gap will close for 250 KW systems anyway.
Three Phase 250 VAC power distribution and switching sys. with 250 KW modules	Development of 250 KW system modules.	No	Three-phase to two-phase failure tolerance mass and cost savings. Cost lower than DC system.	No	Benefits of 300 kg offset by higher costs.
900 VDC power distribution system with switched DC ion drive and either DC/DC converters or DC/AC/DC for radar power/SCF power.	High voltage fault protection and switching circuitry development on array regulation for ion engine beam.	No	Lowest mass system for unmanned/non-maintained vehicles. Mass savings: 10 MW Radar 9,000 Kg 2.5 MV SCF 1,600 Kg Cost higher for first article.	Yes, but	High voltage lethality a critical safety issue for astronaut maintained and tested systems.

Table 2-20. Technology Gap Identification (cont)

DC POWER DISTRIBUTION

Description of Gap	Technical Approach to Gap Closure	Will Gap readily close without special Multimegawatt planning	Will this study plan a Gap closure and justification for this plan	
			Benefit of Closure	Justification
900 VDC system with 1 mm Al conduit overshield and fault tolerance/redundancy.	Develop a safe conduit system which serves also as the Ground Return.  Develop switches for high voltage control at 900 VDC 72 KW ( 100 Amps) switches must not run away thermally at overload.	No	Yes	The high voltage safety issue is not severe for unmanned GEO systems.
		No	Yes	The mass of the system is slightly less than 300 VDC systems - and the safety issue is not severe for unmanned GEO systems.

### SECTION 3

#### CONCLUSIONS

This study looked at missions for the 1990s which might require multimegawatt power levels. Two missions were selected for study: a GEO air traffic control radar illuminator and a LEO space construct facility. The GEO radar appears to be beneficial because of its ability to provide a terminal region redundancy at low cost. One system with a moderate amount of additional capacity can back up the entire CONUS and, with two satellites, the entire U.S. is redundantly covered using the minimum number of orbit slots. The LEO Space Construction facility provides a base for assembly and test of the two radar satellites, as well as the potential for assembling an electrical orbital transfer vehicle. For both missions, argon ion engines were found to have significant benefits for stationkeeping (LEO) and orbital injection (LEO to GEO).

The study also developed beneficial approaches for concentrating photovoltaic systems and potentially low mass power management and distribution systems. The concentrating photovoltaic system, using small, semiparabolic troughs with low light loss, supports the GEO and LEO missions with only one gimbal per array wing. It is tolerant of array pointing errors up to 25 degrees about the yaw axis. Pitch error tolerance is 1 degree, an error easily achieved by today's GEO spacecraft. The power management topology accommodates the ion engines by time-sharing those portions of the power conversion equipment which can be shared, thus minimizing mass. Energy Storage Technology development recommendations are corrosion-resistant, sodium sulfur batteries and flywheel backup systems.

Although GaAlAs planar arrays are projected to cost more than the modular concentrator, their low mass makes them attractive for missions such as the electrical orbital transfer vehicle (TUG). Data which validates the ability of GaAlAs arrays to recover from the full spectrum of particle radiation using both continuous and electrical re-annealing is required to validate the expected performance, which today is based on testing at a limited number of energy levels.

Technologies which do not appear to be as beneficial for multimegawatt systems are:

- a. Large Parabolic Concentrators, including hybrids with Rankine turbines
- b. Planar Silicon Arrays

Arrays are the mainstay of today's technology and will be more expensive than concentrators because of their increased cell area and lower efficiency. They are inferior when compared to concentrators for the self-injected GEO radar spacecraft, because of their susceptibility to radiation.

Large parabolic concentrators, including hybrids with Rankine turbines, are ineffective because of the massive radiators required to dispose of the waste heat generated by the cell inefficiencies. These radiator systems are more massive than small modular concentrators, because the radiators require heat-carrying fluids, tubes, and heat pipes to distribute the heat out to the fins in the redundant manner required for micrometeoroid survivability.

Energy storage technologies which were predicted to be less beneficial include:

- a. Hydrogen/oxygen fuel cells
- b. Current solid plate batteries (NICAD, NiH)
- c. Other high energy density systems ( $ZnBr_2$ , LiMS).

Hydrogen/oxygen fuel cells, with electrolysis units for storage have about the highest theoretical specific energy (joules/kg), but, in practice, the system is massive and inefficient. The surrounding hardware (with provisions for electrolysis with phase changes) and survivability of the fluids and gas systems when exposed to micrometeoroids, decreases achievable specific energies to 66 watt hours/kg. Inefficiencies are less than 50% (including the electrolysis); these make the solar arrays larger than other approaches.

The current systems (NICAD, NiH) all have shorter cycle life and would require significant on-orbit battery restocking for the LEO mission with its 100,000 cycle-life need.

Of the other two high-energy density systems,  $ZnBr_2$  requires pumps and fluid loops, and appears to be less efficient and less capable than the NaS alternative recommended. The LiMS approach does not have active loops but also has probable lower efficiency penalties. Both of these systems have a solid plate electrode, which is perhaps more vulnerable to life cycling degradation than the liquid NaS system.

The power management and distribution system results developed during the study indicate that hybrid AC/DC power management systems, with high voltage arrays driving the ion beam supplies directly and with split AC power converters, are an effective approach. Mass savings of from 10,000 to 30,000 kg would result, compared to more conventional all-AC or -DC approaches. The approach requires that arcing losses from the front face of the solar cells into the plasma be made acceptable by floating the concentrator metal structure at the plasma potential of that portion of the array. The configurations will require study to establish allowable voltages and voltage gradients, and may be mission/orbit dependent. In any event, the cyclo-inverter technology for DC-AC-DC conversion will be developed for the low-voltage discharge supplies, so that in the event array voltages are limited to 100-300 VDC, the high-voltage beam supply can still be accommodated.

Three other Power Management technology requirements emerged from the study:

- a. There is a need for a maintainable, low friction, high efficiency, and space survivable approach for AC and DC rotary joint power transfer.
- b. There is a need for the development of fault-isolating, fault-tolerant, efficient switching for AC and DC power distribution systems. The AC problem is more amenable to solution, because AC current is automatically zero at the crossover point each half cycle and therefore the probability of a thermal runaway in a half cycle at 20 KHz is small, if efficient thyristors are used as the control device. DC distribution will require fast actuating electro-mechanical devices sized to accommodate maximum short-circuit currents during their activation interval.
- c. The DC system may also require the development of high-power DC transistors, if AC development is not accomplished.

## SECTION 4

## REFERENCES

1. SPS Recommended Preliminary Baseline Concept, NASA, Lyndon B. Johnsons Space Center, Jan 25, 1978.
2. Space Industrialization, Opportunities, Markets, and Programs, Contract Report NAS8-32197, Science Application, Inc., April 15, 1978.
3. Jack W. Geis, Concentrating Photovoltaics - A Viable Candidate for the Next Generation of Air Force Satellite Power Systems, 15th Intersociety Energy Conversion Engineering Conference, Seattle, Washington, August 18-22, 1980, pp. 393-387.
4. D.C. Byers and V.K. Rawlin, Electron Bombardment Propulsion System Characteristics for Large Space Systems, presented at the 12th International Electronics Propulsion Conference, Key Biscayne, Fla, 15-17 Nov. 1976, N77-11106.
5. Large Payload Earth-Orbit Transportation with Electric Propulsion. Technical Memorandum 33-793, Jet Propulsion Laboratory.
6. W.P. Glunt, Station Keeping Velocities Required for a Large Space Platform in Geosynchronous Orbit, General Dynamics, Convair Division Memorandum No. 697-9-78-024, 3 April 1978.
7. U.S. Standard Atmosphere, 1976, National Aeronautics and Space Administration, U.S. Government Printing Office, October 1976.
8. A Reference Atmosphere for Patrick AFB, Florida, Annual (1963 Revision), NASA/MSFC Tech. Memo, TMX-53139, 23 September 1964.
9. A. Karemaa, Error Sources and Trajectory Dispersion Simulation Data, General Dynamics Convair Division Report No. GDCA-BKM71-024B, September 1976.
10. J. Jensen, et. al., Design Guide to Orbital Flight, McGraw-Hill Book Co., Inc., New York 1962.
11. TRAJEX Users Guide, General Dynamics, Convair Division Report No. GDC-DBA67-003, Revision 17, July 1979.
12. R.L. Pleasant, Analysis and Optimization of Radiator Systems for Large Heat-Generating Spacecraft, Convair Report CASD-ERR-78-031, December 1978.

13. W.D. Ebeling, D. Rex, U. Bierfischer, Properties of Solar Generators with Reflectors and Radiators, N80-33901, June 1980.
14. S.W. Chi, Introduction to Heat Pipe Theory: An Instruction Manual, School of Engineering and Applied Science, The George Washington University, Washington, D.C., October 1971.
15. David C. Byers, Characteristics of Primary Electric Propulsion Systems, NASA Technical Memorandum 79255, Presented at the 14th International Conference on Electric Propulsion, Princeton, New Jersey, October 13 - November 2, 1979, p. 7.
16. Reference 15, pp. 1-15.
17. David C. Byers, Fred F. Terdan, and Ira T. Myers, Primary Electric Propulsion for Future Space Missions, Prepared for the Conference on Advanced Technology for Future Space Systems, Langley, VA., May 8-11, 1979.
18. William J. Ketchum, Low Thrust Vehicle Concept Study, Contract NAS8-33527, GDC-ASP-80-010, General Dynamics Convair Division, 26 September 1980, pp 4-17.
19. John D. Regetz, Jr., and C.M. Terwilliger, Cost Effective Technology Advancement Directions for Electric Propulsion Transportation Systems in Earth Orbital Missions, 1979, N80-11950; presented at the 14th Interim Conference on Electric Propulsion, Princeton, N.J., October 30 - November 1, 1979.
20. H.Y. Tada and J.R. Carter, Jr., Solar Cell Radiation Handbook, JPL Publication 77-56, Jet Propulsion Laboratory, Pasadena, CA, November 1, 1977.
21. W.L. Crabtree, W.E. Horne, A.C. Day, R.B. Gregor, and L.P. Milliman, Solar Thermophotovoltaic Space Power System, Proceedings of the 15th Intersociety Energy Conversion Engineering Conference, Seattle, Washington, August 18-27, 1980, Vol. 1, p. 381.
22. James W. Mildice, Study of Power Management Technology for Orbital Multi 100 KWe Applications, NASA CR159834, GDC-ASP-80-015, General Dynamics Convair Division, 15 July 1980, p. 3-42.
23. R.L. Pleasant, Upper Stage Avionics Thermal Control, Convair Report CASD-ERR-76-039, December 1976.

24. R.F. O'Neill, et al, A Numerical Procedure for Solution of Radiation and Convection Fin Heat Transfer Problems, Computer Program P5399, Convair Report No. GDCA-BTD71-001, August 1971.
25. R. Loo, G.A. Kamath, and R.C. Knechtlin, Radiation Damage in GaAs Solar Cells, Presented at the 14th IEEE Photovoltaic Specialists Conference, San Diego, CA, January 7-10, 1980.
26. S. Li Sheng, D.W. Schoenfeld, T.T. Chiu, and R.Y. Loo, Effects of Thermal Annealing on the Deep-Level Defects and I-V Characteristics of 200 KeV Proton Irradiated AlGaAs - GaAs Solar Cells, Proceedings of the 15th Intersociety Energy Conversion Engineering Conference, Seattle, Washington, August 18-22, 1980, Vol. I, p. 356.
27. Reference 20, pages 5-23, 6-2, and 3-131.
28. Solar Cell Array Design Handbook, JPL SP43-38, Vol. 1, Jet Propulsion Laboratory, October 1976, p. 2.3-4.
29. Michael J. Mirtick, NASA LeRC, Verbal Communication.
30. Reference 22, pp. A-1 - A-25.
31. Reference 22, p. 3-66.
32. J.A. Rinde, T.T. Chao, and R.G. Stone, Composite Fiber Flywheel for Energy Storage, Lawrence Livermore Laboratory Contract Report, Contract No. W-7405-Eng-48, pp. 25.
33. High Energy Density (HED) Rechargeable Battery for Satellite Applications, CDRL Item 10, 5 November 1980, Contract No. F33615-79-C-2044, Huges Aircraft Corp., pp. 99-100.
34. Reference 22, pp. A3-1 through A3-83.
35. Integrated Power and Attitude Control Study (IPACS), NASA CR-2383, April 1974.
36. 30-Centimeter Ion Thruster Design Manual, NASA Technical Memorandum 79191, June 1979.

APPENDIX A  
MULTIMEGAWATT POWER SYSTEM (MMPS)  
APPLICATION AND PERFORMANCE SHEETS

## MMPS COMPONENT APPLICATION AND PERFORMANCE

1. **COMPONENT**  
Idealized Silicon Solar Cell, Planar Array
2. **BASIC PARAMETERS**  
Efficiency of 16% (May consider Metal, Insulator, Semiconductor (MIS) type construction), 50  $\mu$ m thickness, 200°C self annealing - or somewhat higher if 200°C defect not removable.
3. **STATEMENT OF NEED**  
A planar array cell with long life, high efficiency, low cost
4. **ALTERNATIVE TECHNOLOGY CONCEPTS**  
Gallium Arsenide Cells, concentrators annealed polycrystalline cells, Dendritic Web cells.
5. **SUBSYSTEM REQUIREMENT**  
Annealable in space at high temperatures, therefore, Welds capable of high current, for on-array annealing.
6. **COMPONENT IMPLEMENTATION**  
Basic Spectrolab or Comsat Cell, with lower cost due to process improvements, plus Boron Oxygen defect removed for 200°C self annealing.
7. **ALTERNATIVE IMPLEMENTATIONS**  
Comsat, Spectrolab, ASEC, Solarex implementation of existing cells
8. **COMPONENT PERFORMANCE REQUIREMENTS**  
Cell dimensions, 5x5cm. Planar array blanket assumed to be packaged folded for shuttle launch. 100,000 temperature cycles -65°C to +60°C

A-2

## MMPS COMPONENT APPLICATION AND PERFORMANCE

### 1. COMPONENT

Idealized GaAlAs Planar Array Solar Cell

### 2. BASIC PARAMETERS

Efficiency of 20% (28°C, AMO, CR = 1) 50  $\mu$  meter, low cost substrate, back surface reflector. Tmax at least 125°C for 20 years

### 3. STATEMENT OF NEED

A planar array with very low cost, high efficiency cells may be more effective than concentrators because of the thermal control concentrators require.

### 4. ALTERNATIVE TECHNOLOGY CONCEPTS

Planar Silicon Cells, Cells for Concentrators

### 5. SUBSYSTEM REQUIREMENT

Radiation Insensitivity, (Self annealing), Weldable contacts, up to 100,000 thermal cycles (-65°C to +60°C)

### 6. COMPONENT IMPLEMENTATION

Basically, take the current MIT Lincoln Lab Cell and add production features for low cost, plus development test, back surface reflection, and deposition on a low mass, graphite substrate.

### 7. ALTERNATIVE IMPLEMENTATIONS

Other low cost substrates (not yet demonstrated).

### 8. COMPONENT PERFORMANCE REQUIREMENTS

The cell should be an advanced, low cost low mass version of the MIT/Hughes/Varian work.  
Cell width of 50  $\mu$  meters. Planar blanket packaging in multiple folds for launch environmental protection. Capable of accepting electro statically bonded cover slides and back welded circuit attachment. Possibly capable of circuit self annealing  
Specific weight of 1 gm/cm<sup>3</sup> assumed.

A-3

## MMPS COMPONENT APPLICATION AND PERFORMANCE

1. **COMPONENT** Single Band Gap Gallium Aluminum Arsenide Solar Cells -  
CR = 1 or 2, Germanium Substrate

2. **BASIC PARAMETERS**

Efficiencies demonstrated in the Lab of up to 16%

3. **STATEMENT OF NEED**

Planar Solar Arrays - Low cost Germanium substrate - high efficiency  
plus 30 year life - self annealing

4. **ALTERNATIVE TECHNOLOGY CONCEPTS**

Silicon, GaAlAs with Gallium Arsenide Substrate

5. **SUBSYSTEM REQUIREMENT** Radiation Insensitive,  $T_{HOT RANGE} = 80^{\circ}C$  to  $125^{\circ}C$ ,  
up to 100,000 cycles.  $T_{COLD} = -65^{\circ}C$

6. **COMPONENT IMPLEMENTATION**

Demonstrated by Lincoln Labs in Research Stage

7. **ALTERNATIVE IMPLEMENTATIONS**

Other low cost substrates (not demonstrated to date)

8. **COMPONENT PERFORMANCE REQUIREMENTS**

A translation into production of the present Lincoln Lab cell design.

Capable of withstanding the Shuttle launch environment in a folded blanket  
condfiguration.

A-4

## MMPS COMPONENT APPLICATION AND PERFORMANCE

1. COMPONENT	Single Band Gap Gallium Arsenide Solar Cells - CR=1, GaAs substrate
2. BASIC PARAMETERS	Efficiency of 17-20% in lab. 50 $\mu\text{m}$ thick $T_{\text{max}}$ at least 125 $^{\circ}\text{C}$ for 20 years
3. STATEMENT OF NEED	A planar array cell with very high efficiencies, needed only if the low cost substrate approach cannot be made to work.
4. ALTERNATIVE TECHNOLOGY CONCEPTS	Silicon Cells, concentrator cells. Low cost substrate Gallium Arsenide cell.
5. SUBSYSTEM REQUIREMENT	Radiation insensitivity, self annealing, weldable contacts, electrostatic coverslide bonding, 100,000 cycles -65 $^{\circ}$ to 60 $^{\circ}\text{C}$
6. COMPONENT IMPLEMENTATION	Utilization of the Hughes, Rockwell, or Varian approaches.
7. ALTERNATIVE IMPLEMENTATIONS	Varian, Hughes, and Rockwell processes. (Organo Metallic, and Liquid Phase Epitaxial (LPE)).
8. COMPONENT PERFORMANCE REQUIREMENTS	<p>Advanced, low cost version. Weldable contacts. <math>V_{\text{mp}}</math> Temperature coefficient of .22 MV/C<math>^{\circ}</math>. <math>I_{\text{mp}}/I_{\text{sc}}</math> not strongly dependent on temperature. Coverslide attachment via electrostatic bonding.</p> <p>Capable of withstanding the Shuttle launch environment in a folded balnket package approach.</p>

A-5

## MMPS COMPONENT APPLICATION AND PERFORMANCE

1. **COMPONENT**      Edge Defined, Film Grown (EFG)  
                         or Dendritic Web formed Silicon Solar Cells

2. **BASIC PARAMETERS**

$\eta$  = 18% by lasar re-annealing and regrowing of junction region at AM1.

AMO  $\eta$  = 16% @ 28°C, 14% @ 60°C

3. **STATEMENT OF NEED**

Low cost silicon cells for space usage. Reliable, long lived, capable of 100,000 temperature cycles (-65° to +65°C)

4. **ALTERNATIVE TECHNOLOGY CONCEPTS**

Single crystal or polycrystalline silicon.

5. **SUBSYSTEM REQUIREMENT**

Radiation insensitivity, weldable contacts

6. **COMPONENT IMPLEMENTATION**

Use terrestrial production silicon and lasar annealing/diffusion to make the equivalent of a

7. **ALTERNATIVE IMPLEMENTATIONS**

Several suppliers and universities are developing approaches for very fast ribbon forming systems.

8. **COMPONENT PERFORMANCE REQUIREMENTS**

$\eta$  = 14%, capable of surviving the Shuttle launch environment mounted to a folded solar blanket.

A-5

## MMPS COMPONENT APPLICATION AND PERFORMANCE

### 1. COMPONENT

Amorphous Silicon Solar Cells

### 2. BASIC PARAMETERS

Only lower efficiency demonstrated, but potentially much lower cost.

### 3. STATEMENT OF NEED

Lower cost solar power enhances the competitive position of space missions such as the Space Radar and Construction Station.

### 4. ALTERNATIVE TECHNOLOGY CONCEPTS

Planar arrays with more efficient mono-crystalline silicon or GaAlAs, or concentrating systems

### 5. SUBSYSTEM REQUIREMENT

Radiation insensitivity or self annealing, 100,000 temperature cycles (-65 to +60°C)

### 6. COMPONENT IMPLEMENTATION

Horizontally Multilayered High Voltage Cells <sup>(1)</sup>

Efficiencies to 6% are predicted, assuming one of the 3 implementations matures.

### 7. ALTERNATIVE IMPLEMENTATIONS

Ultrathin active layer "FAN" type cell <sup>(2)</sup> or Tandem amorphous cells <sup>(3)</sup>

1, 2, 3 (References) "14th IEEE Photovoltaic Specialists Conference"

### 8. COMPONENT PERFORMANCE REQUIREMENTS

It is assumed that the shuttle launch packaging of the solar blanket which uses the cells will be accomplished by multiply folding the blanket, so that launch vibration and "g" loading are minimized, as far as the cells themselves are concerned. The cells themselves must be capable of accepting coverslides.

$V_{oc} > .4$ ,  $I_{sc}$ . Because low cost is inherent, width is assumed to be 200-500 meters, driving blanket specific weight up to 2 Kg/M<sup>2</sup>.

A-7

## MMPS COMPONENT APPLICATION AND PERFORMANCE

### 1. COMPONENT

Amorphous Silicon Solar Cells (High Efficiency)

### 2. BASIC PARAMETERS

Only lower efficiency demonstrated, but potentially much lower cost.  
Efficiency increased by laser annealing/diffusion.

### 3. STATEMENT OF NEED

Lower cost solar power enhances the competitive position of space missions such as the Space Radar and Construction Station.

### 4. ALTERNATIVE TECHNOLOGY CONCEPTS

Planar arrays with more efficient mono-crystalline silicon or GaAlAs, or concentrating systems

### 5. SUBSYSTEM REQUIREMENT

Radiation insensitivity or self annealing, 100,000 temperature cycles (-65° to +60°)

### 6. COMPONENT IMPLEMENTATION

Doped amorphous layer deposited and regrown epitaxially.  
Efficiencies to 16% are predicted.  
(Reference) "14th IEEE Photovoltaic Specialists Conference"

### 7. ALTERNATIVE IMPLEMENTATIONS

### 8. COMPONENT PERFORMANCE REQUIREMENTS

It is assumed that the Shuttle launch packaging of the solar blanket which uses the cells will be accomplished by multiply folding the blanket, so that launch vibration and "g" loading are minimized, as far as the cells themselves are concerned. The cells themselves must be capable of accepting coverslides.  
 $V_{oc} \approx .4$ ,  $I_{sc}$ . Because low cost is inherent, width is assumed to be 200-500 meters, driving blanket specific weight up to 2 Kg/M<sup>2</sup>.

A-8

**MMPS COMPONENT APPLICATION AND PERFORMANCE**

**1. COMPONENT**

**Multibandgap One Sun Solar Cells**

**2. BASIC PARAMETERS**

**Efficiencies of 23-25% @ 60°C**

**3. STATEMENT OF NEED**

**A planar array cell with long life, higher efficiency, self annealing at GEO levels.**

**4. ALTERNATIVE TECHNOLOGY CONCEPTS**

**Single bandgap cells, concentrators**

**5. SUBSYSTEM REQUIREMENT**

**Annealable in space, possibly by applying higher temperatures (200-300°C) capable of withstanding 100,000 -65°C to +65°C cycles.**

**6. COMPONENT IMPLEMENTATION**

**Both Varian and Spectrolab have approaches for construction of this type of cell.**

**7. ALTERNATIVE IMPLEMENTATIONS**

**Under study at Varian, Hughes Research, Arizona State University.**

**8. COMPONENT PERFORMANCE REQUIREMENTS**

**Capable of being packaged to withstand the shuttle launch on a foldable blanket.  
5 X 5 cm square cells.**

**9. UNAVAILABLE DATA**

**There is no laboratory data on three bandgap systems as yet, however, theoretical studies indicate that this extension of today's technology should be anticipated but with the provision of high risk.**

6-A

## MMPS COMPONENT APPLICATION AND PERFORMANCE

### 1. COMPONENT

Etched Groove Silicon Concentrator Solar Cell

### 2. BASIC PARAMETERS

Efficiencies of as high as 18% have been demonstrated in the laboratory at 1000 suns.

### 3. STATEMENT OF NEED

A high efficiency, concentrating solar cell should be considered for its benefits. They are: cost reduction, low mass

### 4. ALTERNATIVE TECHNOLOGY CONCEPTS

GaAlAs concentrating cells, planar cell arrays

### 5. SUBSYSTEM REQUIREMENT

Radiation insensitive or self annealable, heat exchanger mounting. (100,000 temperature cycles,  $-65^{\circ}\text{C}$  to  $+160^{\circ}\text{C}$ )

### 6. COMPONENT IMPLEMENTATION

Described in the 14th photovoltaic IEEE specialists conference by Microwave Associates.

### 7. ALTERNATIVE IMPLEMENTATIONS

OCLI concentrator cells, fabricated to NASA standards

### 8. COMPONENT PERFORMANCE REQUIREMENTS

1. The etched grooves shall not cause a loss of reliability (Ref. NTS-II experiment).

The cells will be mounted to a heat exchanger, and in the mounted configuration must be capable of withstanding the shuttle launch environment. Based on our analysis, heat fluxes will be up to 35 watts per 2.0 by 2.0 cm cell.

A-10

<b>MMPS COMPONENT APPLICATION AND PERFORMANCE</b>	
<b>1. COMPONENT</b>	<b>Concentrating GaAlAs Solar Cell, Back Surface Reflector</b>
<b>2. BASIC PARAMETERS</b>	17 to 20% at 50 suns
<b>3. STATEMENT OF NEED</b>	A cell of this type appears to be able to make concentrators cost 10-30% of the cost of Planar Arrays.
<b>4. ALTERNATIVE TECHNOLOGY CONCEPTS</b>	Low cost solar cells in planar arrays, other concentrating approaches.
<b>5. SUBSYSTEM REQUIREMENT</b>	Radiation insensitivity, capable of withstanding 100,000 temperature cycles (-65°C to +160°C)
<b>6. COMPONENT IMPLEMENTATION</b>	Similar to Varian GaAlAs terrestrial cells
<b>7. ALTERNATIVE IMPLEMENTATIONS</b>	Liquid Phase Epitaxial (LPE) or Organometallic Processes
<b>8. COMPONENT PERFORMANCE REQUIREMENTS</b>	The cells will be mounted to a heat exchanger and in the mounted configuration must be capable of withstanding the shuttle launch environment. Based on our analysis, heat fluxes will be up to 25 watts per 2.0 cm by 2.0 cm cell.

II-V

## MMPs COMPONENT APPLICATION AND PERFORMANCE

### 1. COMPONENT

Multibandgap concentrating solar cells.

### 2. BASIC PARAMETERS

Efficiencies of 25-28%, temperature coefficients at  $V_{mp}$  of band gap  $\approx 2 \text{ mv/C}^\circ$

### 3. STATEMENT OF NEED

Highly efficient, low cost power

### 4. ALTERNATIVE TECHNOLOGY CONCEPTS

Plane silicon or GaAlAs concentrating cells, planar single band cells

### 5. SUBSYSTEM REQUIREMENT

Radiation insensitive, capable of withstanding up to 100,000 temperature cycles,

### 6. COMPONENT IMPLEMENTATION

Being developed by Varian under contract to NASA LeRC.

$-85^\circ\text{C}$  to  $+180^\circ\text{C}$

### 7. ALTERNATIVE IMPLEMENTATIONS

Varian Dichroic mirror approach with single band concentrating cells.

### 8. COMPONENT PERFORMANCE REQUIREMENTS

The cells will be mounted to a heat exchanger and in the mounted configuration must be capable of withstanding the shuttle launch environment. Based on our analysis, heat fluxes will be up to 25 watts per 2.0 cm by 2.0 cm cell.

A-12

## MMPS COMPONENT APPLICATION AND PERFORMANCE

1. COMPONENT Silicon/Gallium 50% efficient Solar Concentrator Cells

2. BASIC PARAMETERS 1. Spherical concentrator illuminates a target to a "red hot" 2100°K. At this temperature, the Gallium Silicon cells are theoretically 55° efficient, with 50% perhaps achievable.

3. STATEMENT OF NEED A 50% efficient photovoltaic system is needed to minimize system cost, mass, volume.

4. ALTERNATIVE TECHNOLOGY CONCEPTS The only other known possible 50% efficient system would involve excessive radiator mass.

5. SUBSYSTEM REQUIREMENT

6. COMPONENT IMPLEMENTATION The silicon/GA cells which the illuminator shines upon must be capable of high flux densities. They must have back surface reflectors.

7. ALTERNATIVE IMPLEMENTATIONS

8. COMPONENT PERFORMANCE REQUIREMENTS

The silicon cells should handle the heat flux of about 50% of the energy. Since a concentration ratio of about 2500 is required for 2100 K° illuminator temperature, fluxes of approximately 200 w/cm<sup>2</sup> will be incident on the cell. 100 w<sup>2</sup>/cm must then be handled by the thermal control system, with what would probably be a jet impingement on a heat exchange close to the back of the cell.

A-13

## MMPS COMPONENT APPLICATION AND PERFORMANCE

### 1. COMPONENT

Rankine cycle heat engine

### 2. BASIC PARAMETERS

Terrestrial technology and KIPS technology have developed turbines whose efficiency is 70 to 72% of Carnot maximum.

### 3. STATEMENT OF NEED

Rankine engines could be employed to utilize low quantity waste heat from photovoltaic systems, depending radiator specific weight, they may have benefits.

### 4. ALTERNATIVE TECHNOLOGY CONCEPTS

Pure photovoltaic systems. Fluid systems with rankine pumps.

### 5. SUBSYSTEM REQUIREMENT

Radiation and micrometeoroid environment, 0 g liquification, LEO thermal cycle for space construction

### 6. COMPONENT IMPLEMENTATION

KIPS turbine(s) could be upscaled and used with jet condensers. Scaled point designs for up to 10 KW have been developed.

### 7. ALTERNATIVE IMPLEMENTATIONS

No other space alternative is known for use in conjunction with photovoltaics, although a commercial Barber-Nichols turbine could perhaps be space qualified.

### 8. COMPONENT PERFORMANCE REQUIREMENTS

A-14

## MMPS COMPONENT APPLICATION AND PERFORMANCE

### 1. COMPONENT

Brayton cycle heat engine/alternator

### 2. BASIC PARAMETERS

Input temperature assumed to take only one value -  $T_{HOT} = 1400^{\circ}$  with reflections from Dichroic mirror secondary.  $T_{HOT} = 150^{\circ}C$  with cells at secondary not judged feasible.

### 3. STATEMENT OF NEED

Using reflective mirrors, perhaps 30% of the solar insolation might be utilized in a heat engine system.

### 4. ALTERNATIVE TECHNOLOGY CONCEPTS

Rankine or Stirling Engines, or Photovoltaic "only" systems.

### 5. SUBSYSTEM REQUIREMENT

Low sensitivity to micrometeoroids. Fluids should not be a possible contaminant.

### 6. COMPONENT IMPLEMENTATION

The DIPS and LeRC Brayton turbine developments serve as lower power prototypes which could be upscaled.

### 7. ALTERNATIVE IMPLEMENTATIONS

### 8. COMPONENT PERFORMANCE REQUIREMENTS

The unit should have overall efficiencies of about 25% for a temperature range of from  $+60$  to  $+1100^{\circ}C$ . The attainable specific power from typical combined rotating units, appears to be about 50 W/Kg, and this will be specified.

A-15

## MMPS COMPONENT APPLICATION AND PERFORMANCE

**1. COMPONENT**  
Nickel - Cadmium Electrochemical Storage Battery

**2. BASIC PARAMETERS**  
 Energy Density - 10-25 W-hr/kg  
 Life 5-10 yrs. 30,000 cycles (LEO), 300-900 cycles (GEO)  
 Throughput Efficiency - 75-90%  $V_{oc} = 1.3 \text{ V}$   
 Optimum Temperature -  $0-10^{\circ}\text{C}$

**3. STATEMENT OF NEED**  
 Load management buffer, secondary and backup power during array outages, power source for on-array thermal management/annealing.

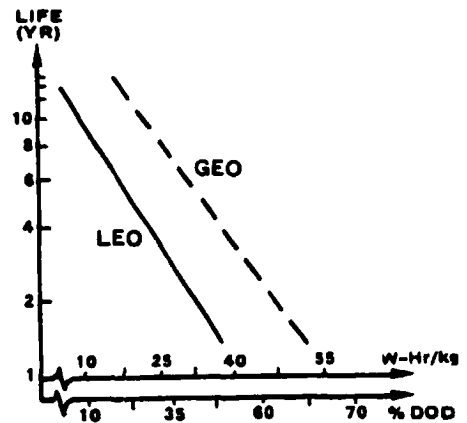
**4. ALTERNATIVE TECHNOLOGY CONCEPTS**  
 Metal-Hydrogen electrochemical  
 Flywheels electromechanical  
 Fuel Cells, regenerative

**5. SUBSYSTEM REQUIREMENT**  
 Occlusion in LEO (38%), radiation and micrometeoroid environment

**6. COMPONENT IMPLEMENTATION**  
 Charge/Discharge unit draws power from secondary bus  
 Batteries on array side of rotary joint to minimize pointing requirements  
 Deep discharge reconditioning for extended life, resistance heater for op below  $-50^{\circ}\text{C}$

**7. ALTERNATIVE IMPLEMENTATIONS**  
 Depth of discharge: varies inversely with useful life. Implies trade-off of transportation against component costs over time. Minimum 10 year weight attained at about 25% discharge depth  
 Regulation: shunt, series, on-array regulation, or  $LC^3$  high efficiency charge control

**8. COMPONENT PERFORMANCE REQUIREMENTS**  
 Load profile: handles intermittent peak power loads (up to 2C without loss of life) for space construction facility  
 Output: Equals array EOL power, for about 0.5 hrs  
 Voltage: Dedicated storage bus allows selection  
 Reliability: Switches for bypass of inoperative cells  
 Control: Microprocessor algorithm based on sensed voltages, temperatures  
 Temperature Range:  $-40^{\circ}\text{C}$  to  $50^{\circ}\text{C}$   
 Working Voltage: 1-1.25 V  
 Acceleration: 5 g's max  
 Vibration: Shuttle launch environment  
 Longer lifetimes not achievable - although benefits from longer life could be significant.



A-16

## MMPS COMPONENT APPLICATION AND PERFORMANCE

**1. COMPONENT**

**Nickel - Hydrogen Electrochemical Storage Battery**

**2. BASIC PARAMETERS**

Energy Density - 30-35 W/hr/kg (H1-H)  
 Life 5-10 yrs. 30,000 cycles (LEO), 900 cycles (GEO)  
 Throughput Efficiency 75-90%  $V_{OC} = 1.36V$

**3. STATEMENT OF NEED Backup for NaS and flywheel.**

Load management buffer, secondary/backup power during array outages, power source for on-array thermal management/annealing

**4. ALTERNATIVE TECHNOLOGY CONCEPTS**

Nickel Cadmium electrochemical  
 Flywheel electromechanical  
 Fuel cell, regenerative

**5. SUBSYSTEM REQUIREMENT**

Occlusion in LEO (38%), radiation and especially micrometeoroid protection

**6. COMPONENT IMPLEMENTATION**

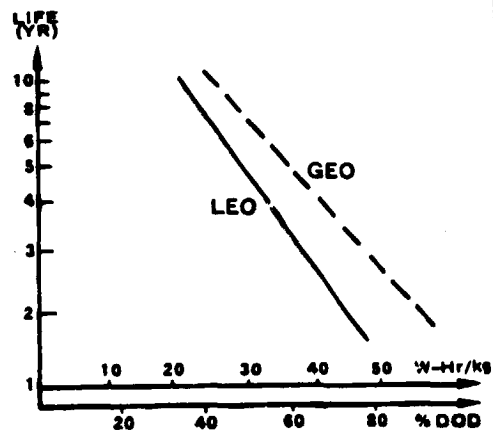
Charge/discharge unit draws power from dedicated bus  
 Batteries on array side of rotary joint to minimize pointing requirements  
 Provisions for protection against punctures or for bypassing cells required

**7. ALTERNATIVE IMPLEMENTATIONS**

Nickel, Hydrogen vs. more materially expensive but lighter Silver-Hydrogen  
 Regulation: shunt, series, on-array or LC<sup>3</sup> high efficiency charge control  
 Depth of discharge varies inversely with useful life. Minimum 10-yr. weight is achieved at about 50% discharge depth.

**8. COMPONENT PERFORMANCE REQUIREMENTS**

Load profile: Handle intermittent peak power (up to 1.5 C w/o loss of life)  
 Output: equals array EOL power for 0.5 hrs  
 Voltage: dedicated storage bus allows selection  
 Reliability: provisions for bypassing failed cells  
 Control: Microprocessor algorithm based on sensed voltage, temperature and pressure  
 Temperature Range: 0<sup>o</sup> to 30<sup>o</sup>C  
 Working Voltage: 1.0 - 1.6 V  
 Shuttle Environment  
 Longer lifetime not achievable - although benefits from longer life could be significant.



A-17

MMPS COMPONENT APPLICATION AND PERFORMANCE

1. COMPONENT

Silver - Zinc Electrochemical Storage

2. BASIC PARAMETERS

Energy Density, 30-50 Whr/kg and perhaps greater

Life - 1-2 yrs; 200-500 cycles GEO only

Throughput Efficiency 70-90%  $V_{oc} = 1.5$

3. STATEMENT OF NEED

Emergency power source, power source for array outage and thermal management/annealing

4. ALTERNATIVE TECHNOLOGY CONCEPTS

Nickel - Cadmium electrochemical

Regenerative fuel cell

Flywheel electromechanical

5. SUBSYSTEM REQUIREMENT

Emergency backup power for radar mission (GEO), radiation and micrometeoroid environment

6. COMPONENT IMPLEMENTATION

Inorganic/organic separator allows extended life compared to earlier cells

60% maximum DOD for rechargeable operation

Charge/discharge unit draws power from dedicated bus

7. ALTERNATIVE IMPLEMENTATIONS

8. COMPONENT PERFORMANCE REQUIREMENTS

One year lifetime with excellent charge retention. Lifetime increase is unlikely

Acceleration: 5 g's

Operating temperature:  $-40^{\circ}\text{C}$  to  $75^{\circ}\text{C}$

Working voltage: 1 to 1.55 V

Charge retention: 1 year at  $25^{\circ}\text{C}$

Shuttle launch environment

8I-A

MMPS COMPONENT APPLICATION AND PERFORMANCE

1. COMPONENT

Silver - Hydrogen Electrochemical Storage

2. BASIC PARAMETERS

Energy Density - 50-70 W. hr/kg

Life 1-10 yrs 8,000 cycles (LEO), 900 cycles (GEO)

Throughput Efficiency 70-90%  $V_{oc} = 1.7V$

3. STATEMENT OF NEED

Load management buffer, secondary/backup power during array outages, power source for on-array thermal mgmt./annealing

4. ALTERNATIVE TECHNOLOGY CONCEPTS

Nickel Cadmium electrochemical

Flywheel electromechanical

Fuel Cell, regenerative

5. SUBSYSTEM REQUIREMENT

Occlusion in(LEO) 39%, radiation and micrometeoroid protection

5. COMPONENT IMPLEMENTATION

Charge/discharge unit draws power from dedicated bus

Batteries on array side of rotary joint to minimize pointing requirements

Provisions for protection against micrometeoroids or bypassing failed cells

7. ALTERNATIVE IMPLEMENTATIONS

Silver - Hydrogen vs. heavier but less expensive Nickel Hydrogen

Regulation: shunt, series, on-array, LC<sup>3</sup> high efficiency regulation

Depth of discharge inversely proportional to battery life; optimum around 75%  
depth of discharge

8. COMPONENT PERFORMANCE REQUIREMENTS

Similar to Nickel - Hydrogen

A-19

## MMPs COMPONENT APPLICATION AND PERFORMANCE

### 1. COMPONENT

Lithium/Transition Metal (e.g. Ti) Sulfide Electrochemical Battery

### 2. BASIC PARAMETERS

Energy Density 150-250 H hr/kg

Life - 300-900 cycles 5-10 yrs. (GEO)

Throughput Efficiency 70-90%  $V_{OC} = 2.1 V$

### 3. STATEMENT OF NEED

Load management buffer, emergency and occlusion power for GEO orbit.

### 4. ALTERNATIVE TECHNOLOGY CONCEPTS

Nickel-Cadmium electrochemical

Metal - Hydrogen electrochemical

Flywheel Electromechanic

### 5. SUBSYSTEM REQUIREMENT

GEO Occlusion (1%), micrometeoroid and radiation environments.

### 6. COMPONENT IMPLEMENTATION

Batteries on array to minimize pointing requirements.

Charge/Discharge unit draws power from dedicated bus to account for large voltage vs. SOC slope for this couple.

### 7. ALTERNATIVE IMPLEMENTATIONS

High temperature lithium/iron sulfide battery (350-450°C)

### 3. COMPONENT PERFORMANCE REQUIREMENTS

Operating temperature:

Working voltage = 1.5 - 2.0

Shuttle launch environment

Deep discharge capability

A-20

## MMPS COMPONENT APPLICATION AND PERFORMANCE

### 1. COMPONENT

Rotary Joint (Transformer)

### 2. BASIC PARAMETERS

5 MW AC continuously rotatable joint arranged as 20 separate 250 KW circuits - repairable on orbit - use pot core design with outside coils. See below.

### 3. STATEMENT OF NEED

Transfer of energy across rotary joint.

### 4. ALTERNATIVE TECHNOLOGY CONCEPTS

Slip rings.

### 5. SUBSYSTEM REQUIREMENT

Array must point at sun; antenna must point at earth.

### 6. COMPONENT IMPLEMENTATION

Rotary transformer connects between resonant converter primaries and load converter secondaries.

### 7. ALTERNATIVE IMPLEMENTATIONS

Rotary capacitor, slip rings.

### 8. COMPONENT PERFORMANCE REQUIREMENTS

Power: 5 mw total per side  
20 transformers rated at 250 KW each per transformer side.

Frequency: 20 KHz

Inductance: Controlled  
parameter

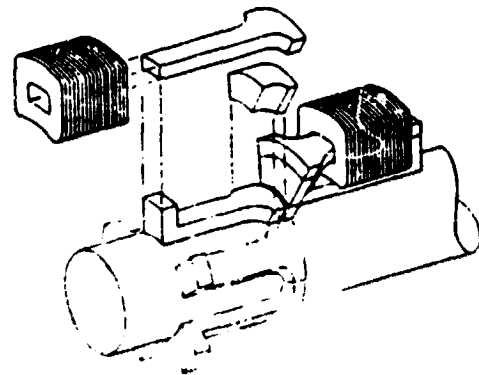
Full Load Torque: TBD

Efficiency: 98%

Specific Mass: 1, Kg/KW

Voltage: 1.000 Vrms

Current: 250A rms per  
circuit.



## MMPs COMPONENT APPLICATION AND PERFORMANCE

1. COMPONENT Payload Connectors - Magnetic

### 2. BASIC PARAMETERS

Voltage (primary) 1 KVRMS, 20 KHz  
Power: Up to 250 KW @ 250 amps.

### 3. STATEMENT OF NEED

Connectors are required to connect individual membrane loads to the distribution matrix. Connectors facilitate maintenance and upgrading as technology improves.

### 4. ALTERNATIVE TECHNOLOGY CONCEPTS

Hardwiring, welding, or regular contact connectors.

### 5. SUBSYSTEM REQUIREMENT

### 6. COMPONENT IMPLEMENTATION

Magnetic connectors offer increased resistance to plasma losses, increased safety and eliminate the need for a separate power transformer in load equipment.

### 7. ALTERNATIVE IMPLEMENTATIONS

Should be the subject of a detailed design study.

### 8. COMPONENT PERFORMANCE REQUIREMENTS

Primary Voltage:	1 KVRMS
Secondary Voltage:	Single or multiple windings per load requirements
Frequency:	60 Hz
Power:	Up to 250 KW
Connect/Disconnect Cycles:	100*
Efficiency:	98%
Circuits:	2
Insulation Resistance:	100 Megohms

\*Not a limitation - could be increased if an increase was required.

## MMPS COMPONENT APPLICATION AND PERFORMANCE

1. COMPONENT Resonant Converter Driver Unit

### 2. BASIC PARAMETERS

Power level 25 KW for Space Construction Facility and Radar with a high modularization level. 250 KW for lowest cost and mass radar system.

### 3. STATEMENT OF NEED

Power distribution converter.

### 4. ALTERNATIVE TECHNOLOGY CONCEPTS

DC distribution.

### 5. SUBSYSTEM REQUIREMENT

High efficiency distribution system required.

### 6. COMPONENT IMPLEMENTATION

Solar arrays drive converter primaries which passes across rotary joint and to load distribution.

### 7. ALTERNATIVE IMPLEMENTATIONS

DC distribution would eliminate need.

### 8. COMPONENT PERFORMANCE REQUIREMENTS

Input Voltage:	300 VDC
Input Power:	25 to 250 KW
Output Voltage:	300 VRMS
Resonance:	Resonant at about 20 KHz with rotary joint internal capacitor and inductor.
Control:	Databus
Efficiency:	98%
Physical:	1.65 Kg/KW for one half of the converter + second order terms in accordance with Figure __.

## MMPS COMPONENT APPLICATION AND PERFORMANCE

1. COMPONENT Load Distribution Switchgear

### 2. BASIC PARAMETERS

Power Level: 10 MW AC total, 25 KW for radar distribution  
Configuration: Electronic crossbar

### 3. STATEMENT OF NEED

Interfaxw parallel lines from rotary joint to load matrix.  
Adaptive load management. Redundance management.

### 4. ALTERNATIVE TECHNOLOGY CONCEPTS

Hardwired system.

### 5. SUBSYSTEM REQUIREMENT

Adaptive load distribution required.

### 6. COMPONENT IMPLEMENTATION

Outputs from the rotary joint need to be distributed throughout the load matrix. Failures of power management equipment on the load side of the joint must be accommodated.

### 7. ALTERNATIVE IMPLEMENTATIONS

Thyristor switches which switch at zero voltage point.

### 8. COMPONENT PERFORMANCE REQUIREMENTS

Power Level: From 25 to 250 KW (may actually be 30 KW so that for compatibility with icn modularity).  
Frequency: 20 KHz  
Inputs: 21 (20 + 1 spare) @ 250 KW  
Outputs: Determined by load matrix for the radar.  
Control: Databus  
Efficiency: 99%.  
Voltage: 1,000 vrms  
Current: 250 A per input X 20 inputs X 2 wings

## MMPS COMPONENT APPLICATION AND PERFORMANCE

1. COMPONENT      Power Management Control Computer System

### 2. BASIC PARAMETERS

Distributed Master/Slave Computer System

### 3. STATEMENT OF NEED

Overall PMS control.

### 4. ALTERNATIVE TECHNOLOGY CONCEPTS

### 5. SUBSYSTEM REQUIREMENT

Yes

### 6. COMPONENT IMPLEMENTATION

All PMS components connect to the control computer.

### 7. ALTERNATIVE IMPLEMENTATIONS

### 8. COMPONENT PERFORMANCE REQUIREMENTS

This control computer will be a distributed computing system with a master computer and many slave computers with fault detection software and hardware. The throughput of a typical slave computer will need to be about 2 MBPS with the master computer operating at about 80 MBPS.

Word length:                      8 bits  
Communication Medium:          Optical or wire databus, or FM RF  
Power Source:                      Master - 1 KVDC  
   Slaves - 20 KHz AC

## MMPs COMPONENT APPLICATION AND PERFORMANCE

1. **COMPONENT** Ion Engine Power Supply (AC input)(50 cm dia. assumed)

### 2. BASIC PARAMETERS

Input is 20 KHz AC, must operate as resonant converter secondary output is to beam and discharge engine inputs.

### 3. STATEMENT OF NEED

Ion engines required for space construction facility station-keeping and boost to GEO for space radar.

### 4. ALTERNATIVE TECHNOLOGY CONCEPTS

Beam supply array switched, DC/DC converters at the engines for discharge supply.

### 5. SUBSYSTEM REQUIREMENT

Supplies must enable possible cooling.

### 6. COMPONENT IMPLEMENTATION

For the split AC system, the ion supplies must operate as the back half of the split inverter system. For 50 cm engine diameter, sizing is approximately 42 KW.

### 7. ALTERNATIVE IMPLEMENTATIONS

Smaller diameter ion engines with smaller power modularization level (35 cm/25 KW).

### 8. COMPONENT PERFORMANCE REQUIREMENTS

Input:	300 RMS, 20 KHz AC Resonant Converter
Total Output:	29 KW/thruster X 108 thrusters (radar)
Efficiency:	97% overall
Physical:	1.65 Kg/KW per module (Figure _)
Beam Output:	900 VDC
Discharge Output:	30 VDC @ 88 amps.
Cooling:	Passive 480 W/Supply Module at 92 KW

## MMPS COMPONENT APPLICATION AND PERFORMANCE

1. **COMPONENT** Ion Engine Power Supplies (DC input)
2. **BASIC PARAMETERS**

Input is directly off of the solar arrays. Beam output is directly from switched array—no isolation required. Discharge supply is to be provided by a DC/DC converter.\*
3. **STATEMENT OF NEED**

Ion engines required for LEO stationkeeping (space construction facility) and boost to GEO (10 MW Radar).
4. **ALTERNATIVE TECHNOLOGY CONCEPTS**

A split AC system with a DC/AC driver module driving a high-voltage beam system. A DC system with a high voltage DC/DC converter for power beam.
5. **SUBSYSTEM REQUIREMENT** Determined by Reliability and Cost/mass minimization.
6. **COMPONENT IMPLEMENTATION**

Single failure tolerant switching for the beam output.  
DC/DC converter for the 30 volt discharge supply.
7. **ALTERNATIVE IMPLEMENTATIONS**

A split AC resonant converter with both beam and discharge supplies.
8. **COMPONENT PERFORMANCE REQUIREMENTS**

Input:	900 VDC
Total Output:	10 megawatts (radar), 750 KW (SCF)
Efficiency:	95% (DC/DC) 99% (switches)*
Physical:	3.3 Kg/KW ← DC/DC converter at modularity level of ion engine
Beam Output:	900 V at 80 amps per thruster (8 for SCF)
Cooling:	1 KW per supply-passive (108 for radar)
Discharge Output:	660 amps at 30 volts.

\*Benefits of a DC/DC converter over switches for the 30 VDC discharge requirement all about 31,000 Kg and \$30M because of transmission line mass.

## MMPs COMPONENT APPLICATION AND PERFORMANCE

1. COMPONENT SCF Energy Storage Switching Controller-Electrical

### 2. BASIC PARAMETERS

Voltage: (In and out) 300 VDC  
Power: 1 megawatt output to SCF facility  
Discharge Time: 1 hour nominal

### 3. STATEMENT OF NEED

A computer-controlled charge/discharge system is required to manage battery or fuel cell electrical energy storage system.

### 4. ALTERNATIVE TECHNOLOGY CONCEPTS

Flywheel energy storage.

### 5. SUBSYSTEM REQUIREMENT

Overall energy storage of one megawatt.

### 6. COMPONENT IMPLEMENTATION

Single failure tolerant switching to ensure reliability.  
No crosstrapping of busses.

### 7. ALTERNATIVE IMPLEMENTATIONS

If this switching approach later proves to be infeasible, regulators at 2.3 Kg/KW could be substituted. This substitution will not affect the trade of DC vs. AC PMS components, which are downstream from the Energy Storage.

### 8. COMPONENT PERFORMANCE REQUIREMENTS

Input/Output Voltage:	300 VDC input, 300 VDC output
Input Current:	55 amps @ 300 VDC
Output Current:	Modularity level of 20/array panel requires 80 amps/output module switch with 40 switches.
Physical:	0.1 Kg/KW
Control:	Databus

## MMPS COMPONENT APPLICATION AND PERFORMANCE

1. COMPONENT Connectors - Mechanical

### 2. BASIC PARAMETERS

Voltage:	1 KVRMS	20 KHz	1,000 VDC
Current:	Up to 80 amps		Up to 80 amps
	AC System		DC System

### 3. STATEMENT OF NEED

Connectors are required to connect individual loads to the distribution matrix and service any failed modules.

### 4. ALTERNATIVE TECHNOLOGY CONCEPTS

Hardwiring or welding.

5. SUBSYSTEM REQUIREMENT Ion engines, space construction facility modules and radar blanket modules should be repairable/serviceable.

### 6. COMPONENT IMPLEMENTATION

### 7. ALTERNATIVE IMPLEMENTATIONS

AC transformer coupling for the AC system design.

### 8. COMPONENT PERFORMANCE REQUIREMENTS

Voltage:	1 KVRMS/1000 VDC
Frequency:	20 KHz
Current:	Up to 80 amps
Connect/Disconnect Cycles:	100
Efficiency:	99.5%
Contacts:	6 (4 hot, 2 shields)
Insulation Resistance:	100 megohms

**GDC/AST 81-019**

**APPENDIX B**  
**DEFINITION OF TECHNOLOGY REQUIREMENTS**  
**AND**  
**TECHNOLOGY PLANS**

---

---

DEFINITION OF TECHNOLOGY REQUIREMENT

---

---

1. TECHNOLOGY REQUIREMENT (TITLE): High bandgap cell, Type I Page 2 of 4

---

---

7. TECHNOLOGY OPTIONS:

AlGaAs is the best high bandgap material to use, because it is almost perfectly lattice-matched to GaAs.

Liquid-phase epitaxy (LPE) has been used to grow some of the best AlGaAs on record, but OM/VPE is better for high throughput solar cell processing.

---

8. TECHNICAL PROBLEMS:

Incorporation of oxygen into AlGaAs, especially with Om/VPE. This is why high bandgap cells have not turned out very well thus far.

---

9. POTENTIAL ALTERNATIVES:

Split the spectrum two ways instead of three, use lower bandgap AlGaAs.

---

PLANNED PROGRAMS OF UNPERTURBED TECHNOLOGY ADVANCEMENT

High bandgap AlGaAs cells are much closer to being realized than, say, the monolithic multijunction cell. These cells could be acceptable by OM/VPE in the early 1980s.

---

TECHNOLOGY REQUIREMENTS

Filters for blocking long wavelength light: reflection  
if the filter does exist and can be obtained from  
Spectrolab, Inc., Santa Rosa, CA, among others.

**ORIGINAL PAGE IS  
OF POOR QUALITY**

LARGE SPACE POWER SYSTEM COMPONENTS CHARACTERISTIC DATA SHEET

PART A - PHYSICAL

COMPONENT NAME <u>High bandgap cell</u>	Page 3 of 4
FUNCTION <u>Efficient conversion of upper part of AMØ spectrum.</u>	

<p><b>PHYSICAL DESCRIPTION</b></p> <p><u>                    </u> - Ag grid</p> <p><u>p+GaAs</u></p> <p><u>2.95 eV AlGaAs window</u></p> <p><u>1.95 eV p AlGaAs</u></p> <p><u>1.95 eV n</u></p> <p><u>GaAs substrate</u></p>	<p><b>PARAMETRIC ANALYSIS RESULTS</b></p> <p>At 50 sun, 125°C, 1.5 µm diff. length</p> <p>4.5 µm grid line width } metal</p> <p>290 µm grid spacing }</p> <p>p-junction depth = 0.7 µm</p>
--	--

**PHYSICAL DEVELOPMENT PROJECTIONS**

CHARACTERISTIC	STATE OF THE ART	PROJECTION FOR 1990	ACHIEVABLE CAPABILITY
Size (cm x cm)	1.5 x 3.0 cm	1.5 x 3.0 cm	large as boule
Thickness (µm)	400 µm	300-400 µm	250 µm
Mass (g)	1.0	0.75-1.0	0.6g for 1.5 x 3 cm
Substrate Thermal Conductivity (W/cm-°K)	0.3	0.3	0.3 (GaAs)
Space Radiation Damage EOL/BOL @10 <sup>16</sup> 1 MeV electron dose	0.5 µm diff. lengths	1.5 µm diff. lengths	perhaps 3 µm diffusion lengths

**METALLIZATION MATERIAL/CONFIGURATION/CHARACTERISTICS**

Ag metal grid on cell. Vacuum solder to package.

**MATERIAL CONSIDERATIONS**

SPACE POWER SYSTEM COMPONENTS CHARACTERISTIC DATA SHEET  
 PART B - PERFORMANCE

COMPONENT NAME High bandgap cell Page 4 of 4

FUNCTIONAL CHARACTERISTICS Photovoltaic conversion at 125°C,  
 50 suns for upper part of AM0 spectrum.

PERFORMANCE DEVELOPMENT PROJECTIONS 125°C, 50 suns, 0.847 cm cell

CHARACTERISTIC	STATE OF THE ART	PROJECTION FOR 1990	ACHIEVABLE CAPABILITY
Open-Circuit Voltage - $V_{oc}$	No data available on this level of spectrum splitting	1.26 V	about 10% higher current and power, with associated gain in efficiency
Maximum Power Voltage - $V_{mp}$		1.5 V	
Short-Circuit Current - $I_{sc}$		0.41 amp	
Maximum Power - $P_{max}$		0.49 watt	
Efficiency - $\eta$		12.8% *	
MTBF - hours			
Temperature Coefficient of Current - $\Delta I_{sc}/\Delta T$			
		0.388	
		0.023%	
		°C	

\* at 1000 W/m² solar power.

---

DEFINITION OF TECHNOLOGY REQUIREMENT

---

1. TECHNOLOGY REQUIREMENT (TITLE): TYPE II Page 1 of 4

Orange-Red Response Solar Cell (650-900  $\mu$ m)

2. TECHNOLOGY CATEGORY: Photovoltaic converters

3. OBJECTIVE/ADVANCEMENT REQUIRED: >30% efficiency

---

4. CURRENT STATE OF ART: GaAs solar cells can presently be fabricated with acceptable efficiencies for this task.

---

5. DESCRIPTION OF TECHNOLOGY:

Cell for mid-range of spectrum.

Organometallic vapor-phase epitaxy (OM/VPE) should be used to grow a GaAs junction on an N+ GaAs substrate. Then an AlGaAs window (bandgap >2 eV or so) should be grown on top.

---

6. RATIONALE AND ANALYSIS:

GaAs is ideally suited for this range of the spectrum. AlGaAs with Al concentration >50% is sufficient for window.

---

DEFINITION OF TECHNOLOGY REQUIREMENT

---

1. TECHNOLOGY REQUIREMENT (TITLE): Mid-spectrum cell, Type II Page 2 of 4

---

7. TECHNOLOGY OPTIONS:

A GaAs cell is best suited for this range of the spectrum. Technology is fairly well developed because GaAs is presently used as a full-spectrum cell, so no other material is likely to replace GaAs.

Liquid phase epitaxy (LPE) can be used to fabricate GaAs solar cells but OM/VPE is best for reproducible, high throughput cell growth.

---

8. TECHNICAL PROBLEMS:

Presently, some oxygen can find its way into the AlGaAs window with OM/VPE, but this may not be a severe limitation.

Ohmic contacts could be better on p+ GaAs (which always caps the AlGaAs window), used in p on n cells, which are easier to fab.

---

9. POTENTIAL ALTERNATIVES:

This is the assist III-V cell to fabricate and is likely to be used in any spectrum-splitting scheme, unless a more difficult technology were employed (e.g., Si and AlGaAs for 2-cell spectrum splitting).

---

10. PLANNED PROGRAMS OR UNPERTURBED TECHNOLOGY ADVANCEMENT

GaAs solar cell is now close to realizing its full potential. This component will be ready before either the high bandgap (Type I) AlGaAs cell, or the low bandgap (Type III) cell.

---

11. RELATED TECHNOLOGY REQUIREMENTS

Cover slides for heat (long wavelength light) rejection. The technology for this does exist (See #11 under Type I cells).

LARGE SPACE POWER SYSTEM COMPONENTS CHARACTERISTIC DATA SHEET

PART A - PHYSICAL

COMPONENT NAME <u>Mid-spectrum cell, Type II</u>		Page 3 of 4	
FUNCTION <u>Efficient conversion of middle part of AMØ spectrum</u>			
PHYSICAL DESCRIPTION  <u>                    </u> - Ag metal grid <u>p+ GaAs</u> <u>&gt;2 eV AlGaAs window</u> <u>p-GaAs</u> <u>n-GaAs</u> <u>GaAs substrate</u>		PARAMETRIC ANALYSIS RESULTS  A+ 50 suns, 125°C, 1.5 µm diff, length  4.5 µm gridline width } metal 290 µm grid spacing } p-junction depth=0.7 µm	
PHYSICAL DEVELOPMENT PROJECTIONS			
CHARACTERISTIC	STATE OF THE ART	PROJECTION FOR 1990	ACHIEVABLE CAPABILITY
size (cm x cm)	1.5 x 3.0 cm	1.5 x 3.0 cm	large as boule
thickness (µm)	400 µm	300-400 µm	250 µm
mass (g)	1.0	0.75-1.0	0.6g for 1.5x 3 cm
substrate thermal conductivity(W/cm K)	0.3	0.3	0.3 (GaAs)
Space Radiation Damage (EOL/BOL)@10 <sup>16</sup>	1 µm diff lengths	1.5 µm diff lengths	perhaps 3 µm diffusion lengths
electron dose			
METALLIZATION MATERIAL/CONFIGURATION/CHARACTERISTICS			
Ag metal grid on cell. Vacuum solder to package.			
MATERIAL CONSIDERATIONS			

LARGE SPACE POWER SYSTEM COMPONENTS CHARACTERISTIC DATA SHEET  
PART B - PERFORMANCE

COMPONENT NAME Mid-spectrum cell, Type II Page 4 of 4

FUNCTIONAL CHARACTERISTICS Photovoltaic conversion at 125°C,  
50 suns for middle part of AM0 spectrum.

PERFORMANCE DEVELOPMENT PROJECTIONS 125°C, 50 suns, 0.847 cm cell

CHARACTERISTIC	STATE OF THE ART	PROJECTION FOR 1990	ACHIEVABLE CAPABILITY
Voltage - $V_{mp}$ Open Voltage - $V_{oc}$ Current Capacity - $I_{sc}$ Peak Load - $P_{max}$ Efficiency - $\eta$ Reliability MTFB (Hours)	no data on a spectrum - split all but present results are not far from the 1990 projections at right	.774v .927v .408 amp .296 watt 7.8%*	about 10% higher current and power with associated gain in efficiency
- $I_{mp}$ Current - $I_{mp}$ $\Delta\eta/\Delta C$		.383 amp .0145% °C	

\* as % of total solar power

---

DEFINITION OF TECHNOLOGY REQUIREMENT

---

1. TECHNOLOGY REQUIREMENT (TITLE): Type III Page 1 of 4  
IR Response Solar Cell (900 nm - 1200 nm)

2. TECHNOLOGY CATEGORY: Photovoltaic Converter

3. OBJECTIVE/ADVANCEMENT REQUIRED: >30% efficiency

---

4. CURRENT STATE OF ART: Some GaAsSb cells have been made, but technology is primitive. Si alternative is, of course, well developed.

---

5. DESCRIPTION OF TECHNOLOGY:

Low bandgap, low-voltage cell.

Organometallic vapor-phase epitaxy (OM/VPE) should be used to grow a 1.11 eV GaAs<sub>0.73</sub>Sb<sub>0.27</sub> junction lattice-graded to a GaAs substrate.

An appropriate AlGaAs window (bandgap > 1.5 eV or so) should be grown on top.

---

6. RATIONALE AND ANALYSIS:

Low bandgap cell should convert low-energy photons, i.e., reduce "red loss."

---

---

DEFINITION OF TECHNOLOGY REQUIREMENT

---

---

1. TECHNOLOGY REQUIREMENT (TITLE): Low bandgap cell, Type III Page 2 of 4

---

---

7. TECHNOLOGY OPTIONS:

This study will center on the OM/VPE-grown GaAsSb cell lattice-graded to GaAs, having 1.11 eV bandgap at 30°C. Silicon is an obvious alternative to GaAsSb and would present fewer process problems, but since Varian is better equipped to study III-V cells, this study will center on GaAsSb.

---

8. TECHNICAL PROBLEMS:

Defects arising from lattice-constant graded layers. Also, GaAsSb growth by OM/VPE or any technique is not well developed.

---

9. POTENTIAL ALTERNATIVES:

Silicon cell, as described in #7.

---

10. PLANNED PROGRAMS OR UNPERTURBED TECHNOLOGY ADVANCEMENT

Work on lattice-constant grading and on GaAsSb epitaxy is in progress.

---

11. RELATED TECHNOLOGY REQUIREMENTS

Nothing that other solar cells do not require.

---

LARGE SPACE POWER SYSTEM COMPONENTS CHARACTERISTIC DATA SHEET

PART A - PHYSICAL

COMPONENT NAME <u>Low bandgap cell, Type III</u>		Page 3 of 4	
FUNCTION <u>Efficient conversion of long-wavelength part of AM0 spectrum.</u>			
PHYSICAL DESCRIPTION  <div style="border: 1px solid black; padding: 2px; margin-bottom: 5px;"> </div> <p style="margin-left: 20px;">- Ag grid</p> <p style="margin-left: 20px;"><u>p+ GaAs</u></p> <p style="margin-left: 20px;"><u>&gt; 1.5 eV AlGaAs window</u></p> <p style="margin-left: 20px;"><u>p-GaAsSb</u></p> <p style="margin-left: 20px;"><u>n-GaAsSb</u> <u>and grading layer</u></p> <p style="margin-left: 20px;"><u>GaAs substrate</u></p>		PARAMETRIC ANALYSIS RESULTS  At 50 suns, 125°C, 1.5 μm diff. length  4.5 μm grid line width } metal 290 μm grid spacing }  p-junction depth = 0.7 μm	
PHYSICAL DEVELOPMENT PROJECTIONS			
CHARACTERISTIC	STATE OF THE ART	PROJECTION FOR 1990	ACHIEVABLE CAPABILITY
Size (cm x cm)	1.5 x 3.0 cm	1.5 x 3.0 cm	large as boule
Thickness (μm)	400 μm	300-400 μm	250 μm
Mass (g)	1.0	0.75-1.0	0.6 g for 1.5x3 cm
Substrate thermal conductivity (W/cm-°K)	0.3	0.3	0.3 (GaAs)
Space Radiation Damage (EOL/BOL) @ 10 <sup>16</sup> 1 MeV electron dose	< 1.0 μm diff. lengths	1.5 μm diff lengths	Perhaps 3 μm diff. lengths
METALLIZATION MATERIAL/CONFIGURATION/CHARACTERISTICS			
Ag metal grid on cell. Vacuum solder to package.			
MATERIAL CONSIDERATIONS			

ORIGINAL PAGE IS  
OF POOR QUALITY

LARGE SPACE POWER SYSTEM COMPONENTS CHARACTERISTIC DATA SHEET  
PART B - PERFORMANCE

COMPONENT NAME <u>Low bandgap cell, Type III</u>		Page <u>4</u> of <u>4</u>	
FUNCTIONAL CHARACTERISTICS <u>Photovoltaic conversion at 125°C, 50 suns for long wavelength part of AM0 spectrum.</u>			
PERFORMANCE DEVELOPMENT PROJECTIONS <u>125°C, 50 suns, 0.847 cm cell</u>			
CHARACTERISTIC	STATE OF THE ART	PROJECTION FOR 1985	ACHIEVABLE CAPABILITY
Voltage Level - $V_{mp}$ Peak Voltage - $V_{oc}$ Current Capacity - $I_{sc}$ Peak Load - $P_{max}$ Efficiency - $\eta$ Reliability MTBF - Hours  - $I_{mp}$ Current - $I_{mp}$ $\Delta\eta/^\circ C$	GaAsSb cells (1.15 eV bandgap at 30°C) have been grown with lattice-constant grading to GaAs, but efficiency is poor due to dislocations.	0.45 V 0.57 V 0.31 amp 0.13 watt 3.42% *  0.287 amp <u>0.011%</u>  °C	about 10% higher current and power, with associated gain in efficiency.

\* as % of total solar power.

**DEFINITION OF TECHNOLOGY REQUIREMENT**

1. TECHNOLOGY REQUIREMENT (TITLE): \_\_\_\_\_ Page 1 of 4

Full-Spectrum Response Multibandgap Monolithic

2. TECHNOLOGY CATEGORY: Photovoltaic Converters

3. OBJECTIVE/ADVANCEMENT REQUIRED: high-efficiency conversion at air mass 0 and space operating condition

4. CURRENT STATE OF ART: Single-junction GaAs cells with AlGaAs windows are being produced.

5. DESCRIPTION OF TECHNOLOGY:

Organometallic vapor-phase epitaxial (OM/VPE) growth of 3-cell monolithic stack as shown at right. Substrate is  $\approx 400 \mu\text{m}$  thick and the active layers and lattice-constant grading add another 35-40 microns.

	Ag grid
	p+ GaAs
window →	2.76 eV AlAsSb, P
J1 {	2.01 eV AlGaAsSb, P
	2.01 eV, n
tunnel jcn {	n+
	p+
J2 {	1.54 eV, AlGaAsSb, P
	1.54 eV, n
tunnel jcn {	n+
	p+
J3 {	1.19 eV GaAsSb, P
	1.19, n and
	lattice grading
	n+ GaAs substrate

6. RATIONALE AND ANALYSIS:

OM/VPE has been used for uniform, reproducible growth of III-V materials. It holds the best promise for future high-throughput systems. GaAs substrates are being produced in growing numbers for a variety of applications.

---

---

DEFINITION OF TECHNOLOGY REQUIREMENT

---

---

1. TECHNOLOGY REQUIREMENT (TITLE): Multibandgap cell Page 2 of 4

---

---

7. TECHNOLOGY OPTIONS:

If lattice constant grading proves to give unacceptably high defect density, bulk sensory crystals may be developed which could serve as substrates with arbitrary lattice constant. They would be much more expensive than GaAs.

---

8. TECHNICAL PROBLEMS:

Lattice constant grading now gives too high a defect density. Also, any kind of III-V alloy with Al presently grown has an oxygen problem. Al is necessary for a wide bandgap range.

---

9. POTENTIAL ALTERNATIVES:

Two-junction cells, lattice matched to binary III-V substrates (e.g., AlGaAs on GaAs) can be fabricated but will be less efficient than the proposed AlGaAsSb cell.

---

10. PLANNED PROGRAMS OR UNPERTURBED TECHNOLOGY ADVANCEMENT

Present work aimed toward improving lattice-constant grading, growing AlGaAs, GaAsSb, etc., growing good tunnel junctions, fabricating good GaAs and AlGaAs solar cells. These "pieces" are not yet good enough for MJ cell to be attempted.

---

11. RELATED TECHNOLOGY REQUIREMENTS

Successful fabrication of each vital "piece" of the multi-junction cell, see (10).

LARGE SPACE POWER SYSTEM COMPONENTS CHARACTERISTIC DATA SHEET

PART A - PHYSICAL

COMPONENT NAME <u>Multibandgap cell</u>		page 3 of 4	
FUNCTION <u>high-efficiency conversion, AMO</u>			
PHYSICAL DESCRIPTION		PARAMETRIC ANALYSIS RESULTS	
AlGoAsSb cell on GaAs, see drawing in (5), P. 1		4.5 $\mu\text{m}$ grid line width } metal- 290 $\mu\text{m}$ grid spacing } lization for 50 suns, 125°C, 1.5 $\mu\text{m}$ diff. length  p-layer thickness=0.7 $\mu\text{m}$ n-layer thickness=1.0 $\mu\text{m}$ (except bottom)	
PHYSICAL DEVELOPMENT PROJECTIONS			
CHARACTERISTIC	STATE OF THE ART	PROJECTION FOR 1990	ACHIEVABLE CAPABILITY
size (cm x cm)	1.5x3.0 cm	1.5 x 3.0 cm	large as boules
thickness ( $\mu\text{m}$ )	400 $\mu\text{m}$	300-400 $\mu\text{m}$	250 $\mu\text{m}$
Mass (g)	1.0g	0.75-1.0g	0.6g for 1.5 x3 cm
Substrate thermal conductivity(W/cm <sup>2</sup> K)	0.3	0.3	0.3 (GaAs)
Space Radiation Damage EOL/BOL @10 <sup>16</sup> 1 MeV elec. dose	0.5 $\mu\text{m}$ diff. lengths	1.5 $\mu\text{m}$ diff lengths	perhaps 3 $\mu\text{m}$ diff. lengths
METALLIZATION MATERIAL/CONFIGURATION/CHARACTERISTICS			
Ag metal grid on cell. Cell is vacuum-soldered to package.			
MATERIAL CONSIDERATIONS			
Some solders could be jeopardized at too high a cell temperature (e.g., Ag-Su eutectic volts at 221°C).			

LARGE SPACE POWER SYSTEM COMPONENTS CHARACTERISTIC DATA SHEET  
PART B - PERFORMANCE

COMPONENT NAME Multibandgap cell Page 4 of 4

FUNCTIONAL CHARACTERISTICS High-efficiency photovoltaic conversion at 125°C, 50 suns

PERFORMANCE DEVELOPMENT PROJECTIONS

CHARACTERISTIC	STATE OF THE ART	PROJECTION FOR 1990	ACHIEVABLE CAPABILITY	
Maximum Voltage - $V_{mp}$	low bandgap GaAsSb cells, lattice-graded to GaAs, have been grown but efficiency is poor due to dislocation.	2.8 v	2.9v	
Open Circuit Voltage - $V_{oc}$		3.3 v	3.3 v	
Current Capability - $I_{sc}$		.33 amp	.409 amp	
Maximum Power - $P_{max}$		.92 watt	1.02 watt	
Efficiency - $\eta$		24%	26.5%	
Reliability				
MTBF (Hours)				
Maximum Current - $I_{mp}$			.318 amp	.394 amp
$\Delta\eta/\Delta C$		.056%/°C	.04	

## DEFINITION OF TECHNOLOGY REQUIREMENT

1. TECHNOLOGY REQUIREMENT (TITLE): Modular Small Aperture Page 1 of  
Concentrator.
2. TECHNOLOGY CATEGORY: \_\_\_\_\_
3. OBJECTIVE/ADVANCEMENT REQUIRED: For 25% efficient multibandgap  
cells, a design having 1 Kg/m<sup>2</sup> specific mass, capable of  
holding the cell temperature below 125°C.
4. CURRENT STATE OF ART: Study activity to develop concepts and  
conduct trade studies.

### 5. DESCRIPTION OF TECHNOLOGY:

Activity is under way to develop multibandgap cells with the required efficiency at about 125°C. Low light loss modular concentrator designs with single reflections should be examined to develop geometries with a high degree of isolation uniformity over the cell surface and pointing error insensitivity. The 100 cm<sup>2</sup> aperture is sized to permit passive low cell temperature, a reasonable cell size for handling and manufacture. It also allows for two cell geometries should the multibandgap cell fail to become available.

### 6. RATIONALE AND ANALYSIS:

The required small concentrators represent the least costly approach for meeting the 1990's power needs. Cost will be of utmost significance in enabling the large power missions, since they must compete with alternate terrestrially-based solutions. Further, the modular concentrators should be safer, may have lower plasma losses, should be less sensitive to radiation, and should be more compatible with DOD threat survivability needs.

DEFINITION OF TECHNOLOGY REQUIREMENT

1. TECHNOLOGY REQUIREMENT (TITLE): Modular Small Aperture Page 2 of Concentrator.

7. TECHNOLOGY OPTIONS:

Develop the concentrator module using one of several geometries such as:

1. Modular Nested Trough
2. Modular Off-Axis Parabola
3. Modular Small Cassegrainian

8. TECHNICAL PROBLEMS:

- a. Optical design for lowest light loss, most even insolation across the cell face, and
- b. Thermal mirror radiator design for lowest mass at 125°C cell temperature.

9. POTENTIAL ALTERNATIVES:

- a. A thermophotovoltaic module
- b. Planar arrays.

10. PLANNED PROGRAMS OR UNPERTURBED TECHNOLOGY ADVANCEMENT:

NASA and DOD plans for development in this area appear to have settled initially on modular cassegrainian solutions. Light losses which may be avoidable result. Further study is required to limit losses.

11. RELATED TECHNOLOGY REQUIREMENTS:

- a. Multibandgap cell development.
- b. Truss beambuilder development.

**ORIGINAL PAGE IS  
OF POOR QUALITY**

DEFINITION OF TECHNOLOGY REQUIREMENT	No.
1. TECHNOLOGY REQUIREMENT (TITLE): <u>Modular Small Aperture Concentrator.</u>	Page 3 of 3
12. TECHNOLOGY REQUIREMENTS SCHEDULE:	
CALENDAR YEAR	
SCHEDULE ITEM	'9   '90   '91   '92   '93   '94   '95
TECHNOLOGY CONCEPT PROOFING	
φA Further Concept Studies	
φB Design Studies (2)	
LDEF Test Article Dev.	
LDEF Flight Evaluation	
FLIGHT PROGRAM	
Flight Article Design and Fabrication	
Space Construction Development in Space	
Space Assy - Operational Hardware	
13. USAGE SCHEDULE:	
TECHNOLOGY NEED DATE	TOTAL
NUMBER OF LAUNCHES	
14. REFERENCES	
<p>1. Concentrating Photovoltaics - A viable candidate for the next generation of Air Force Satellite Power Systems, Jack W. Geis, Proceedings of the 15th Intersociety Energy Conversion Conference, Vol. 1, page 363.</p>	
15. LEVEL OF STATE OF THE ART:	
<p>1. Basic phenomena observed and reported</p> <p>② Theory formulated to describe phenomena</p> <p>③ Some portions of the theory tested by physical experiment or mathematical model</p> <p>4. Pertinent functions or characteristic demonstrated, e.g., material, component</p>	<p>5. Component or breadboard-tested in relevant environment in laboratory</p> <p>6. Model tested in aircraft environment</p> <p>7. Model tested in space environment</p> <p>8. New capability derived from a much lesser operational model</p> <p>9. Reliability upgrading of an operational model</p> <p>10. Lifetime extension of an operational model</p>

2652 22

DEFINITION OF TECHNOLOGY REQUIREMENT

1. TECHNOLOGY REQUIREMENT (TITLE): Low Mass Gallium Page 1 of 3  
Arsenide Planar Array Blanket and Cells

2. TECHNOLOGY CATEGORY: Power Generation

3. OBJECTIVE/ADVANCEMENT REQUIRED: A Low-Mass Gallium Arsenide Blanket  
for use in East Electric Transfer (Space Tug) missions.

4. CURRENT STATE OF ART: 8-12 mill cells for blankets.

5. DESCRIPTION OF TECHNOLOGY:

50 micrometer thick gallium arsenide cells on a Kapton blanket.

6. RATIONALE AND ANALYSIS:

This appears to be the lowest mass approach for this mission, and, when combined with on-array annealing, is a viable technology for missions which spend extended times in the radiation belts.

DEFINITION OF TECHNOLOGY REQUIREMENT

1. TECHNOLOGY REQUIREMENT (TITLE): Low Mass Gallium Arsenide Page 2 of 3  
Planar Array Blanket and Cells

7. TECHNOLOGY OPTIONS:

1. 50 micrometer thick cells with 50 micrometer thick coverslides.
2. 50-100 micrometer coverslides with very thin 10 micrometer deposited Gallium Arsenide cells.

6. TECHNICAL PROBLEMS:

Fabricating and handling the cells prior to blanket installation.

9. POTENTIAL ALTERNATIVES:

Heavier modular concentrators.

10. PLANNED PROGRAMS OR UNPERTURBED TECHNOLOGY ADVANCEMENT:

Gallium Arsenide technology may not continue for other missions because of its high cost.

11. RELATED TECHNOLOGY REQUIREMENTS:

None.



DEFINITION OF TECHNOLOGY REQUIREMENT

1. TECHNOLOGY REQUIREMENT (TITLE): Space Fabricated Truss Page 1 of 3  
for Solar Array Support

2. TECHNOLOGY CATEGORY: Power Generation

3. OBJECTIVE/ADVANCEMENT REQUIRED: Fabrication of Truss Beams  
in Space for Support of Solar Array Modules Made by a Robotic Beambuilder.

4. CURRENT STATE OF ART: Deployable beams in development at General Dynamics.  
Fabricated beams developed at MSFC/Grumman.

5. DESCRIPTION OF TECHNOLOGY:

Trusses made by a robotic truss beambuilder which fabricates, from rolls of graphite epoxy material, truss members with a low mass per unit length ( $< 1$  Kg/m).

6. RATIONALE AND ANALYSIS.

Beambuilders utilizing aluminum and graphite epoxy have been studied extensively by Grumman and General Dynamics. The beams themselves should weigh about half as much as comparable deployable beams with heavy fitting and hinges. Total mass savings are about 15 to 20% of the total array mass.

DEFINITION OF TECHNOLOGY REQUIREMENT

1. TECHNOLOGY REQUIREMENT (TITLE): Space Fabricated Truss Page 2 of  
for Solar Array Support

7. TECHNOLOGY OPTIONS:

Alternate materials exist with varying degrees of strength.

8. TECHNICAL PROBLEMS:

An aluminum beam fabricator has been demonstrated.

9. POTENTIAL ALTERNATIVES:

1. Deployable trusses (about 100% heavier).
2. Aluminum Space Fabricated Trusses (about 50% heavier for the same strength).

10. PLANNED PROGRAMS OR UNPERTURBED TECHNOLOGY ADVANCEMENT:

Plans for this technology exist but are on hold at this time.

11. RELATED TECHNOLOGY REQUIREMENTS.

1. Astronaut-Controlled Transporter and Installer for Space-Installed Photovoltaic Array Modules.

**DEFINITION OF TECHNOLOGY REQUIREMENT** No.

1. TECHNOLOGY REQUIREMENT (TITLE): Space Fabricated Truss for Solar Array Support Page 3 of 3

**12. TECHNOLOGY REQUIREMENTS SCHEDULE:**

SCHEDULE ITEM	YEAR																			
	1	2	3	4	5	6	7	8	9	10	11	12	13	14	15	16	17	18	19	
<b>TECHNOLOGY</b>																				
Key Beambuilder Sub-system Development	_____				▽															
Beambuilder System					_____				▽											
Mission Equipment Development					_____															
Space Fabricated Demo Module									_____											
Space Demonstration of Demo									_____											

**13. USAGE SCHEDULE:**

TECHNOLOGY NEED DATE	1	2	3	4	5	6	7	8	9	10	11	12	13	14	15	16	17	18	19	TOTAL	
NUMBER OF LAUNCHES																					

**14. REFERENCES**

Final Report - Space Construction Automated Fabricated Experiment Definition Study (SCAFEDS) - Contract NAS9-15310 - General Dynamics/Convair Division.

- 15. LEVEL OF STATE OF THE ART:**
- |   |  |
|---|--|
| <ul style="list-style-type: none"> <li>1. Basic phenomena observed and reported</li> <li>2. Theory formulated to describe phenomena</li> <li>3. Theory tested by physical experiment or mathematical model</li> <li>4. Pertinent functions or characteristic demonstrated, e.g., material, component</li> </ul> | <ul style="list-style-type: none"> <li>5. Component or breadboard-tested in relevant environment in laboratory</li> <li>6. Model tested in aircraft environment</li> <li>7. Model tested in space environment</li> <li>8. New capability derived from a much lesser operational model</li> <li>9. Reliability upgrading of an operational model</li> <li>10. Lifetime extension of an operational model</li> </ul> |
|---|--|

## DEFINITION OF TECHNOLOGY REQUIREMENT

1. TECHNOLOGY REQUIREMENT (TITLE): Flywheel Inertia Page 1 of 3  
Storage Module

2. TECHNOLOGY CATEGORY: Energy Storage

3. OBJECTIVE/ADVANCEMENT REQUIRED: A 20-year LEO cycle life energy  
storage system.

4. CURRENT STATE OF ART: Flywheels for automobiles will have specific  
energies of 20-40 wt-hr/kg.

### 5. DESCRIPTION OF TECHNOLOGY:

Kevlar 49<sup>®</sup> composite flywheel rotor, with magnetic bearings and  
brushless DC motor generator.

### 6. RATIONALE AND ANALYSIS:

The 80,000 eclipse cycles the Space Construction Facility will see over its 20-year life make a storage medium which has extended cycle life beneficial life cycle mass would be lowest for this approach, for a relatively low risk system.

DEFINITION OF TECHNOLOGY REQUIREMENT

1. TECHNOLOGY REQUIREMENT (TITLE): Flywheel Inertia Page 2 of 3  
Storage Modules

7. TECHNOLOGY OPTIONS:

The rotor design can be axially wound, or perhaps a brush type. The axial winding would be safer—probably a significant discriminator.

8. TECHNICAL PROBLEMS:

The entire system requires a predesign study to validate the concept. In addition, the angular momentum interaction will require opposing modules to avoid unfavorable spacecraft interaction.

9. POTENTIAL ALTERNATIVES:

Sodium sulfur liquid mode batteries.

10. PLANNED PROGRAMS OR UNPERTURBED TECHNOLOGY ADVANCEMENT:

DOE automobile technology will develop the rotor designs, but NASA funding is required for the magnetic bearing activity and for the thermal aspects of the motor/generator design.

11. RELATED TECHNOLOGY REQUIREMENTS:

This activity is related to control of the structure bending modes and angular orientation.

DEFINITION OF TECHNOLOGY REQUIREMENT																	No.		
1. TECHNOLOGY REQUIREMENT (TITLE): <u>Flywheel Inertia Storage Module</u>																	Page 3 of 3		
12. TECHNOLOGY REQUIREMENTS SCHEDULE:																			
YEAR																			
SCHEDULE ITEM	1	2	3	4	5	6	7	8	9	10	11	12	13	14	15	16	17	18	19
TECHNOLOGY																			
Concept Definition Studies	█	█																	
Prototype Development			█	█															
Prototype Accelerated Life Testing					█	█	█												
Flight Article Development								█	█	█									
IOC In-Space Module Evaluation											▽	█							
Operational Deployment Availability																			▽
13. USAGE SCHEDULE:																			
TECHNOLOGY NEED DATE																			TOTAL
NUMBER OF LAUNCHES																			
14. REFERENCES																			
Flywheel components for satellite applications, A.R. Millner, Lincoln Laboratory. Technical Note 1978-4, Massachusetts Institute of Technology.																			
15. LEVEL OF STATE OF THE ART:																			
1. Basic phenomena observed and reported									5. Component or breadboard-tested in relevant environment in laboratory										
2. Theory formulated to describe phenomena									6. Model tested in aircraft environment										
3. Theory tested by physical experiment or mathematical model									7. Model tested in space environment										
4. Pertinent functions or characteristic demonstrated, e.g., material, component									8. New capability derived from a much lesser operational model										
									9. Reliability upgrading of an operational model										
									10. Lifetime extension of an operational model										

3852-98

## DEFINITION OF TECHNOLOGY REQUIREMENT

1. TECHNOLOGY REQUIREMENT (TITLE): Sodium Sulfur Batteries Page 1 of 3

2. TECHNOLOGY CATEGORY: Energy Storage

3. OBJECTIVE/ADVANCEMENT REQUIRED: High Specific Energy  
(100-150 Wt-hr/kg) batteries - with very

high cycle life - 10,000-30,000 cycles.

4. CURRENT STATE OF ART: NiCad and NiH batteries at 10-30 wt-hr/kg and  
5,000 cycles.

### 5. DESCRIPTION OF TECHNOLOGY:

Liquid sodium sulfur batteries operating at 300-400°C have the potential to be able to sustain many cycles and have high specific energies. However, the development of corrosion-proof container platings using rutile titanium, molybdenum, or chromium, followed by extensive life-cycle testing is required.

### 6. RATIONALE AND ANALYSIS:

Batteries operating with liquid electrolytes have the potential for extended cycle life, and this study has shown there would be significant mass and cost benefits from this development (about a 50% life-cycle cost and mass savings).

ORIGINAL PAGE IS  
OF POOR QUALITY

DEFINITION OF TECHNOLOGY REQUIREMENT	
1. TECHNOLOGY REQUIREMENT (TITLE):	Sodium Sulfur Batteries Page 2 of 3
7. TECHNOLOGY OPTIONS:	Alternative platings and alternative seals.
8. TECHNICAL PROBLEMS:	1. Thermal control to stabilize the batteries at their operating temperature, after a frozen launch. 2. Proof-of-cycle life.
9. POTENTIAL ALTERNATIVES:	Flywheel inertia energy storage.
10. PLANNED PROGRAMS OR UNPERTURBED TECHNOLOGY ADVANCEMENT:	The Air Force high energy density battery storage program should develop this technology.
11. RELATED TECHNOLOGY REQUIREMENTS:	Development of mostly passive thermal control systems.

**DEFINITION OF TECHNOLOGY REQUIREMENT** No.

1. TECHNOLOGY REQUIREMENT (TITLE): Sodium Sulfur Batteries Page 3 of 3

**12. TECHNOLOGY REQUIREMENTS SCHEDULE:**

SCHEDULE ITEM	YEAR																		
	1	2	3	4	5	6	7	8	9	10	11	12	13	14	15	16	17	18	19
<b>TECHNOLOGY</b>																			
Battery Cell Development	█	█																	
Accelerated Life Cycle Testing			█	█															
Phase II Cell Design					█														
Accelerated Life Cycle Testing						█	█												
Flight Article Development								█	█	█									
Proof Flight/Module Tests											█	█							

**13. USAGE SCHEDULE:**

TECHNOLOGY NEED DATE	1	2	3	4	5	6	7	8	9	10	11	12	13	14	15	16	17	18	19	TOTAL	
NUMBER OF LAUNCHES																					

**14. REFERENCES**

High Energy Density (HED) Rechargeable battery for satellite applications. Contract F33615-79-C-2044, Hughes Aircraft Company. Quarterly Meeting.

**15. LEVEL OF STATE OF THE ART:**

- |   |  |
|---|--|
| <ol style="list-style-type: none"> <li>1. Basic phenomena observed and reported</li> <li>2. Theory formulated to describe phenomena</li> <li>3. Theory tested by physical experiment or mathematical model</li> <li>4. Pertinent functions or characteristic demonstrated, e.g., material, component</li> </ol> | <ol style="list-style-type: none"> <li>5. Component or breadboard-tested in relevant environment in laboratory</li> <li>6. Model tested in aircraft environment</li> <li>7. Model tested in space environment</li> <li>8. New capability derived from a much lesser operational model</li> <li>9. Reliability upgrading of an operational model</li> <li>10. Lifetime extension of an operational model</li> </ol> |
|---|--|

## DEFINITION OF TECHNOLOGY REQUIREMENT

1. TECHNOLOGY REQUIREMENT (TITLE): Astronaut Controlled Page 1 of 3  
Transporter and Installer for Space Assembled Photovoltaic Array Modules

2. TECHNOLOGY CATEGORY: Power Generation

3. OBJECTIVE/ADVANCEMENT REQUIRED: Photovoltaic Array modules must be installed onto the truss support frame to facilitate their final use in generating power.

4. CURRENT STATE OF ART: Solar Array panels are all installed and interconnected terrestrially.

### 5. DESCRIPTION OF TECHNOLOGY:

After the truss frame work has been fabricated and interconnected by the Space Construction Facility (SCF) crew, a machine is required to transport the array modules from the cargo containers attached to the SCF, out onto the truss frame. There, they must be attached at both ends to the truss members and electrically connected.

### 6. RATIONALE AND ANALYSIS:

The routine task of transporting Photovoltaic Array modules and then attaching them to the truss framework requires a machine to assist with the transportation and installation. The degree of robotics could be minimal, human direction of the process is a distinct possibility.

**DEFINITION OF TECHNOLOGY REQUIREMENT**

1. TECHNOLOGY REQUIREMENT (TITLE): Astronaut Controlled Page 2 of 3  
Transporter and Installer for Space Installed Photovoltaic Array Modules

7. TECHNOLOGY OPTIONS:

Human vs. robotic control requires study. Time and motion analysis is needed. Modules might come attached in widths equal to the width between truss beams, or, the machine might attach modules at their final location. One machine may span the trusses, or two may be used.

8. TECHNICAL PROBLEMS:

This requirement requires a full-scale study to begin its implementation.

9. POTENTIAL ALTERNATIVES:

The entire assembly process could be done entirely by astronauts—but probably more expensively.

10. PLANNED PROGRAMS OR UNPERTURBED TECHNOLOGY ADVANCEMENT:

None.

11. RELATED TECHNOLOGY REQUIREMENTS:

Space-fabricated truss for solar array support.

DEFINITION OF TECHNOLOGY REQUIREMENT												No.								
1. TECHNOLOGY REQUIREMENT (TITLE): <u>Astronaut-Controlled</u>												Page 3 of 3								
<u>Transporter and Installer for Space Installed Photovoltaic Array Modules</u>																				
12. TECHNOLOGY REQUIREMENTS SCHEDULE:																				
												YEAR								
SCHEDULE ITEM	1	2	3	4	5	6	7	8	9	10	11	12	13	14	15	16	17	18	19	
TECHNOLOGY																				
Design Concept Studies																				
Phototype Machine Development																				
Truss Framework Fabrication Using Truss																				
Hard Mockup (Terrestrial) Developmental Testing and Refinement of Operational Transporter Flight Article Dev.																				
Proof of Concept Flight Demonstration																				
										Beam Builder Available										
										Installation Complete										
13. USAGE SCHEDULE:																				
TECHNOLOGY NEED DATE																				TOTAL
NUMBER OF LAUNCHES																				
14. REFERENCES																				
Space Construction Automated Fabrication Experiment Definition Study (SCAFEDS) Part IV. Contract NAS 9-15310. General Dynamics/Convair Division.																				
15. LEVEL OF STATE OF THE ART:																				
1. Basic phenomena observed and reported																				
2. Theory formulated to describe phenomena																				
3. Theory tested by physical experiment or mathematical model																				
4. Pertinent functions or characteristic demonstrated, e.g., material, component																				
										5. Component or breadboard-tested in relevant environment in laboratory										
										6. Model tested in aircraft environment										
										7. Model tested in space environment										
										8. New capability derived from a much lesser operational model										
										9. Reliability upgrading of an operational model										
										10. Lifetime extension of an operational model										

8052-92

## DEFINITION OF TECHNOLOGY REQUIREMENT

1. TECHNOLOGY REQUIREMENT (TITLE): Fault Tolerant, Low Mass Page 1 of 3  
DC Switching and Fault Isolation Matrix
2. TECHNOLOGY CATEGORY: Power Management and Control
3. OBJECTIVE/ADVANCEMENT REQUIRED: A fault tolerance, low mass  
switching matrix - single or dual fault tolerant - with on-array  
regulation capability.
4. CURRENT STATE OF ART: DC low power switching using electromechanical  
components.

### 5. DESCRIPTION OF TECHNOLOGY:

Single and dual failure-tolerant designs for efficient, DC power on-array regulation are required for Ion Engine Beam Supply voltage control. Ideally, the limited short-circuit current capability of the array - along with a limited complement of electromechanical switches - can be used to meet the requirements.

### 6. RATIONALE AND ANALYSIS:

Single and dual failure-tolerant designs for electromechanical DC switches for fault isolation and on-array ion engine beams supply regulation would be heavy. AC masses are also high. Approaches which are low mass - and utilize the short-circuit capability of the array - may enable this technology. Benefits were shown to be significant mass savings if a hybrid approach using both regulated DC and AC for the systems can be developed.

**DEFINITION OF TECHNOLOGY REQUIREMENT**

1. **TECHNOLOGY REQUIREMENT (TITLE):** Fault Tolerant, Low Mass Page 2 of 3  
DC Switching and Fault Isolation Matrix

**7. TECHNOLOGY OPTIONS:**

1. Transistor or electromechanical switches.
2. Single or dual failure tolerant.

**8. TECHNICAL PROBLEMS:**

1. The specific ion engine beam voltage range of regulation requirements should be developed.
2. A circuit-analysis-study should be conducted to validate the regulation approach, redundancy approach, and reliability goals to be targeted toward a more massive, all AC or all DC power management and control system, with AC or DC switches.

**9. POTENTIAL ALTERNATIVES:**

**10. PLANNED PROGRAMS OR UNPERTURBED TECHNOLOGY ADVANCEMENT:**

An on-array regulation study is actively under way.

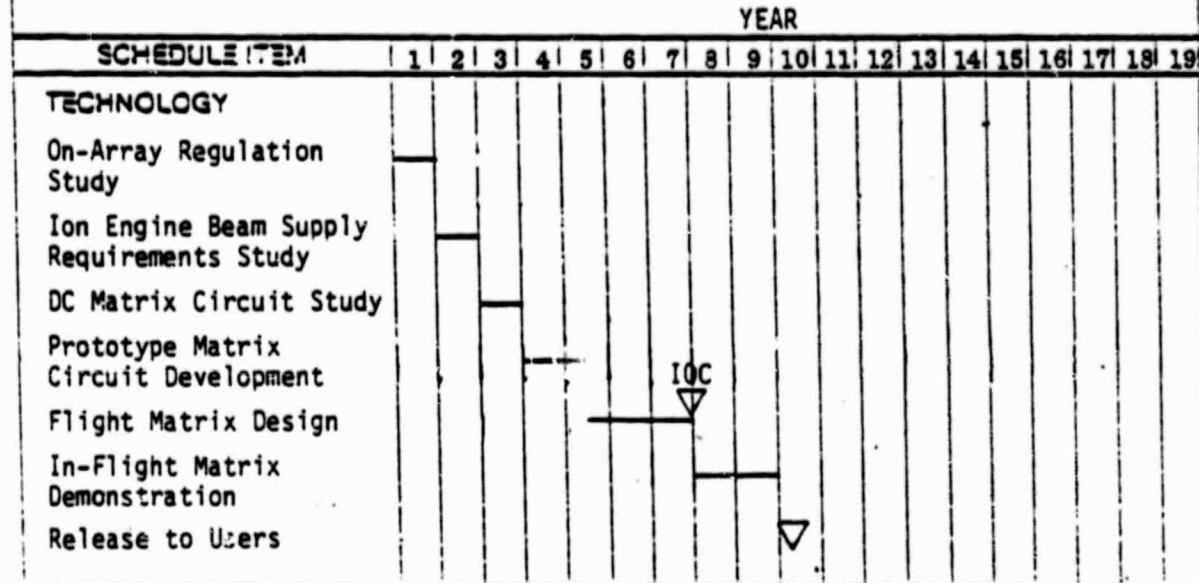
**11. RELATED TECHNOLOGY REQUIREMENTS:**

Ion engine beam supply voltage, current, and regulation goals.

<b>DEFINITION OF TECHNOLOGY REQUIREMENT</b>	<b>No.</b>
---	------------

1. TECHNOLOGY REQUIREMENT (TITLE): <u>Fault Tolerant, Low Mass DC Switching and Fault Isolation Matrix</u>	Page 3 of 3
--	-------------

<b>12. TECHNOLOGY REQUIREMENTS SCHEDULE:</b>
--



<b>13. USAGE SCHEDULE:</b>
----------------------------

TECHNOLOGY NEED DATE																					TOTAL
NUMBER OF LAUNCHES										1	1	1	1								

<b>14. REFERENCES</b>
-----------------------

- |   |  |
|---|--|
| <b>15. LEVEL OF STATE OF THE ART:</b> <ol style="list-style-type: none"> <li>1. Basic phenomena observed and reported</li> <li>2. Theory formulated to describe phenomena</li> <li>3. Theory tested by physical experiment or mathematical model</li> <li>4. Pertinent functions or characteristic demonstrated, e.g., material, component</li> </ol> | <ol style="list-style-type: none"> <li>5. Component or breadboard-tested in relevant environment in laboratory</li> <li>6. Model tested in aircraft environment</li> <li>7. Model tested in space environment</li> <li>8. New capability derived from a much lesser operational model</li> <li>9. Reliability upgrading of an operational model</li> <li>10. Lifetime extension of an operational model</li> </ol> |
|---|--|

## DEFINITION OF TECHNOLOGY REQUIREMENT

1. TECHNOLOGY REQUIREMENT (TITLE): Fault Tolerant AC Page 1 of 3  
Switching and Fault Isolation Matrix

2. TECHNOLOGY CATEGORY: Power Management and Control

3. OBJECTIVE/ADVANCEMENT REQUIRED: 25 KW Sized Modules must be  
switched to achieve fault tolerance.

4. CURRENT STATE OF ART: DC low power switch on today's satellites using  
electromechanical switches.

### 5. DESCRIPTION OF TECHNOLOGY:

AC user loads require a switch matrix interconnecting them to the AC buses, so that user faults or array/DC to AC converter faults can be switched out, with the remainder of the system continuing to operate correctly. Because high frequency AC changes direction quickly and each half cycle, thyristors can be used as these switches without the risk of thermal runaway in the event of a fault.

### 6. RATIONALE AND ANALYSIS:

By modularizing the AC power management and control system to connect Solar Array Modules directly to the DC to AC split cycle converter modules, DC fault isolation switching can be avoided. This means that heavy fault isolating electromechanical single-failure tolerant switches can be eliminated from the system, enabling a low-mass switching system.

DEFINITION OF TECHNOLOGY REQUIREMENT

1. TECHNOLOGY REQUIREMENT (TITLE): Fault Tolerant AC Page 2 of 3  
Switching and Fault Isolation Matrix

7. TECHNOLOGY OPTIONS:

1. Thyristor switches or electromechanical switches.
2. Single or dual failure tolerant.

8. TECHNICAL PROBLEMS:

The required degree of redundancy should be established by a reliability analysis for 100 KWe to 10 MWe systems.

9. POTENTIAL ALTERNATIVES:

Electromechanical switches used in a DC distribution system.

10. PLANNED PROGRAMS OR UNPERTURBED TECHNOLOGY ADVANCEMENT:

Single and dual failure DC fault correcting and isolating switches for 5 KWe level switching.

11. RELATED TECHNOLOGY REQUIREMENTS:

25 KWe split cyclo converters for AC power management and distribution.

DEFINITION OF TECHNOLOGY REQUIREMENT																		No.	
1. TECHNOLOGY REQUIREMENT (TITLE): <u>Fault Tolerant AC Switching and Fault Isolation Matrix</u>																	Page 3 of 3		
12. TECHNOLOGY REQUIREMENTS SCHEDULE:																			
YEAR																			
SCHEDULE ITEM	1	2	3	4	5	6	7	8	9	10	11	12	13	14	15	16	17	18	19
<b>TECHNOLOGY</b>																			
Reliability Requirement Study	-----																		
Prototype Switch Development	-----																		
Flight Article Development	-----																		
Flight Demonstration Ready for Users	-----																		
					▼														
								▼											
13. USAGE SCHEDULE:																			
TECHNOLOGY NEED DATE																			TOTAL
NUMBER OF LAUNCHES																			
14. REFERENCES																			
15. LEVEL OF STATE OF THE ART:																			
1. Basic phenomena observed and reported									5. Component or breadboard-tested in relevant environment in laboratory										
2. Theory formulated to describe phenomena									6. Model tested in aircraft environment										
3. Theory tested by physical experiment or mathematical model									7. Model tested in space environment										
4. Pertinent functions or characteristic demonstrated, e.g., material, component									8. New capability derived from a much lesser operational model										
									9. Reliability upgrading of an operational model										
									10. Lifetime extension of an operational model										

## DEFINITION OF TECHNOLOGY REQUIREMENT

1. TECHNOLOGY REQUIREMENT (TITLE): AC 25 KWe Power Cyclo Page 1 of 3  
Converters for AC Power Distribution

2. TECHNOLOGY CATEGORY: Power Management and Control

3. OBJECTIVE/ADVANCEMENT REQUIRED: Operational 85 KW DC/AC and AC/DC  
split cycloconverter modules.

4. CURRENT STATE OF ART: ]2 KWe DC/DC Cyclo Converters are operational  
in the laboratory.

### 5. DESCRIPTION OF TECHNOLOGY:

25 KW DC/DC Cyclo Converter development is currently under way. This technology activity should be completed and then extended to include split cyclo converter design, ultimately leading to array located DC/AC converters using rotary joint transformers for reliable, frictionless power transfer.

### 6. RATIONALE AND ANALYSIS:

Development of this conceptual approach will enable AC power distribution and split cyclo converters. These save system mass whenever one DC-AC converter can drive two AC-DC user supplies when compared to two DC/DC converters. Also, frictionless rotary power transfer across the spacecraft orientation drive and power transfer assembly rotary joint is enabled by these modules when rotary transformers are used.

DEFINITION OF TECHNOLOGY REQUIREMENT

1. TECHNOLOGY REQUIREMENT (TITLE): AC 25 KWe Power Cyclo Page 2 of 3  
Converters for AC Power Distribution

7. TECHNOLOGY OPTIONS:

A. A transistorized Power Converter.

B. A power converter utilizing SCRs.

Also, utilization of the rotary transformer.

8. TECHNICAL PROBLEMS:

Minimizing series inductive reactance so that the resonant cyclo converter will function correctly.

9. POTENTIAL ALTERNATIVES:

DC to DC Boost Buck Regulators, CUK DC/DC Converters.

10. PLANNED PROGRAMS OR UNPERTURBED TECHNOLOGY ADVANCEMENT:

25 KWe Power Converter prototype development.

11. RELATED TECHNOLOGY REQUIREMENTS:

Rotary Transformer, Orientation Drive, and Power Transfer Assembly (ROTODAPT).

DEFINITION OF TECHNOLOGY REQUIREMENT		No.																			
1. TECHNOLOGY REQUIREMENT (TITLE): <u>AC 25 KWe Power Cyclo Converters for AC Power Distribution</u>		Page 3 of 3																			
12. TECHNOLOGY REQUIREMENTS SCHEDULE: NEEDED FOR ION ENGINE INJECTION AND STATIONKEEPING AND MULTIMEGAWATT MISSION USES:																					
YEAR																					
SCHEDULE ITEM	1	2	3	4	5	6	7	8	9	10	11	12	13	14	15	16	17	18	19		
TECHNOLOGY																					
25 KW DC/DC Module Development	█	█	█																		
Split DC/AC - AC/DC Module Development			█	█																	
Testing of Rotary Transformer Coil Sections in 25 KW DC/AC/DC Converter			█	█																	
Flight Article Development																					
Proof Flight Testing																					
IOC																					
13. USAGE SCHEDULE:																					
TECHNOLOGY NEED DATE																					TOTAL
NUMBER OF LAUNCHES										1	1	1									
14. REFERENCES																					
Study of Power Management Technology for Orbital Multi 100 KWe Applications, Report CR 159834, Contract NAS 3-21757, J. W. Mildice, General Dynamics/Convair Division.																					
15. LEVEL OF STATE OF THE ART:																					
1. Basic phenomena observed and reported										5. Component or breadboard-tested in relevant environment in laboratory											
2. Theory formulated to describe phenomena										6. Model tested in aircraft environment											
3. Some portions of the theory tested by physical experiment or mathematical model.										7. Model tested in space environment											
4. Pertinent functions or characteristic demonstrated, e.g., material, component										8. New capability derived from a much lesser operational model											
										9. Reliability upgrading of an operational model											
										10. Lifetime extension of an operational model											

8652-72

## DEFINITION OF TECHNOLOGY REQUIREMENT

1. TECHNOLOGY REQUIREMENT (TITLE): Rotary Transformer Page 1 of 3  
Orientation Drive, and Power Transfer Assembly (ROTODAPT)

2. TECHNOLOGY CATEGORY: Power Management and Control

3. OBJECTIVE/ADVANCEMENT REQUIRED: Operational Modular ROTODAPTS  
with 25 KWe coil power transfer capability.

4. CURRENT STATE OF ART: Low power DC slip ring ODAPTS used on  
Geosynchronous Spacecraft.

### 5. DESCRIPTION OF TECHNOLOGY:

A ROTODAPT is required to transfer power transfer between the solar arrays  
~~which must be oriented so their aperture plane faces the sunlight, and~~  
the spacecraft bodies, which are required to point toward the earth.  
The ROTODAPT would consist of a rotary transformer, to enable low friction  
power transfer, dual redundant coaxial bearings, and a servo drive system.

### 6. RATIONALE AND ANALYSIS:

The use of a rotary transformer for power transfer across the rotary  
joint enables low friction transfer with low arcing risk. Spacecraft  
distribution and array distribution voltage can be as high as possible;  
the slip rings will not limit this voltage. Outside coil design enables  
easy maintenance and passive thermal control.

## DEFINITION OF TECHNOLOGY REQUIREMENT

1. TECHNOLOGY REQUIREMENT (TITLE): Rotary Transformer, Orientation Drive, and Power Transfer Assembly (ROTODAPT) Page 2 of 3

### 7. TECHNOLOGY OPTIONS:

1. A "pot coil" design with both coils on the outside for easy maintenance and passive, low mass heat rejection.
2. A coaxial coil design.

### 8. TECHNICAL PROBLEMS:

1. Assuring that transformer inefficiencies and forces caused by the rotary transformer air gap are minimized.
2. Interfacing with the orientation drive mechanical hardware compatibility, including its redundant bearing tolerances.

### 9. POTENTIAL ALTERNATIVES:

1. DC ODAPT with slip rings.
2. AC ODAPT with slip rings and no rotary transformer.

### 10. PLANNED PROGRAMS OR UNPERTURBED TECHNOLOGY ADVANCEMENT:

100 KWe technology activity with low voltage DC slip rings.

### 11. RELATED TECHNOLOGY REQUIREMENTS:

25 KWe cyclo converter development with the ODAPT rotary transformer used as the cyclo converter inductive element.



### DEFINITION OF TECHNOLOGY REQUIREMENT

1. TECHNOLOGY REQUIREMENT (TITLE): Slip Ring Orientation Drive Page 1 of 3 and Power Transfer Assembly (Slip Ring ODAPT)(Rotary Joint)
2. TECHNOLOGY CATEGORY: Power Management and Control
3. OBJECTIVE/ADVANCEMENT REQUIRED: If ROTODAPTS are not developed, DC slip rings capable of arcless, megawatt transfer must be developed.
4. CURRENT STATE OF ART: Low power DC slip ring ODAPTS.

#### 5. DESCRIPTION OF TECHNOLOGY:

This is an extension of today's slip ring design - except pressurization is required to enable high voltages, and meteoroid protection of the pressurization system is also required (modular pressure vessels).

#### 6. RATIONALE AND ANALYSIS:

If, for some unexpected reason, AC power management and distribution are not developed, or, when ion engine beam supplies can be supplied directly from DC on-array regulated sources - avoided power converters completely - then this technology is required.

DEFINITION OF TECHNOLOGY REQUIREMENT

1. TECHNOLOGY REQUIREMENT (TITLE): Slip Ring Orientation Drive Page 2 of 3  
and Power Transfer Assembly (ODAPT)

7. TECHNOLOGY OPTIONS:

- A. Wet Ring
- B. Dry Ring
- C. Axial or Radial Rings

8. TECHNICAL PROBLEMS:

Axial brush ring may not be topologically compatible with dual redundant bearings - requiring extra redundancy.

9. POTENTIAL ALTERNATIVES:

Rotary transformer, orientation drive, and power transfer assemble (ROTODAPT).

10. PLANNED PROGRAMS OR UNPERTURBED TECHNOLOGY ADVANCEMENT:

Air Force high voltage slip ring development up to 25 KWe.

11. RELATED TECHNOLOGY REQUIREMENTS:

- 1. Ion engine beam voltage supply delta regulation.
- 2. On-array DC power regulation.

**DEFINITION OF TECHNOLOGY REQUIREMENT** No.

1. TECHNOLOGY REQUIREMENT (TITLE): Slip Ring Orientation Drive and Power Transfer Assembly (Slip Ring ODAPT) Page 3 of 3

**12. TECHNOLOGY REQUIREMENTS SCHEDULE:**

SCHEDULE ITEM	YEAR																		
	1	2	3	4	5	6	7	8	9	10	11	12	13	14	15	16	17	18	19
<b>TECHNOLOGY</b>																			
Modularity Design Study of High Power ODAPT	█																		
Prototype Development of ODAPT Ring Modules Design, Fabrication and Test		█	█																
Flight Article ODAPT Development				█	█	█	█	▽											
Proof Flight Demonstration								█	█	█									

**13. USAGE SCHEDULE:**

TECHNOLOGY NEED DATE	1	2	3	4	5	6	7	8	9	10	11	12	13	14	15	16	17	18	19	TOTAL	
							▽														
NUMBER OF LAUNCHES								1		1			1				1				

**14. REFERENCES**

High Voltage, High Power Solar Power Systems Study, LMSC-D715836, 15 April 1980.

**15. LEVEL OF STATE OF THE ART:**

- |   |  |
|---|--|
| <ul style="list-style-type: none"> <li>1. Basic phenomena observed and reported</li> <li>2. Theory formulated to describe phenomena</li> <li>③ 3. Theory tested by physical experiment or mathematical model</li> <li>4. Pertinent functions or characteristic demonstrated, e.g., material, component</li> </ul> | <ul style="list-style-type: none"> <li>5. Component or breadboard-tested in relevant environment in laboratory</li> <li>6. Model tested in aircraft environment</li> <li>7. Model tested in space environment</li> <li>8. New capability derived from a much lesser operational model</li> <li>9. Reliability upgrading of an operational model</li> <li>10. Lifetime extension of an operational model</li> </ul> |
|---|--|

DEFINITION OF TECHNOLOGY REQUIREMENT

1. TECHNOLOGY REQUIREMENT (TITLE): Power System Control Page 1 of 3  
Computers (Failure Tolerant)

2. TECHNOLOGY CATEGORY: Power Management and Control

3. OBJECTIVE/ADVANCEMENT REQUIRED: Single Failure or Dual Failure  
Tolerant Control Computers to Control the Power Switching

4. CURRENT STATE OF ART: Power is generally controlled from ground  
stations.

5. DESCRIPTION OF TECHNOLOGY:

Distributed, single, or dual failure tolerant processors which send commands to switch matrix drivers which control the switching of the user loads.

6. RATIONALE AND ANALYSIS:

The power system itself will be single or dual failure tolerant; therefore, the processor(s) controlling it should have the same level of redundancy.

**DEFINITION OF TECHNOLOGY REQUIREMENT**

**1. TECHNOLOGY REQUIREMENT (TITLE):** Power system Control Page 2 of 3  
Computers (Failure Tolerant)

**7. TECHNOLOGY OPTIONS:**

1. Distributed processors connected as a federated system to provide single or dual failure tolerant processors.
2. Single package processors with single failure tolerant designs.

**8. TECHNICAL PROBLEMS:**

Architectural and software studies are required to define failure detection and correction strategies.

**9. POTENTIAL ALTERNATIVES:**

None.

**10. PLANNED PROGRAMS OR UNPERTURBED TECHNOLOGY ADVANCEMENT:**

Significant activity is already under way in this area at MSFC for DC system concepts. It should be expanded to include Hybrid System Design.

**11. RELATED TECHNOLOGY REQUIREMENTS:**

Hybrid AC/DC Power System Development.

DEFINITION OF TECHNOLOGY REQUIREMENT																	No.		
1. TECHNOLOGY REQUIREMENT (TITLE): <u>Power System Control</u>																	Page 3 of 3		
Computers (Failure Tolerant)																			
12. TECHNOLOGY REQUIREMENTS SCHEDULE:																			
CALENDAR YEAR																			
SCHEDULE ITEM	1	2	3	4	5	6	7	8	9	10	11	12	13	14	15	16	17	18	19
TECHNOLOGY																			
Simulation Studies of Power	█	█																	
Management Failure Detection and Isolation Strategies - Processor Requirements Definition																			
Prototype Processor Development			█	█															
Software Development					█	█													
Flight Critical Fabrication							▽												
							IDC												
13. USAGE SCHEDULE:																			
TECHNOLOGY NEED DATE																			TOTAL
NUMBER OF LAUNCHES																			
14. REFERENCES																			
1. Study of Power Management Technology for Orbital Multi 100 KWe Applications, Report CR 159834, Contract NAS 3-21757, J. W. Mildice, General Dynamics/Convair Division.																			
15. LEVEL OF STATE OF THE ART:																			
1. Basic phenomena observed and reported									5. Component or breadboard-tested in relevant environment in laboratory										
2. Theory formulated to describe phenomena									6. Model tested in aircraft environment										
3. Theory tested by physical experiment or mathematical model									7. Model tested in space environment										
4. Pertinent functions or characteristic demonstrated, e.g., material, component									8. New capability derived from a much lesser operational model										
									9. Reliability upgrading of an operational model										
									10. Lifetime extension of an operational model										

8652-98

GDC/AST 81-019

APPENDIX C  
TECHNOLOGY PLANS



III-V MULTIJUNCTION SOLAR CELLS AND  
III-V SOLAR CELLS FOR SPECTRUM SPLITTING  
AT AIR MASS 0

by

Timothy J. Maloney and Bruce R. Cairns

Prepared for General Dynamics, Convair Division



## 1. TASK I - MONOLITHIC EPITAXIAL MULTIJUNCTION SOLAR CELL

### 1.1 AlGaAsSb Multijunction Cell

A monolithic epitaxial III-V multijunction solar cell should have all junctions lattice matched to one another in order to avoid excessive lattice defects. If possible, the epitaxial stack should also be lattice matched to a binary III-V substrate, but this can severely restrict the junction bandgap range. The best junction series occur in the quaternary system AlGaAsSb (which allows higher bandgap windows than, say, AlGaInAs) for lattice constants in between those of GaAs and InP. A lattice-constant grading layer could allow such a stack to be grown on a GaAs or InP substrate, and a substantial amount of work on graded lattice constants has been and is being done. There is a slight chance that the development of bulk ternary materials will allow substrate material of arbitrary lattice constant to be used.<sup>1</sup> The best multijunction bandgap series in AlGaAsSb at typical operating temperatures in space was found to be (30°C bandgaps) 1.19-1.54-2.01 eV, which is accomplished by growing junctions of GaAs<sub>.8</sub>Sb<sub>.2</sub>, Al<sub>.22</sub>Ga<sub>.78</sub>As<sub>.82</sub>Sb<sub>.18</sub>, Al<sub>.58</sub>Ga<sub>.42</sub>As<sub>.83</sub>Sb<sub>.17</sub>, and finally a 2.76-eV window layer of AlAs<sub>.85</sub>Sb<sub>.15</sub>. This has a lattice constant of 5.73 Å, closer to GaAs (5.64 Å) than to InP (5.87 Å). High-bandgap tunnel junctions are grown in between the cell junctions. The tunnel junctions are taken to be perfect in these calculations, but one could subtract, say, 0.1V per tunnel junction from the maximum power voltage to get an idea of their effect.

A multijunction cell-modeling program was developed using the single-cell program of L. James<sup>2</sup> as a building block. The basic cell program has 29 independent variables,



nine of which are set for each junction in the multijunction program. Thus the multijunction model has  $29 + 9(n-1)$  independent variables, where  $n$  is the number of junctions. Among these are the carrier diffusion lengths in the p and n layers of each junction, which one would like to be as long as possible. At present such diffusion lengths are about 0.5 micron or less, but one would expect better values by 1990. The effect of radiation in space is unknown, but the diffusion lengths are likely to be somewhat degraded, although it is known that III-V materials are less susceptible to radiation damage than silicon. Moreover, Heinbockel, et al<sup>3</sup> have argued that the high operating temperature of GaAs solar cells in space could allow the radiation damage to be annealed out. Our study was done using two different diffusion lengths for all layers -- 3 microns and 1.5 microns. Junction thicknesses were optimized for each diffusion length (about 0.7-1 micron for 1.5-micron diffusion length and 1-1.3 micron for 3-micron diffusion length). The bottommost layer can be almost arbitrarily thick, and 30 microns has been used in this work.

Calculations were done for Air Mass 0 (AM0) at 1, 2, 3, 10, 100, 500 and 1000 suns and at temperatures between 50 and 250°C. Results are presented in tables and figures as follows: Table I, efficiency, 3-micron diffusion length; Figure 1, graph of efficiencies; Table II, maximum power voltage and current, 3 microns; Table III, efficiency, 1.5 micron; Figure 2, graph of efficiencies and Table IV, maximum power voltage and current, 1.5 micron. A one-third-inch cell is specifically considered in all cases, but intrinsic quantities such as efficiency do not change much with cell size or shape.



Other remarks about the AlGaAsSb multijunction solar cell appear in the attached General Dynamics forms.

TABLE I

AlGaAsSb 3-junction Cell Efficiency, 3-micron Diffusion Length.

	T °C	50	75	100	125	150	175	200	225	250
C suns										
1		25.6	24.2	22.6	20.9	19.3	17.5	16.0	14.3	12.6
2		26.5	25.2	23.6	22.0	20.4	18.8	17.4	15.7	14.1
3		27.0	25.7	24.2	22.6	21.1	19.5	18.1	16.5	14.8
10		28.5	27.3	26.0	24.6	23.1	21.7	20.2	18.9	17.4
100		30.6	29.8	28.6	27.4	26.2	24.9	23.9	22.7	21.3
500		31.0	30.3	29.3	28.3	27.3	26.2	25.3	24.3	23.1
1000		30.5	29.9	28.9	28.0	27.0	26.0	25.2	24.1	23.1

FIGURE 1

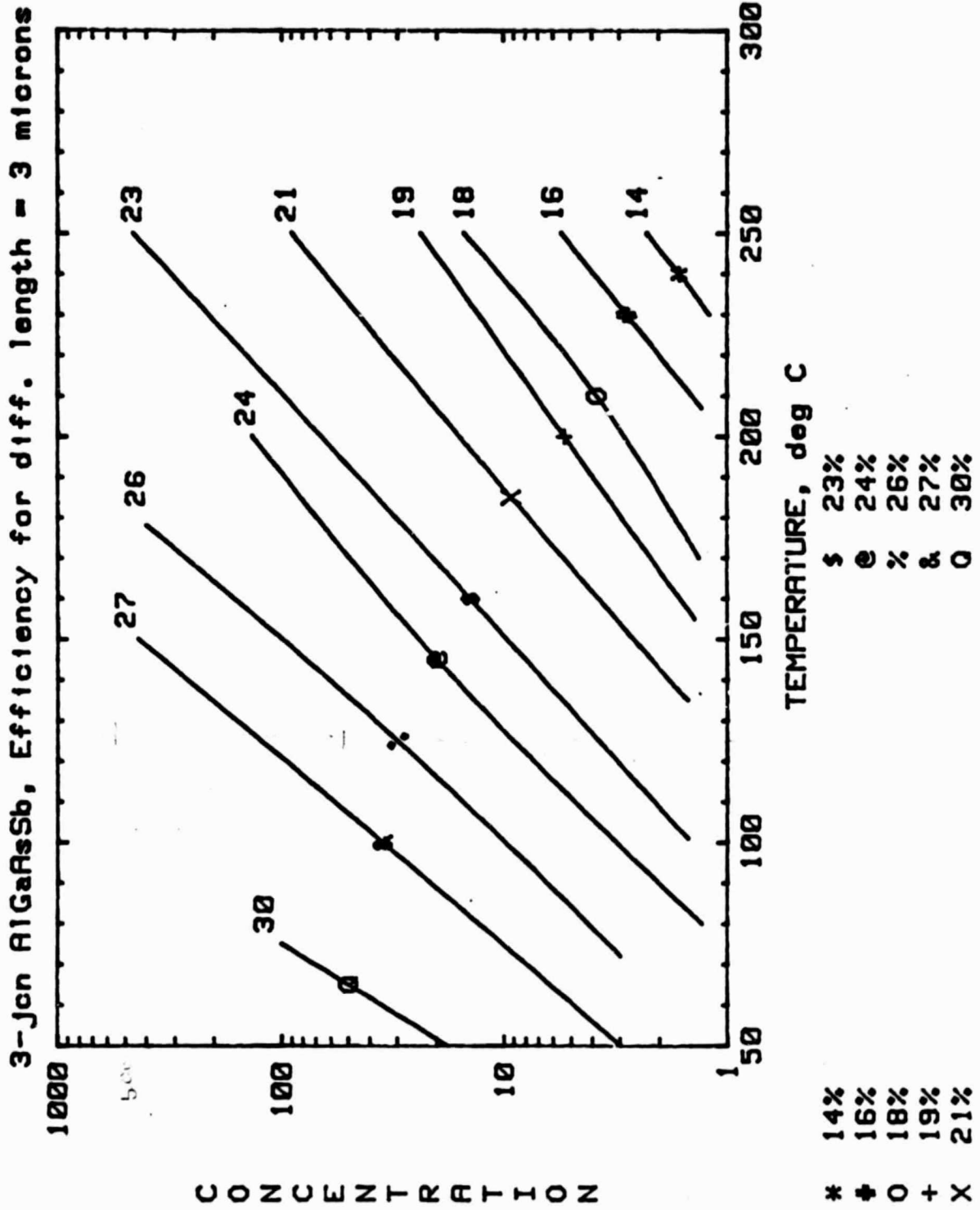


TABLE II  
 AlGaAsSb 3-junction Cell for 1/3-inch Cell  
 Max. power V(volts), Max. Power I (amps), for Diffusion Length = 3  $\mu$ m

	T °C	50	75	100	125	150	175	200	225	250
C suns										
1		2.84V .0069A	2.64 .0070	2.46 .0070	2.25 .0071	2.11 .0070	1.96 .0068	1.73 .0070	1.62 .0067	1.38 .0070
2		2.94 .0137	2.77 .0139	2.58 .0139	2.38 .0141	2.23 .0139	2.05 .0140	1.87 .0140	1.76 .0140	1.56 .0140
3		2.99 .0206	2.77 .0212	2.62 .0211	2.47 .0210	2.31 .0210	2.09 .0210	1.92 .0220	1.78 .0210	1.56 .0220
10		3.14 .0690	3.00 .0690	2.81 .0700	2.63 .0710	2.48 .0710	2.34 .0710	2.24 .0690	2.00 .0720	1.87 .0710
100		3.38 .689	3.24 .699	3.09 .706	2.96 .704	2.81 .711	2.67 .712	2.57 .708	2.40 .719	2.33 .696
500		3.52 3.35	3.39 3.40	3.27 3.41	3.13 3.45	3.00 3.46	2.87 3.48	2.79 3.46	2.66 3.48	2.46 3.57
1000		3.46 6.73	3.35 6.79	3.25 6.78	3.09 6.89	2.97 6.92	2.85 6.96	2.72 7.05	2.67 6.88	2.55 6.91

ORIGINAL PAGE IS  
OF POOR QUALITY

TABLE III  
AlGaAsSb 3-Junction Cell

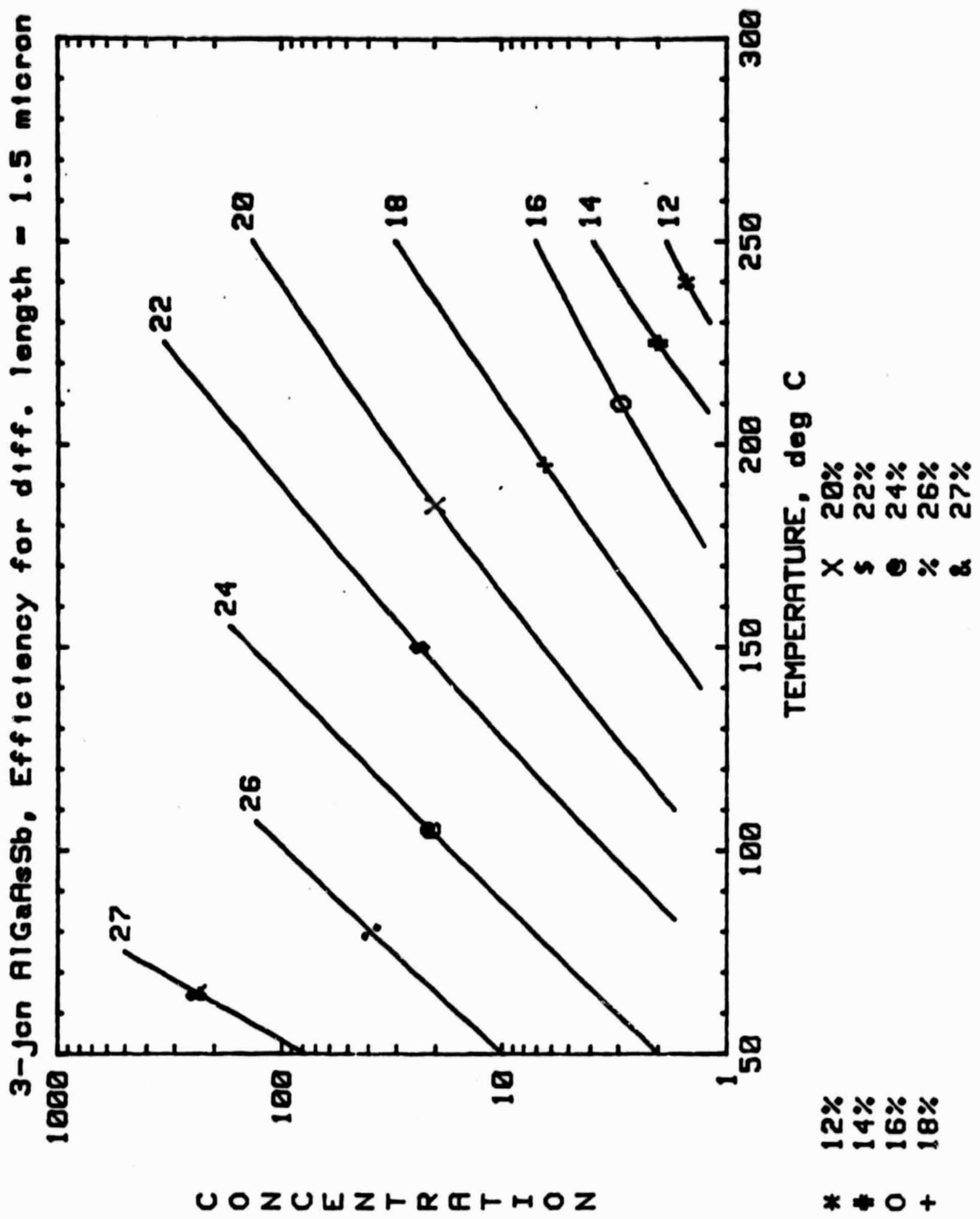
Efficiency (%), Diffusion Length = 1.5  $\mu$ m

C suns	T °C	Efficiency (%)									
		50	75	100	125	150	175	200	225	250	
1		23.2	21.8	20.2	18.9	17.4	15.8	14.4	12.9	11.3	
2		24.0	22.9	21.4	19.8	18.3	17.0	15.6	14.0	12.7	
3		24.5	23.4	21.9	20.4	19.1	17.7	16.3	14.9	13.4	
10		25.9	24.8	23.5	22.2	20.8	19.5	18.4	17.0	15.6	
100		27.7	26.9	25.9	24.8	23.7	22.4	21.5	20.4	18.9	
500		28.0	27.2	26.4	25.5	24.4	23.5	22.7	21.7	20.7	
1000		27.5	26.8	25.9	25.0	23.9	23.1	22.4	21.5	20.4	

TABLE IV  
 AlGaAsSb 3-Junction Cell  
 Max. power V (volts), Max. Power I (amps) for 1/3-inch cell, Diffusion Length = 1.5  $\mu$ m

	T °C	50	75	100	125	150	175	200	225	250
C suns										
1		2.83 .0062	2.67 .0062	2.52 .0061	2.28 .0063	2.08 .0064	1.91 .0063	1.70 .0065	1.54 .0064	1.42 .0061
2		2.96 .0123	2.75 .0126	2.59 .0126	2.44 .0123	2.26 .0123	2.02 .0128	1.92 .0124	1.648 .0130	1.53 .0126
3		3.00 .0187	2.80 .019	2.61 .019	2.49 .019	2.30 .019	2.12 .019	1.94 .019	1.75 .019	1.64 .019
10		3.11 .064	2.98 .064	2.82 .063	2.68 .063	2.46 .065	2.33 .064	2.15 .065	2.00 .065	1.84 .065
100		3.38 .626	3.24 .633	3.11 .634	2.96 .638	2.80 .644	2.65 .644	2.54 .644	2.37 .655	2.17 .664
500		3.47 3.07	3.30 3.14	3.25 3.10	3.13 3.10	3.04 3.06	2.88 3.10	2.74 3.16	2.66 3.11	2.52 3.12
1000		3.43 6.09	3.28 6.22	3.20 6.16	3.02 6.29	2.86 6.36	2.77 6.34	2.70 6.33	2.57 6.35	2.54 6.11

FIGURE 2





## 2.0 TASK II - III-V CELLS FOR SPECTRUM SPLITTING

### 2.1 Type I Short Wavelength AlGaAs Cell

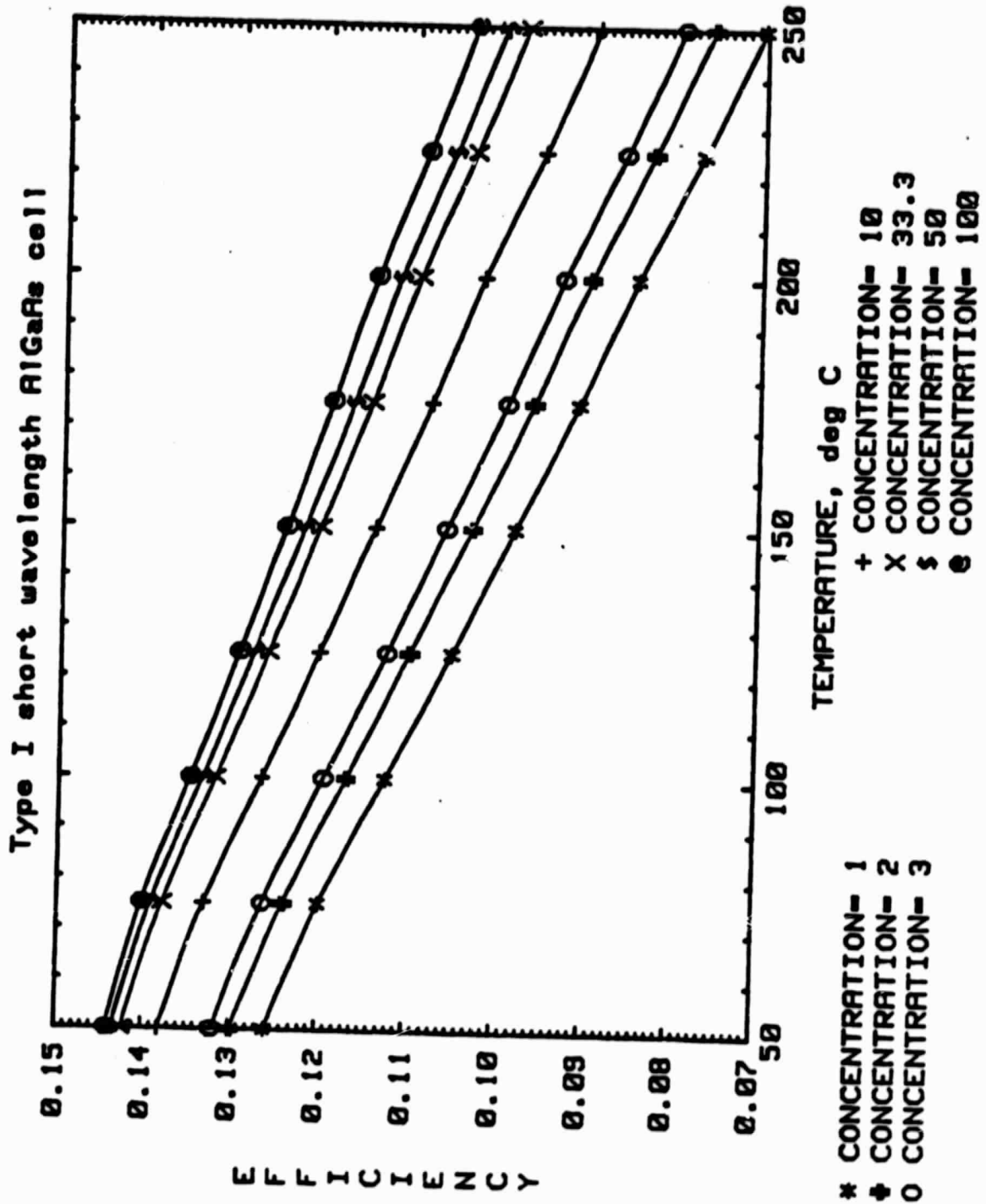
An  $\text{Al}_{.4}\text{Ga}_{.6}\text{As}$  solar cell (30°C bandgap of 1.91 eV) with an  $\text{Al}_{.93}\text{Ga}_{.07}\text{As}$  window of 2.95 eV is proposed as the Type I cell. Efficiency as a function of temperature and concentration is plotted in Fig. 3 for the 350-650 nm part of the AM0 spectrum. Efficiency is calculated as a fraction of total solar power in these graphs, so that efficiencies of the three cells can be added to compute system efficiency. A 1.5-micron diffusion length has been used for all these cells. Since 125°C, 50 suns has been suggested as a likely operating point for solar cells, the complete I-V curve for that operating point is shown in Fig. 4. Table V gives cell performance data at 125°C, 50 suns, for Types I, II, and III spectrum split cells. Remarks about using cover slides for heat rejection are in Section 3.1.4.

Figure 5 shows the efficiency versus temperature and concentration for monochromatic light. Here a 1-sun concentration was taken to be the power in the AM0 band from 1.91 eV to the usual window cutoff of 3 eV. It was found for Type I cells that optimal efficiency was achieved for monochromatic light at 0.13 eV above the bandgap.

### 2.2 Type II Medium Wavelength GaAs Cell

The 650-900 nm AM0 spectrum is well suited to a GaAs solar cell, and it is therefore suggested for Type II. Figure 6 shows efficiency versus temperature and concentration for this cell. The I-V curve for 50 suns, 125°C, is shown in Fig. 7.

FIGURE 3



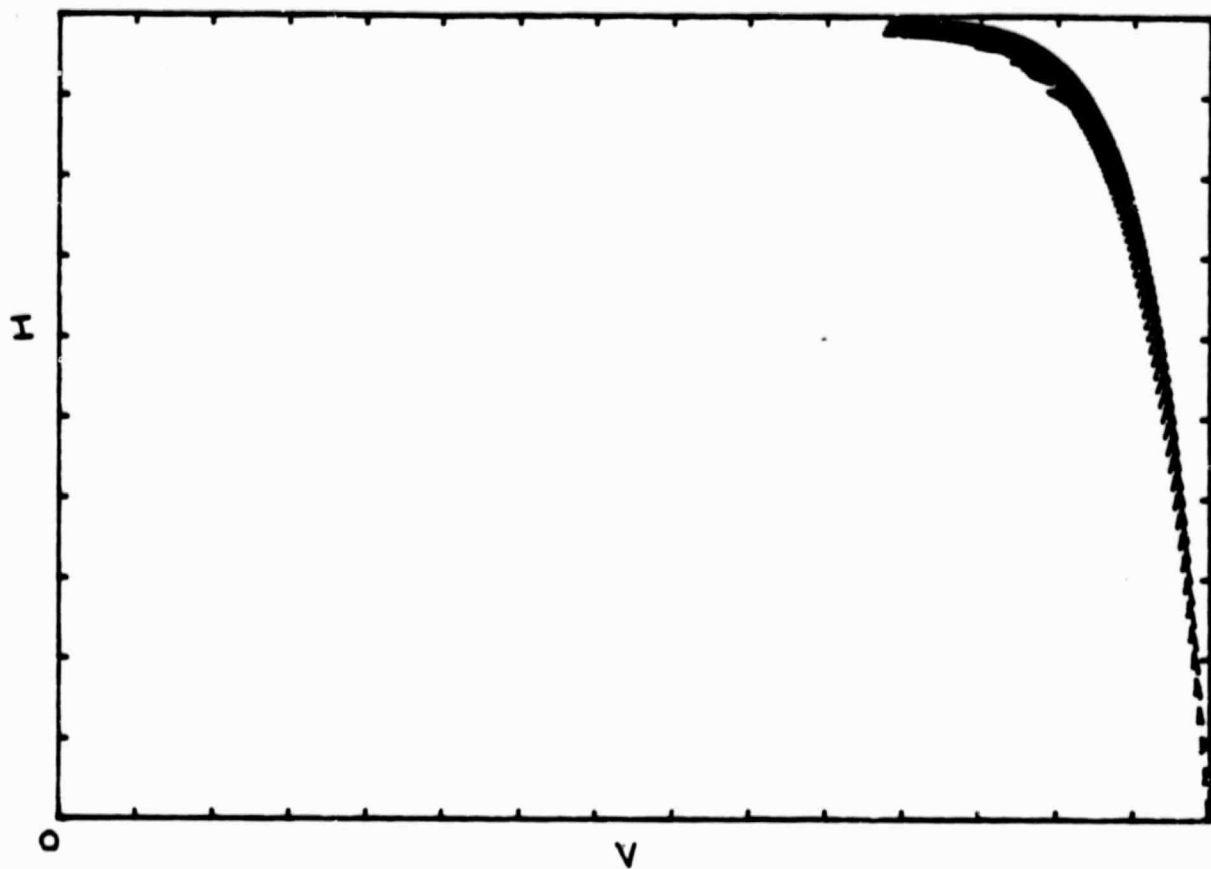


FIGURE 4 I-V curve for Type I cell, 50 suns and 125°C.  
(See Table V for current and voltage scales,  
and Fig. 10 for a discussion of I-V curve  
details.)

TABLE V

Spectrum-Split Cell Data for 125°C, 50 suns\*

	$V_{oc}$ , volt	$I_{sc}$ , amp	$V_{max}$	$I_{max}$	$\frac{ff}{ff}$	$\frac{Eff.}{Eff.}$
Type I, AlGaAs	1.50	.409	1.26	.387	.798	.128
Type II, GaAs	.927	.408	.774	.383	.782	.078
Type I, GaAsSb	.567	.311	.452	.287	.735	.034

\* One-third-inch cell used.

FIGURE 5

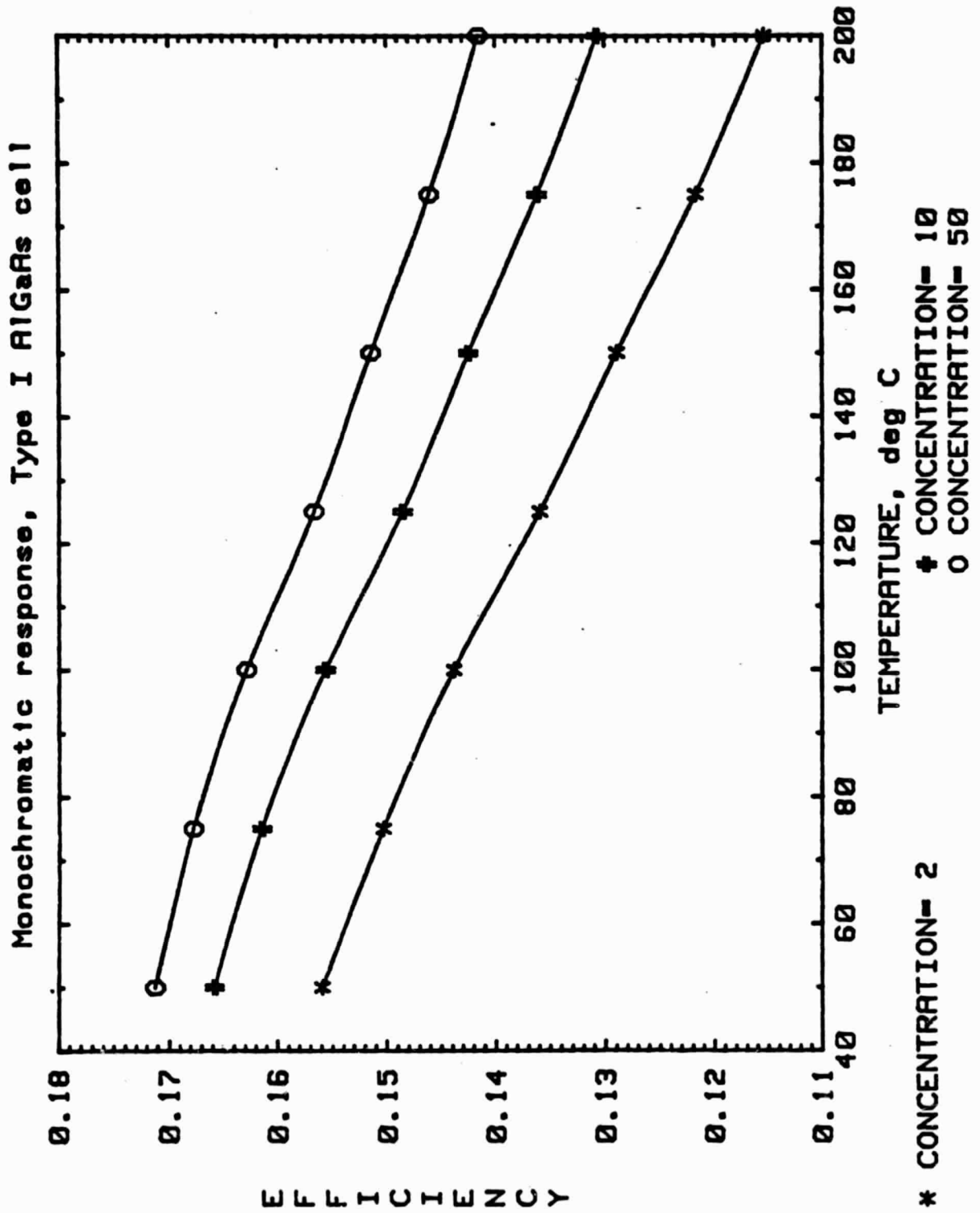
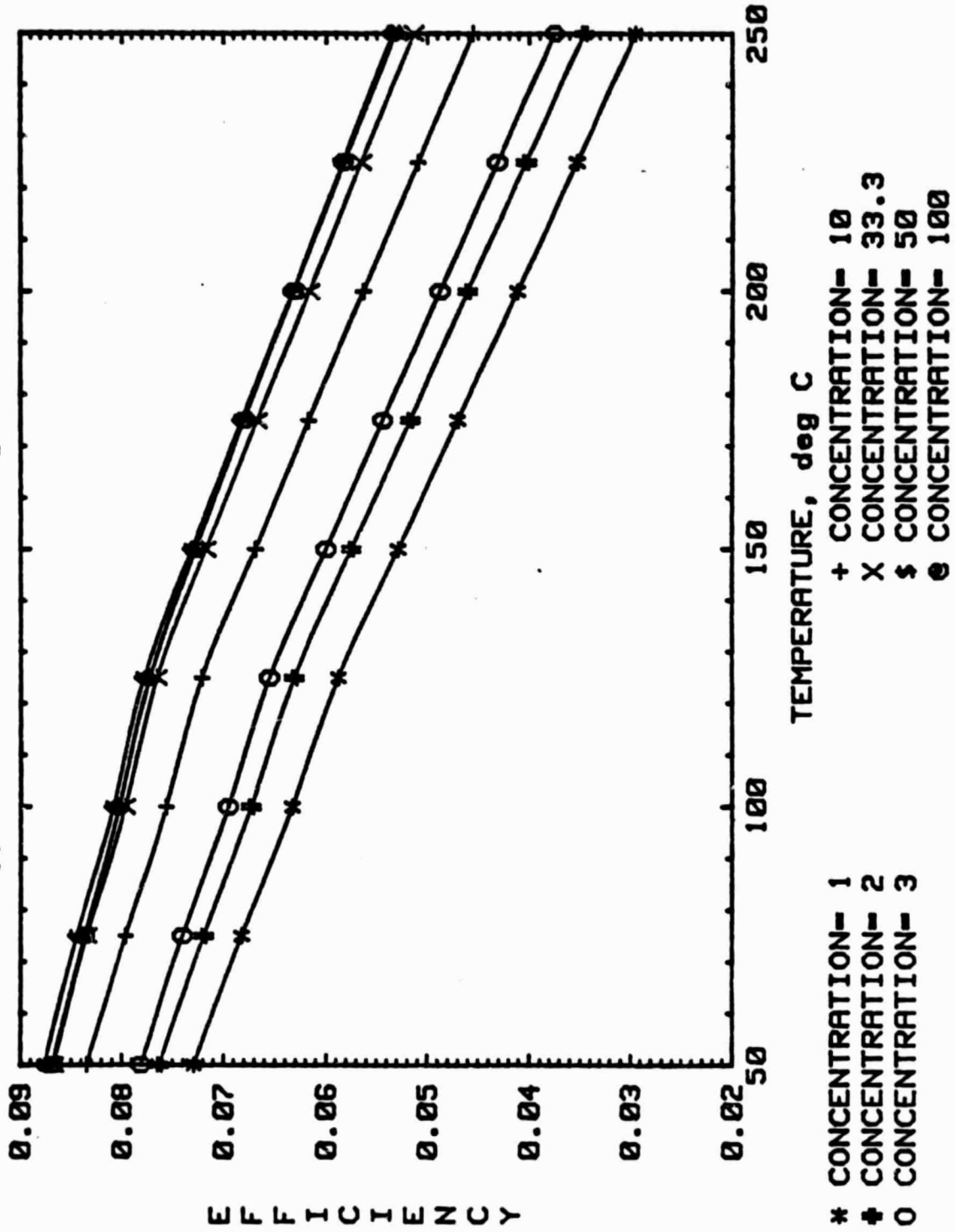


FIGURE 6

Type II medium wavelength GaAs cell



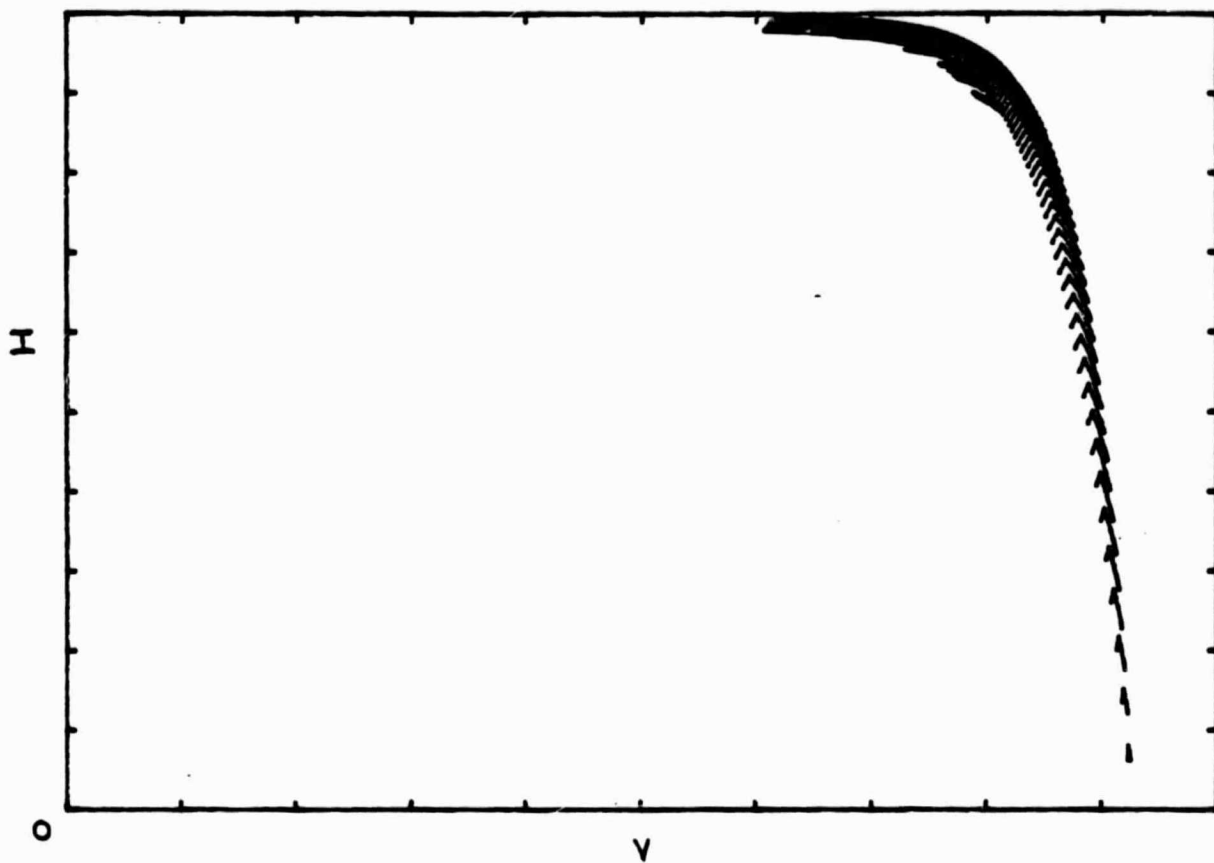


FIGURE 7 I-V curve for Type II cell, 50 suns and 125°C.  
(See Table V for current and voltage scales and  
Fig. 10 for a discussion of I-V curve details.)

Efficiency versus temperature and concentration for monochromatic light (1 sun being the power in the AM0 band from 1.38 eV to 1.91 eV) is shown in Fig. 8. In Type II cells, the optimal efficiency was achieved for monochromatic light at 0.10 eV above the bandgap.

### 2.3 Type III Long Wavelength GaAsSb Cell

The 900-1200 nm AM0 band is probably best suited for a silicon solar cell, but since Varian is best equipped to evaluate III-V solar cells, this analysis was done for a GaAs<sub>0.73</sub>Sb<sub>0.27</sub> cell having 1.11-eV bandgap at 30°C. Figure 9 shows the efficiency versus temperature and concentration. The I-V curve for 50 suns, 125°C, is in Fig. 10.

Efficiency versus temperature and concentration for monochromatic light (1 sun being the AM0 power from 1.03 to 1.38 eV) is shown in Fig. 11. Optimal efficiency was achieved with the monochromatic light 0.07 eV above the bandgap for Type III cells.

FIGURE 8

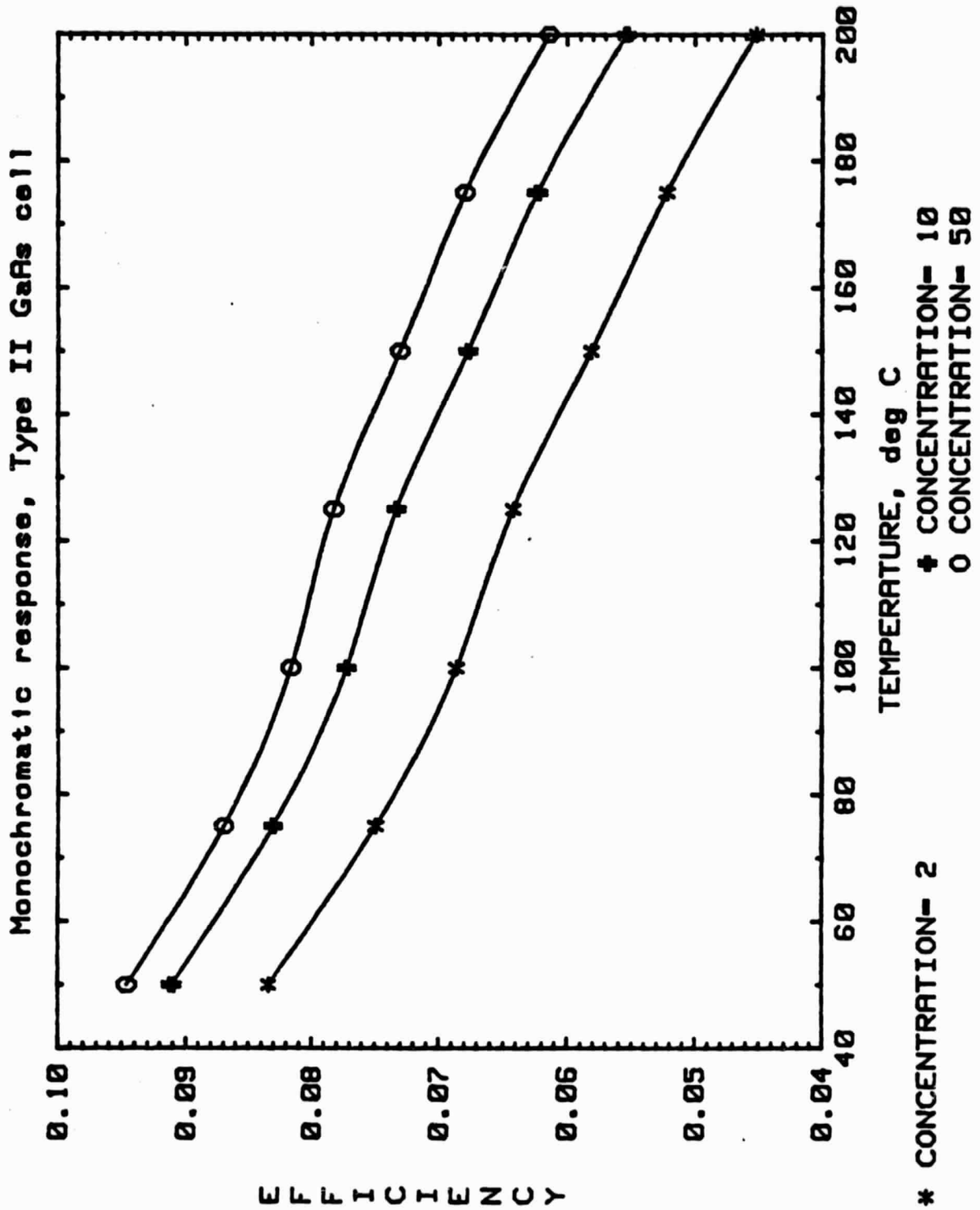
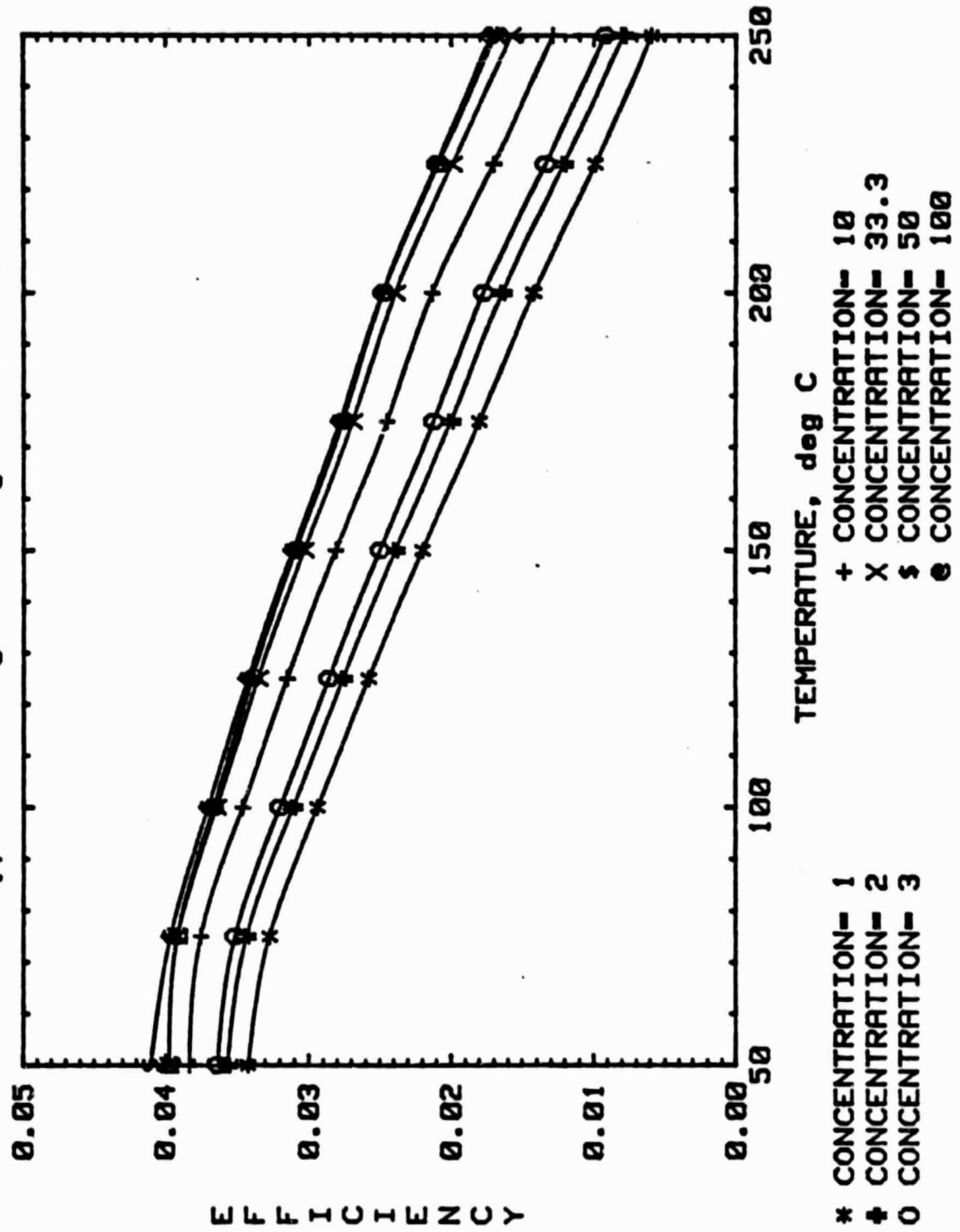


FIGURE 9  
Type III long wavelength GaAsSb cell



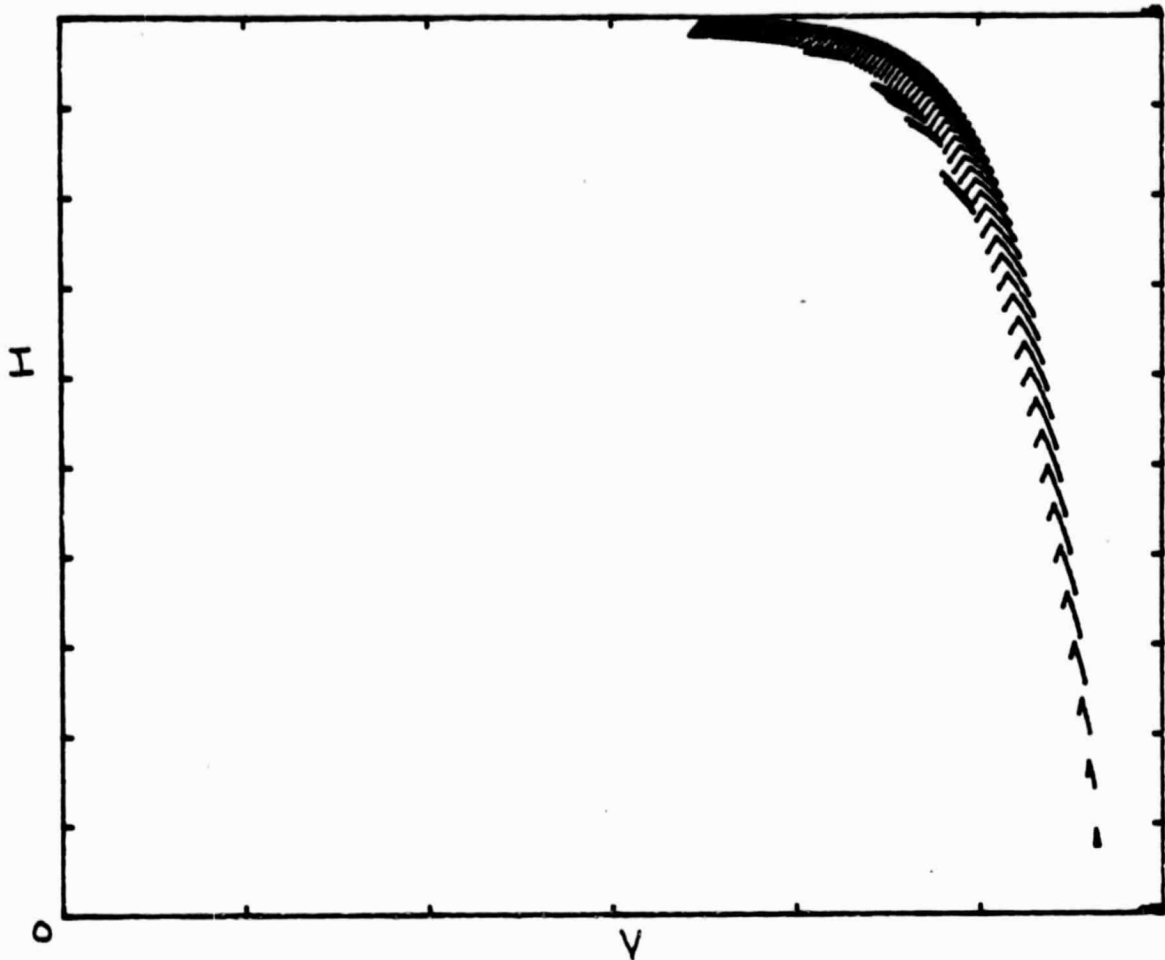
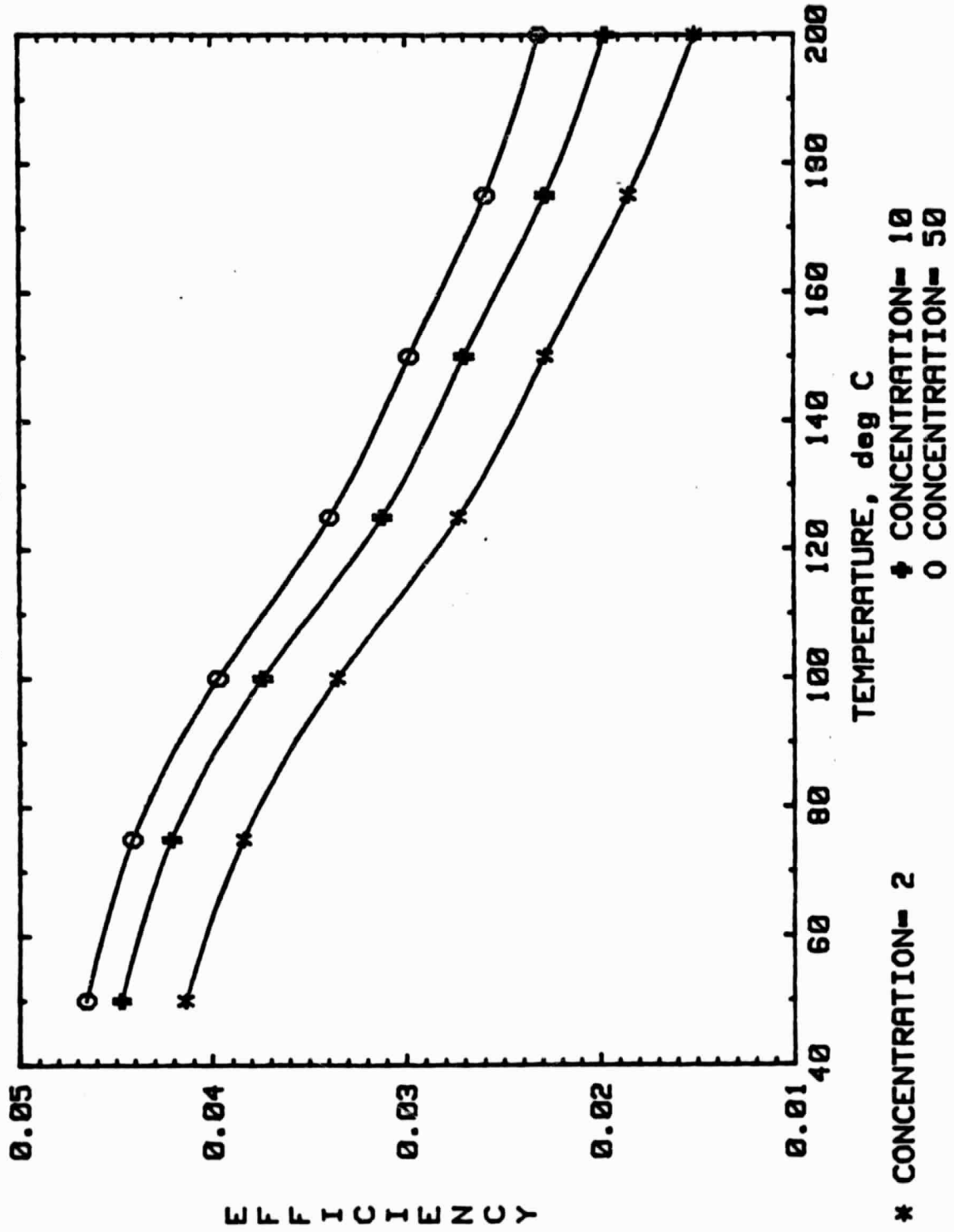


FIGURE 10 I-V curve for Type III cell, 50 suns and 125°C.  
(See Table V for current and voltage scales.)

The outside envelope of the set of curves represents the I-V curve of the junction itself, with no series resistance. The curve through the points of the inverted V's includes sheet resistance losses. The curve through the inside edge of the V's includes the voltage drop through the ohmic contact resistance, blockage of light by the metallization, and loss of current in the junction under the metallization. The curve drawn inside the set of 10 bunched curved lines is the terminal I-V curve. It includes losses due to the resistance of the grid contact metallization. The maximum power point is at the point where the lines are most closely bunched together.

FIGURE 11

Monochromatic response, Type III GaAsSb cell





### 3.0 TASK III - SOLAR CELL MANUFACTURING AND COST PROJECTIONS

#### 3.1 Multijunction Solar Cell Manufacturing Processes

Multijunction solar cell manufacturing can be divided into four major component process areas as shown in Table VI. Each of these areas influences the performance and cost of the cells. High volume, commercial equipment is available for many processes; however, several processes, such as epitaxial growth and packaging, require in-house-designed equipment to meet specific cell design and system requirements. The cells are processed in wafer form until step 12 where they are cut into individual cells. This process would be used if cells were processed today; however, various improvements will undoubtedly be introduced by 1990. The following discussion will describe several of the most important processes.

##### 3.1.1 GaAs Substrate Preparation

In this cost study, we will consider the epitaxial multijunction stack to be lattice matched or lattice-constant graded to a GaAs substrate. Single crystal GaAs substrates of the size required are available from either liquid encapsulation Czochralski (LEC) or horizontal Bridgmen growth. Varian grows high quality LEC ingots 2.5 inches in diameter weighing 1.5 kgm. It is very likely that ingots at least 3 inches in diameter weighing 4-5 kgm will be available by 1990. Rectangular ingots are being grown by horizontal Bridgmen which can supply wafers that are 1.25 inches x 1.75 inches, and this size will also be significantly increased by 1990. Polycrystalline GaAs, which



TABLE VI

SOLAR CELL MANUFACTURING PROCESS FLOW

- I. GaAs SUBSTRATE PREPARATION
  1. Polycrystalline GaAs Growth
  2. Single Crystal GaAs Growth
  3. Slice into GaAs Substrates and Polish
  
- II. ACTIVE LAYER EPITAXIAL GROWTH
  4. Organometallic Vapor Phase Growth
  
- III. CELL FABRICATION
  5. SiO<sub>2</sub> Deposition
  6. Front Contact Photolithography
  7. Front Contact Metal Evaporation
  8. Front Contact Metal Lift
  9. Back Contact Evaporation
  10. Front and Back Contact Alloy
  11. Plate Front Contact
  12. Cut Wafer into Individual Cells
  13. Etch to Remove SiO<sub>2</sub> and GaAs Contact Layer
  14. Deposit Antireflection Coating
  15. Test at One Sun
  
- IV. CELL PACKAGING
  16. Solder Solar Cell to Baseplate
  17. Solder Interconnect Metal to Solar Cell Front Contact and Baseplate
  18. Test at Concentration
  19. Attach Cover Glass with Transparent Adhesive
  20. Test at Concentration



contains the n-type dopant (Sn, Te, etc.), is used as the starting material for both of these growth techniques.

Single crystal GaAs ingots are sliced on a multiblade saw into wafers .020 inch thick. The wafers are then lapped and chemically-mechanically polished to remove saw damage and provide flat, smooth, damage-free surfaces required for high yield epitaxial growth. Final wafer thickness is .016 inches. This will also be very nearly the thickness of the multijunction solar cell. Because they are large-area devices, GaAs cells are susceptible to breakage during processing. It would probably not be cost effective to produce thinner cells because of reduced yield. However, the possibility of reducing the thickness to .010-.012 inches would be investigated during early stages of production to determine the exact yield and net cost effect.

### 3.1.2 Solar Cell Active Layer Epitaxial Growth

In the organometallic vapor phase epitaxy process, the wafers are placed on a susceptor which is heated, and  $H_2$  gas containing various organometallic compounds, hydrides such as  $AsH_3$ , and dopant gases are passed over the wafers. Chemical reactions result in deposition of the active layers on the wafer surface. It is a continuous process in which the compositions of the various layers are determined by the chemical inputs to the gas transport system. The organometallic process can employ larger reactors than are presently used, can handle a variety of wafer sizes, and give smooth wafer surfaces which are important for photolithography during cell fabrication. The main challenge with organometallic growth is to control material



properties to meet the desired cell efficiencies.

### 3.1.3 Solar Cell Fabrication

Following active layer growth, the wafers are metallized, cut into individual cells, covered with the antireflection coating, and tested at one sun for acceptable performance. Most of these processes use cost-effective, high-volume, semiconductor industry equipment. The processes must be carefully controlled in order to obtain high yields. A low specific contact resistance is essential for high cell efficiency, and this property is monitored during fabrication.

The AR coating will most likely be either  $\text{Si}_3\text{N}_4$  or  $\text{TiO}_2$ .  $\text{Si}_3\text{N}_4$  is currently used and is deposited by a plasma deposition process.  $\text{TiO}_2$  has been developed experimentally as an AR coating and will probably be available by 1990 for production if required.

### 3.1.4 Solar Cell Packaging

The cell packaging procedure consists of attaching the cell to a cell support structure (baseplate) and interconnect metallization and installing a cover glass. The GaAs cell is soldered to a baseplate which provides solder connections to the front and back cell contacts. The cell baseplate can then be mounted to the array by either a solder or mechanical connection. This baseplate could be made part of the array structure so that it would not add extra weight. The baseplate could be metallized alumina approximately .020 inch thick and rectangular in shape so it could easily insert into a pattern of open matching spaces



containing the overall system interconnect metallization. The cell would be soldered to the baseplate using vacuum solder, and a metal leadframe interconnect could be soldered from the front contact of the cell to the baseplate in the same manner.

A cover glass for radiation protection would be attached to the soldered GaAs cell using a space-approved transparent adhesive such as Dow Corning 93-500. III-V solar cells appear to be more resistant to radiation damage than silicon cells and could probably use a .004 inch thick  $MgF_2$  or blue-red-coated ceria-doped microsheet cover for light weight. This gives excellent transmission and perhaps 0.5-1.5% power enhancement when bonded to the GaAs cell AR coating of  $TiO_2$ . An alternate cover to be tried would be .006-.012 inch thick fused silica with antireflection and UV rejection coatings. The expected transmission is the same; however, this is a thicker cover which adds weight. A blue-red coating which would reflect most of the IR above  $1.0 \mu m$  would be very useful for heat rejection in this high concentration system. Reduced heat transfer through the cell would simplify attachment of the cell to the array.

The cell-baseplate assembly would be tested at concentration to select those units for glass covers and tested again after cover attachment. This should result in a high yield of good cells attached to the array.

### 3.2 Projected Solar Cell Costs

III-V solar cell costs are presently very high because the cell technology is still undergoing considerable



development and high volume facilities do not exist at this time. Future costs will depend largely on the extent of engineering efforts given to III-V and the volume of cells required. Extensive engineering programs can develop high-volume processes in all areas -- materials, fabrication and packaging. In addition, progress on volume production by 1990 of GaAs integrated circuits and optoelectronic devices will have significant impact on some of the costs, such as substrates and quite possibly epitaxial growth. Government and private funding for terrestrial GaAs cells could have a large impact as well.

The major areas requiring development to lower solar cell costs for large power arrays are epitaxial material and packaging components and technology. Considerable commercial equipment already exists for fabrication, yet largely remains to be developed for materials and packaging. High-volume fabrication equipment will also continually be developed for the general semiconductor market. The major focus in fabrication should be aimed at high-yield processes using existing equipment. As these processes are more clearly defined, any high-volume fabrication equipment not available can be developed.

Low-cost solar cell wafers, including substrate and epitaxial layers, are absolutely essential for low-cost cells. This is important as it relates to the basic cost of materials as well as fabrication costs, which are greatly reduced by processing large wafers containing numerous cells per wafer. Bulk GaAs ingots of 3" diameter and 5-10 kgm will be required for low-cost substrates. Organometallic epitaxial growth will need multiwafer run



capability, with fast turnaround time. The amount of material required for sizable cell power production will be very large. For example, the production of 4 MW/year would require ~1 million in<sup>2</sup> of epitaxial wafers. It is obvious that high-volume processes are required to handle these quantities of wafers at reasonable labor and capital equipment costs.

Packaging costs can be a significant percentage of the total costs. Not only can package components be expensive, but they can critically affect yield, initial performance, and reliability of solar cells, all of which can have sizable cost implications if not carefully considered. Packaging materials and fabrication techniques for these materials determine the package component costs.

The potential for obtaining low-cost solar cells can be demonstrated by comparison to a very similar industry -- namely, optoelectronics for LED devices. The optoelectronics industry has clearly shown that GaAs and related compounds (GaAsP, GaP) can be greatly cost-reduced through volume processing of the materials. In addition, the optoelectronics industry has shown that materials (substrates and epitaxial growth) and packaging are the dominant cost factors. The optoelectronics GaAsP processes are quite similar to solar cells in kind and only differ in specific details. Both require GaAs substrates, epitaxial growth, fabrication of metallized devices, testing of unpackaged devices, packaging and final test. The yield and cost considerations for solar cells will be very similar to optoelectronics devices. We have compared our basic cost estimate, where possible, to available costs from the LED industry and found them con-



sistent. If the market develops as expected, the costs will be achievable. These costs also assume a continuous market for GaAs cells and an 80% learning curve as volume increases.

Cost projections are based on a method used for calculating terrestrial cell costs and adding 30% for special costs related to space cells. These special costs cover additional documentation and quality control tests required for space cells. The packaged cell costs also incorporate cover glass quotes and associated assembly costs from two potential vendors. Aside from these two considerations, cost estimates are similar to those done for terrestrial cells.

For this contract, the following specific assumptions are used:

1. Concentration ratios of 50 and 100
2. Operating temperature of 150°C
3. Theoretical efficiency of 22.5%, although there will probably be a 1% difference in efficiency from 50-100 suns. This was not considered.
4. Average actual power output at 90% of theoretical
5. AM0 solar power of 1.353 kW/M<sup>2</sup>
6. Cell size. This was not specified, but individual cells might be on the order of 1.5 cm x 3 cm.
7. 15% of cell covered by busbar metal for contact to package components.
8. Loss of 10% of the epitaxial material due to wafer edges not usable as part of a cell.
9. Overall cumulative yield of 60.5% of assembled good cells out of potential cells obtainable from wafers entering the epitaxial process.
10. Cell costs at selling prices to array manufacturer from an outside supplier.



#### 11. 1980 \$ values.

From these assumptions and terrestrial cell cost projections, cost curves were generated as a function of cumulative cell production for packaged cells at 50x and 100x concentration ratios. The packaged cell cost includes all soldering operations and cover glass attachment required for a unit which could be mounted to an array. These projections follow an 80% learning curve. These curves are shown in Fig. 12 for cumulative power levels from 1 to 1000 MW. The upper curves for both concentration ratios assume technology and material costs similar to today's optoelectronic industry. The lower curves assume a 50% reduction in these costs. For example, present wafer sizes are small (2-3 in<sup>2</sup>) compared to those obtained from potential 3" diameter ingots (7 in<sup>2</sup>). Similar improvements in epitaxial, fabrication, and packaging throughput could bring about lower costs.

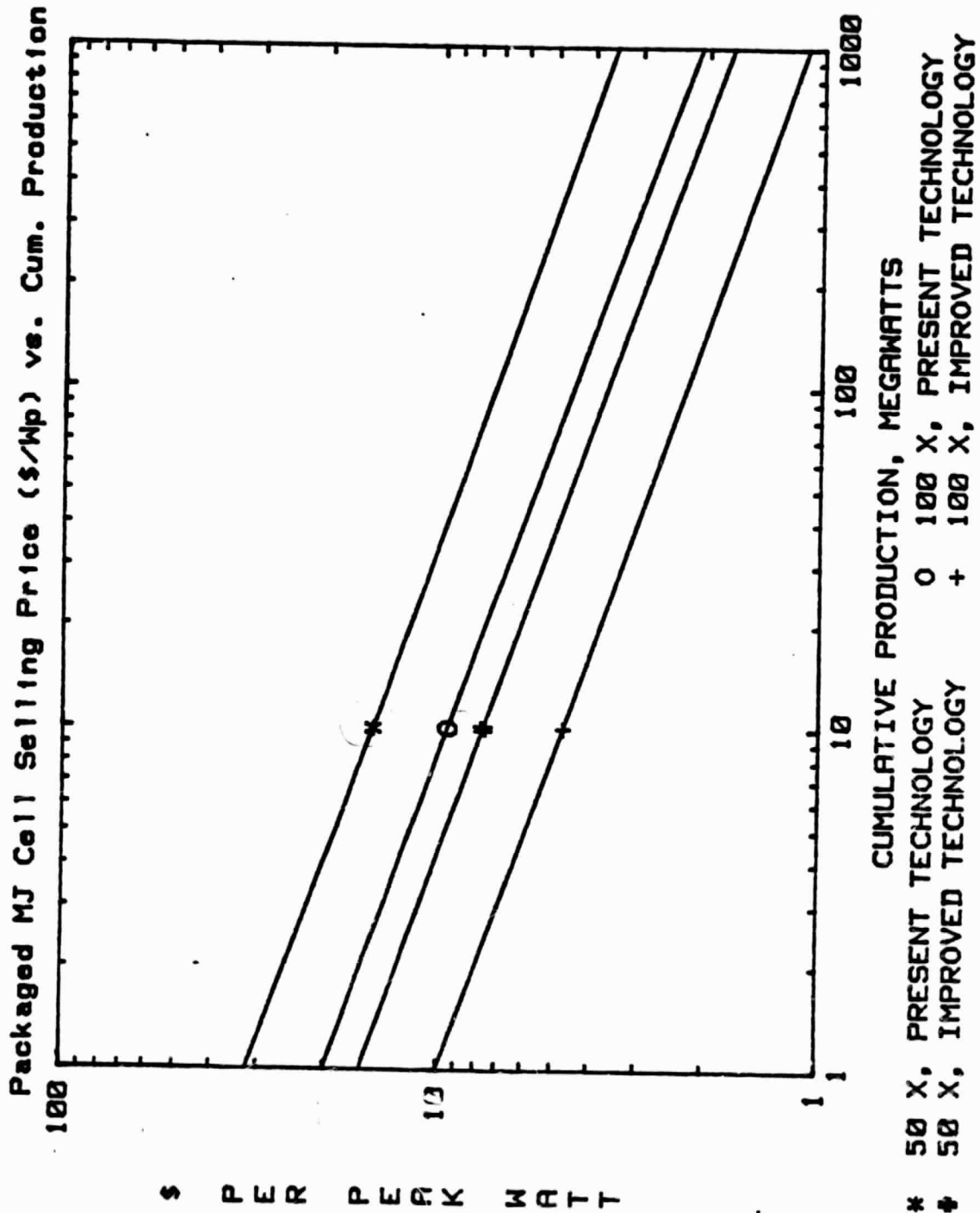
Several conclusions may be made from these curves and discussion:

1. Costs in \$/Wp (Wp = peak watt) at high-power volumes can be greatly reduced from present space solar cell costs.
2. Higher concentration ratios strongly lower cost due to the high cost of GaAs material and packaging materials such as cover glasses.
3. Volume has a strong impact both from the standpoint of the learning curve as well as technology breakthroughs which occur for sizable markets.



4. To meet these costs, all areas of solar cell development will need strong support, but materials and packaging in particular.

FIGURE 12





#### REFERENCES

1. K. Bachmann, et. al., "Melt and Solution Growth of Bulk Single Crystals of Quaternary III-V Alloys," Prog. Crystal Growth Charact. 2, 171-206 (1979).
2. L. James et. al., "High Performance GaAs Photovoltaic Cells for Concentrator Applications", Final Report, Sandia Contract No. 05-4413 (1977).
3. J. H. Heinbockel, et. al., "Simultaneous Radiation Damage and Annealing of GaAs Solar Cells", Proc. 14th IEEE Photovoltaic Specialists' Conf., San Diego (1980).

## REFERENCES

1. Pleasant, R. L., "Analysis and Optimization of Radiator Systems for Large Heat-Generating Spacecraft," Convair Report CASD-ERR-78-031, December 1978.
2. Chi, S. W., "Introduction to Heat Pipe Theory: An Instruction Manual," School of Engineering and Applied Science, The George Washington University, Washington, D.C., October 1971.
3. Pleasant, R. L., "Upper Stage Avionics Thermal Control," Convair Report CASD-ERR-76-039, December 1976.
4. O'Neill, R. F., et al, "A Numerical Procedure for Solution of Radiation and Convection Fin Heat Transfer Problems, Computer Program P5399," Convair Report No. GDCA-P-71-001, August 1971.